ISAS - INTERNATIONAL SCHOOL
FOR ADVANCED STUDIES

OPTICAL AND UV SPECTROSCOPY OF Be/SHELL AND SUPERGIANT STARS

Thesis submitted for
the
Degree of
Philosphiae Doctorate

CANDIDATE:
Levent DENIZMAN

SUPERVISOR :
Prof. Margherita HACK

ASTROPHYSICS SECTOR

ACADEMIC YEAR 1987-1988

TRIESTE

SSA - SCUOLA
TERNAZIONALE
SUPERIORE
TUDI AVANZATI
TRIESTE
Strada Costiera 11

CONTENTS

I.GENERAL ASPECTS OF Be/SHELL STARS.

I.1.INTRODUCTION

After the discovery of the first Be star in 1866 by A. Secchi,these stars and their puzzling properties attracted a great curiosity of the astronomers for more than one century.The first catalogues of Merrill and Burwell (1933, 1943, 1949, 1950) contain 1088 Be stars.Lastly Wackerling (1970) listed nearly 3000 of them; anyhow the list of the Be stars is far from being complete,and new Be stars are still being discovered among the bright B stars, which were thought to be normal B stars.

According to the classification scheme of Jaschek et al. (1980), a Be star was defined as a nonsupergiant object of B type that has exhibited a Balmer line emission at least once.From this classification supergiants were excluded even though many of them exhibit H alpha in emission.Later we will discuss the consequences of this exclusion.This distinction of Be stars from supergiants is primarly based on the great difference in absolute magnitudes of these two groups.The Be stars form a large subset of the B stars,about 20 %, having a maximum frequency at spectral type B2-B3.

The following classification of Jaschek et al.(1980)was based on the descriptions of many spectra of Be stars, taken at an arbitrary phase.Furthermore the material used was taken at the same dispersion in order to have a homogenous data set; the catalogue includes 140 stars, and reports with all changes

occured in the last 20 years.

GROUP 1:The objects of this group were characterized by the FeII emissions. Emission features were permanent (over 20 years) except in few cases where sometimes they were absent.This group of stars exhibited also emission in the Balmer lines of hydrogen up to the higher members.Members of this group were found from spectral types B0 to B6 with a maximum frequency at B2.The earliest stars of this group(B0 and B0.5) showed emission filling for Balmer lines and some of them HeI 5876(A) line in emission.FeII lines in emission were stronger in the early spectral types and weaker towards the later ones.There were only four stars which were later than spectral type B3.The emission lines showed long term variability both in FeII and hydrogen.It seems that there was a rule that whenever H emission lines were strong FeII lines were also strong. After the maximum intensity of the emissions, FeII emissions faded faster than the Balmer emission.

They also remarked that luminosity class of members of this group was difficult to ascertain for the earliest stars because of the fill-in.But in generally they are dwarfs except four of them which are giants.These possible giants also exhibited H core and metallic shell lines and P Cygni profiles in the Balmer lines.Lastly; forty four stars, 31 % of the total sum, belonged to this group ;which on the other hand represents 52 % of all the early type stars (B0 - B5) in their

catalogue.

GROUP 2:The objects of this group exhibited emissions in H alpha and H beta, with sharp cores of which half were permanent during the 20 year period (H shell).Members of this group were found between spectral types B3 and B8 (one exception at B2) with a maximum at B3.In the later types of this group the H beta emission consists in a central emission superimposed on a broad absorption line.Luminosity classes for the members of this group was generally V, with one exception which was IV.Thirteen stars, 9 % of the whole sample, belonged to this group.The emission lines and the sharp cores exhibited time variability.

GROUP 3:The objects in this group exhibited emissions in H alpha and H beta only, dark cores in the higher Balmer lines (hydrogen shell lines) and narrow metallic absorption lines.They extend from spectral types B5 to A0 with a maximum frequency at B8.The absorption lines corresponded mostly to FeII and TiII but their presence was clearly incompatible with the classification based on the HeI lines.The spectrum of the metals ,resembles that of supergiants of luminosity class I ,however it was difficult for Jaschek et al.(1980) to assign a spectral type and the only rule was that it never seemed to be earlier than the type attributed on the basis of the He lines.Since the number of the metallic lines observed in the spectra later than B9 spectral type increases with spectral type, classifications based on the helium lines becomes

practically impossible.

The spectrum of the metallic lines generally was variable, both in intensity and in line richness.The intensity of the SiII lines did not correspond to that of FeII in a normal supergiant and that of MgII lines behaved irregularly.This group seemed to be an extension of group 2 towards later spectral types.There were seven objects in the group representing 5 % of the total sample.

GROUP 4:The objects in this group exhibited emission permanently.In the earlier spectral type members of this group the emission was visible in H alpha and H beta and very occasionally in the earliest types in H gamma as a weak central emission on a broad absorption line.Towards the later spectral types the emission features were present only in H alpha and H beta as a central emission on a broad absorption line.In the later types of this group the emission was present only in H alpha and appears as a central emission.The range of these objects was varying from spectral types B3 to A0 with a maximum around B8.As regarding the luminosities, half of the stars considered were dwarfs and half were in IV or III luminosity classes.Forty stars belonged to this group ,29 % of the whole sample.

GROUP 5:the objects of this group changed from B to Be or vice versa during the period of study and some of them even underwent two changes(Be-->B-->Be or B-->Be-->B).Emission was present in H alpha and H beta and exceptionally in H

gamma.Except in one case there was no strong evidence for FeII emission lines during the Be phases.There were stars of this type between spectral types B1 and A0, but their number tended to decrease towards later types.Roughly half of the stars were off the main sequence.A total of 37 objects belong to this group.

In the following section we will discuss the current models and their difficulties to reproduce the observations.This discussion will give only the main outlines of these models for the explanation of the Be phenomena.

I.2.POSSIBLE MODELS TO GENERATE Be/Shell SPECTRA

The recent observational data in UV,and Xrays gave evidence that standard models are not able to describe the high energy spectrum of normal B stars, and they fail also for normal stars of other spectral types too.As an example they cannot represent the hot chromospheric-coronal regions which surrounds stellar photospheres and/or it is not possible to generate with them the macroscopic outward flow of the atmosphere, the stellar wind, where measured velocities pass progressively outward through subthermal, thermal and superthermal values.In a thermodynamic sense this "wind" is a simple mass flux from the star; thus even a normal real star is an open thermodynamic system while the standard model refers to a closed system,where the "degree of opennes"can be measured by the size of the mass flux observed from the star.Also this standard aproach fail to represent the low energy spectrum of Be stars because such models cannot produce those very extended ,low velocity dynamic regions lying above the photosphere which are colder than the temperatures predicted under radiative equilibrium(RE); moreover far UV and X ray observations suggests that there are some regions hotter than RE permits.Particularly at certain phases of their variations,these regions in Be stars show stronger mass flow than do the same regions in the B stars.

Now let's see the current approach to explain the Be phenomena.Three models are rather successful,in a certain

degree, in explaining Be/shell stars.Harmenec (1982) had outlined these models and remarked one more important aspect: according to his approach classification which was done by Jaschek et al. (1980) was limited a priori to "normal conventional" Be stars, i.e. stars of luminosity classes V to III, and there is still no general agreement about the nature of the Be phenomena hence all such classifications must be more or less descriptive.The possibility that the hydrogen emission observed in the spectra of apparently very different objects had always the same physical cause and that the differences between these objects are caused only by continuosly varying physical and/or geometrical parameters should seriously be considered, along with all other concepts.He proposed that it will be more promising to study Be stars in the context of all early type emission objects including supergiants,P Cygni stars,Beta Cep objects,WR stars ,symbiotic stars and novae.Such a viewpoint is not new; infact it was expressed already by Struve (1942).As an example we can give Wackerling's catologue which includes all of these objects.In particular if we consider the case of supergiants very little is known about their long term spectral variability. However their radial velocity and photometric variations do seem to be rather similar to what is observed for Be III-V stars(Sterken 1977., Sterken and Wolf 1978 or Rufener et al. 1978,Denizman and Hack 1988).Thus to exclude the supergiants from consideration probably will lead from

time to time to inconsistencies.

i]The Rotational Model (RM) proposed originally by Struve(1931)

The basic assumption of the model is that Be stars are rotationally unstable at equator and eject matter, which forms envelopes and gives rise to the emission lines.RM is thus based on the assumption that a rapid axial rotation is a common property of all Be stars, a property which these stars gained during their contraction towards the ZAMS. Let's see the observational evidences in favour of this model.Different shapes of the lines are easily explained by the aspect effect: Be stars with single-peaked narrow emission lines have also sharp absorption lines and are understood as rapidly rotating objects seen roughly pole-on.Also the observed direct proportionality of the width of the hydrogen emission lines to their wavelength ,first recognized by Curtis (1923) agrees well with RM.

The great disadvantage of this model is that it offers no clear explanation of the variations observed.It only could explain light and spectral variations with typical cycles around one day.However for explaining the long-term E/C,RV and V/R variations of emission lines, some other mechanisms had to be considered.Already Struve (1931) suggested a possibility to explain the cyclic V/R variations by the assumption that the envelope has a form of an elliptical ring whose line of apsides rotates slowly in space.Later Mc Laughlin (1961) tried

to formulate this model mathematically and showed that it gives correct amplitudes of the RV variations.Huang (1973a) enlarged Mc Laughlin's ideas and computed also emission profiles of the ring assuming that the ring is optically thin for line radiation.However it was not clear how such a narrow ring, arbitrarily tilted with respect to the observer could produce the deep shell lines (Marlborough 1976).At the same time Kriz (1976,1979a,b) using more realistic physical assumptions with a geometrically thick elliptical envelope was able to reproduce the observed profiles as well as their V/R and RV variations quite reasonably.According to Harmanec (1982) this model seems promising but the long-term E/C variations are much less understood and it is possible that several different types of these variations exist.One more important problem to be solved is the following: Be/shell stars are rotating fast but not at the break-up velocities so rotation only cannot be responsible from the outflow of the matter.

A new approach to RM have been done by Baade (1981).He suggested to interpret Be stars as analogs of Beta Cep objects subjected to a rapid axial rotation and developed a crude theory of non-radial pulsations of rapidly rotating stars.He succeded to explain the 1.37 day periodicity of RV and V/R variations of 28 C Ma as a non-radial pulsation with waves travelling opposite to the sense of rotation.

ii]The Model of Radial Outflow of Matter(OM).

Gerasimovic (1934, 1935) was the first to introduce this concept of radial outflow of matter as an alternative for explaining the presence of emission lines in the spectra of Be stars.His proposal was that in luminous stars like supergiants and P Cyg stars, the acceleration due to radiation pressure must outweight gravitation hence resulting a formation of a steady expanding envelope which he called a "non-static chromosphere".In less luminous rapidly rotating Be stars this radiative dissipation is largely helped by stellar rotation.

Assuming that the envelope is expanding with decreasing velocity he was able to explain qualitatively the central absorptions in double peaked emissions and even the long term V/R changes as consequences of varying optical thickness of the expanding envelope.Recently Doazan et al. (1980 a,b,c) modified these old ideas of Gerasimovic; they have proposed that the Be phenomena is only an enhancement of the chromosphere-corona complex which should exist around every star.The basic difference of their model from those of the other supporters of OM, is that the mass loss from the stars in these cases is not due to the radiatively driven stellar wind.They have accepted the concept of Thomas (1973) and Cannon and Thomas (1977) that the flux of the matter is provocated by subatmospheric nonthermal storage of energy.So their model of a radially expanding envelope of Gamma Cas (Doazan et al. 1980) predicted correctly the presence of highly ionized lines in the UV spectrum and of the X ray

emission which should originate in the high temperature regions close to the star.The H I emission should originate in the cooler outer layers of the envelope, where the expansion velocity is decreasing outwards as in Gerasimovic's model.However they had problems in reproducing the observed hydrogen emission in the optical region, where the calculated densities are lower than satisfactory values.

Snow et al. (1979) suggested another modification of OM. They assumed the radiatively driven stellar wind model and a velocity field with expansion velocity increasing outwards.In their model the hydrogen emission originates near the stellar surface where the velocity is low ; the UV shell lines like FeIII with expansion velocities around 100 km/s are formed above these layers.Finally the high velocity SiIV and NV lines ,in some cases originate in the outer layers of the envelope, where both the acceleration of the expanding matter and the degree of ionization have increased substantially.Their main difficulty can be stated like that:The resulting line profiles from all available theoretical profiles of the H I lines originating in the expanding atmospheres which use radiatively driven stellar wind (Kunacz 1980) differ substantially from the profiles observed in Be stars.

iii]The Binary Model proposed by Kriz and Harmanec 1975.

This model assumes that the Be envelope is formed by the matter transfered to the B star from the other component

of the binary system.Now let us outline probable scenarios for this model.

Mode 1; can be defined as follows; an envelope is formed within the corresponding Roche lobe.To provide space enough for the envelopes with dimensions several times larger than the radius of a B star the orbital periods of such systems must be relatively long.Surely the period is not the only important parameter; the masses of both components must also play an important role and specially the mass ratio which may control the rate and the type of mass exchange.Also the appearance of the real systems depends on which one of the component stars dominates on the optical spectrum.Thus this simple picture can be almost arbitrarily complicated.As an example; if the mass transfer is strong enough ,the emission may be associated with hot spots, especially in extremely short period systems such as dwarf novae (Mode 2).

It seems that most of Be stars with double emission lines do not originate in this manner.Another consequence of a rapid mass transfer can cause a substantial mass loss from the system.In principle such material can form an outer envelope around the whole system (Mode 3).So no apparent restriction of the orbital period of such binary can be predicted, because the mass loss will be probably connected also with a substantial loss of angular momentum which can result in a system with a short orbital period.Further complications in real systems can be produced by combinations of several modes.

Besides the formation of the envelope the other component may be responsible for the long term RV and V/R variations observed for many Be stars.Computations by Kriz and Harmanec (1975) showed that the envelope around the gainer produced by a variable mass transfer may have the form of an elliptical ring whose line of apsides slowly rotates due to the perturbing force of the secondary component. Thus BM can explain the origin of the elliptical envelope, infact Castle (1977) developed a whole grid of models including those corresponding to mode 3 and confirmed the applicability of the model to Be stars and pointed out that elliptical disks can produce radial velocity-excitation gradients of either sign.It also seems that the secondary may be responsible even for the long-term E/C variations of Be stars.

There are two main objections raised against BM;namely i]the negative result of the search of duplicity in several Be stars, ii] if all Be stars were semidetached binaries one must observe eclipsing binaries among them.

We would like to conclude these introductory remarks with some notes taken from Plavec M.(1987).A very important trend can also be recognized: the growing realization that the Be stars are not an isolated group of objects, as they appeared to be at the time of the Struve-Mc Laughlin-Huang elliptical ring model.In the stellar wind model (OM), the Be stars are a continuation of the Oe stars; the strong radiative push provided by the high luminosity OB supergiants is

believed to be partly provided by the rapid rotation in the less luminous Be stars.

The binary model implies that in the wide sea of various types of interacting binaries, there are cases where by chance the mass gainer happens to be a B star, that is, provides enough ionizing photons to create Balmer emission lines radiated from the accretion disk.The hypothesis of non-radial pulsations stresses the affinity of the Be stars to their other neighbours in the H-R diagram, namely to the pulsating Beta Cephei stars.And the model of the chromosphere-corona complex (OM) dominated by the non-radiative energy flux from the deeper layers of the star, as supported by Thomas, Doazan and others ,stresses explicitly that the Be phenomena is only an enhancement of a structural complex which should exist in all stars.

I.3.THE PRESENT RESEARCH

The aim of this research can be summarized as follows:

Up to now I.A.U. organized two symposia and one colloquium on the Be phenomena.Many researchers contributed with theoretical models and observational results.These meetings revealed the fact that there is still no clear understanding of the Be phenomena.Its' physical and geometrical causes are far away from being clear.

To search the Be phenomenon two observational strategies can complete one another: The first one is to observe extensively a large number of objects in order to permit future researchers to trace the historical behaviour of each object, based on the good statistics and deductive research.The other one is to observe individual objects for detailed inductive study, in order to gather information on the fundamental parameters (and therefore evolutionary stage) and on their short and long term variability in order to obtain physical insight on the reason of their variability, or in other words the origin of the Be phenomenon.

In this research we gathered stars which have different spectral types and luminosity classes, but all of them exhibiting Be phenomena.Some of our program stars are well known and already being classified by Jaschek et al. (1980) but others (one Herbig Be star and three Late B and A supergiants) are not.So, here we study a number of selected Be/shell stars and Be supergiants observed several times at

several epochs of the year, for understanding the envelope and shell by means of the Balmer line profiles, radial velocity distribution/varability, Balmer line progression,emission line variability and for deriving the fundamental stellar parameters by the study of the underlying stellar spectrum. These fundamental parameters such as spectral type effective temperature and effective gravity of Be/shell stars are quite uncertain because of the spectroscopic variability of these stars.Besides the optical spectra, we also secured UV spectra of the program stars in order to get information about the envelopes of the stars.Another important aspect of our research is to put light on the Be characteristics of Late B-A supergiants.Underhill(1982) remarked that, the long time spectral variations and envelopes of these stars are very poorly known.

Up to now very few researchers made a detailed comparison of the late B-A supergiants and Be spectra in the UV region (Snow et al. 1979).Also we applied a detailed analysis to a large number of resonance lines of the program stars,observed at different epochs.These lines generally formed outside of the photosphere and give important clues to velocity fields, mass loss and superionization in the atmospheres of these stars.At the same time UV continuum and it's comparison with Kurucz models is done for every star except supergiants where the interstellar extinction is very high.By having spectra taken at the different epochs we tried to study short and long

time variability in the UV resonance lines and UV continuum.

All the data processing for optical and UV spectra were carried out with an European standard software which maximizes the confidence to the measurements.Some of the used programs and their modifications are specially developed for our study.

II.OBSERVATIONS, DATA PROCESSING AND BIBLIOGRAPHY OF THE PROGRAM STARS.

II.1.THE OBSERVATIONS

II.1.1.The visual spectra

All the visual observations were carried out with the 1.52 meter telescope of the Haute-Provence Observatory.Spectrograms obtained at the Coude' spectrograph, at 12.4 and 20 A/mm reciprocal dispersions, are marked GB and GA respectively. III aF hypersensitized plates and IIa0 baked Kodak plates were used respectively for the region 5000-6700 and 3400-5000 angstroms. Table II.1 gives the basic data for the program stars and the log of the visual spectra are given in Table II.2.In appendix I the same data are presented for selected supergiants (respectively, Table 1,Table 2).

II.1.2.The Ultraviolet spectra

The UV high dispersion spectra of the program stars were secured from the VILSPA Data Bank Madrid,Spain.Spectra were generally well exposed and with a good S/N ratio and in the region 1250 A to 3100 A. The log of the UV spectra are presented in Table II.3. for the Be stars and Table 9 for the selected supergiants.

II.2.THE DATA PROCESSING

II.2.1.The visual spectra

The photographic material was digitized with the Perkins-Elmer PDS 1010 A digital microdensitometer of Trieste Astronomical Observatory.We give a short description of the

machine and SCANSALOT control software.For full reference to PDS and SCANSALOT specifications it is recommended to apply to Perkins-Elmer original user manuals.

The PDS (1010 A model) is a 2D mechanical scanning machine with a maximum scanning speed of 50 mm/sec on either axis.The scanning format is 250 mm* 250 mm. The digitization resolution is 1 micron.The standard scanning apertures are selected by the user from circular, square and rectangular formats of various sizes, depending on the particular slit and optical gain combination selected among the available ones.Astronomical spectra are usually scanned through a rectangular slit.The slit height is set by the effective height of the spectrum band.Astronomical spectra are usually digitized at a 5 microns step.The PDS machine can be operated in the transmittance or density mode.In the density mode, which was used for the digitization of our plates, an analog logarithmic converter is used between the detector and the analog digital converter, allowing the user to extend standard PDS digitization up to maximum density 4, with a typical density error 0.02.

The PDS machine is computer controlled through the standard SCANSALOT softwere.This software allows full control of the machine.The scanned data are stored on a magnetic tape in SCANSALOT standard format, in records of 3919 data/record.Pds digitization of the Astronomical spectra for ELSPEC/11 (Pasian et.al. 1982) interactive spectrogram

processing package, is carried out by executing five standard parallel scans on the spectrogram.These scans correspond to five consistent data files containing, with respect to the target spectrum, the lower plate fog, the lower wavelength reference spectrum and the target spectrum,the upper wavelength reference spectrum and the upper plate fog. ELSPEC/11 software accepts PDS SCANSALOT standard density data.To set properly the PDS in density mode it is used a suitable neutral filter to enhance the photomultiplier dynamics and the zero density is obtained on a region of the plate not exposed to the light.Of course the plate support should be aligned so as to ensure the best focus all over the scanning range.

The PDS digitization of the exposure calibration plates of the spectrograms for ELSPEC/11 processing is carried out by exactly the same PDS setting which is used previously to digitize the stellar spectrograms.Of course PDS must be refocused and readjusted to zero electronics on the calibration plate under scanning.Then the scanning operation can be carried by a raster perpendicular to the dispersion axis of the exposure calibration plates.The origin of this raster should set to one suitable line of the wavelength reference spectrum present on the calibration plates.Each scan of the raster thus includes one full series of exposure calibration levels at the wavelength corresponding to the current scan origin. The interscan distance was set to 100 A

for the blue and 200 A for the red plates.

The monochromatic exposure versus density calibration which was used through this work, is implemented in ELSPEC/11 by program DEXCAL which runs normally on a Textronix 4010/1 interactive graphic terminal.This program inputs no more than 20 observed densities versus log(exposure) data pairs and computes the second order canonical polynomial least squares fit of the Baker transform of observed densities versus log(exposure) data in the density range 0.001 to 4.0. DEXCAL accepts data directly from user terminal keyboard operated manually or interactively from the density calibration scan displayed on the user terminal screen.The calibration levels should be selected in a regularly increasing or decreasing sequence.For each selected level the user must enter the corresponding log(exposure) level.In this work H beta corresponding scan was used for the exposure calibration of the blue plates and H alpha corresponding scan for the red ones. The exposure calibration error as estimated through the residuals of the poynomial is fit typically about 2 %.The total expected error in intensity measurements is about 5 %.

The wavelength calibration is carried out by fitting the nominal prism or grating dispersion function by means of a fourth order canonical polynomial least squares fit of the laboratory wavelengths of selected reference spectral lines to their observed abscissae.This operation normally requires two reference spectra parallel to the target spectrum placed

between them, in order to compansate for the wavelength offset due to the unavoidable angular misalignment of the PDS scan axis with respect to the spectrum axis.The wavelength calibration is performed by program WLCAL, the auxilary program RLASS is required to prepare the list of laboratory wavelength identification file.WLCAL inputs an ELSPEC standard PDS data file of a wavelength reference spectrum, processes the data and outputs one RSX11M sequential formatted file containing the calibration label, coefficients and auxilary data.

The spectrum linearization is performed by mapping the density above fog of the spectrum to linear exposure by means of the calibration coefficients generated by programs DEXCAL and WLCAL. ELSPEC/11 provides program SPCAL for implementing the lineariziation of the target and eventually of the sky background spectra which runs on a standard alphanumeric terminal.

For removing the plate fog it is recommended to average together the upper and the lower fog files, if available, which can be done by means of program PDSMAT.Then SPCAL built-in plate fog removal facility carries out a data smoothing, a fourth order canonical polynomial least squares fit, then rejects all data exceeding 3.5 standard deviations above the fit and fits again the remaining data.SPCAL prompts for the input of all files required by the operational option selected by the user and outputs an ELSPEC/11 standard

CALIBRATED SPECTRUM data file.The output data can be monitored by means of programs SPVER and plotted by means of program SPPLOT.

The normalization to continuum of a spectrum is implemented by interpolating the assigned continuum points by means of a cubic spline and then dividing the spectrum by the fitted continuum.The continuum points are defined interactively by means of a program SPCONT.This program outputs an RSX11M sequential formatted file containing the file label and the selected continuum points.For the operation of the normalization to continuum, program SPNORM is used.This program accepts as input calibrated standard ELSPEC spectrum and continuum data file which was created by SPCONT.

The reduction to sun of spectral wavelengths is carried out by program VELRAD, which is used to compute the velocity correction needed, followed by program SPVCAL to shift the wavelength data by the appropriate velocity correction for computing the corrected radial velocities.

The measurement of the spectral parameters can be performed with three different procedures;

i]semi-manual measurement of symmetric non-blended gaussian lines,

ii]optimum measurement of symmetric blended gaussian or lorenz lines,

iii]optimum measurement of non-symmetric blended gaussian or lorentz lines.

In this work, the third procedure by means of program SALPAR is used.But before applying this program the lines which will be measured are extracted interactively from calibrated,linearized,normalized and heliocentricly corrected ELSPEC spectra by means of program SPLASS.This program displays on the user terminal the current PDS record and allows the user to select interactively and to extract a sequence of no more than 75 spectral lines for succesive analysis with program SALPAR.A graphical scheme for visual data processing is presented in Figure II.1.The total measurement accuracy of this standard data reduction was estimated to be 0.8 km/s in radial velocities.The average total error of the radial velocities, obtained by fitting line-parameters is typically around 2 km/s.

II.2.2.The UV spectra

The UV data obtained from the IUE data bank are registered on magnetic tapes and listed with the program IUELAB.For the whole data processing IUEOAT PLOTTING PROCEDURE Vax/Vms Version 1.1 (Allochio C.,Morossi C. and Ramella M. 1983) is used.This procedure consists from the following steps:

i]Reading data from the magnetic tapes.After mounting the magnetic tape on the available magnetic tape unit one can read one and/or several files depending his/her choice.The output file is automatically named as INPUT.DAT;1 , and so on.

ii]Conversion to standard file.In this second step

copied IUE file transfered to standard OAT formatted file.Procedure asks which type of image is under study, normally the INPUT.dat file contains various 'y' records such as a]the Gross spectrum, b]the interorder background, c]the Net spectrum, d] the ripple corrected spectrum for the high resolution spectra, e]the Absolutely calibrated spectrum for the low resolution spectrum.Selection can be done according to the type of IUE spectrum available.In any case for the users IUEOAT has a very useful HELP service which explains clearly every step.

iii]Absolute flux calibration.This step simply divides the Y axis values by the exposure time.

iv]The plotting.This last step gives a complete flexibility of plotting with the available hardware, some explanatory notes are given as follows:

It is not possible to have the whole spectrum on the same plot, so the plot must be divided in three steps.It is recommended first of all to plot the whole spectrum in a compact wavelength scale for determining the best Y axis scale. Different types of 'Y' scales can be adopted in the next steps to take into account the differences in the intensity of the observed flux with wavelength. The maximum, minumum and mean 'Y' values are stored in the file and typed during the plotting.In most cases, (if there are no strong variations in the data as spikes or strong emission lines) one half of the mean 'Y' value is a reasonable 'Y' step.

In this research after the third step of the IUEOAT, a personal software library and it's modifications are used for further analysis (Sedmak G. 1987). In summary, programs and the description of their functions are given schematically in Figure II.2.This specially developed software gave us a very important and efficient tool for data analysis in IUE spectra.After the calibration of the IUE spectra the program GETORD divides the complete spectrum into desired orders.These orders can be seen visually on the terminal with the use of the program IUESHOW or can be plotted.By means of the program IUECONT, interactively continuum points are selected.This program normalizes the spectrum to the continuum by interpolating the assigned continuum points by means of a cubic spline and then divides the spectrum by the fitted continuum.The desired spectral lines can be selected interactively with the program IUELIN.The output files of the program IUELIN contain selected lines which are ready to be measured by ELSPEC as explained previously.

We have corrected the wavelength scale with the interstellar lines.Maximum correction in the wavelength scale was around 30 km/s.Our total expected error in the radial velocity measurements is about 50km/s for edge velocities, 25 km/s for central wavelength velocities and 0.1 angstrom for equivalent widths.

Because of having stars from quite different spectral types and luminosity classes, in order to carry out this

numerical and comparative research we have analysed the following UV multiplet lines:Si IV (UV1), C IV (UV1), Al III (UV1),Fe III (UV34),Mg II (UV1),Si II (UV1,2,3),C II (UV1),Al II(UV2), He II(H),Fe II (UV1,2,3).For the Si IV, C IV, Al III, Fe III and Mg II lines we present the measurements in detail, but for the rest of the lines only central absorption radial velocity and blue edge velocities are given.In our measurements of edge velocities unlike other researchers, such as Snow et al. (1979), Slettebak and Carpenter (1983), Grady et al.(1987) we fitted asymmetric Gaussian profiles to the measured lines so specially for the late B and A UV spectra we tried to avoid blending of the lines.

II.3.SHORT BIBLIOGRAPHY FOR THE Be PROGRAM STARS.

In this section a short summary of the bibliography of the program stars are presented.List of the publications is secured by a network between the ASTRONET pole of OAT with Strasbourg data center.Some of these publications will be discussed and compared with the observed data in the following sections.

II.3.1.HD 22192 (Psi PER)

This star was classified as group I in Jaschek et al. (1980) classification and observed by many astronomers.Campbell (1895) reported first H alpha emission, later Merril and Burwell (1943) listed this star as a Be star, according to them the spectrum did not seem to be variable.Roman and Morgan (1950) mentioned that this star is possibly a member of the Alpha Per cluster.Gray and Marlborough (1974) reported that HD 22192 presented a very prominent H alpha emission feature, I/Ic=5.8, with a narrow (nearly FWHM=1 A) central core.Kitchin (1976) has determined the envelope model and the radius of the emission region of six Be stars, including this star where R(em.)=16.5 R(*).Later Kogure et al. (1978) developed a model for estimating the envelope thickness and other related parameters.They had studied the formation of the shell absorption lines in the H Balmer lines of the shell stars.For Psi Per they estimated the equatorial radii R(eq.)/R(*)=4.5, and the mass of the envelope M(gas)/M(o)=2.3 * 10**-11. Baliunas et al. (1975) found long

term variations in the H alpha line of the star by comparing their photometry with that of Andrew (1968).Later Cester et al. (1977) listed HD 22192 as having variable H alpha.Slettebak and Reynolds (1978) had obtained photoelectric scans of H alpha in the spectra of 35 bright Be stars during five observing periods in 1975-1977.They have shown that HD 21292 was variable in equivalent width from night to night. Polidan (1976) presented this star as an unusual shell star with emission at O I 7774 and IR CaII triplet.Peter (1976) found Te=1.5 * 10**4 K and <log g>=3.3 for this star.Molnar (1975) found reasonable agreement for Psi Per, between OAO2 Si and C line strengths and those calculated from model atmospheres.The substantially displaced Si IV 1400 A Line found by Lamers and Snow (1978), made this star the LEAST LUMINOUS B DWARF known to have a wind.Later Snow et.al. (1979) studied this star by Copernicus UV data.They noted shell expansion velocity of 93 km/s which was based on the Fe III 1131.9 and 1129.2 lines. This relatively high outward velocity could be linked to the substantial wind which was present.Pollitsch (1981) carried out simple model calculations in order to demonstrate how shell properties (geometry, density gradient and rotation) influence the emission profiles in Be stars.He derived the following parameters for HD 22192: spectral type, B5 V; vsini(H_α)=400 km/s; R(e,H_α)/R(*)=4.5.

The same year Snow (1981) studied the Copernicus scans

of the Si III and Si IV resonance lines in the spectra of 22 early B stars, 19 of which were known to have Be characteristics.He estimated 7.63 * 10**-11 M⊙ 1/yr for the mass loss of Psi Per.One year later Fontaine et al. (1982) presented H alpha line profiles for 25 emission line and shell stars, 10 of them also were observed in H beta where HD 22192 exhibited a strong double emission.Slettebak (1982) published spectral type and rotational velocity of this star; his spectral classification was made by using standard stars, with line broadening which matched that of the program star as close as possible.He found very different results from the previous cases; spectral type B 5 IIIe shell with vsini=280 km/s.We give some notes from his original study:"The spectrum of this star which is probably a member of the Alpha Per cluster, has not changed appreciably and presents sharp double emission of Halpha, with R=V :the other Balmer lines have sharp absorption cores.The FeII lines are also double peaked emission, but V(violet component) is less strong than R (red component). Numerous sharp and faint metallic shell absorption lines are also visible." Hubert-Delplace et al. (1979) stated that the shell became fainter and the FeII emission was weaker on their plates at the end of 1976.The strength of H alpha emission changed little in 1975-1977 (Slettebak 1978) and was still the same in December 1980, with double emission and V=R (Andrillat and Fehrenbach 1982)." Later Slettebak and Carpenter (1983) studied high dispersion

UV spectra of this star; from the analysis of Si IV 1393, C IV 1548 and Al III 1854 lines they have estimated following values:R(*)/R(ɵ)=6, Mbol=-3.5 mag, Te=15000 K. Lastly, in 1986 Marlborough and Peters, studied superionization in Be stars of different types including HD 22192.

II.3.2.HD 184279(V 1294 AQL)

This star is listed as group V star with B 0.5 spectral type, and was first studied in 1929 by Merrill and Burwell.They have noticed dark and narrow H lines and two very bright edges in H beta.Later Swings and Struve (1943) observed broad Hydrogen and He I lines with normal intensity without emission at H beta in 1942 and they have concluded that the shell had completely dissappeared. Merrill (1951) saw extremely weak and diffuse H and He I lines on a spectrum taken that year, while Lynds (1959) found variations in brightness over 3 months.Svolopoulos (1975) had studied four spectra of this star.He presented equivalent widths and Io/Ic ratios of some spectral lines, then by using Norris and Bascheck (1970) models he calculated model equivalent widths with Te=23000 ; log g=4.0 and He/H ratio 0.08.He found small differences between the observed and calculated equivalent widths for the selected He I lines (4026, 4471,4713 and 5876).These lines can be considered to a large extent to be of stellar origin (Struve and Wurm 1938).Hubert-Delplace and Hubert (1979) noted three distinct phases in the recent life of this star: 1955-1960 B phase, 1963-1970 faint Be phase,

1973-1976 strong Be/shell phase. Ballereau and Hubert-Delplace (1982) had published their observations since 1976.They have noted large variations of radial velocities of the lines over four years.The lines of all elements presented variations of radial velocity with a cycle of about four years.From 1973 to 1977, the shell was essentially seen in H, HeI and FeIII.The lines of these elements were strengthened in 1975 when an inverse P Cyg profile was observed in H beta.Later after 1978 Mg II and FeII shell line components were present in addition to the former shell lines.Then in 1979-1980 Mg II, Ni II, CaII and SiII lines exhibited shell components.They have noticed a Balmer progression in 1980 when the radial velocities were negative.According to their measurements other elements -FeIII, FeII, MgII, CaII, NiII- exhibited similar radial velocity variations.

The behaviour of the line profiles were also interesting.From September 1976 to November 1979 the H and HeI line profiles showed important changes.They have observed a P Cygni profile in H beta in 1976-1977 when the radial velocities of the shell lines were negative, than an inverse P Cygni profile was observed in 1978-1979 when the radial velocities were positive, with a strong emission peak in July 1979.Later in 1980 H beta presented a P Cyg profile again. They have also observed a faint emission component in H gamma which was absent in H delta.The higher members of the Balmer series of H were more asymmetric than the lower ones,

FeIII.In 1975-1976 brightness increased again without reaching the former value.Alvarez and Schuster (1981) measured a decrease of 0.4 magnitudes in brightness between June 1977 and May 1978 to reach 7.2 magnitudes.Lastly Horn et al. (1982) published the light variations of HD 184279 in the past 50 years.

Grady, Bjorkman and Snow (1987) presented the the results of UV survey of stellar winds in 62 Be and 43 normal B stars including HD 184279 and HD 22192. Ballerau and Chauville (1987) had presented the visual observations between July 12 and August 1 ,1985.They concluded a presence of a shock wave progressing from the star's surface towards the external layers of the shell.

II.3.3.HD 183656 (V923 AQL)

This star was classified as group I like HD 22192 in Jaschek classification and it's shell spectrum was first noticed by Harper (1937).Then Bidelman (1950) called attention to the interesting shell spectrum of this star including strong Fe II and other metallic lines.The Balmer lines of H exhibited sharp and deep central absorption components which might be seen up to very high members of the series.A weak flanking emission was visible on either side of the absorption core at H beta with the violet component somewhat weaker than the red one.No significant differences were visible between October 1958 and November 1981.Because of the prominent shell features Bidelman(1950)failed to estimate a luminosity class

especially in 1979 when the radial velocities were very positive.They have noted also that the He I lines were very strong and sharp absorptions during the whole cycle, 4471, 4026 3965, 3888, 3820 are particularly enhanced.The profile variations were similar to those of the higher Balmer lines.One interesting note from their study was that in October 1976 all the H and He lines were double.The fainter and the blue shifted secondary components were more visible in the UV region, and very clearly observable for H9, H10 and He I 4471 A.The difference between these two components was 76 km/s.

In this period the equivalent widths and central depths of the lines had a similar behaviour.There was a decrease from the middle of 1976 to the middle of the 1977 where they have reached minima when the radial velocities were at the minimum.Then these two parameters increased by a factor up to two in the middle of the 1979 and after decreased again.Between the middle of 1978 and the middle of 1979, He I lines decreased more rapidly than H.

The photometric behaviour of HD 184279 can be summarized as follows: Tempesti and Patriarca (1976) have published the photometric variations of this star from 1950.Their measurements showed a decrease of brightness between 1968 and 1975 with a pronounced minumum in 1973.At that epoch Ballerau et al. (1982) observed a strengthening of emission and the apperance of a shell with H, He I and

for this star.

Vojkhanaskaya (1976) concluded that the behaviour of the relative intensities of the red and violet emission components that border H alpha and H beta, and the slopes of the Balmer progression at different phases in the radial velocity curve yielded by the shell, suggest that this object belong to the group of the cyclic V/R variables, the cycle being appearently longer than 20 years; the longest yet known among such objects.Lynds (1960) reported light variations nearly 0.1 magnitudes with a characteristic period of about 0.86 days.

Ringuelet and Sahade (1981) had analyzed the visual spectra of this star in detail.Here we want to give some notes from their research.Their observations appeared to correspond to the epoch when the shell was entering the positive velocity phase.They have concluded that the stellar spectrum suggested the same spectral type that had been previously assigned namely, somewhere around B5, which they inferred from the intensity of He I and the barely visible Si II lines.They have estimated the luminosity class of this star to be V, i.e. the central object with an Te=15 * 10**3 K.The shell spectrum displayed lines of H, CaII, Na I and of metals, which were identified as Mg I, Cr II, Ti II, Ni II, Mn II and Fe II.The lines were sharp in contrast to the broadened photospheric profiles of H and He I, and asymmetrical with extended violet wings.The stronger features could be resolved into several

components.The H lines exhibited an extremely deep core which originates in the shell. Ringuelet and Sahade (1981) have detected two components ;for n> 8 these components are not distinguishable anymore.Besides these two, that they have called "main components" ,other components might also be present located to the violet of the other two, and which yielded consistent radial velocities.Therefore, they have considered that the shell displays only three components in H.When they plotted the radial velocities of these three components versus the quantum number n, they observed that the two main components of the core yielded Balmer progressions with opposite slopes while the the most violet displaced feature displayed a mean radial velocity of -39.5 km/s.

It is interesting to note that the strongest lines of Fe II (mult. 38 and 74), clearly exhibited two components with radial velocites of about 40 km/s and -15 km/s respectively.The other Fe II lines were single and their mean radial velocity was -19.8 km/s.The lines of Ni II appeared single, but the strongest gave velocities of about -15 km/s, while those that were weaker yielded velocities of -20 km/s.Na I displayed two components at approximately -40 km/s and -20 km/s respectively. Ca II lines behaved similar to Na I.

Several faint emissions,-some of them were associated with the strongest metallic lines and with C II-, could be detected along the whole spectrum. H alpha exhibited the shell absorption core bordered by two strong emission

components of about the same intensity.The emission had an overall width of 660 km/s and covered the broad stellar line that was seen in higher members of the Balmer series.They have examined the H alpha emission and concluded that different parts of the profile were formed under different conditions and they have described the profile as though they were actually dealing with the two superimposed emission profiles.At H beta the narrower emission was barely visible while the broad emission seemed to be absent.Later Slettebak and Carpenter (1983) studied UV high dispersion spectra of this star.Their estimated values for HD 183656 from analysis of Si IV and C IV lines were the followings: R(*)/R(⊙)=5, Te=14000 K, V =600 km/s for Si IV, V =300 km/s for C IV, mass loss derived from Si IV --> 2.6 * 10**-11, from C IV --> 6.8 * 10**-11 M⊙/yr.

Lastly we will deal with the research of Ringuelet et al. (1984) which was based on simultaneous IUE and ground based observations.They have tried to estimate the spectral type and luminosity class of this star with 1980 and 1981 observations using the Balmer discontinuity region where both the stellar and the shell discontinuity were clearly detectable.

Ringuelet et al.(1984) have reported that M.A.Cerruti,in 1981 obtained the colours B-V=0.0, U-B=-0.364 at the same epoch of their observations:these values correspond to the classification obtained from the Balmer

discontinuity due to the envelope, that is, to a late B (B9) giant.In conclusion they have classified this star as a giant of spectral type later than B5.Thus this result caused them to change the idea that HD 183656 was a member of the group of V/R variables.The visual spectrum was similar to that previously observed by Ringuelet and Sahade(1981). Again the shell spectrum was observed in the lines of H, Na I, Mg II, Si II, Ca II, and Ni II. All H lines again displayed the narrow and deep profile characteristic of shell, superimposed upon broad stellar lines.H alpha, H beta and H gamma had emission components.The Balmer lines of H could be seen up to H 33 and the Balmer discontinuity exhibited the effect of the envelope.

The UV spectra presented characteristics similar to the UV spectra of other Be stars of the similar spectral type. Si IV and C IV exhibited broad resonance lines with no outstanding asymmetry. They have identified Fe, Ni, Cr, Si, C, Mg, and O elements in the spectra.Fe II had the richest spectrum of all ions.

II.3.4.HD 193182

HD 193182 was classified as group III in the Jaschek classification, there are no recent detailed spectroscopic analysis of this star.Merrill (1952) described a series of spectra of this star covering the period 1921-1950.He found that it is one of the relatively few examples of stars which have stable shells, since no changes have been detected over the whole period of observation.The shell was exceptionally

rich , with very sharp lines of H and neutral and ionized metals.This star is generally classified as A0, but Struve (1944) noted that very broad, shallow lines of He I might be present, arising in a fast rotating B star underlying the shell.Uesugi (1970) estimated vsini=200 km/s.Pollitsch (1981) found vsini=340 km/s and $R(e,H_{\alpha})/R(*)=3.0$

II.3.5.HD 200775

This star is not classified by Jaschek et al.(1980).There is a large bibliography for this Herbig Be star which is closely associated with the nebulosity complex NGC 7023 .We summarize here some selected papers.

Strom et al. (1972) had done a quantitative spectrophotometric study of the Herbig Ae and Be stars associated with nebulosity.They have noted H emission through H eps, double peaked emission at H beta with red peak slightly stronger, H gamma through H eps showed P Cygni profiles, vsini< 80 km/s from the visual spectrum of this star.Walker et al. (1980) had studied the extinction towards HD 200775 and NGC 7023.They suggested that a three-component dust model was necessary to explain their observations:i]fine grains for UV extinction, ii]large grains for the optical region and possibly a mantle which was responsible for the diffuse absorption and very broad structure.Davis et al. (1983) had estimated the rotational velocities of 15 Herbig Ae/Be stars, including this star and they have noted that those objects with nominal optical spectral types between B5 and A0 showed a

frequency distribution of vsini values significantly different from that of normal Be stars in this spectral type range; the Herbig emission stars must have significantly smaller intrinsic values.Infact their estimation for HD 200775 vsini<100 km/s.Viotti et al. (1977) had studied objective prism spectra of objects known to have large UV and/or X ray fluxes.They noted a marked Balmer excess and H alpha emission for HD 200775 and called attention to the similarity of this star with X Per, which was known as the optical counterpart of the X ray source 3 UO352 +30, as being a low luminosity B3e star with large IR excess and peculiar optical and UV energy distribution.They observed this star on August 2 1976.The Balmer discontinuity was D=-0.14 and H alpha was strongly in emission.The Balmer absorption lines could be distinguished from H gamma to H 13 while H beta was not visible.A very weak emission feature was present at the position of the [Fe II] 4287 line.Baschek et al. (1982) had analyzed high dispersion spectra of this star.By comparing the depths in the wings of H gamma and H delta and the equivalent widths of He I lines with predictions from model atmospheres, they found Te=17000 K and log g=3.6, corresponding to a spectral type B3 V.They have noted also the unusual weakness of IS absorption features 4430 A and 2200 A.Finkenzeller (1985) had studied rotational velocities, spectral types and forbidden lines of Herbig Ae/Be stars including HD 200775 .He estimated vsini=60 km/s and spectral type B3e.Lastly Koppen et al. (1982) had

published data on the Balmer emission lines of this star.They have observed symmetric profiles of H alpha, H beta and H gamma with central absorption dips in H alpha and H beta.They had done numerical calculations of the level populations of H in order to explain the observed H alpha/H beta, H gamma/H beta and H delta/H beta line ratios.Then they have concluded that the Balmer emisson lines are produced in a compact and fairly dense (10**9 cm**-3) envelope.

Table and Figure captions

Table II.1.Basic observational data for Be/shell program stars.

Table II.2.Visual data for the Be/shell program stars.

Table II.3.UV data for the Be/shell program stars

Figure II.1.Scheme of the visual data procession at ASTRONET pole of OAT.

Figure II.2.Schematic description of the UV data procession at the ASTRONET pole of the OAT.

Table II.1.Basic observational data for program stars.

HD number

HD 22192
Coord. (1950) R.A=03h 32m 55.5s Dec.=+48 01 41.4
Corod. (2000) R.A=03h 36m 29.2s Dec.=+48 11 34.9
Galactic coord. l=149 deg. b=-06.09 pm=+0.008, -0.024
Spectral type=B5 Ve
Mag.(ph,V)= 4.17 V? 4.23
other catalog names

SKY# 5462	SAO 38980	AG +48 418	UBV M 40947
EM*MWC 69	BD+47 857	GC 4287	*PSI PER

HD 184279
Coord. (1950) R.A=19h 31m 07.2s Dec.=+03 39 07.8
Coord. (2000) R.A=19h 33m 36.9s Dec.=+03 45 40.8
Galactic coord. l=41.15 b=-07.62 pm=+0.019, +0.001
Spectral type=B0.5 IVe
Mag.(ph,V)= 6.97 6.94
other catalog names

SKY# 36460	SAO 124788	AG +03 2493	UBV 16584
EM*MWC 319	BD+03 4065	GC 27016	V 1294 AQL

HD 183656
Coord. (1950) R.A=19h 28m 02.9s Dec.=+03 20 19.1
Coord. (2000) R.A=19h 30m 32.9s Dec.=+03 26 39.7
Galactic coord. l=40.51 b=-07.09 pm=+0.013, -0.003
Spectral type=A0 e
Mag.(ph,V)= 6.02 6.05
other catalog names

SKY# 36333	SAO 124704	AG +03 2476	UBV 16552
EM*MWC 988	BD+03 4043	GC 26937	V 923 AQL

HD 193182
Coord. (1950) R.A=20h 15m 36.9s Dec.=+39 26 15.1
Coord. (2000) R.A=20h 17m 25.1s Dec.=+39 35 37.3
Galactic coord. l=77.08 b=+02.25 pm=+0.004, -0.008
Spectral type=Ap e
Mag.(ph,V)= 6.42 6.51
other catalog names

SKY# 38279	SAO 69764	AG +39 2089	UBV 17578
EM*MWC 632	BD+39 4115	GC 28211	GCRV 15097

HD 200775
Coord. (1950) R.A=21h 00m 59.7s Dec.=+67 57 55.5
Coord. (2000) R.A=21h 01m 36.8s Dec.=+68 09 48.1
Galactic coord. l=104.07 b=+14.19 pm=+0.007, -0.006
Spectral type=B2 Ve
Mag.(ph,V)= 7.73 7.42
other catalog names

SKY# 39953	SAO 19158	AG +67 924	UBV 18252
EM*MWC 361	BD+67 1283	GC 29401	GCRV 13255

Table II.2.Visual data for the Be/shell program stars.

Star name	Spectrog.	Emul.	DD,MM, YY	U.T.	J.D.(2400000 +)
HD 22192	GB 9063	IIIaFH	30/11/1985	21:15	46400.390
	GB 9066	IIa0ch	02/12/1985	24:55	46402.543
	GB 9067	"	" " "	25:09	46402.553
	GB 9117	"	20/01/1986	21:19	46451.391
	GB 9119	"	" " "	21:58	46451.418
	GA 7326	IIIaFH	08/10/1986	27:27	46712.647
	GA 7327	"	" " "	28:15	46712.681
	GA 7618	"	18/07/1987	24:58	46995.537
	GB 9587	IIa0ch	20/07/1987	25:39	46997.566
HD 184279	GB 9189	IIa0ch	05/06/1986	24:12	46587.512
	GB 9207	"	26/07/1986	09:10	46637.887
	GA 7252	IIIaFH	" " "	24:45	46638.537
	GA 7254	"	27/07/1986	34:15	46639.923
	GA 7258	"	31/07/1986	03:35	46642.655
	GB 9548	IIa0ch	11/05/1987	27:30	46927.648
	GA 7547	"	15/05/1987	25:53	46931.581
	GB 9581	"	12/07/1987	24:14	46989.515
	GA 7616	IIIaFH	14/07/1987	23:27	46991.482
HD 183656	GB 9188	IIa0ch	02/06/1986	25:27	46584.564
	GA 7251	IIIaFH	26/07/1986	22:30	46638.443
	GA 7255	"	28/07/1986	23:32	46640.459
	GA 7256	IIa0ch	" " "	25:05	46640.550
	GB 9208	"	" " "	33:46	46640.912
	GA 7541	"	13/05/1987	25:58	46929.584
	GA 7544	"	14/05/1987	24:30	46930.523
	GA 7545	IIIaFH	" " "	25:52	46930.580
	GB 9582	IIa0ch	12/07/1987	25:24	46989.564
	GA 7615	IIIaFH	13/07/1987	24:52	46990.541
HD 193182	GA 7259	IIIaFH	01/08/1986	22:15	46644.430
	GB 9209	IIa0ch	" " "	12:20	46644.017
	GA 7260	IIIaFH	02/08/1986	23:20	46645.482
	GB 9210	IIa0ch	03/08/1986	11:15	46645.972
	GA 7542	IIaoch	13/05/1987	20:32	46929.520
	GA 7543	"	14/05/1987	23:21	46930.473
	GB 9584	"	13/07/1987	22:02	46990.421
	GA 7617	IIIaFH	18/07/1987	22:27	46995.438
HD 200775	GA 7262	IIIaFH	04/08/1986	12:04	46647.003
	GA 7263	IIa0ch	" " "	26:32	46647.606
	GA 7325	"	08/10/1986	25:32	46712.566
	GA 7329	IIIaFH	10/10/1986	23:27	46714.479
	GA 7330	IIa0ch	11/11/1986	25:03	46715.545
	GA 7546	"	15/05/1987	24:10	46931.505
	GA 7548	IIIaFH	16/05/1987	22:50	46932.450
	GB 9580	IIa0ch	10/07/1987	24:14	46987.510
	GA 7613	IIIaFH	11/07/1987	34:54	46988.954

Table II.3.Ultra-Violet data for the Be shell program stars.

Star name	Spectrum	Year	Day	Beg. U.T. hh:mm	Exp. Time mm:ss
HD 22192	SW 5926	1979	205	13:39	03:34
	SW15513	1981	322	09:15	04:00
	LW 9832	1981	033	02:10	02:30
	LW11990	1981	322	09:23	02:30
HD 184279	SW17840	1982	245	18:22	26:00
	SW18118	1982	269	14:14	15:00
	SW18119	1982	269	15:17	30:00
	LW14076	1982	245	17:51	20:00
	LW14270	1982	269	15:17	30:00
	LW16866	1983	267	17:25	20:00
HD 183656	SW17550	1982	213	11:48	13:00
	SW21152	1983	267	15:47	23:00
	LW13827	1982	213	12:07	07:10
HD 193182	SW 5952	1979	207	08:32	45:00
	SW 5953	1979	207	09:47	60:00
	SW18153	1982	272	13:50	50:00
	SW18154	1982	272	15:17	30:00
	LW14294	1982	272	14:46	25:00
HD 200775	SW 9836	1980	231	19:45	140:00
	SW 9837	1980	231	23:15	152:00
	LW 8548	1980	231	18:41	60:00
	LW 8549	1980	231	22:10	60:00

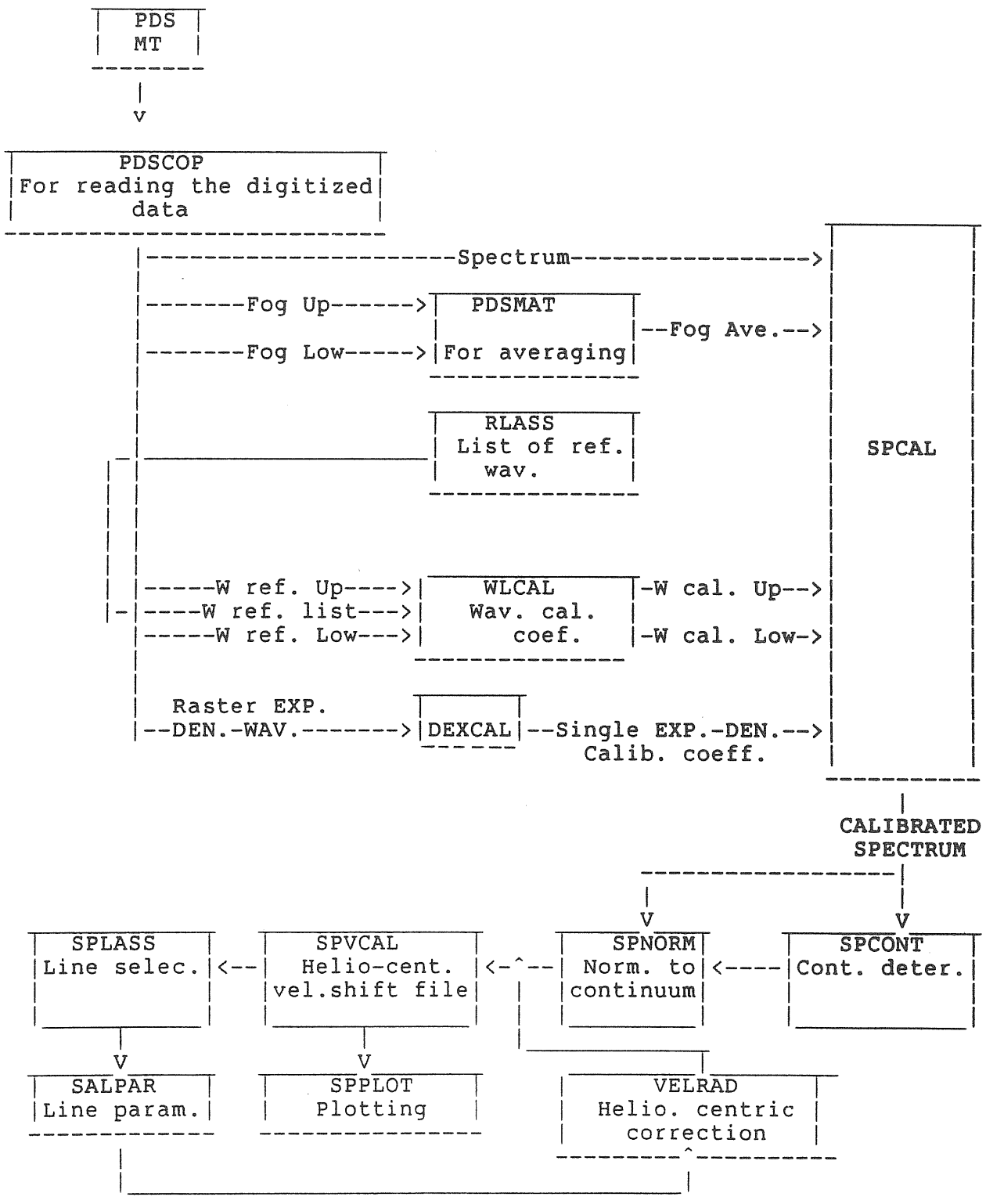
PDS
MT
PDSCOP
For reading the digitized data
Spectrum
Fog Up
Fog Low
PDSMAT
For averaging
Fog Ave.
RLASS
List of ref. wav.
SPCAL
W ref. Up
W ref. list
W ref. Low
WLCAL
Wav. cal. coef.
W cal. Up
W cal. Low
Raster EXP.
DEN.-WAV.
DEXCAL
Single EXP.-DEN. Calib. coeff.
CALIBRATED SPECTRUM
SPLASS
Line selec.
SPVCAL
Helio-cent. vel.shift file
SPNORM
Norm. to continuum
SPCONT
Cont. deter.
SALPAR
Line param.
SPPLOT
Plotting
VELRAD
Helio. centric correction

FIGURE II.1

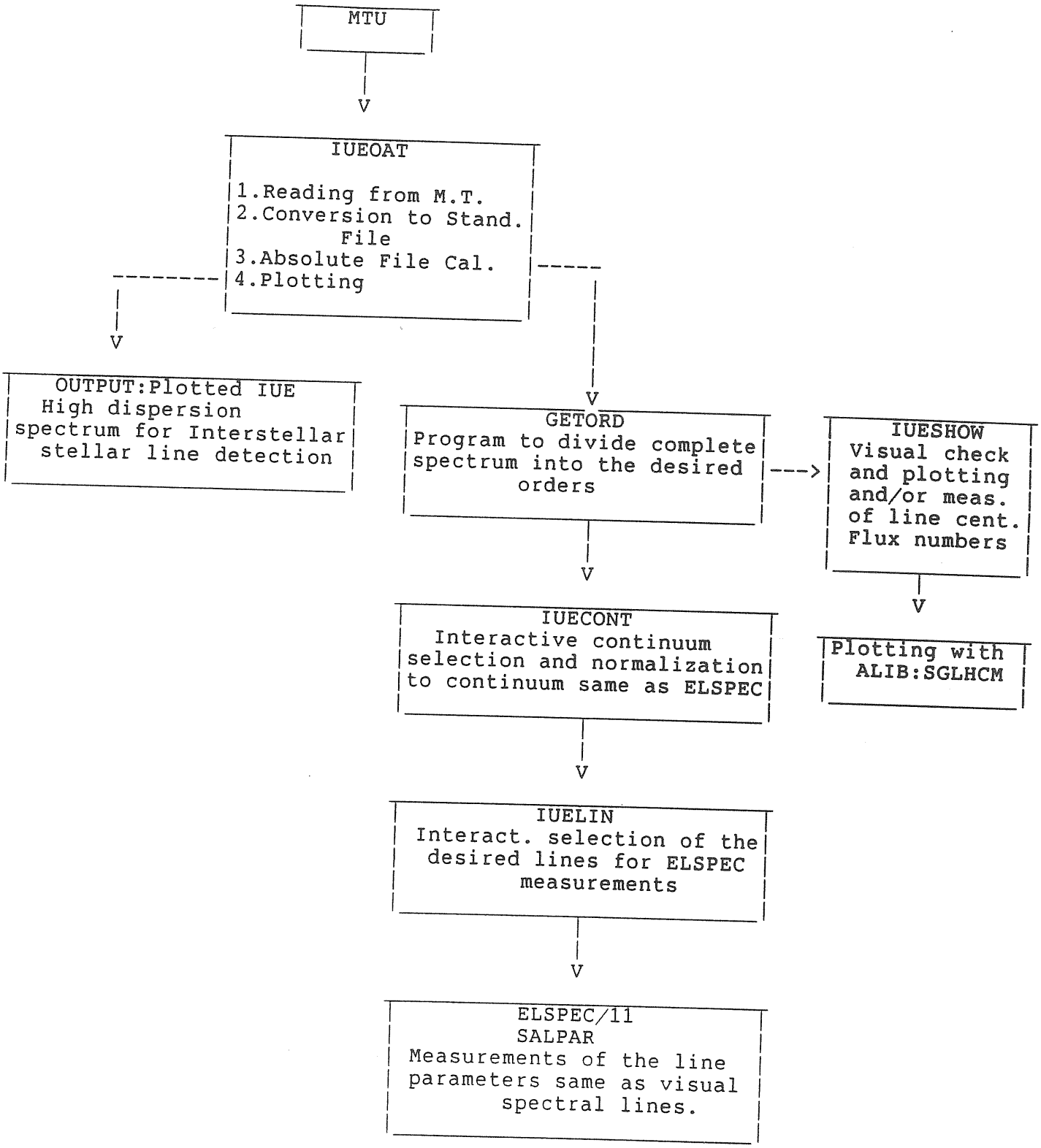
MTU
IUEOAT
1.Reading from M.T.
2.Conversion to Stand. File
3.Absolute File Cal.
4.Plotting
OUTPUT:Plotted IUE High dispersion spectrum for Interstellar stellar line detection
GETORD
Program to divide complete spectrum into the desired orders
IUESHOW
Visual check and plotting and/or meas. of line cent. Flux numbers
Plotting with ALIB:SGLHCM
IUECONT
Interactive continuum selection and normalization to continuum same as ELSPEC
IUELIN
Interact. selection of the desired lines for ELSPEC measurements
ELSPEC/11
SALPAR
Measurements of the line parameters same as visual spectral lines.

FIGURE II.2

III.OUR SPECTRAL OBSERVATIONS OF THE PROGRAM STARS

III.1.The Visual Spectra

In this section we will give a detailed description of the visual spectra of the program stars.But before proceding we would like to give some definitions for the recognition of the Be/shell spectra.Surveys of Be star spectra reveal a very large variety of emission line profiles (Dachs,1987). So we will limit ourselves with the profiles which were observed frequently and will give a short interpretation of them in terms of motions in the cool envelope regions.

i]Symmetric double-peak profiles:

Fairly symmetric, double-peak emission line profiles are the simplest case of relatively weak emission lines, frequently observed in the high-order Balmer lines if emission is detectable and often also at H alpha, at least when vsini> 100...150 km/s. According to the observations (Ebbets(1981),Fontaine et al. (1982),Barker (1983a),Dachs et al. (1986a),Peters (1986) and Dachs et al. (1986b), maximum peak separation occurs for the faintest emission lines and is always less than 2vsini of the star.For larger equivalent widths of the emission peak the separation rapidly decreases.These observations are in good agreement with predictions of the rotating disk model (See Pollistch,1981). In it's simplest version of an optically thin line-emitting disk the double-peak structure is already observed as a direct consequence of the velocity distribution of the emitting atoms

in the disk, leading to velocity crowding at the projected velocities of the outer edges of the disk.

So far as this model is correct, central depressions in many double-peak profiles are not caused by self-absorption in the envelope and for this case they must not be called "shell" components of the emission lines.

ii]"Wine bottle" profiles:

These profiles can be observed with a sufficiently high spectral resolution on the flanks of strong singly peaked or doubly peaked Balmer emission lines, usually in the form of inflexions.Some examples for this type of profile were recorded first for pole-on Be stars (i.e.having small vsini) at resolutions of about 20 km/s (Kogure,1969;Andrillat and Fehrenbach,1982).Both Kogure (1969) and Hanuschik (1986a) interpreted inflexions in the flanks of emission line profiles as a superposition of a faint narrow emission line upon wider emission line, pointing to a composite structure of the envelope.Kogure (1969) successfully fitted a wine bottle type H beta profile measured for 11 Cam to a theoretical profile calculated for a model envelope divided into two concentric, thin narrow gaseous rings surrounding the star in it's equatorial plane and separated by a large gap.

Poeckert and Marlborough (1979) showed that the well known broad emission line wings observed in particular for H alpha in the spectra of many Be stars are usually ascribed to the result of electron scattering of the line photons.

iii]Asymmetric emission profiles:

Asymmetric double-peak emission lines are usually described by their V/R ratio, defined as the ratio of violet-side to red-side peak intensities above the continuum in the units of continuum intensity.For singly peaked asymmetric emission lines, the corresponding designations may be "blue-dominated" if the short wavelength part of the line is significantly more intense than the long wavelength part, or "red dominated" for the opposite case.

Again in the frame work of the rotating disk model, asymmetry of an emission line profile can be explained by radial motions superimposed upon rotation.Following Struve who considered expansion to be a natural feature of line-emitting envelopes around Be stars (Struve,1931), most theoretical line profile calculations based on the disk model assume at least slow expanding motion through the disk in addition to rotation.As a result to this approach only symmetric or red-dominant emission profiles are obtained (Kogure,1969; Poeckert and Marlborough,1978a,b,1979).Kogure (1969) obtains a symmetric profiles because he assumes a "static envelope": Poeckert and Malborough (1979) obtain a red winged emission and asymmetric absorption with the asumption of a slowly expanding envelope.

However observations of blue-dominated asymmetric emission line profiles seem to force theoreticians to accept the hypothesis that inflow through the line-emitting envelope

can occur as well as outflow (Delplace,1970a,Hubert-Delplace et al.,1983).Temporary inward motion through a disk shaped circumstellar envelope may be thought to be part of a large scale circulation system including the stellar wind region (Dachs et al., 1986a).

iv]Shell lines and shell components:

Emission lines with central shell components can be taken to be distinguished from central depression in ordinary double-peak emission lines mentioned previously by the following two related properties (Merrill, 1949; Kogure and Hirata,1982):

a]Measured at sufficiently high spectral resolution central cores of shell lines are distincly deeper than the centres of rotationally broadened photospheric absorption lines of normal B type stars of the same spectral class, while the centres of normal double-peak emission lines always remain above the level of the stellar absorption lines.

b]Cores of the shell absorption lines are V-shaped,i.e. posses sharp minima while central depressions in ordinary double-peak emission lines are U shaped.

Evidently both of these two properties are to be explained by the assumption that shell line cores are produced by self-absorption of line radiation at and near the velocity of the core.Recent calculations of theoretical line profiles by Rybcki and Hummer (1983) and by Horne and Marsh (1986) demonstrated that the expected transition from U-shaped line

centers in double-peak emission lines are produced in optically thin rotating disks and V-shaped line cores (or M-shaped line profiles) are obtained for emission from optically thick disks.

Structure and breaks in the flanks of emission line profiles can be taken to indicate a multi-component structure of cool circumstellar envelope.

If the spectra of certain Be stars, ever since their discovery, permanently show the presence of narrow shell absorption cores in their Balmer emission lines and in addition also in numerous metallic lines, then these stars are properly called "shell" stars.For many other Be stars, shell absorption cores are observed in their emission-line spectra only during relatively short transient phases of their spectral variations.Following Merrill (1952) it is customary to call such phases "shell episodes".In order to explain shell episodes again in the framework of the rotating disk model for Be star envelopes one has to assume that during the shell episodes, the optical density in the disk for line radiation or the scale height of the disk or both increase for some time in such a way that the mean optical density of the line of sight to the star becomes sufficiently large in the line centre to produce shell absorption cores, as discussed by Hirata and Kogure (1984).

III.1.1.HD 22192

H alpha profiles of this star exhibited a double-peak

emission with a central absorption component which was variable in intensity.Little asymmetry was observed in emission wings which were extending between - 800 to +800 km/s.These wings were variable in extension.H beta exhibited a similar profile to H alpha. The main difference was that wide stellar absorption components were distinguishable for H beta while H alpha profiles were completely filled with emission so there were no trace of stellar components.Table III.1.1.1 presents measured line parameters for H alpha and H beta of HD 22192.

H gamma profiles were composed of a wide stellar component which was extending from -1200 to +1200 km/s and a central absorption.This narrow central absorption component exhibited variations in intensity, full band widths on the continuum(FBWC) and equivalent widths.H gamma exhibited also weak emission components on both sides of this narrow component.H delta and H epsilon profiles were similar to H gamma but there were no trace of these emission components as H gamma; for both of them (H delta and H epsilon)narrow components presented time variation in line parameters.Figures III.1.1.1 to III.1.1.5 presents H alpha, beta, gamma, delta, and epsilon profiles respectively.

H Balmer series lines were visible up to n=17 and narrow components were also present in all H lines with diminishing central depths for higher quantum numbers.As it was discussed before narrow components superimposed to H alpha

and H beta profiles can be called "shell components" with certain conditions. HD 22192 behind the sharp M-shaped profiles for H alpha and H beta, presented "shell effect" in optical continuum, by forming a secondary Balmer jump.

He I lines were without narrow components.He I 4471 and Mg II 4481 lines exhibited variable profiles, also He I 5875 was very wide and variable. Ca II 3933, 3968 and Na I 5889,5895 lines were weak.One another interesting property of this star was that Fe II lines exhibited a double-peak emission profiles with narrow absorption components at the center.Only Fe II 4923 presented a P Cygni profile.Some selected lines of HD 22192 are presented through figures III.1.1.6 to III.1.1.8.Line list given in figure captions.

In order to check the time variations of the envelope and shell, central intensities,FBWC,equivalent widths and radial velocites of the narrow components were measured (Table III.1.1.2).The measured line parameters were plotted against log (EP+IP) of each line for all program stars.The excitation and ionization potential values of the lines were taken from Moore (1972) and given for line groups in figure captions.

Radial velocities displayed a variation with time, specially He I lines which were without narrow components.For example He I lines had positive velocities at JD=451.4(2446000.+) respect to the other two spectra.At JD=997.6 all measured velocities were slightly-in the range of

mesurement errors- more positive than the other two nights, specially Fe II lines (Figure III.1.1.9).In the red part of the spectra no variation was recognizable (Figure III.1.1.10).

In the case of relative intensities, the narrow components of H lines decreased at JD=451.4 (shell absorption increased relative to the other two blue spectra) ; although the rest of the lines showed no significant difference (Figure III.1.1.11). On the red part of the spectra only Na I lines exhibited a notable difference while other lines remained the same (Figure III.1.1.12).

Variation of the equivalent widths were similar to the variation of the relative intensities.The spectrum taken at the JD=451.4 presented a maximum for H line equivalent widths, while other lines were remaining more or less equal.Only blue part of the spectral lines was plotted because at the red side lines were generally in emission with central absorption over the continuum (Figure III.1.1.13).Radial velocities of the Balmer lines versus n quantum numbers are presented in Figure III.1.1.14.All three spectra displayed similar behavior; at the JD=997.6 higher Balmer lines showed more dispersion than other epochs.

At JD=712.6 H alpha emission components reached their maximum in equivalent width and in FBWC.At the same time the central depression was diminished to it's minumum observed value.Unfortunately for the same date no blue spectra were available to see the variation of the narrow components.H beta

emission components also exhibited variability in equivalent width and central depth.A notable V/R variation was observed although the central absorption didn't change significantly.

Table and Figure captions.

Figure III.1.1.1.H alpha profiles of HD 22192.In this figure x axis gives the radial velocity and y axis gives relative intensity in continuum units, every interval on the y axis corresponds to 0.5 units.

Figure III.1.1.2.H beta profiles of HD 22192 where every interval on the y axis corresponds to 0.2.

Figure III.1.1.3.H gamma profiles of HD 22192 same scale as previous figure.

Figure III.1.1.4.H delta profiles of HD 22192 same scale as previous figure.

Figure III.1.1.5.H epsilon profiles of HD 22192 same scale as previous figure.

Figure III.1.1.6.He I 4009, 4026, 4143, 4471, Mg II 4481, Fe II 4923 lines of HD 22192. X axis gives the wavelength and y axis relative intensity, every interval corresponds to 0.2 units.

Figure III.1.1.7.Fe II 5018 , 5169, 5234, 5316, lines of HD 22192.Same as previous figure.

Figure III.1.1.8.Fe II 5362 and Na I 5890, 5895 lines of HD 22192.Same as previous figure.

Figure III.1.1.9.RVs versus log (EP+IP) of HD 22192, for blue spectra. Typical log (EP+IP) values for group of lines are followings: H I=(1.373-1.358), He I=(1.657-1.648), Ca II=(0.496-0.492), Si II=1.353 , Fe II=(0.906-0.943), Na I=(0.320-0.322).

Figure III.1.1.10.Same as previous figure for red spectra.

Figure III.1.1.11.Relative intensities versus log (EP+IP) of HD 22192 for blue spectra.

Figure III.1.1.12.Same as previous figure for red spectra.

Figure III.1.1.13.EQWs versus log (EP+IP) of HD 22192 for blue spectra.

Figure 111.1.1.14.Radial velocities of the Balmer lines versus "n" quantum number for HD 22192.

Table III.1.1.1.Measured spectral parameters of H alpha and H beta emission components of HD 22192.

Table III.1.1.2.Measured spectral line parameters of absorption the lines of HD 22192.

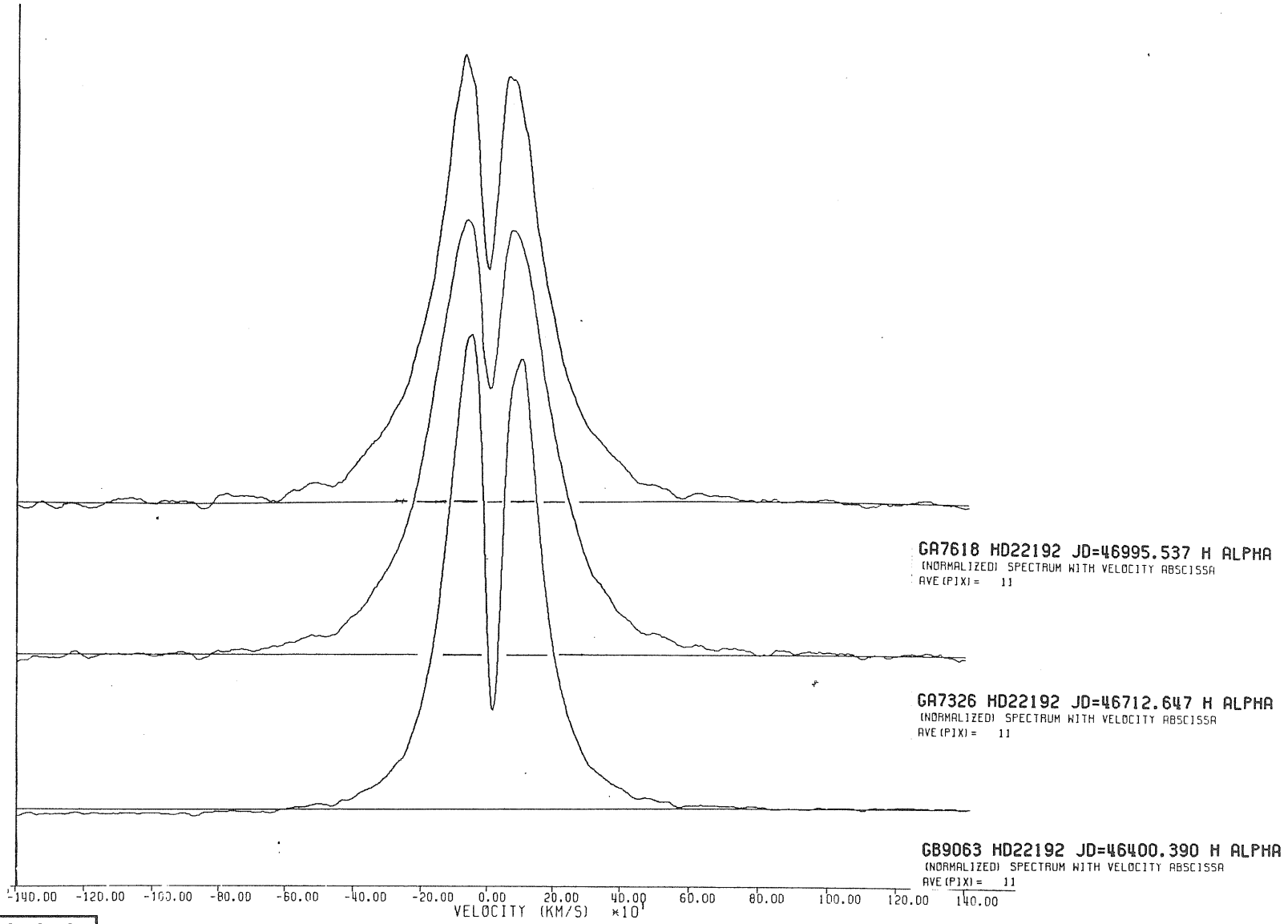

FIGURE III.1.1.1

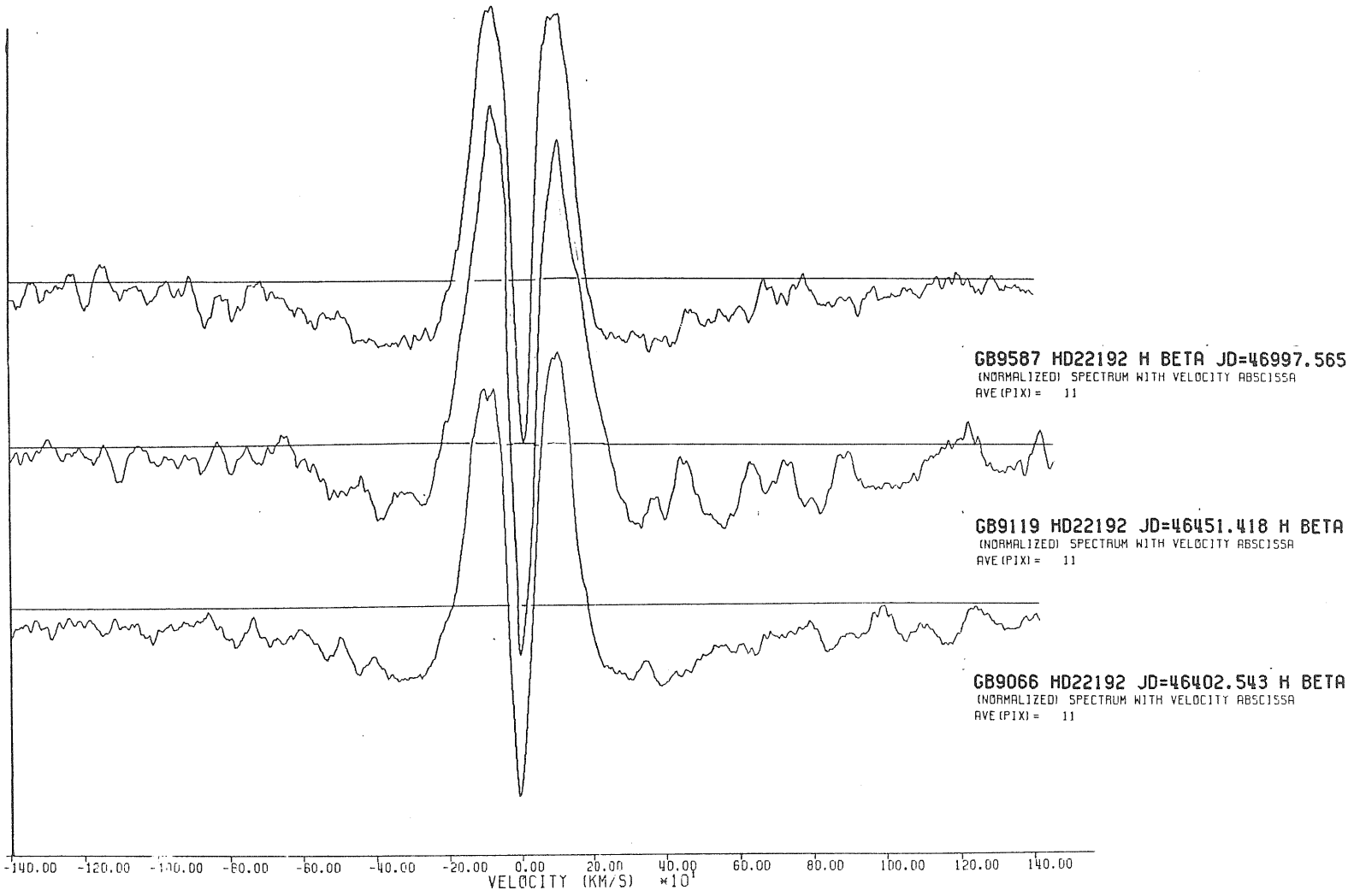

FIGURE III.1.1.2

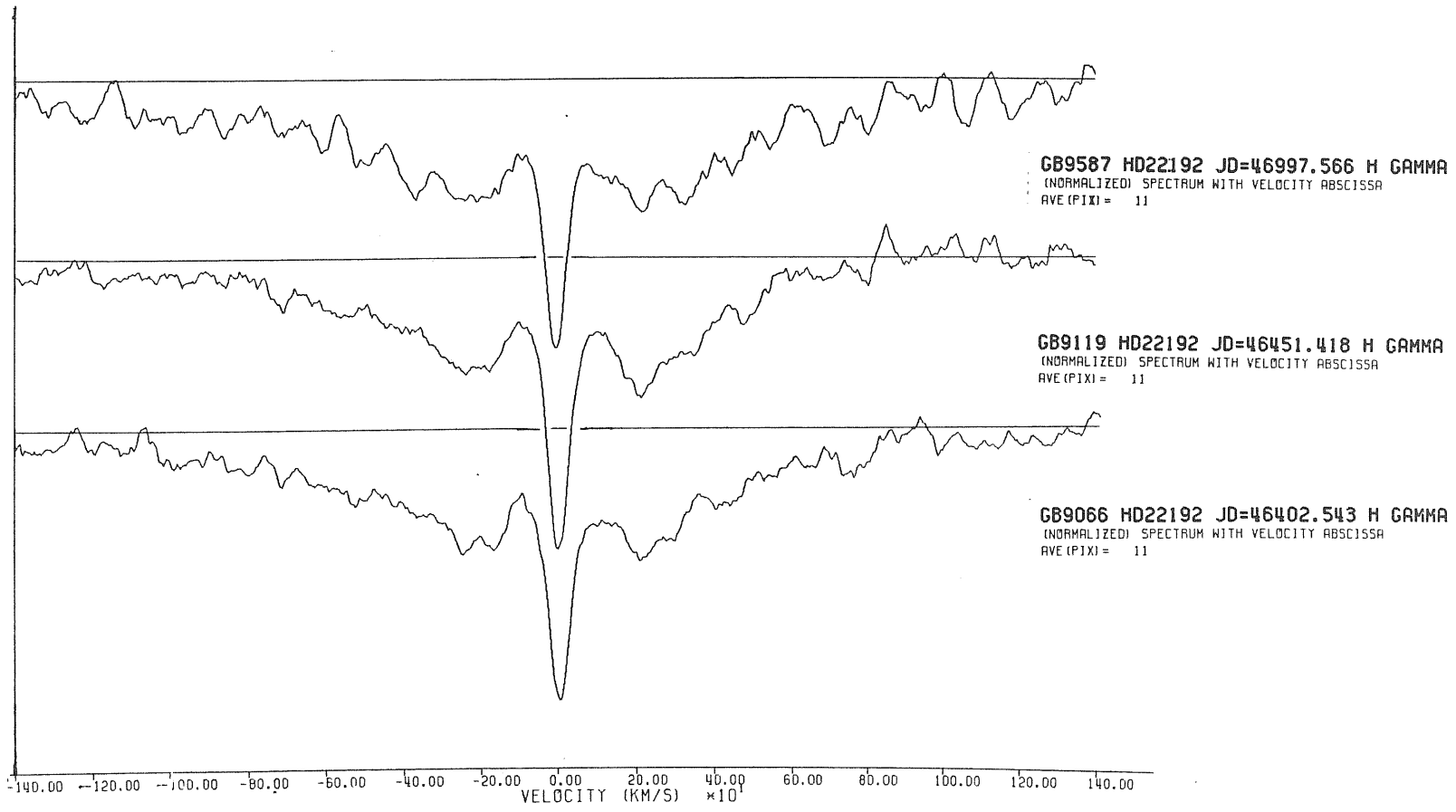

FIGURE III.1.1.3

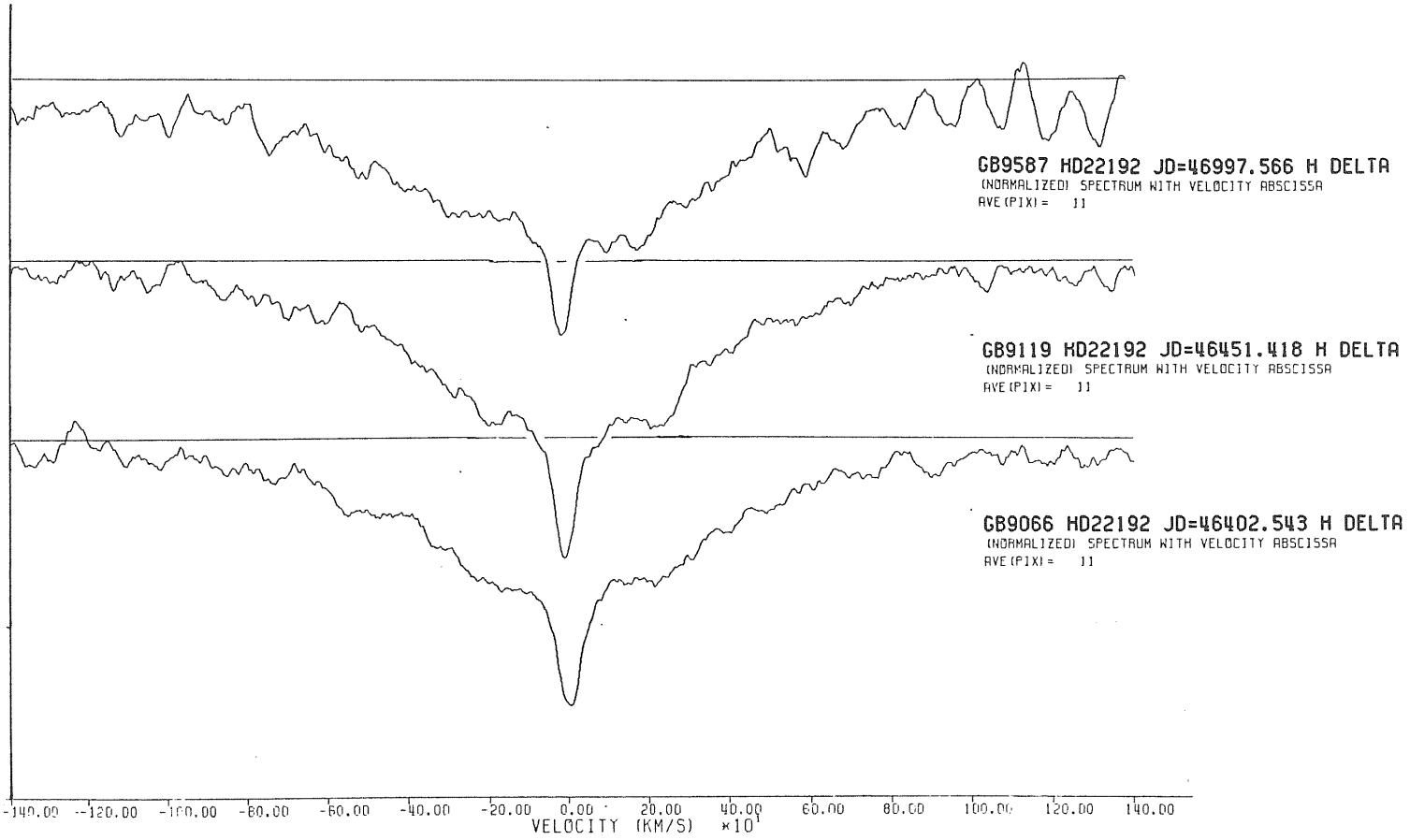

FIGURE III.1.1.4

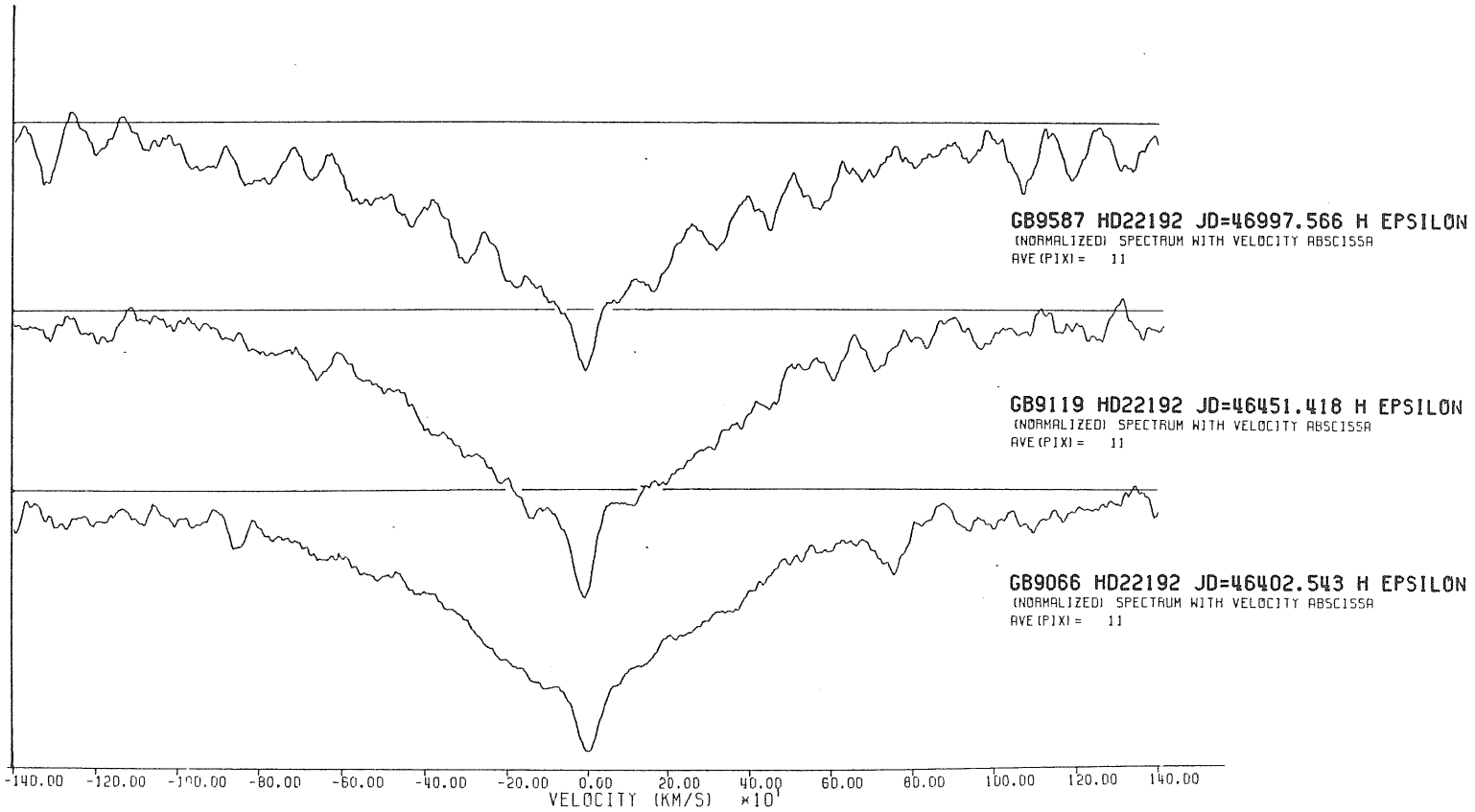

FIGURE III.1.1.5

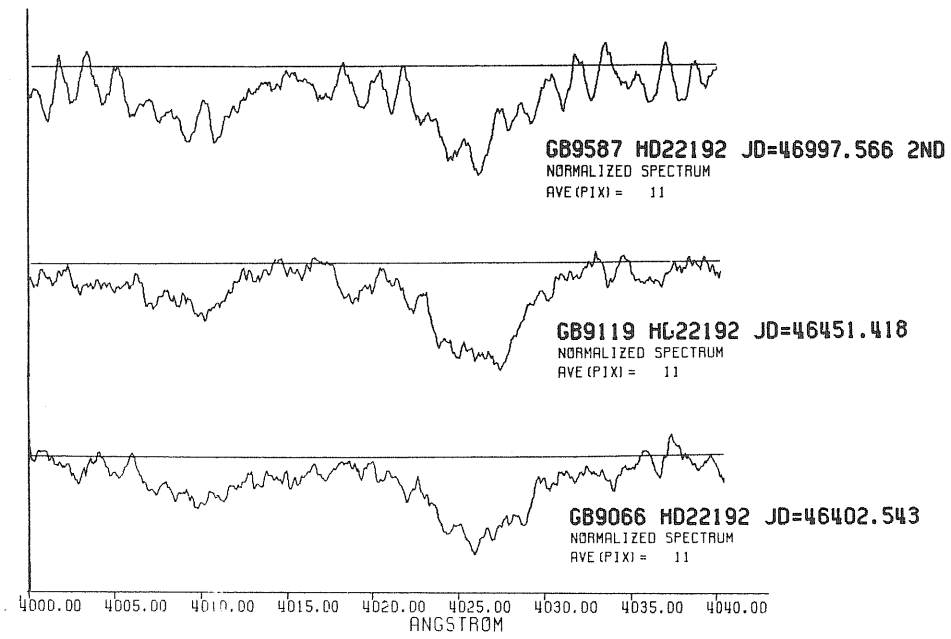

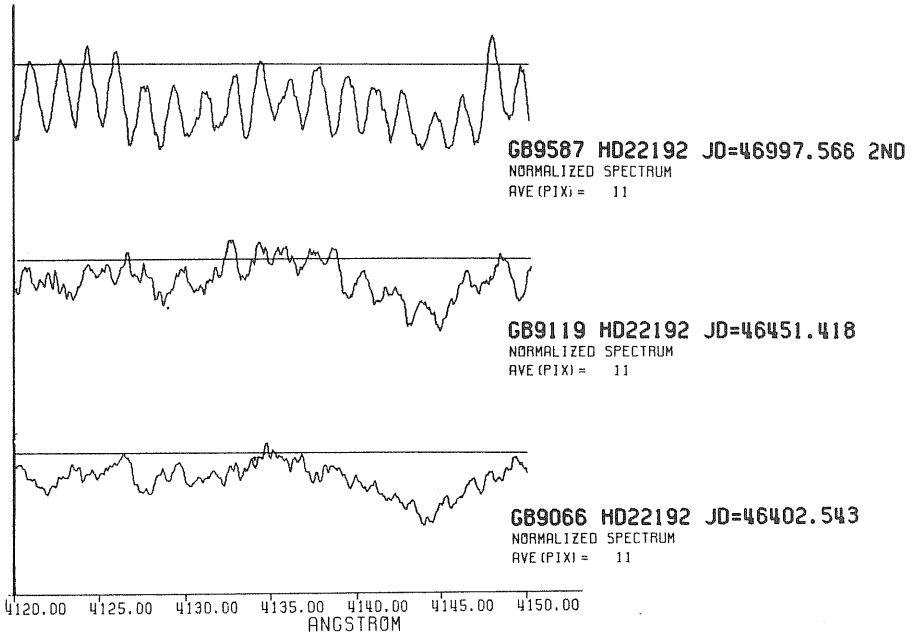

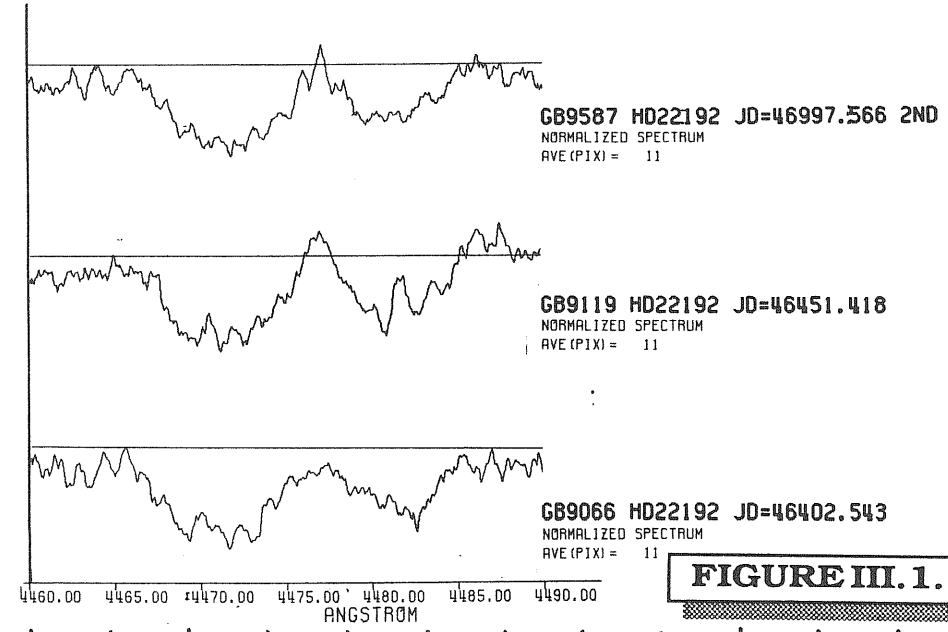

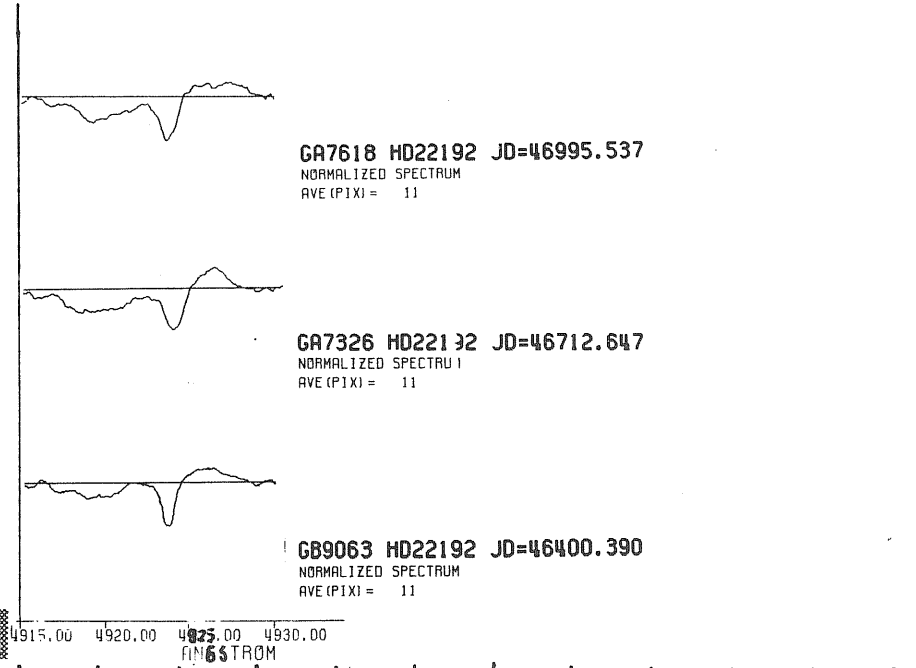

FIGURE III.1.1.6

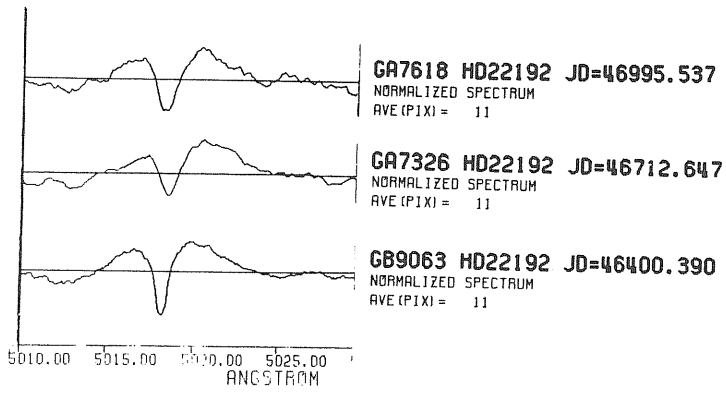

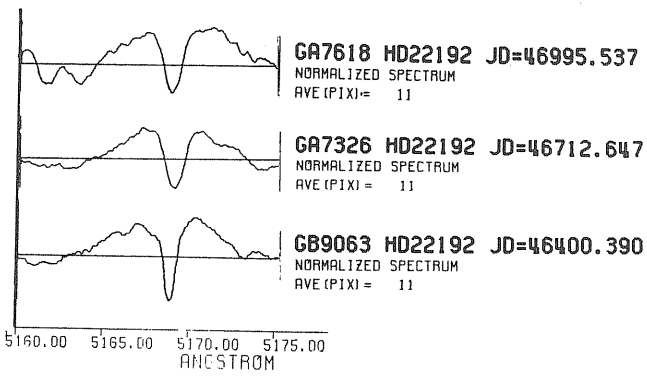

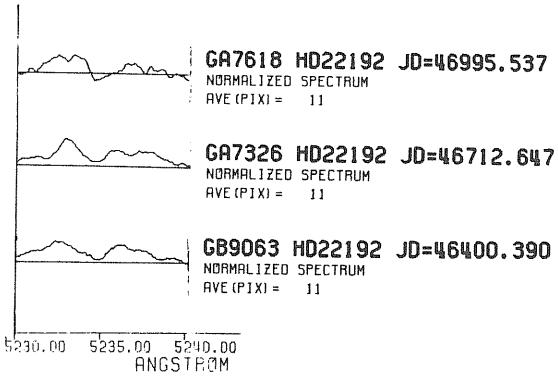

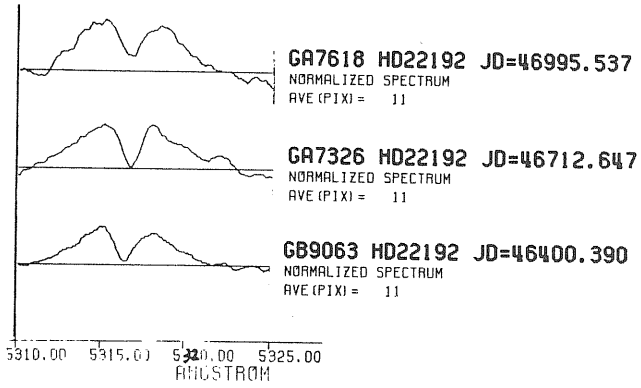

FIGURE III.1.1.7

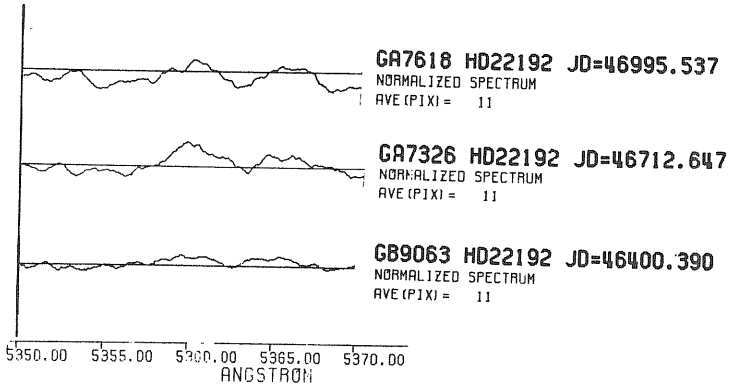

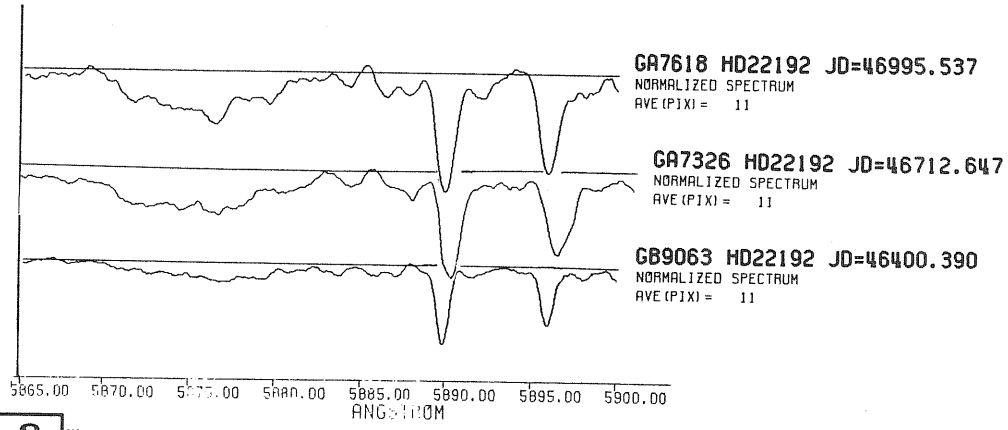

FIGURE III.1.1.8

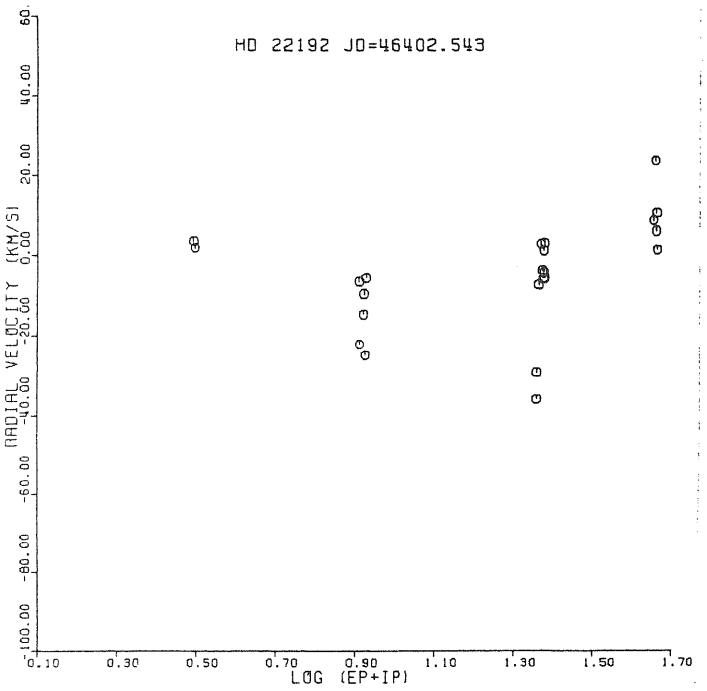

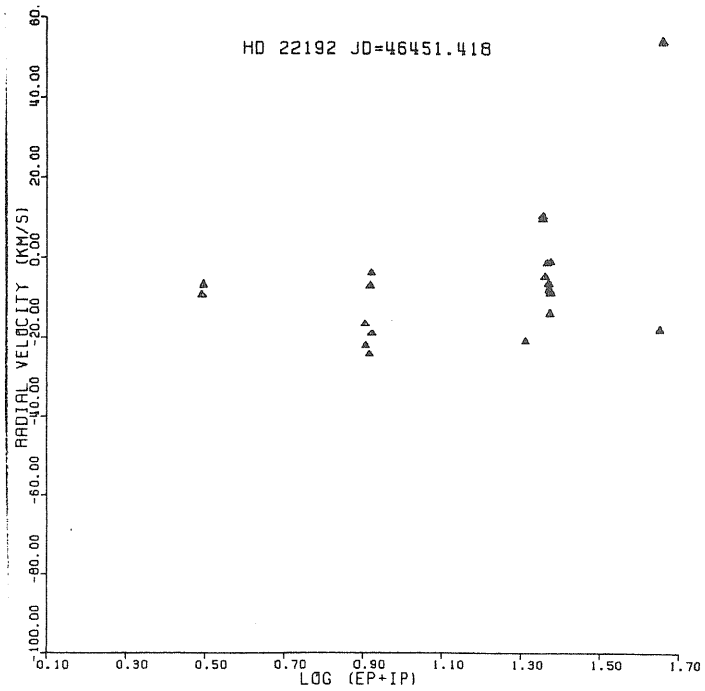

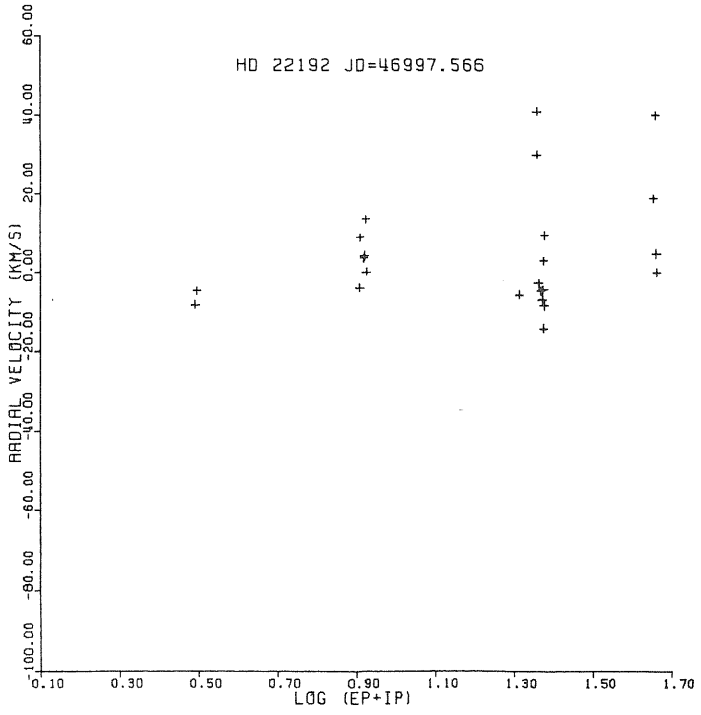

FIGURE III.1.1.9

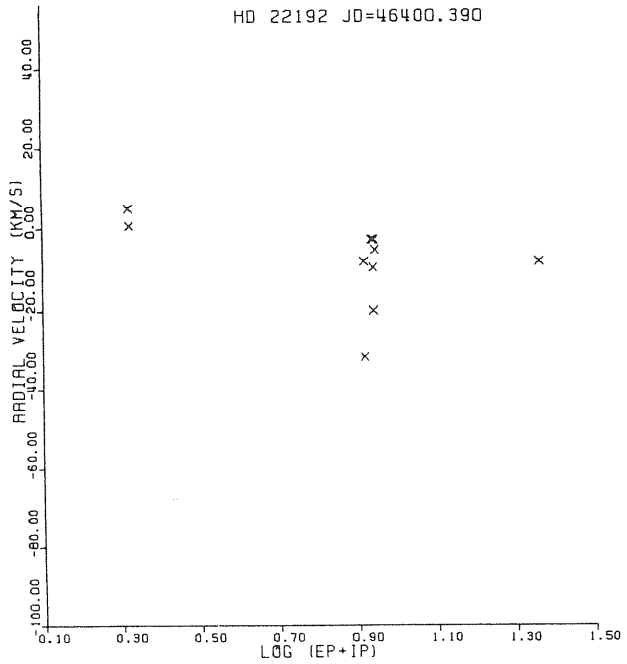

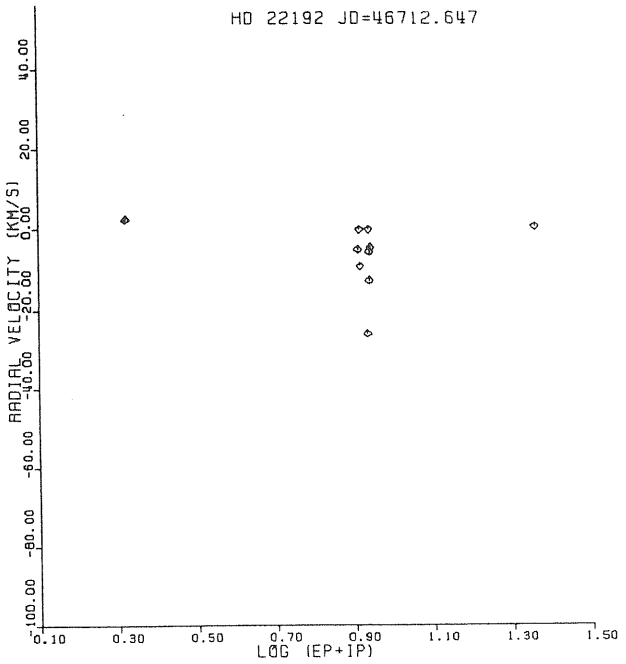

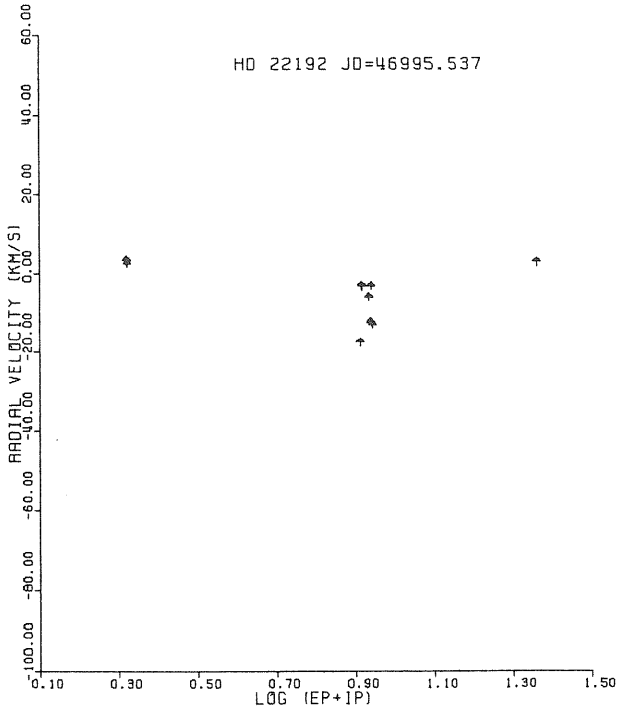

FIGURE III.1.1.10

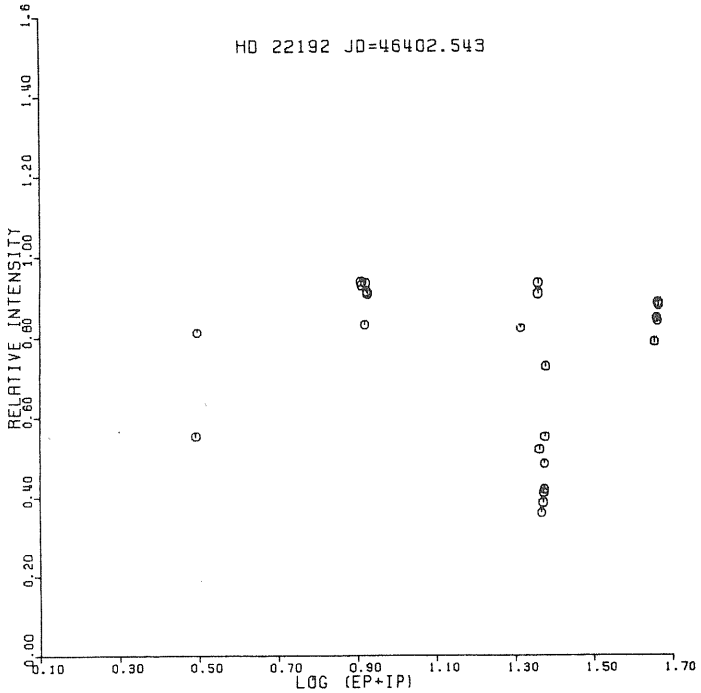

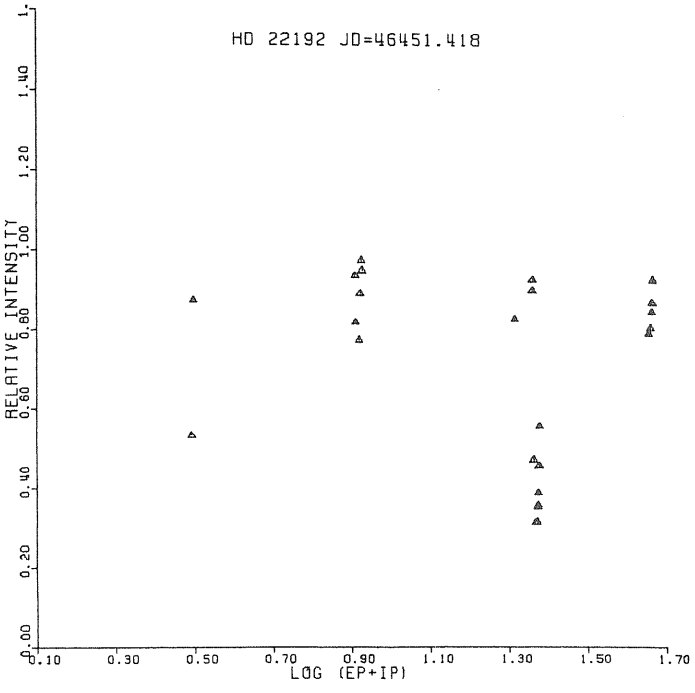

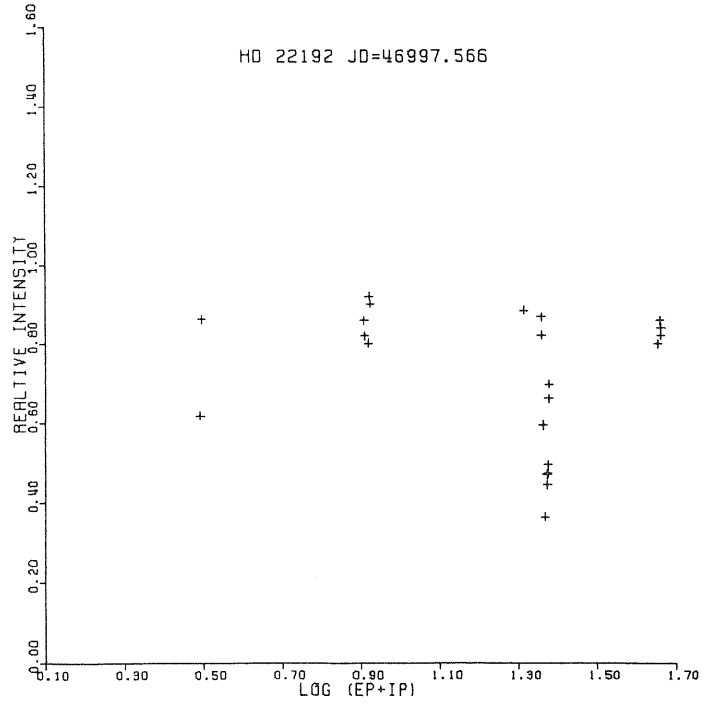

FIGURE III.1.1.11

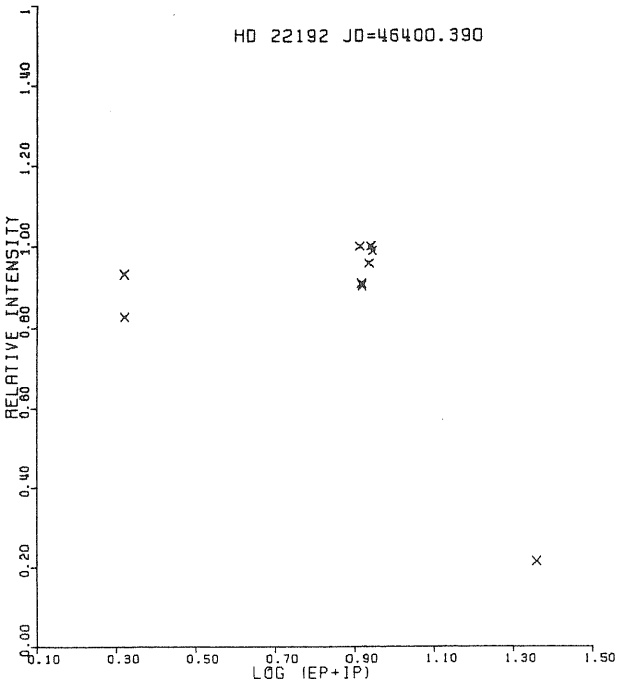

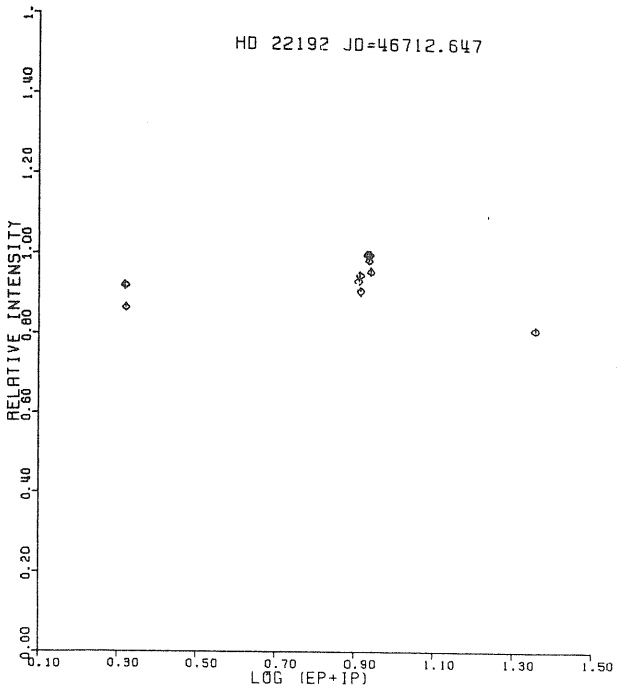

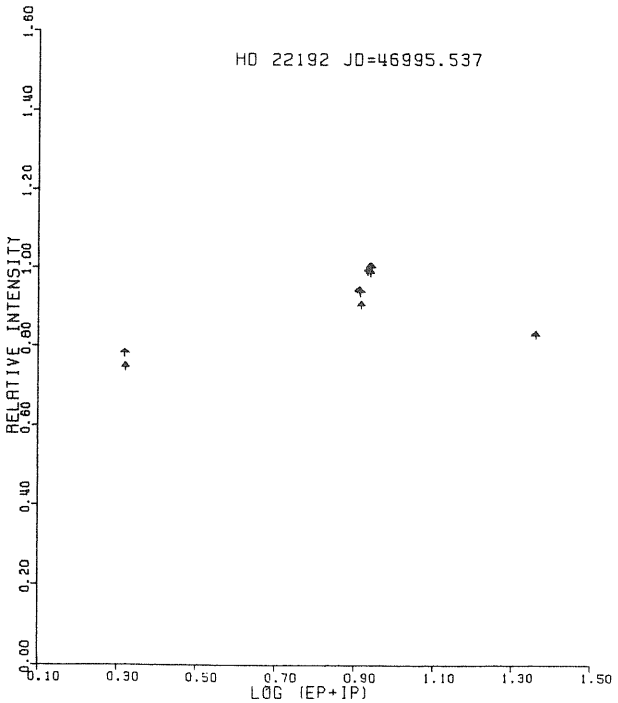

FIGURE III.1.1.12

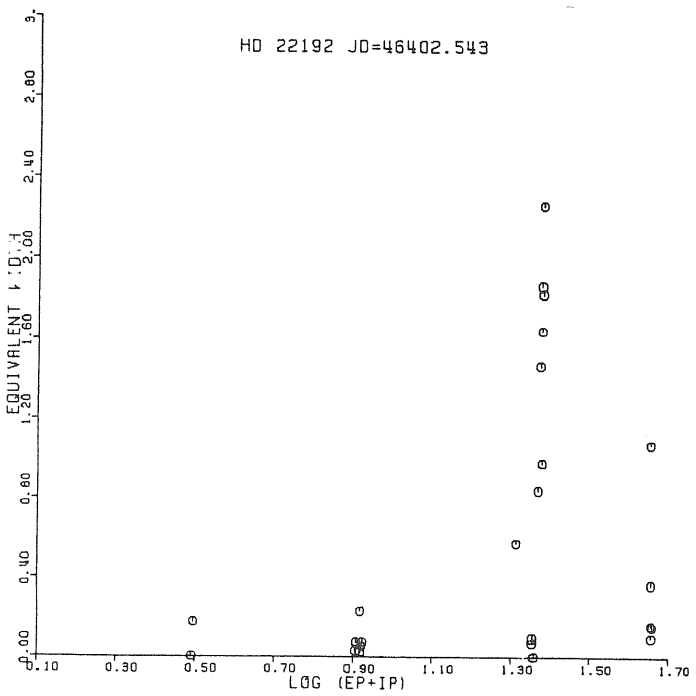

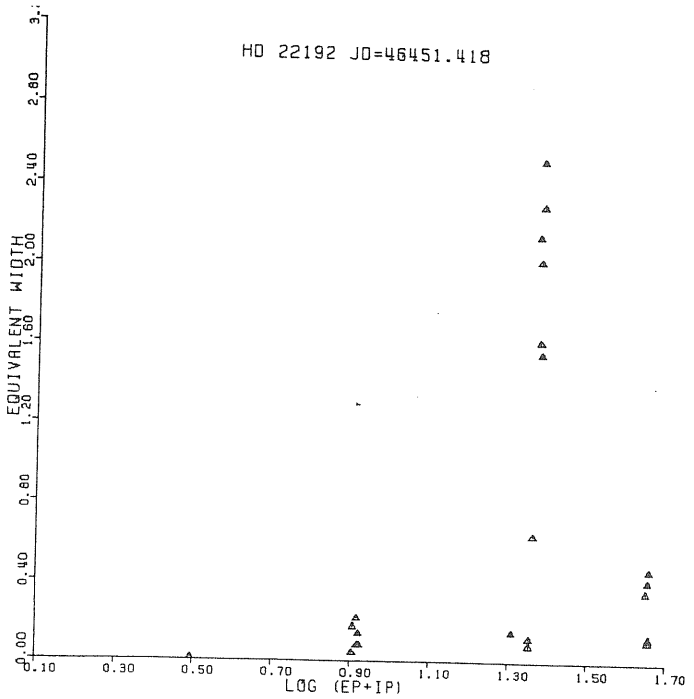

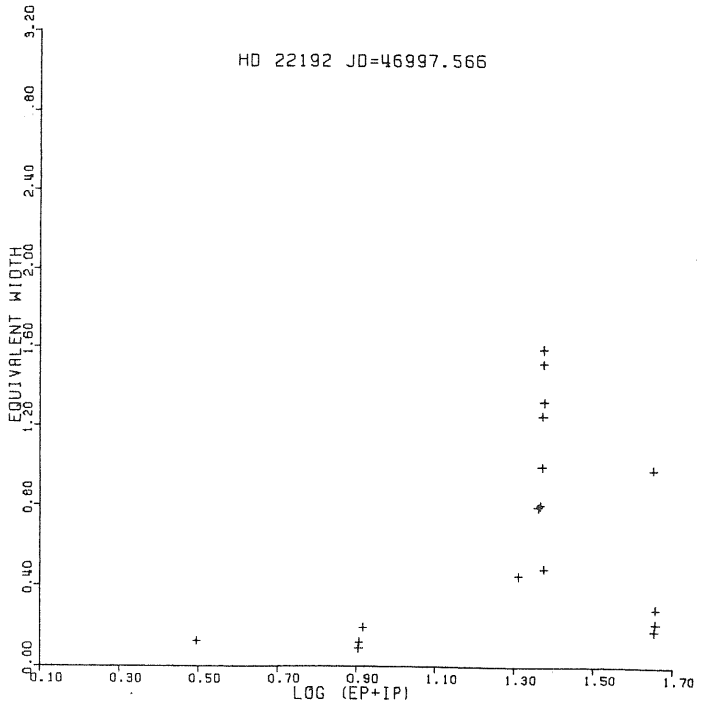

FIGURE III.1.1.13

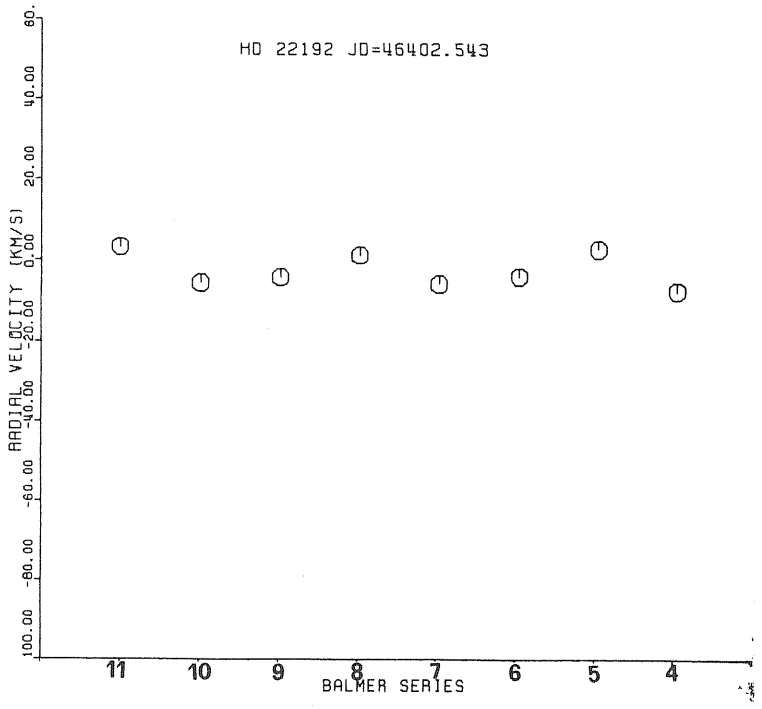

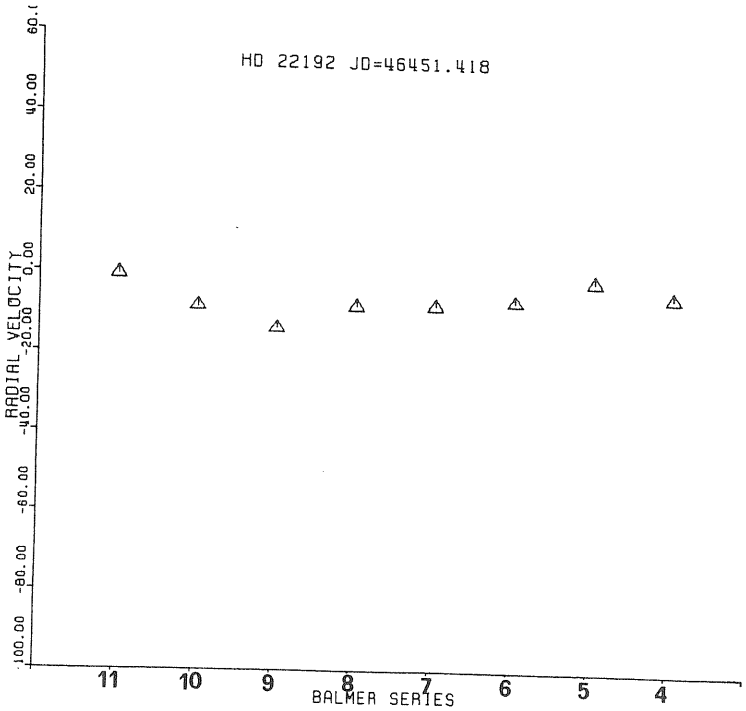

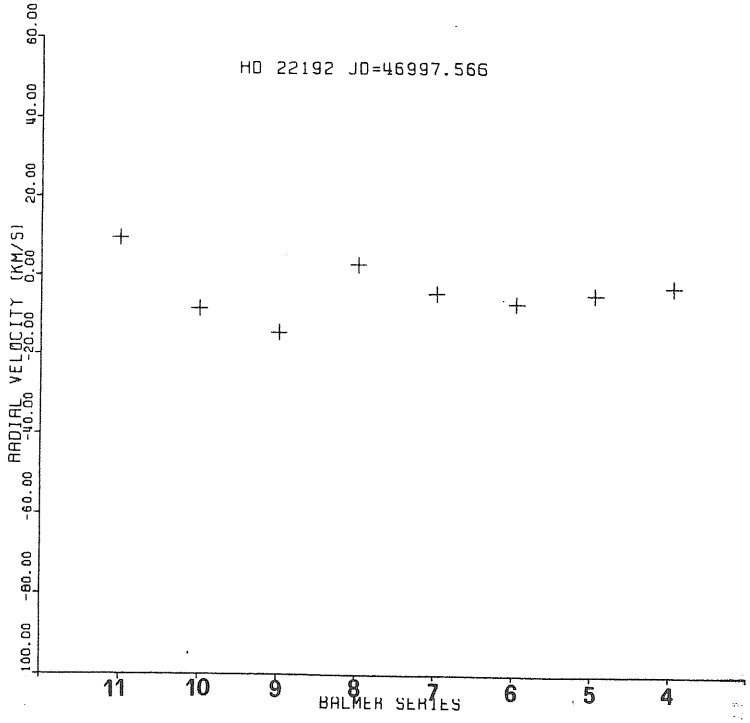

FIGURE III.1.1.14

Table III.1.1.1.Spectral measurements of the H alpha and H beta emission components of HD 22192.

	J.D.	OBSERVED WAVELENGTH(A)	EQW (A)	DEPTH	FBWC (A)	HWC(B) (A)	HWC(R) (A)
alpha							
	46400.390	6561.3	3.7	3.0	2.5	1.7	0.8
		6564.4	3.8	2.9	2.7	1.1	1.6
	46712.647	6561.1	6.0	2.8	4.2	2.6	1.8
		6564.2	4.2	2.8	3.8	0.9	2.9
	46995.537	6561.1	5.3	2.9	3.7	2.2	1.5
		6564.2	4.6	2.7	3.3	0.9	2.4
beta							
	46402.543	4859.9	0.7	0.5	2.4	1.3	1.1
		4862.7	0.8	0.6	2.4	1.1	1.3
	46451.418	4859.8	1.2	0.8	2.8	1.7	1.1
		4862.5	1.0	0.8	2.7	1.2	1.5
	46997.566	4860.0	0.9	0.7	2.7	1.6	1.1
		4862.7	0.8	0.6	2.5	1.1	1.5

NOTE:EQW=Equivalent width,DEPTH=Central intensity of the fitted asymmetric gaussian emission profiles,FBWC=Full band width on the continuum including both emission components of double-peak emission profile,HWC(B)=Half width on the continuum; the total width of the blue emission component on the continuum,HWC(R)=Half width on the continuum;the total width of the red emission component on the continuum.

Table III.1.1.2.Measured spectral line parameters of absorption the lines of HD 22192.

HD 22192			JD= 46402.543					JD= 46451.418					JD= 46997.566				
ELEMENT	MULT.	λ(LAB)Å	λ(OBS)Å	Ic	FBWC(Å)	EQW(Å)	RV(km/s)	λ(OBS)Å	Ic	FBWC(Å)	EQW(Å)	RV(km/s)	λ(OBS)Å	Ic	FBWC(Å)	EQW(Å)	RV(km/s)
H 16	3	3703.9	3704.2	0.8	2.6	0.3	30.8	3704.1	0.6	5.5	1.1	21.3	3704.3	0.7	2.4	0.3	35.1
H 15	3	3712.0	3711.9	0.8	5.1	0.6	- 3.8	3711.8	0.6	4.7	0.9	-13.7	3712.1	0.8	3.0	0.4	11.4
H 14	3	3721.9	3721.8	0.7	5.6	0.9	-13.5	3721.9	0.5	8.3	1.9	- 2.7	3721.9	0.7	4.4	0.3	- 4.1
H 13	3	3734.4	3734.4	0.7	12.9	2.2	- 1.5	3734.3	0.5	9.2	2.3	- 7.7	3734.3	0.6	4.8	1.0	- 4.7
H 12	2	3750.2	3750.0	0.6	7.4	1.6	-10.7	3750.0	0.5	9.0	2.2	-13.4	3750.1	0.8	9.6	1.0	- 3.4
H 11	2	3770.6	3770.6	0.5	9.0	2.1	- 0.4	3770.6	0.4	8.0	2.4	- 3.2	3770.5	0.5	7.1	1.7	-13.2
H 10	2	3797.9	3797.8	0.5	7.4	1.9	- 7.2	3797.7	0.4	11.9	3.6	-13.4	3797.2	0.5	3.7	0.9	-17.4
H 9	2	3835 4	3835.4	0.5	6.1	1.4	- 1.1	3835.2	0.4	10.0	3.1	-13.4	3835.2	0.5	9.7	2.3	-11.1
H 8	2	3889.1	3889.1	0.4	7.8	2.3	1.2	3889.0	0.4	7.9	2.5	- 7.9	3889.1	0.5	5.8	1.5	2.9
He I	58	3926.5	3926.6	0.9	2.7	0.2	1.5	3927.5	0.9	3.6	0.1	70.4	-	-	-	-	-
Ca II K	1	3933.6	3933.7	0.8	1.9	0.2	1.7	3933.6	0.9	1.5	0.1	- 6.6	3933.6	0.9	1.8	0.1	- 4.7
Ca II H	1	3968.5	3968.5	0.6	-	-	3.3	3968.4	0.5	-	-	- 8.9	3698.4	0.6	-	-	- 8.3
H eps	1	3970.1	3970.0	0.4	6.3	1.9	- 5.6	3970.0	0.4	5.0	1.6	- 7.5	3970.0	0.5	4.6	1.3	- 4.5
He I	55	4009.3	4009.4	0.9	1.8	0.1	10.6	4010.0	0.9	1.8	0.1	54.6	4009.3	0.5	2.7	0.2	4.7
H delta	1	4101.7	4101.7	0.4	4.8	1.5	- 3.7	4101.7	0.3	5.9	2.0	- 6.2	4101.6	0.5	3.5	1.0	- 6.8
Si II	3	4128.1	4127.7	0.9	2.2	0.1	-29.2	4128.2	0.9	2.5	0.1	10.8	4128.5	0.8	-	-	29.9
Si II	3	4130.9	4130.4	0.9	1.1	0.1	-35.7	4131.0	0.9	2.4	0.1	9.9	4131.5	0.9	-	-	40.9
He I	53	4143.8	4143.8	0.9	2.1	0.2	6.1	4144.5	0.9	6.3	0.5	54.4	4143.8	0.8	3.2	0.3	4.6
Fe II	28	4178.9	4178.6	0.9	2.1	0.1	-22.0	4178.6	0.8	2.0	0.2	-21.7	4179.0	0.8	1.3	0.1	8.8
Fe II	27	4233.2	4233.1	0.9	0.9	0.0	- 6.5	4232.9	0.9	1.4	0.0	-16.0	4233.1	0.9	1.2	0.1	- 4.0
H gam	1	4340.5	4340.5	0.4	2.6	0.8	2.8	4340.5	0.3	6.3	2.2	- 1.1	4340.4	0.4	2.5	0.8	- 4.7
He I	51	4387.9	4388.3	0.9	5.0	0.4	23.7	4389.3	0.8	4.4	0.4	90.7	4388.5	0.9	2.5	0.2	39.9
He I	14	4471.5	4471.6	0.8	10.2	1.1	8.7	4471.2	0.8	3.5	0.3	-17.6	4471.8	0.8	9.8	1.0	18.7
Mg II	4	4481.1	4482.4	0.8	6.6	0.6	85.1	4480.8	0.8	1.8	0.2	-20.5	4481.0	0.9	7.8	0.5	- 5.7
Fe II	38	4522.6	4522.6	0.9	1.7	0.1	- 5.6	4522.4	1.0	3.1	0.1	-18.6	-	-	-	-	-
Fe II	38	4549.5	4549.3	0.9	1.3	0.1	-24.7	4549.4	1.0	2.4	0.1	- 3.7	4549.7	0.9	-	-	13.3
Fe II	38	4583.8	4583.7	0.9	0.7	0.0	- 9.4	4583.7	0.9	1.6	0.1	- 6.8	4583.9	0.9	-	-	4.1
Fe II	37	4629.3	-	-	-	-	-	-	-	-	-	-	-	-	-	-	-
H beta	1	4861.3	4861.2	0.5	-	-	- 7.2	4861.3	0.5	-	-	- 4.5	4861.3	0.5	-	-	- 2.7
Fe II	42	4923.9	4923.7	0.8	2.8	0.2	-14.3	4923.5	0.8	2.0	0.2	-23.9	4924.0	0.8	2.0	0.2	3.4
H beta	1	4861.3	4861.2	0.2	-	-	- 8.4	4861.3	0.8	-	-	0.4	4861.4	0.8	0.9	-	2.7
Fe II	42	4923.9	4923.4	0.9	1.2	0.1	-31.9	4923.8	0.9	2.5	0.1	- 9.3	4923.9	0.9	1.9	0.1	- 3.6
Fe II	42	5018.4	5018.3	0.9	1.0	0.1	- 8.4	5018.4	1.0	1.3	0.0	- 0.2	5018.4	0.9	1.5	0.1	- 3.4
Fe II	42	5169.0	-	-	-	-	-	5168.9	0.1	1.8	0.1	- 5.2	5168.7	0.9	1.0	0.0	-17.7
Fe II	49	5197.6	5197.5	1.0	-	-	- 5.7	5197.4	1.0	2.4	0.1	- 4.6	5197.3	-	-	-	-13.3
Fe II	49	5234.6	5234.6	-	-	-	- 3.0	5234.4	-	-	-	-12.8	4234.4	1.0	1.2	0.0	-12.8
Fe II	49	5276.0	5275.9	1.0	0.7	0.04	- 3.0	5275.5	-	-	-	-26.0	5275.9	1.0	0.5	0.0	- 6.3
Fe II	49	5316.6	5316.3	-	-	-	-20.0	5316.5	-	-	-	- 5.6	5316.6	-	-	-	- 3.5
Fe II	48	5362.9	5362.7	-	-	-	-10.0	5362.9	1.0	0.6	0.0	- 0.2	5362.6	-	-	-	-12.4
Na I	1	5890.0	5890.0	0.8	1.8	0.2	0.5	5890.0	0.9	2.7	0.2	2.5	5890.0	0.8	2.4	0.3	2.5
Na I	1	5895.9	5896.0	0.9	1.8	0.0	4.9	5896.0	0.9	2.5	0.1	2.2	5896.0	0.8	2.4	0.3	3.3

III.1.2.HD 184279

Two H alpha profiles of this star are presented in Figure III.1.2.1 obtained at nearly one year interval.The first profile exhibited a double-peak emission with a red component much stronger than the violet, and a blue shifted central absorption (-37 km/s) at JD=639.9.Wings of the emission profiles were extending from -400 km/s to +300 km/s.Second profile which was observed at JD=991.5 presented again a double-peak emission with approximately V=R and a strong central absorption with a radial velocity of +44 km/s.First sign of a multi-component structure in the envelope of the HD 184279 is seen in the H alpha profiles , specially the second one.Figure III.1.2.2 presents four H beta profiles with a high variability.The fist profile was a typical P Cygni profile ,with a red emission wing and a blue shifted strong narrow absorption component with a radial velocity about -29 km/s (JD=587.5).In the second profile the emission component was diminished and the absorption component was widened.The radial velocity of the absorption component was more negative, -67 km/s.Time interval between two observations was nearly 50 days.At JD=931.6, the third profile HD 184279 exhibited an asymmetric absorption profile where the narrow component increased it's central depth and with extended red wing.Radial velocity of the absorption component was +46 km/s.Last profile of this figure taken at JD=989.5 presented emission wing at the red side of the absorption component which displayed +45

km/s as a radial velocity.

Similarly, profile changes were observed for H gamma, delta, and epsilon lines; without emission components except H gamma which presented a very weak emission component at the red wing of the central absorption (Figures III.1.2.3 to III.1.2.5).Table III.1.2.1 lists the measured line parameters for HD 184279.Balmer series of HD 184279 could be seen up to n=14 for the first two observations (JD=587.5, and 637.9).Shell effect was not visible for these two spectra; but for the last two the Balmer series was visible up to n=16, and shell effect was present; specially for JD=991.9 it was very evident.The time variation of the other line profiles specially He I can be seen from the Figures III.1.2.6 to III.1.2.9.

Figure III.1.2.10 presents measured radial velocities versus log (IP+EP) of each line.At JD=587.5 with the exception of few lines, generally all the radial velocities were negative.At JD=637.9 the radial velocities were more negative than previous values, specially He I lines, although Ca II lines remained approximately the same.But at JD=931.6 there was an enormous increase in the radial velocities; all of them except few had positive values.Lastly at JD=989.6 HD 184279 presented a relative decrease in the velocities for Ca II, He I and some Fe III lines, but H lines were still positive.For the red part of the spectra (Figure III.1.2.11) at JD=639.9 all the radial velocities were negative.We note here that on

the same night H alpha presented a blue shifted narrow absorption component.But at JD=991.5, when H alpha exhibited double-peak emission with central absorption with positive velocity, all the rest of the velocities were positive except Na I.

Now let's give a look at the relative intensities (Figure III.1.2.12) and equivalent widths (Figure III.1.2.13) in the blue part of the spectra.Ca II, metals and He I lines didn't present a big variation in intensity and in equivalent width between JD=587.5 and 637.9 although H lines slightly decreased in central intensities and increased in equivalent widths.But at JD=931.6 we see an evident decrease in the relative intensities of all lines except Ca II and obviously an increase in equivalent widths.At JD=989.5 some metal lines returned to their previous values but the H lines were still at the same values.For the red spectra, Na I lines remained the same but metals and He I lines increased their central depths and equivalent widths between JD=639.9 and JD=991.5 (Figure III.1.2.14 and III.1.2.15).Radial velocities of the Balmer lines were plotted against the n quantum number (Figure III.1.2.16).At the JD=637.9 a Balmer progression, and at JD=931.6 and JD=989.5 an inverse Balmer progression was observed.

Before concluding the description visual observational results for HD 184279, it is better to recall the past activity of this star.Ballereau and Hubert-Delplace (1982),

had published observations of this star since 1976 which we have outlined in the previous chapter.Their conclusion was that the lines of all elements presented variations over four years.Past activity can be given as follows:1955-1960 Be phase, 1963-1970 faint Be/shell, 1979-1980 strong Be/shell phase. Later Ballerau and Chauville (1987) confirmed a pseudo-periodic variations.Also they remarked short time (days) variations in spectral line profiles (double-peak absorption).In our observations, similar to their's ,H 11 and H 12 presented a double-peak absorption at JD=637.9 with an average velocity difference between the two absorption components approximately 200 km/s.The same phenomenon was already remarked by Ballerau and Hubert-Delplace (1982) with a radial velocity difference of about 76 km/s.Furthermore according to Ballerau and Chauville (1987) at JD=259.5 HD 184279 exhibited positive radial velocities for narrow components indicating a strong shell.In anology with 4 years possible period of Ballerau and Hubert-Delplace (1982), the same phase of strong shell with positive velocities should be repeated at about JD=7719.5.Our observations show that at JD=6931.6 a strong shell with positive radial velocities occured.This happened approximately 1.8 years before the supposed 4 year period, hence contradicting the suggested pseudo-period.So we observed two distinct phases Be (JD=587.5) and "Be/shell episode" (JD=931.6) with an interval of 0.94 yrs. Furthermore we do not know the exact date of the

beginning of the "Be/shell episode" so this interval can be even smaller.

In their original research Ballerau and Chauville (1987) discussed that the double structures of Balmer lines, assuming the presence of a transient shock wave in the envelope of the star.They have assumed that this doubling and dephasing between half depth withs of the first Balmer lines originated from a shock wave progressing from the star's surface towards the external layers of the shell.According to their observations this transient phenomenon- appearence, development and disappearence of a discrete component with strong negative RV in shell lines of Balmer series spread over 5 days.They couldn't be able to determine accurately it's limits in time, their uncertainty was about 0.5-1 day.Moreover they couldn't determine whether the velocity of this wave was constant or increases linearly, nor according to which law. Ballerau and Chauville (in preparation) determined the internal and external semi-major axis of the possible elliptical-rotating disk surrounding this star, 2.1 R(*) and 15.1 R(*) respectively from RV variations measured on H beta between 1976 and 1984.

Table and Figure captions.

Figure III.1.2.1.H alpha profiles of HD 184279.Same as figure III.1.1.1, only difference is every interval on the y axis corresponds to 0.2 units.

Figure III.1.2.2.H beta profiles of HD 184279.Same as previous figure.

Figure III.1.2.3.H gamma profiles of HD 184279.Same as previous figure.

Figure III.1.2.4.H delta profiles of HD 184279.Same as previous figure.

Figure III.1.2.5.H epsilon profiles of HD 184279.Same as previous figure.

Figure III.1.2.6.He I 4009, 4026 and Ca II 3933 lines of HD 184279.

Figure III.1.2.7.He I 4387, 4471, Mg II 4481 lines of HD 184279.

Figure III.1.2.8.He I 4923, O II 4638, C III 4650.

Figure III.1.2.9.He I 5015, 5875, 6678 and Na I 5889, 5895.

Figure III.1.2.10.RVs versus log (EP+IP) of HD 184279 for blue spectra. Typical log(EP+IP) values for group of lines are followings:H I=(1.373-1.358), He I=(1.657-1.648), Ca II=(0.498-0.492), O II=(1.684-1.731), Mg II=1.309, Si III=(1.607), C III=1.788, Fe III=(1.283-1.285)

Figure III.1.2.11.Same as previous figure for red spectra.

Figure III.1.2.12.Relative intensities versus log(EP+IP) of HD 184279 for blue spectra.

Figure III.1.2.13.Same as previous figure for red spectra.

Figure III.1.2.14.EQWs versus log(EP+IP) of HD 184279 for blue spectra.

Figure III.1.2.15.Same as previous figure for red spectra.

Figure III.1.2.16.Radial velocities of Balmer lines versus "n" quantum number for HD 184279.

Table III.1.2.1.Measured spectral line parameters of the absorption lines of HD 184279.

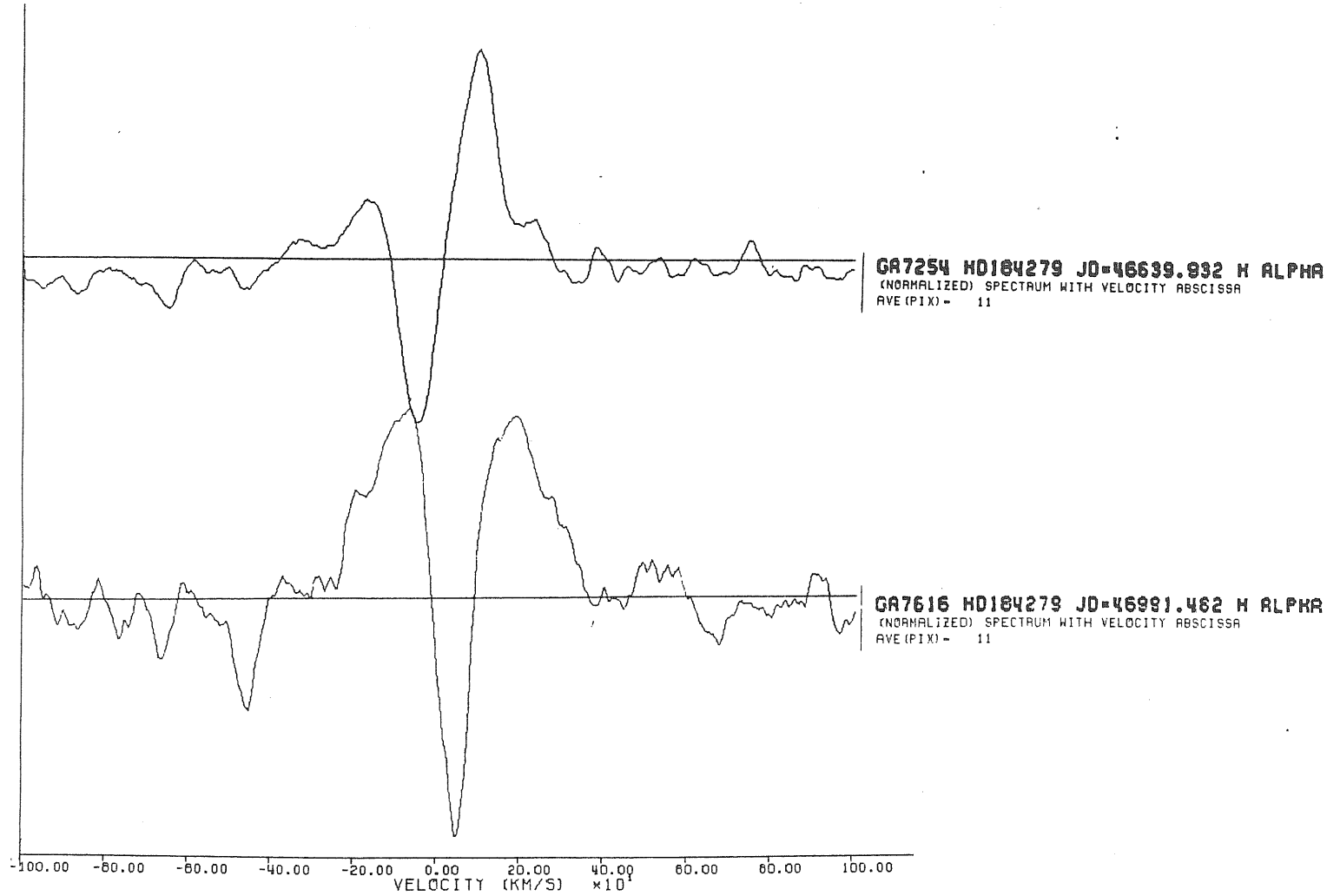

FIGURE III.1.2.1

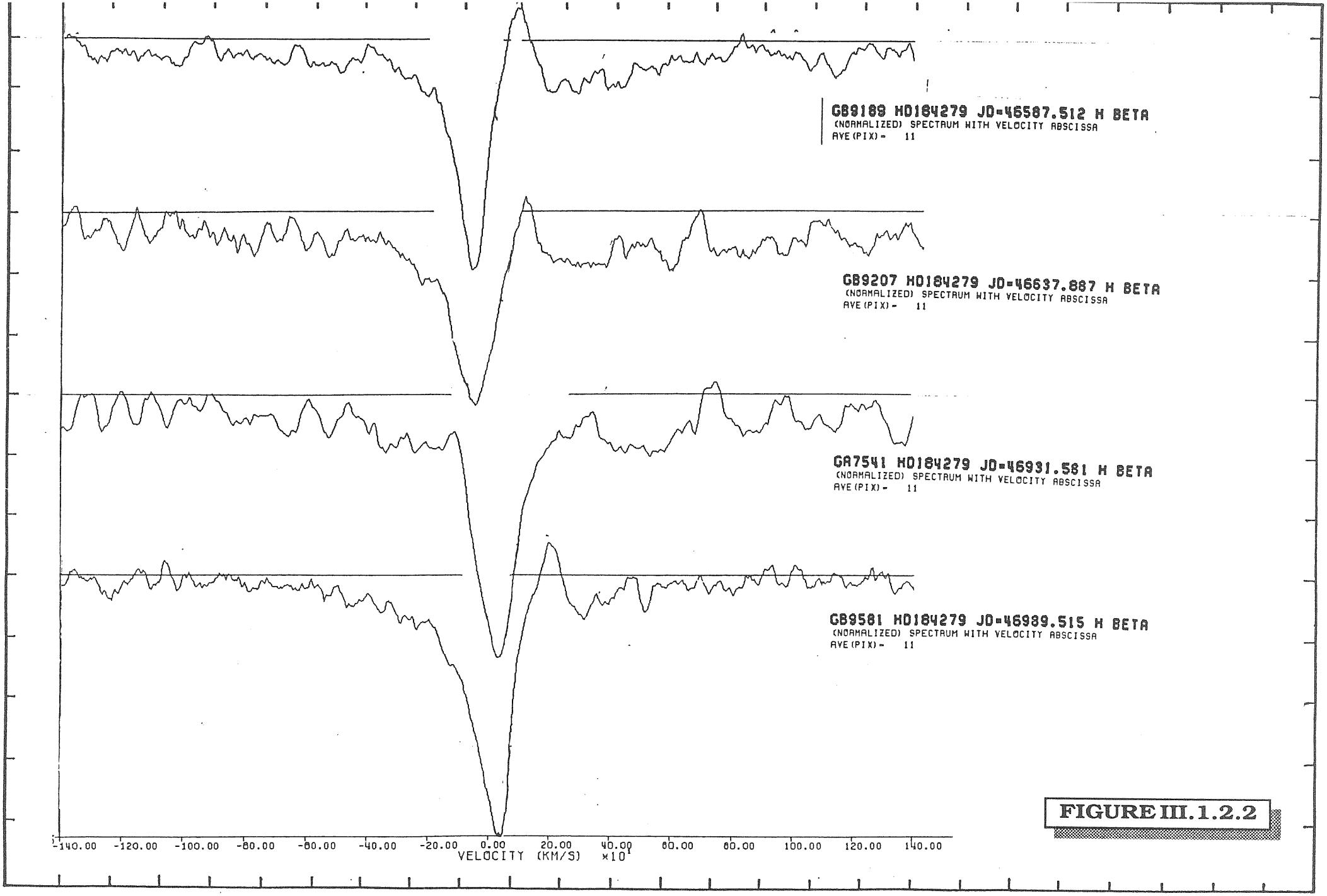

FIGURE III.1.2.2

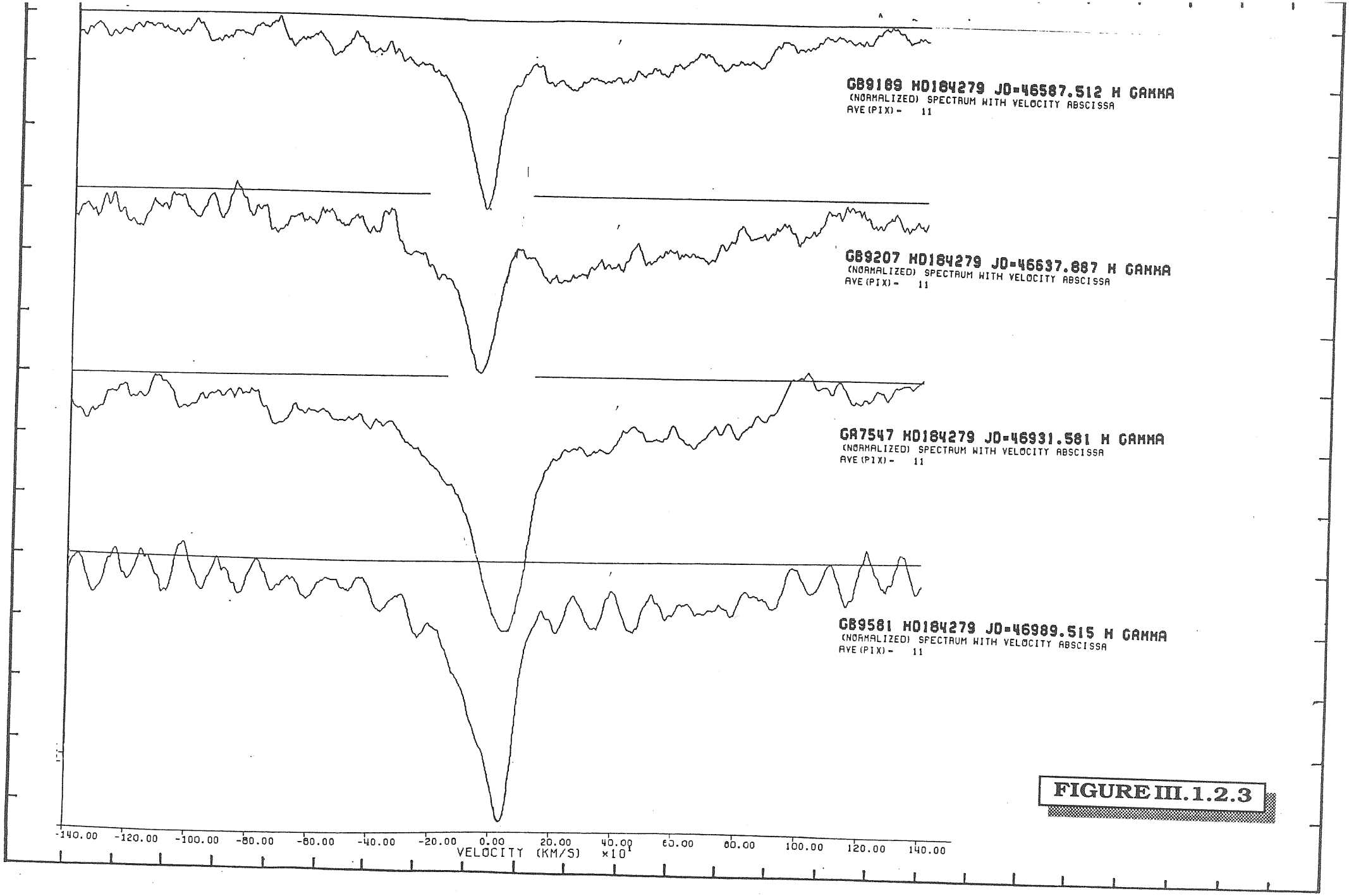

FIGURE III.1.2.3

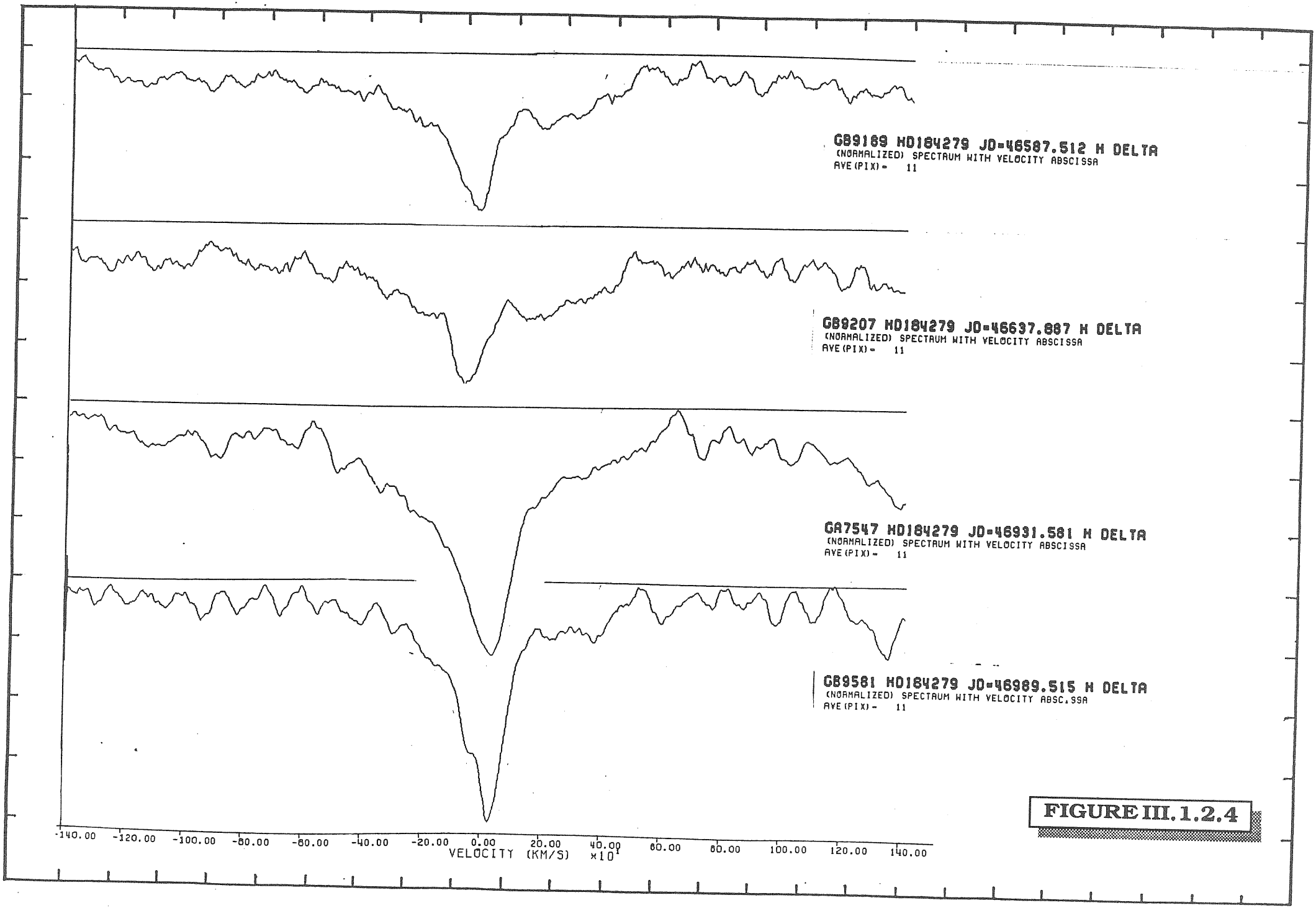

FIGURE III.1.2.4

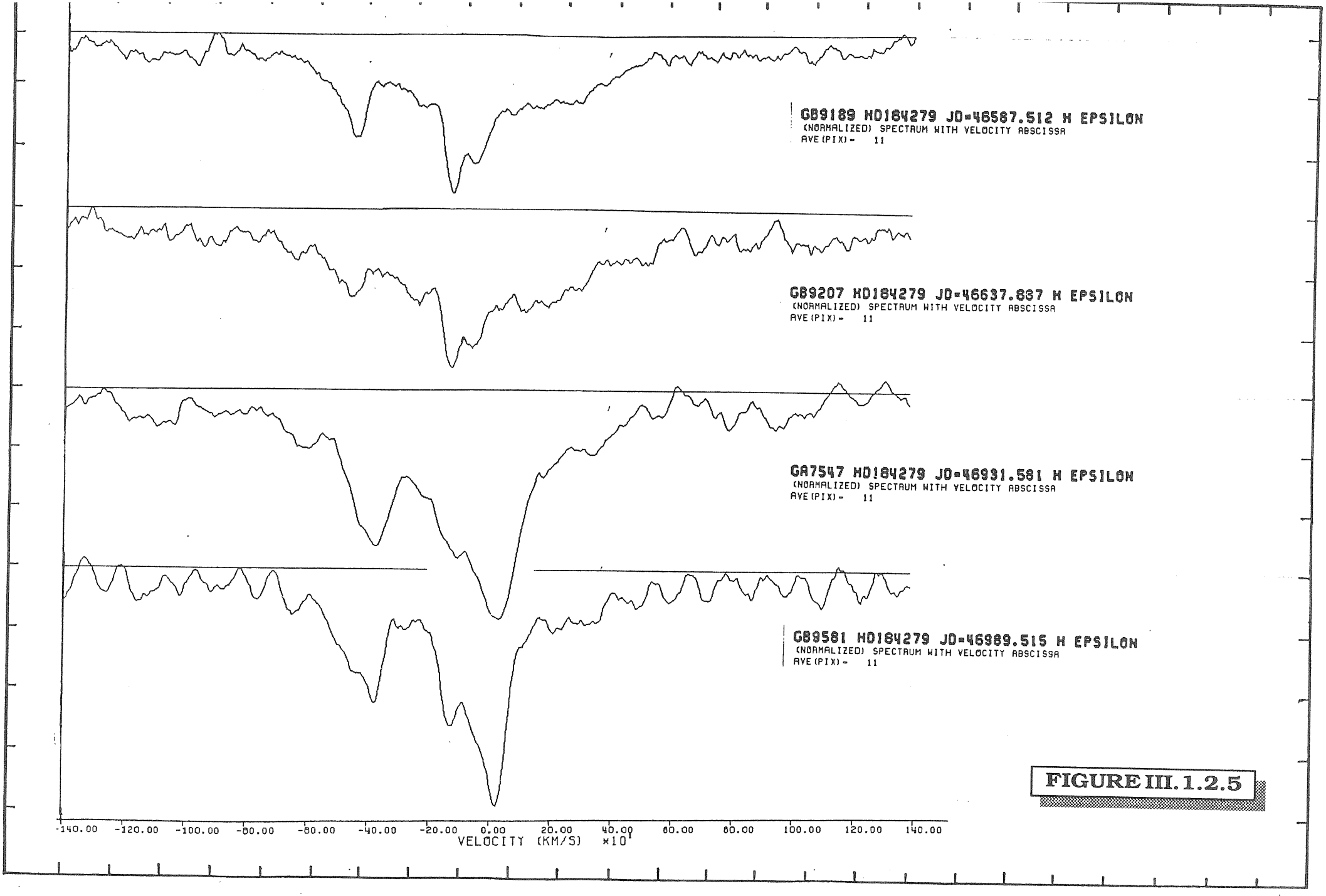

FIGURE III.1.2.5

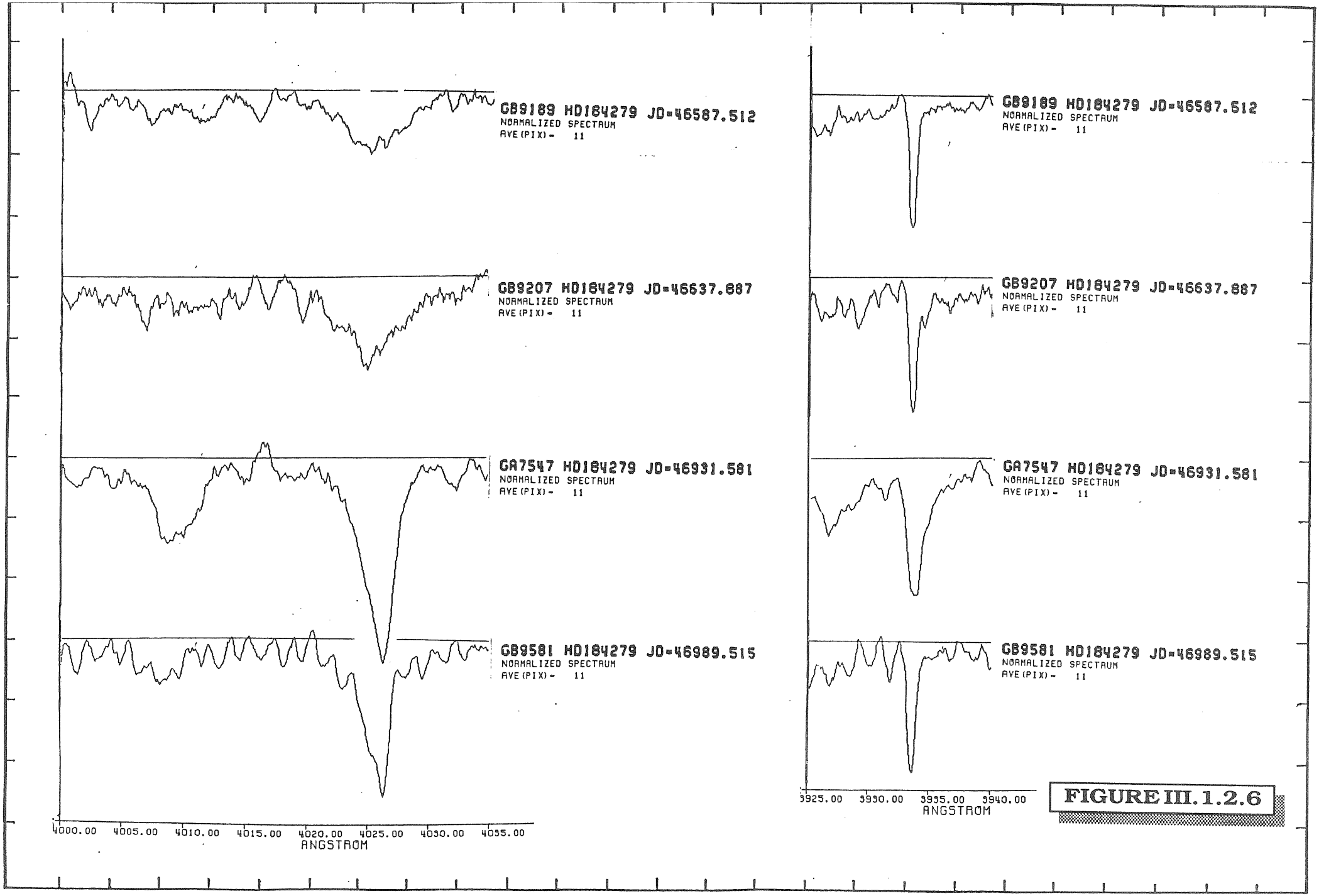

FIGURE III.1.2.6

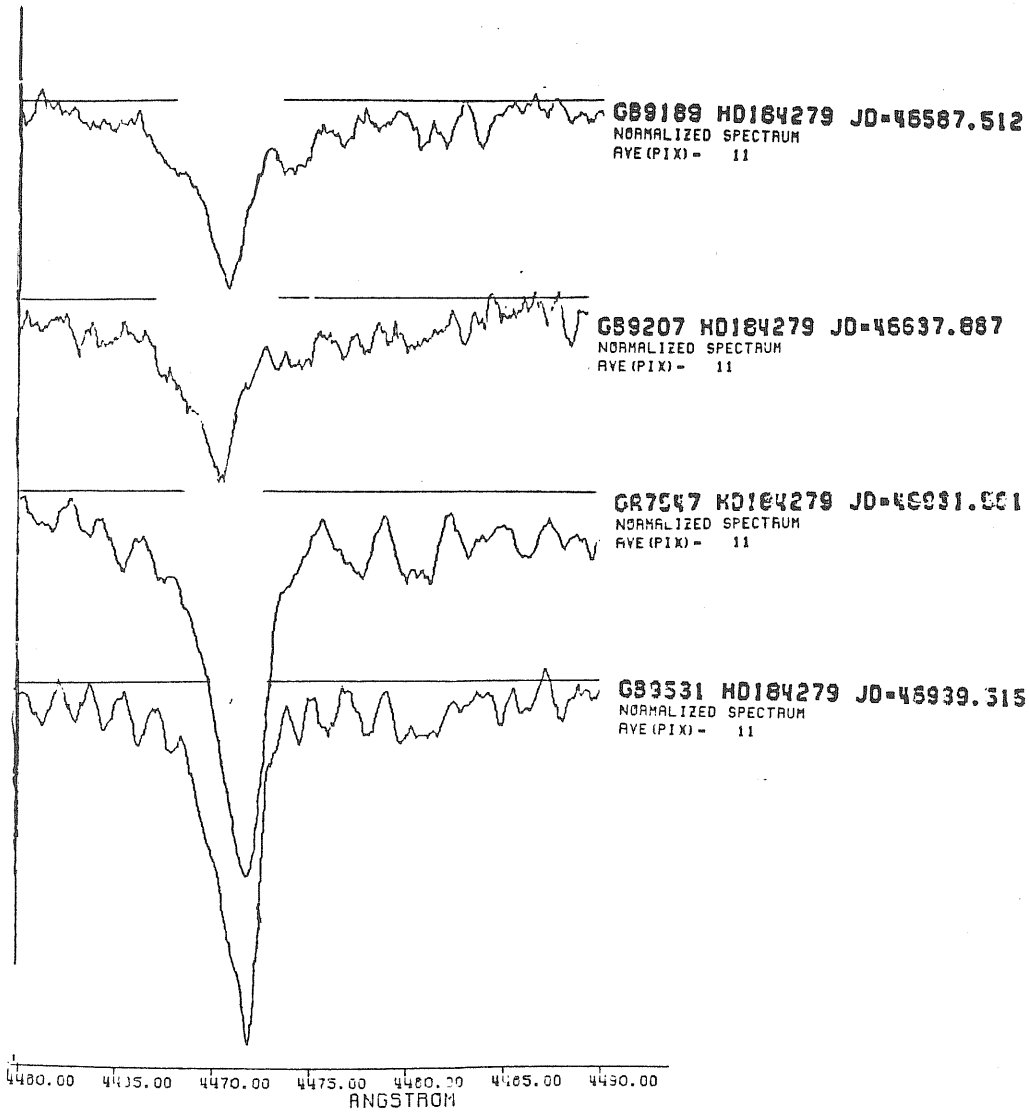

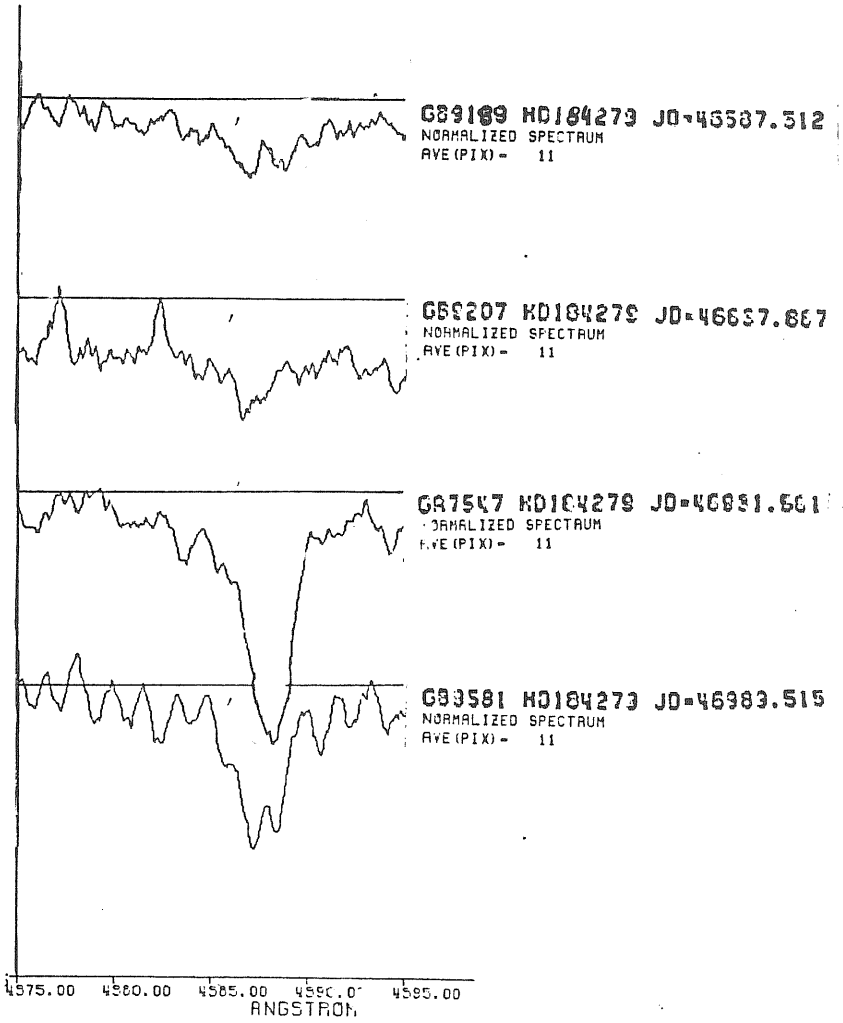

FIGURE III.1.2.7

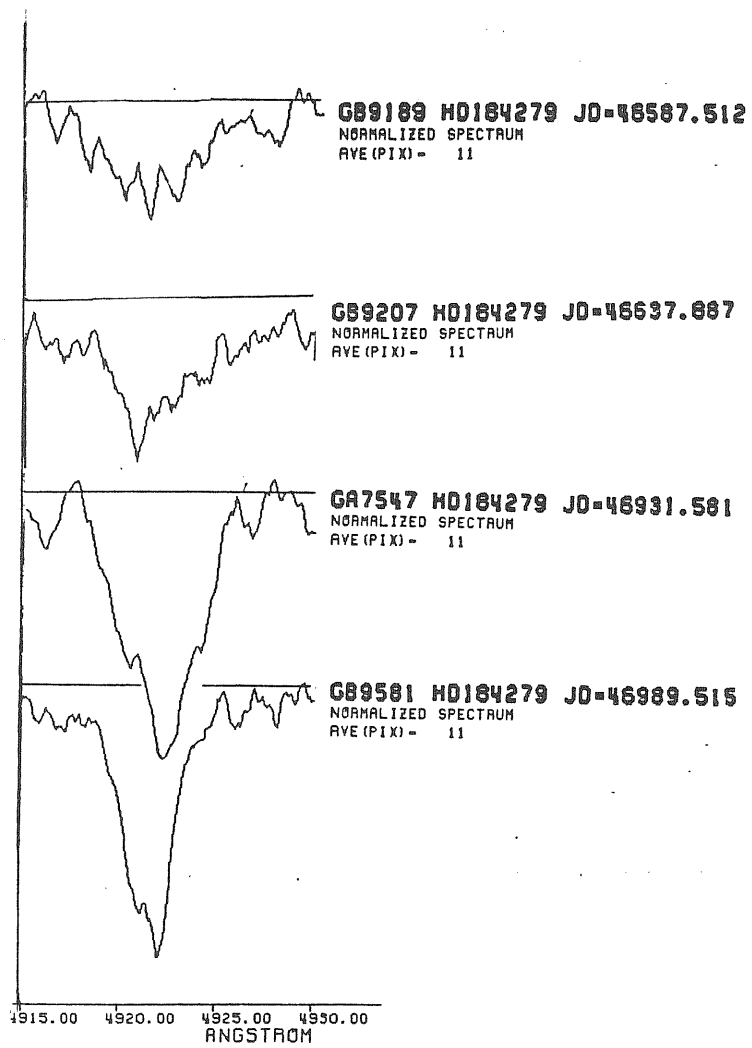

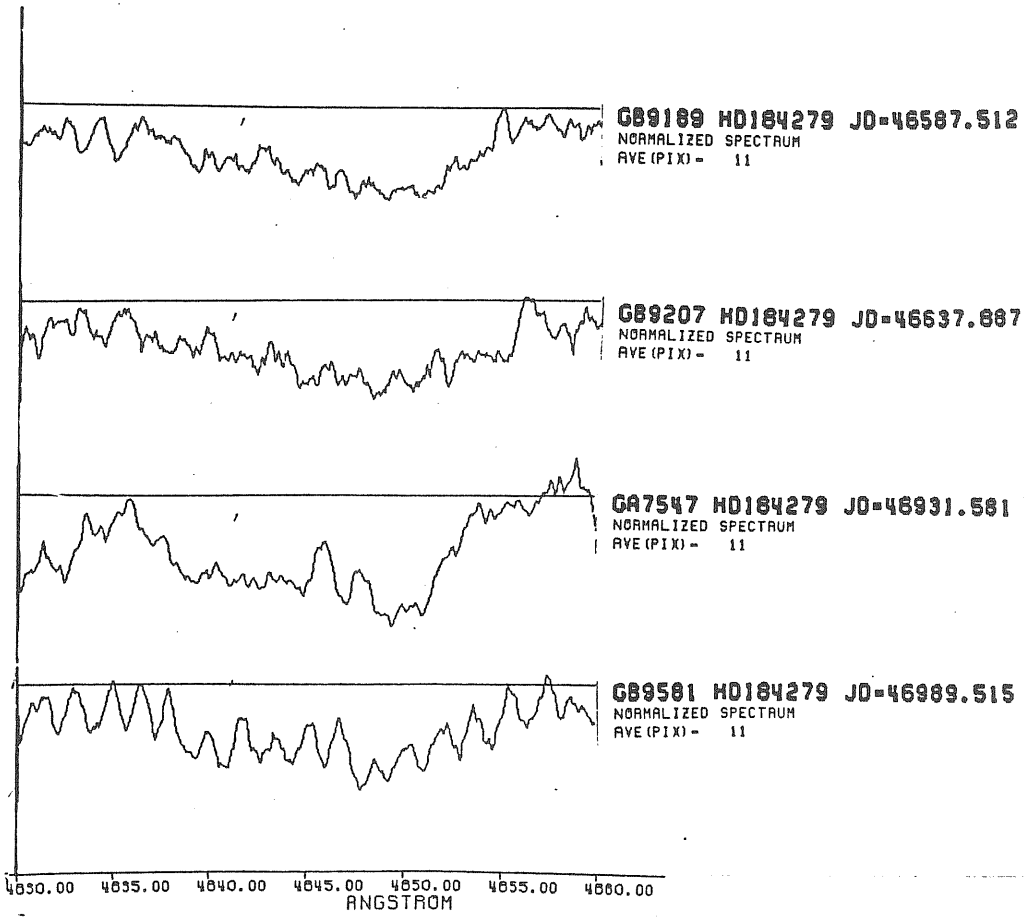

FIGURE III.1.2.8

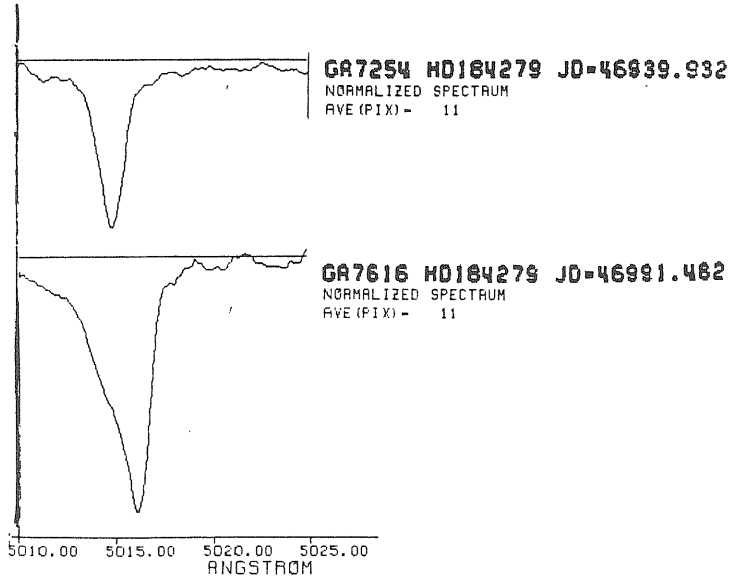

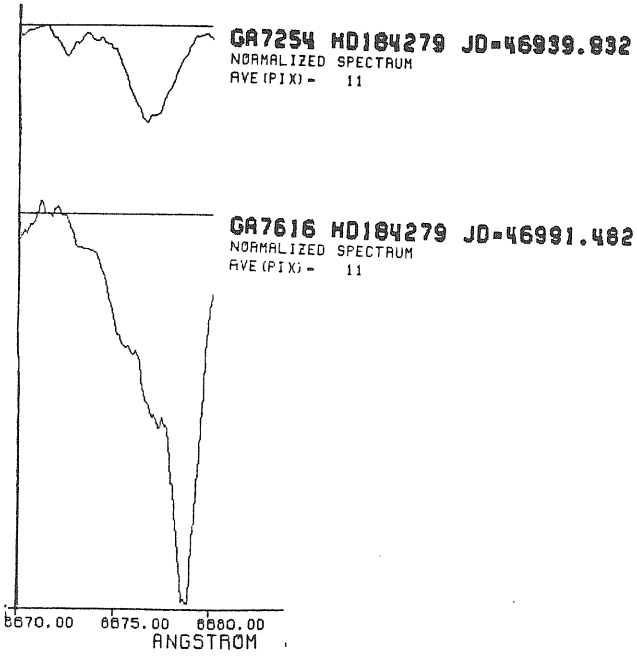

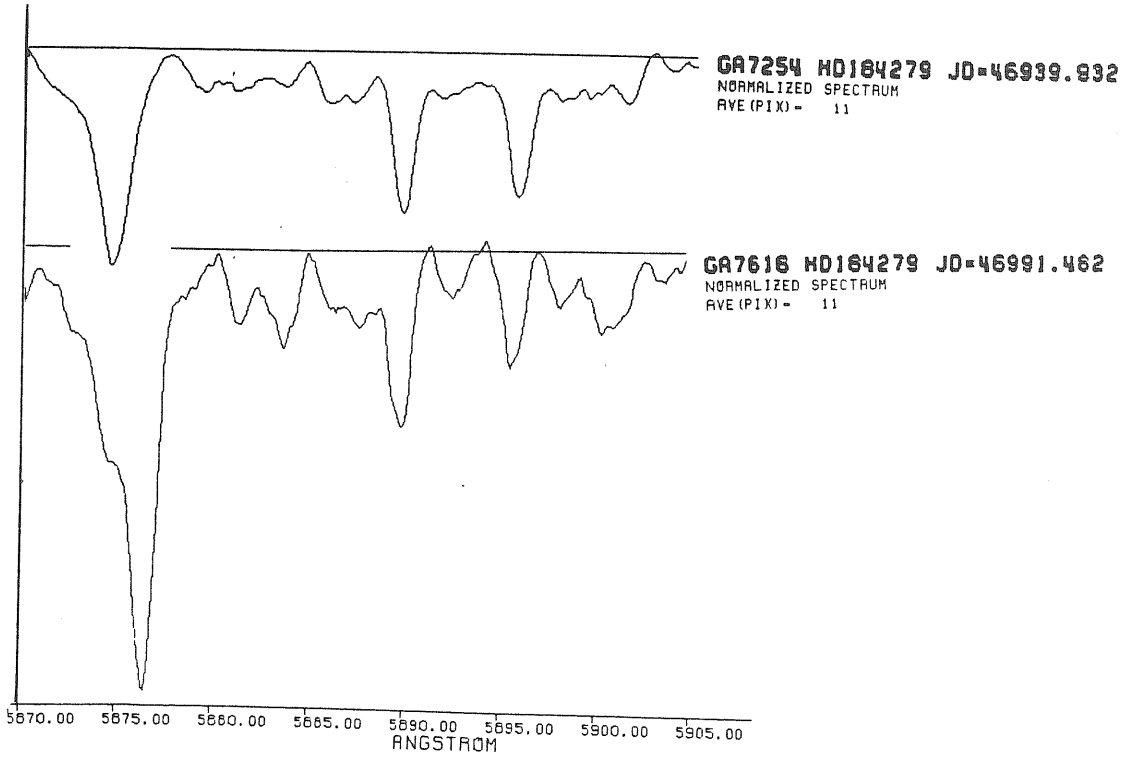

FIGURE III.1.2.9

FIGURE III.1.2.10

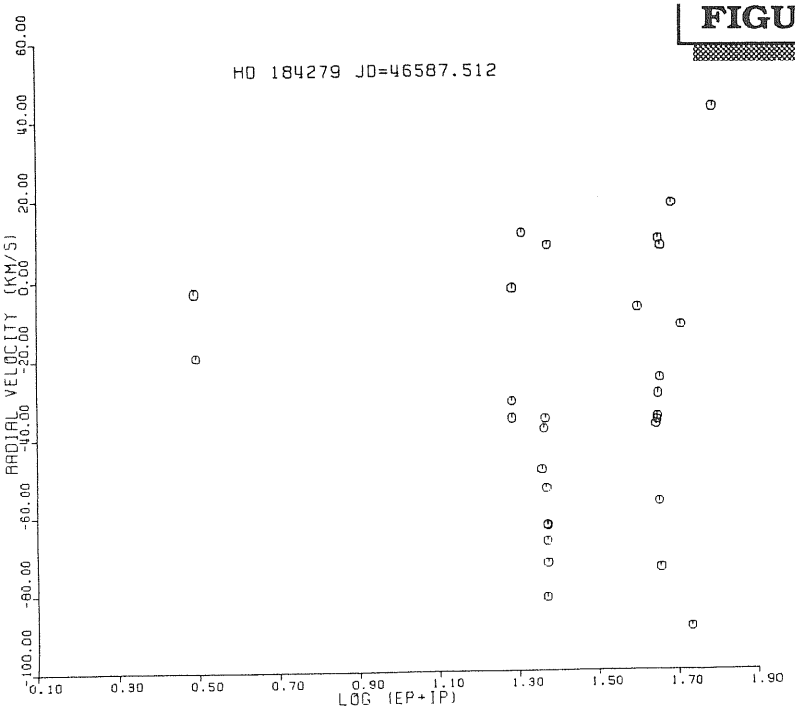

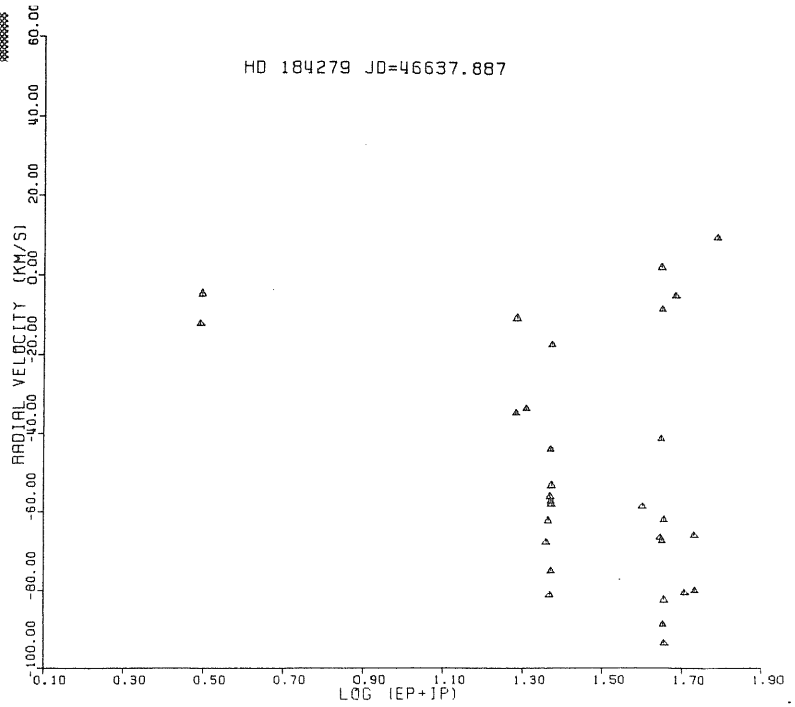

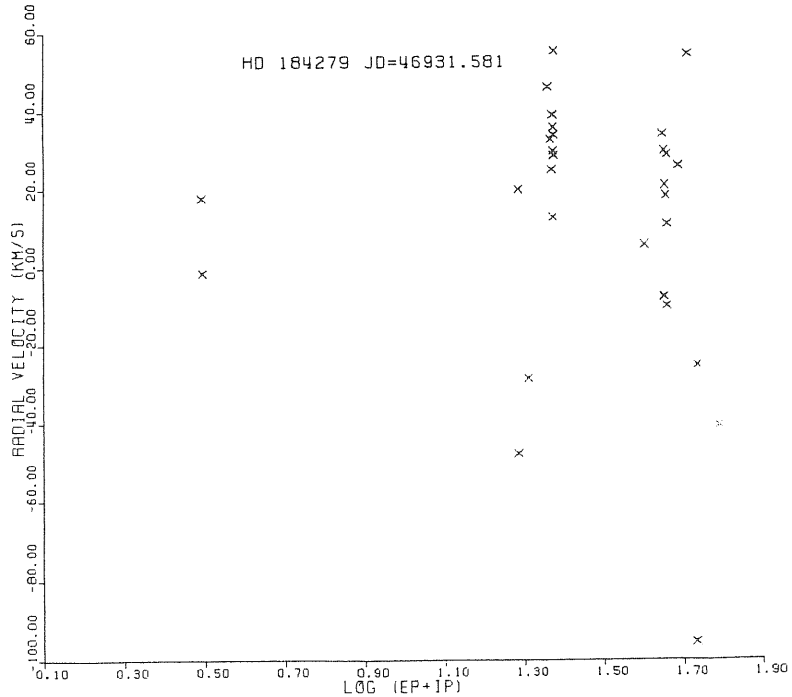

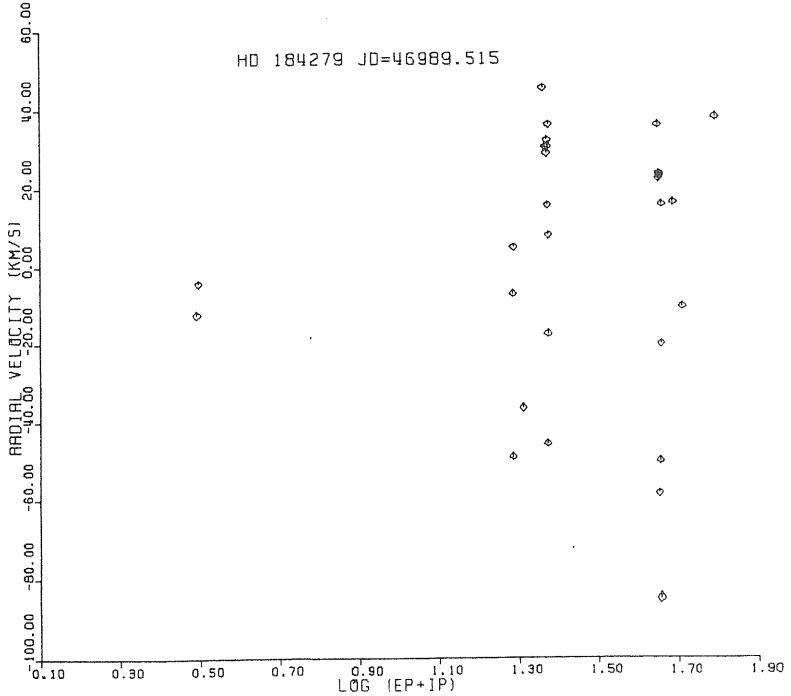

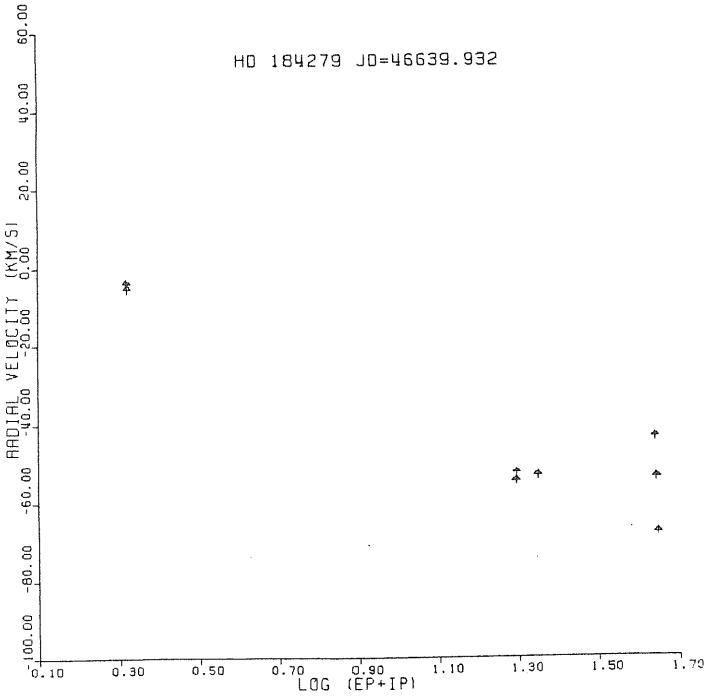

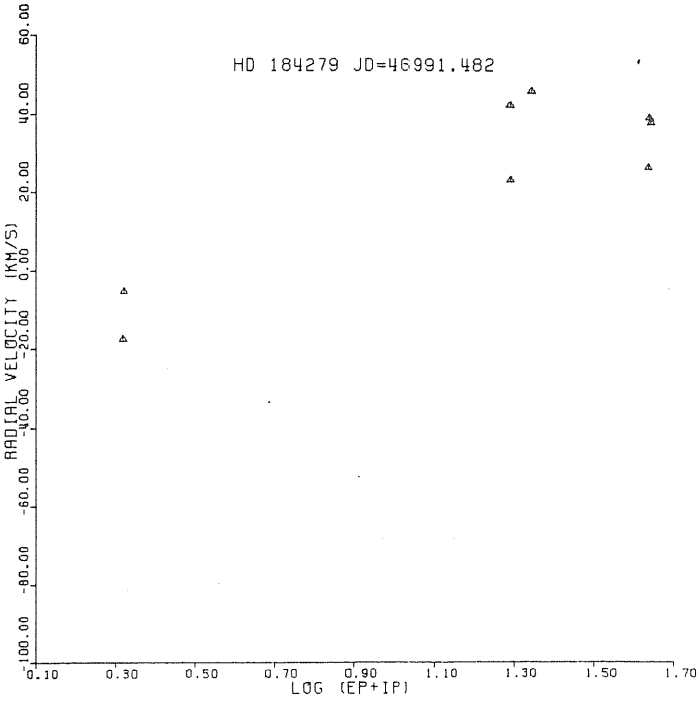

FIGURE III.1.2.11

FIGURE III.1.2.12

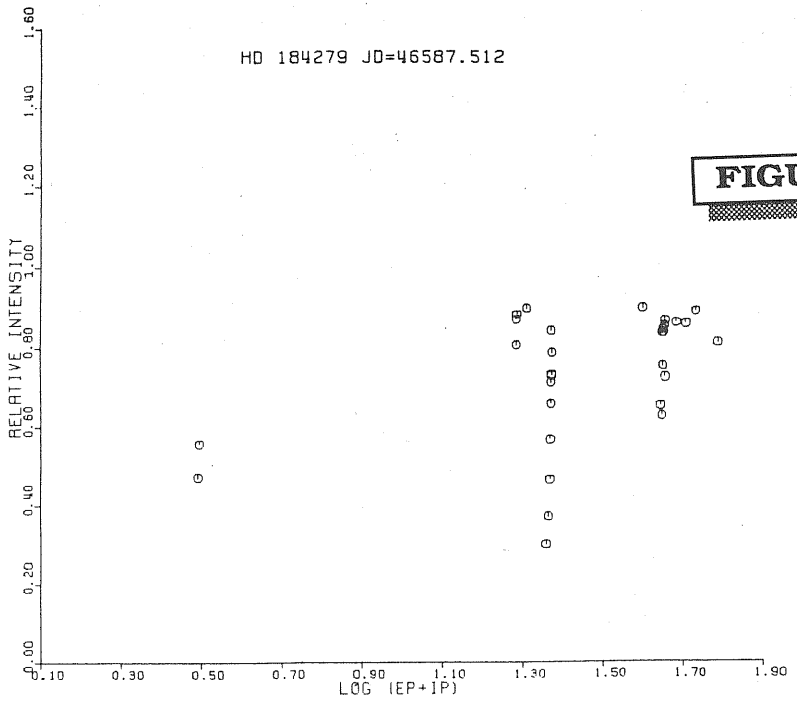

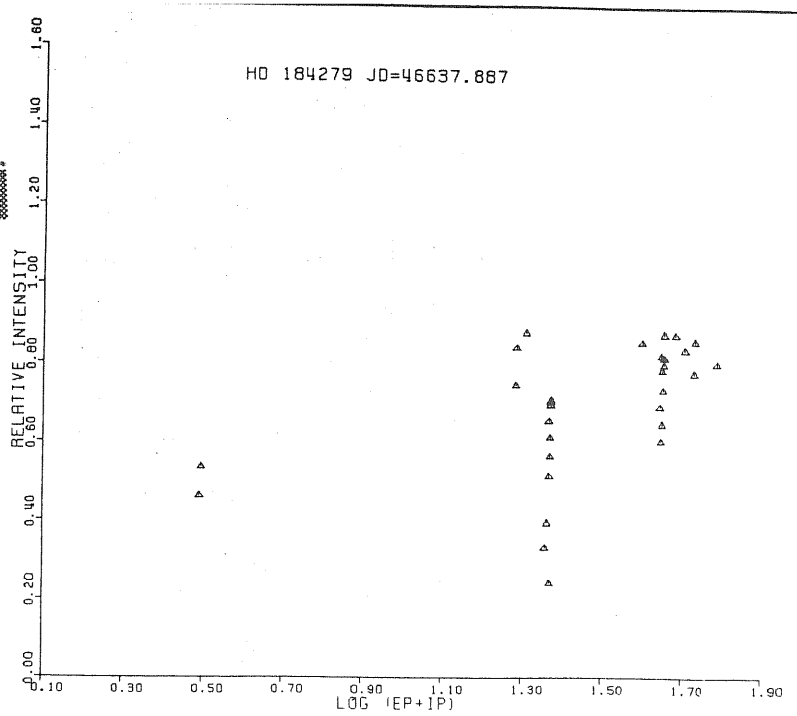

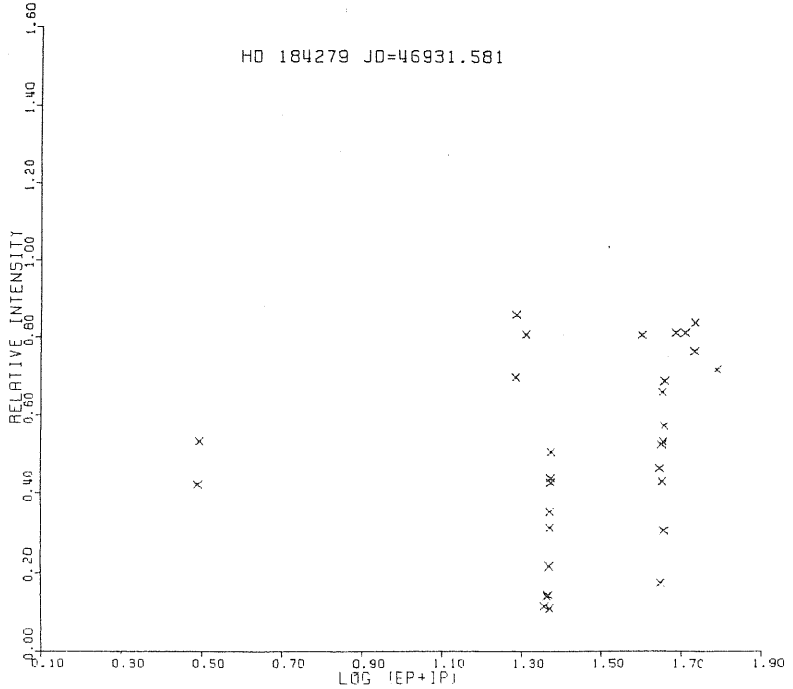

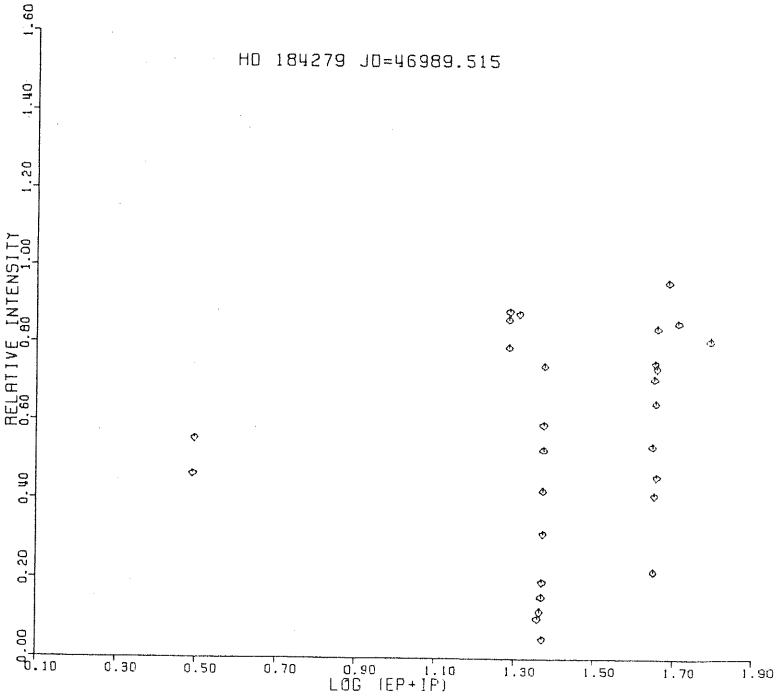

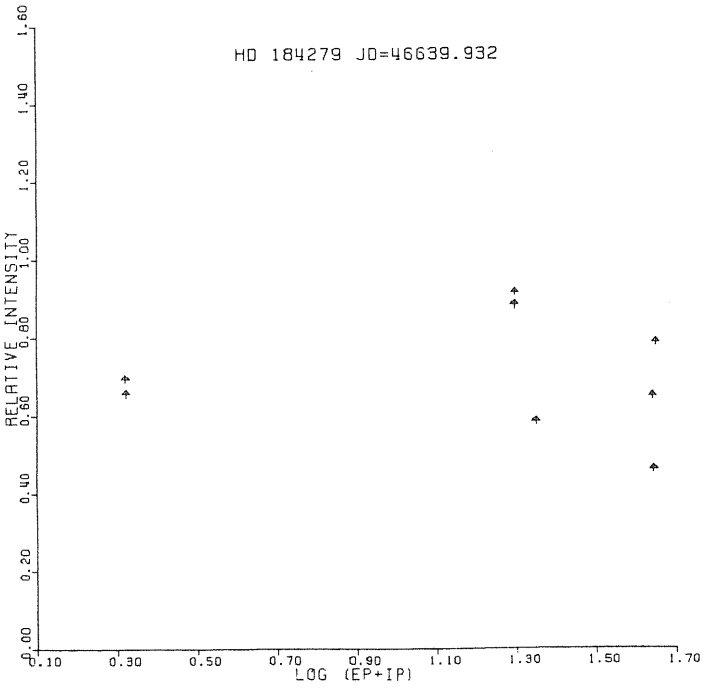

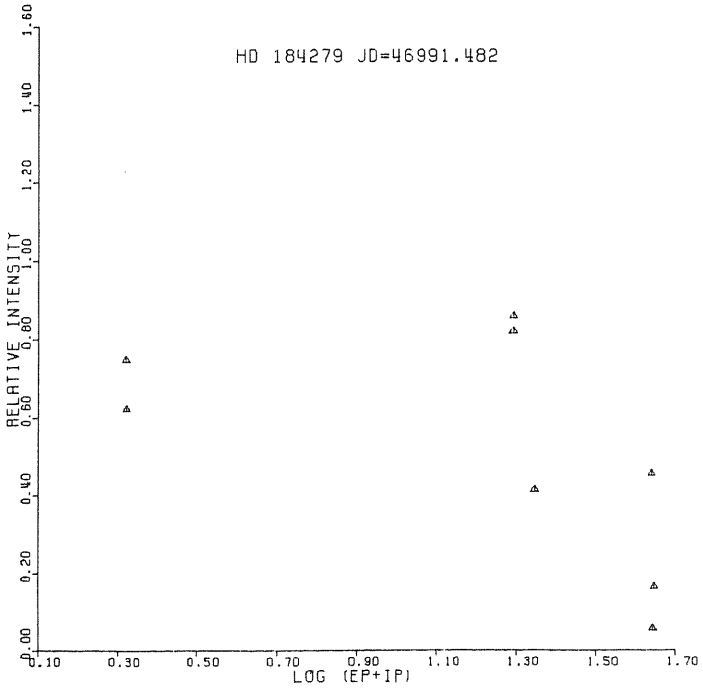

FIGURE III.1.2.13

FIGURE III.1.2.14

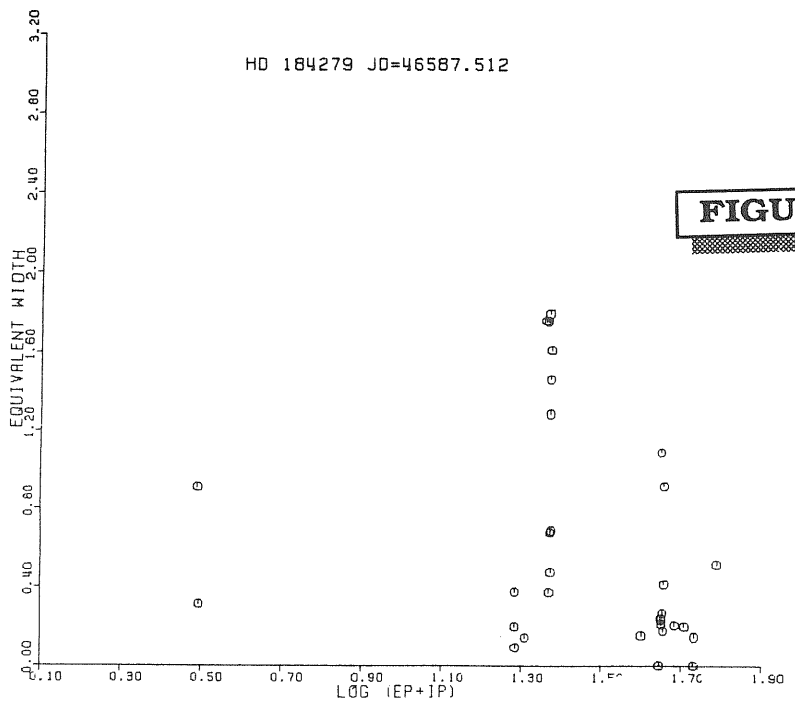

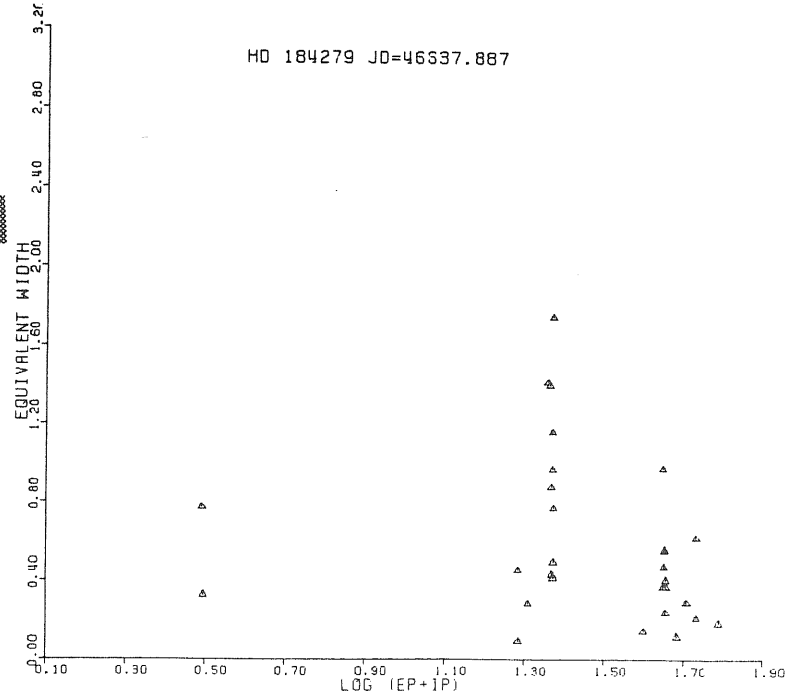

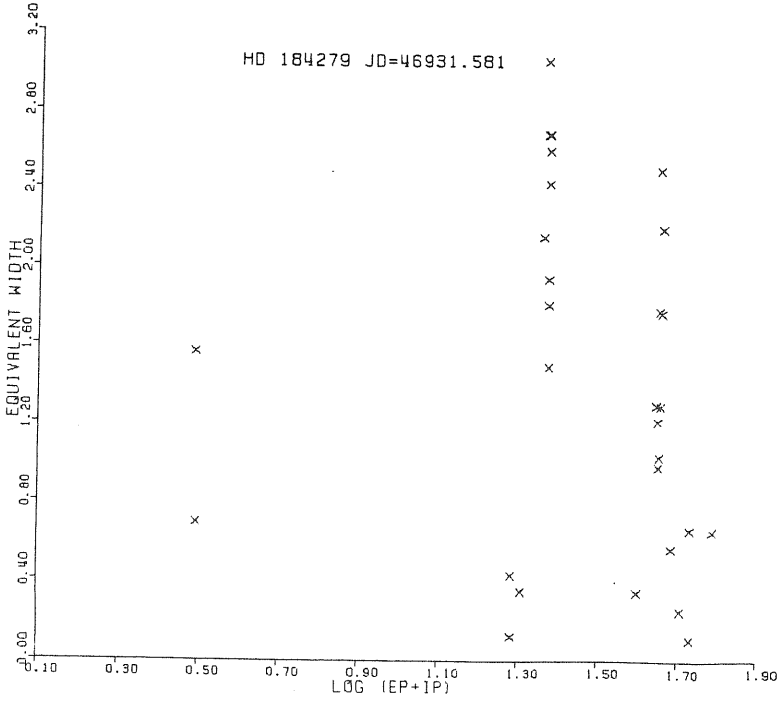

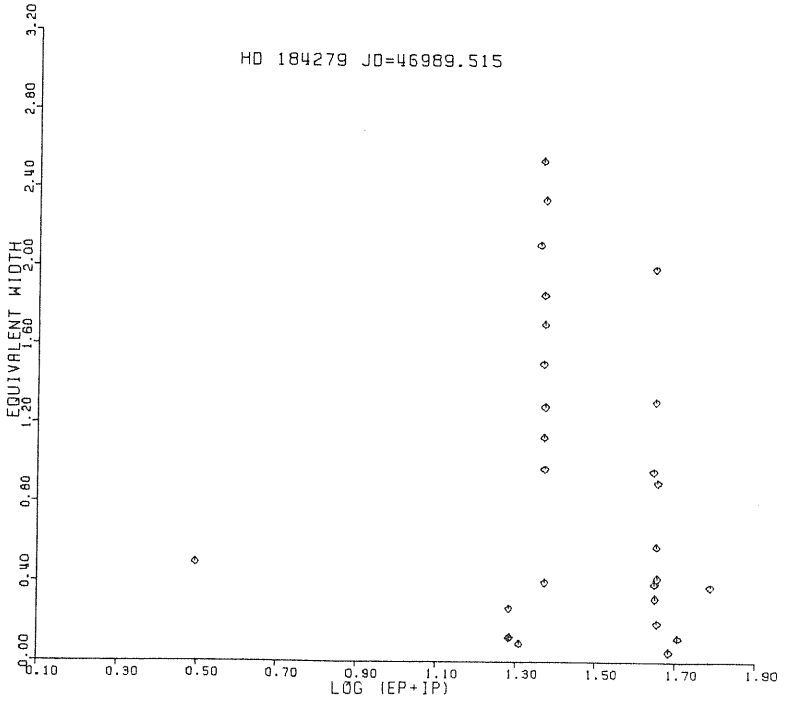

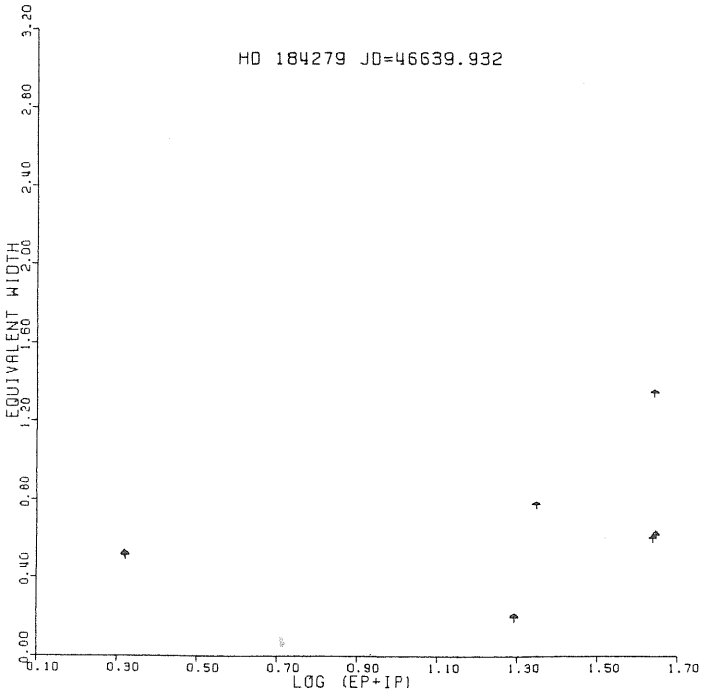

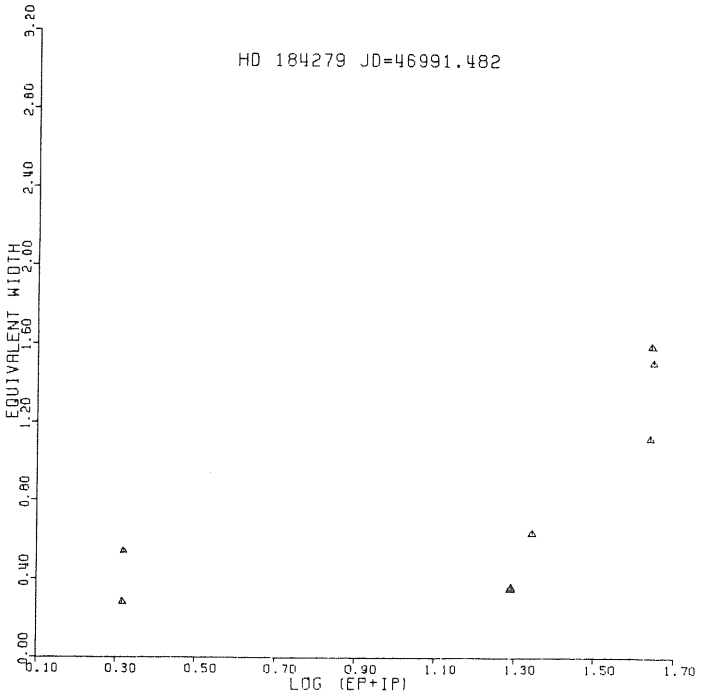

FIGURE III.1.2.15

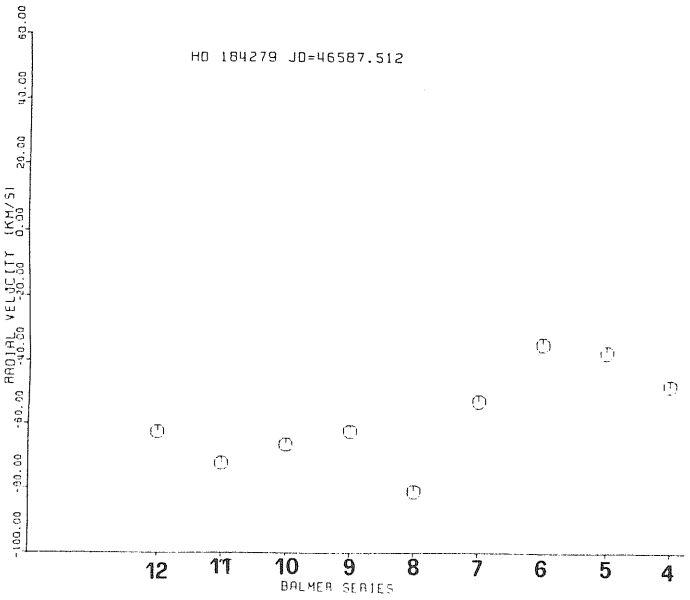

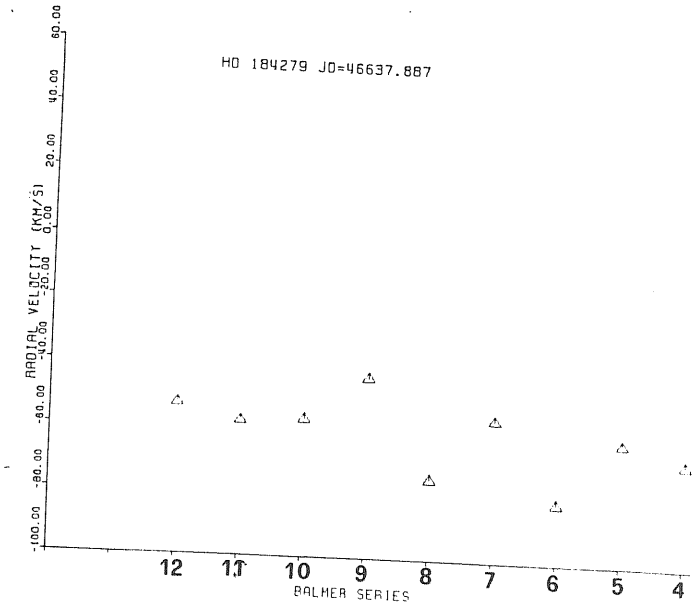

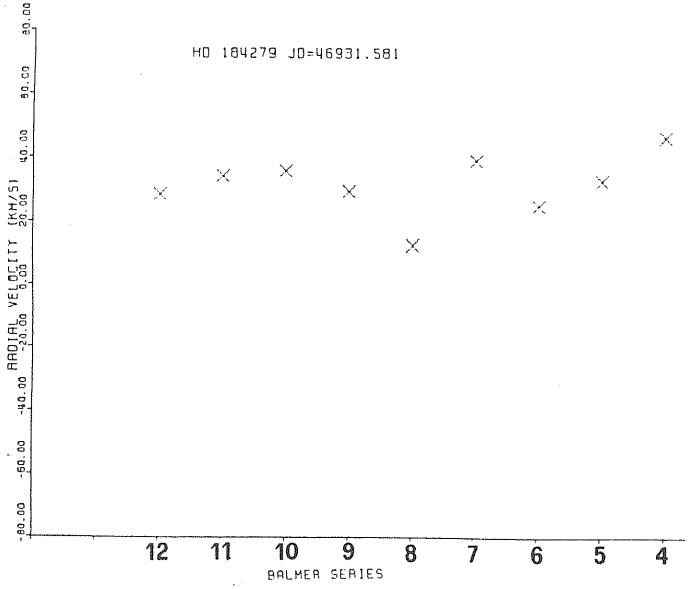

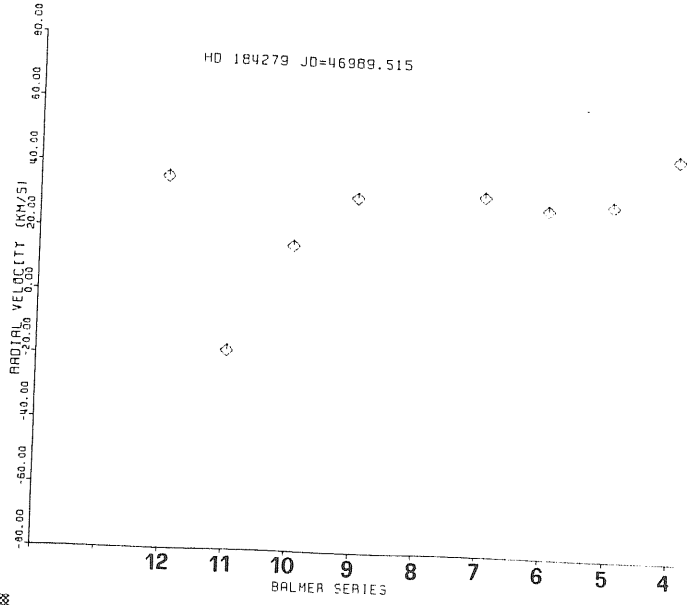

FIGURE III.1.2.16

Table III.1.2.1. Measured spectral line parameters of the absorption lines of HD 184279.

HD 184279			JD= 46587.512					JD= 46637.887					JD= 46931.581				
ELEMENT	MULT	λ(LAB)Å	λ(OBS)Å	Ic	FBWC(Å)	EQW(Å)	RV(km/s)	λ(OBS)Å	Ic	FBWC(Å)	EQW(Å)	RV(km/s)	λ(OBS)Å	Ic	FBWC(Å)	EQW(Å)	RV(km/s)
H 13	3	3734.4	3734.5	0.8	6.4	0.7	8.0	3734.2	0.7	5.3	0.8	-17.2	3735.1	0.5	6.0	1.5	55.3
H 12	2	3750.2	3749.4	0.7	3.5	0.5	-62.6	3749.5	0.7	3.4	0.5	-53.1	3750.5	0.4	6.3	1.8	28.4
H 11	2	3770.6	3769.7	0.7	12.0	1.6	-72.2	3769.9	0.7	2.8	0.4	-58.2	3771.1	0.4	6.9	1.9	33.9
H 10	2	3797.9	3797.1	0.7	4.7	0.7	-66.5	3797.2	0.6	5.0	1.0	-57.2	3798.4	0.4	7.5	2.4	35.8
H 9	2	3835.4	3834.6	0.7	8.6	1.5	-62.4	3834.8	0.6	8.1	1.8	-44.0	3835.8	0.3	7.5	2.6	29.6
H 8	2	3889.1	3888.0	0.8	3.1	1.3	-81.1	3888.1	0.2	3.1	1.2	-75.1	3889.2	0.1	6.0	2.7	12.7
Ca II	1	3933.7	3933.4	0.6	1.4	0.3	-19.3	3933.6	0.5	1.4	0.3	- 4.4	3933.7	0.5	3.0	0.7	- 1.3
He I	5	3964.7	3964.2	0.7	-	-	-37.0	3963.8	0.7	-	-	-66.7	3965.2	0.5	4.9	1.3	34.2
Ca II	1	3968.5	3968.4	0.5	3.5	0.9	- 3.0	3968.3	0.5	1.4	0.8	-11.9	3968.7	0.4	5.4	1.6	17.8
H eps	1	3970.1	3969.4	0.6	1.3	0.4	-53.1	3969.3	0.5	1.8	0.4	-56.0	3970.6	0.2	6.8	2.7	38.8
He I	55	4009.3	4009.4	0.9	6.3	0.4	7.6	4008.0	0.6	2.6	0.2	-93.6	4009.1	0.7	5.1	1.8	-10.0
He I	18	4026.$\frac{2}{4}$	4025.4	0.7	6.6	0.9	-73.5	4025.3	0.9	6.1	0.4	-82.6	4026.5	0.3	6.3	2.2	11.0
O II	10	4069.6	4068.4	0.9	2.8	0.2	-88.8	4068.6	0.9	3.0	0.2	-80.1	4069.3	0.8	1.3	0.1	-25.2
Si IV	1	4088.9	4088.7	0.9	2.8	0.2	-11.6	4087.8	0.8	3.6	0.3	-80.6	4089.6	0.8	2.7	0.3	54.6
H delta	1	4101.7	4101.3	0.9	6.8	1.8	-35.3	4100.6	0.7	5.2	0.9	-81.2	4102.1	0.1	6.2	2.7	24.9
He I	16	4120.8	4120.9	0.9	2.7	0.2	9.4	4120.7	0.8	4.4	0.5	- 7.8	4120.7	0.7	5.8	1.0	- 7.5
He I	53	4143.8	4143.4	0.9	2.4	0.2	-25.2	4142.9	0.8	4.1	0.4	-62.1	4144.2	0.6	6.1	1.3	28.7
H gamma	1	4340.5	4339.9	0.4	5.6	1.8	-37.8	4339.6	0.4	4.6	1.4	-62.2	4340.9	0.1	7.1	3.1	32.7
O II	16	4351.3	-	-	-	-	-	4350.3	0.8	5.6	0.6	-65.9	4349.9	0.7	5.7	0.7	-95.6
Fe III	4	4365.6	4365.5	0.9	1.6	0.1	- 2.3	4365.4	0.8	1.354	0.1	-10.2	4364.9	0.9	1.8	0.1	-48.0
He I	51	4387.9	4387.1	0.8	3.3	0.3	-56.8	4386.6	0.7	4.2	0.6	-89.0	4388.2	0.5	4.4	1.0	18.3
Fe III	4	4419.6	4419.1	0.8	3.8	0.4	-30.8	4419.1	0.8	3.6	0.5	-34.8	4419.9	0.7	2.9	0.4	19.8
Fe III	4	4431.0	4430.4	0.9	3.1	0.2	-35.1	-	-	-	-	-	-	-	-	-	-
He I	14	4471.5	4470.9	0.6	5.5	1.1	-35.9	4470.9	0.6	4.9	1.0	-41.3	4471.9	0.2	6.0	2.5	29.8
Mg II	4	4481.1	4481.3	0.9	2.9	0.1	11.1	4480.6	0.9	4.8	0.3	-33.6	4480.7	0.8	3.7	0.4	-28.4
Si III	2	4567.9	4567.8	0.9	3.1	0.2	- 7.1	4567.0	0.9	2.0	0.1	-58.6	4568.0	0.8	3.7	0.4	5.8
O II	1	4638.9	4639.1	0.9	3.0	0.2	18.3	4638.8	0.9	1.9	0.1	- 4.5	4639.3	0.8	6.0	0.6	5.9
C III	1	4650.2	4650.8	0.8	5.4	0.5	42.8	4650.3	0.0	1.9	0.2	9.9	4649.5	0.7	4.7	0.7	-40.7
He I		4713.4	4712.5	0.8	2.9	0.2	-55.6	4713.4	0.8	4.2	0.4	2.4	4713.3	0.5	5.1	1.2	- 7.5
H beta		4861.3	4860.6	0.3	4.6	1.8	-48.3	4860.2	0.3	4.2	1.4	-67.7	4862.1	0.1	4.9	2.2	46.0
He I		4921.9	4921.5	0.8	1.9	0.2	-29.2	4920.8	0.7	3.1	0.6	-67.4	4922.3	0.4	6.2	1.8	21.0

Table III.1.2.1.(continued)

HD 184279 JD= 46989.515

ELEMENT	MULT.	λ(LAB)Å	λ(OBS.)Å	Ic	FBW(Å)	EQW(Å)	RV(km/s)
H 13	3	3734.4	3734.5	0.7	3.1	0.4	7.5
H 12	2	3750.2	3750.6	0.6	4.7	1.0	35.7
H 11	2	3770.6	3770.4	0.5	5.4	1.3	-17.9
H 10	2	3797.9	3798.1	0.4	3.9	1.1	15.0
H 9	2	3835.4	3835.8	0.3	5.0	1.7	30.2
H 8	2	3889.1	3888.5	0.5	5.0	2.3	-46.1
Ca II	1	3933.7	3933.6	0.6	2.2	0.5	-4.5
He I	5	3964.7	3965.2	0.5	4.2	1.0	35.5
Ca II	1	3968.5	3968.3	0.5	-	-	-12.6
H eps	1	3970.1	3970.5	0.2	4.6	1.9	31.7
He I	55	4009.3	4008.1	0.8	2.5	0.2	-85.1
He I	18	4026.$^{2}_{4}$	4026.6	0.5	3.4	0.9	15.2
O II	10	4069.6	-	-	-	-	-
Si IV	1	4088.9	4088.7	0.9	1.7	0.1	-11.1
H delta	1	4101.7	4102.7	0.2	3.6	1.5	28.3
He I	16	4120.8	4120.0	0.8	2.6	0.3	-58.9
He I	53	4143.8	4143.5	0.7	3.2	0.4	-20.5
H gamma	1	4340.5	4340.9	0.1	5.8	2.5	29.9
O II	16	4351.3	-	-	-	-	-
Fe III	4	4365.6	4365.6	0.9	2.1	0.1	4.3
He I	51	4387.9	4387.2	0.7	3.3	0.6	-50.6
Fe III	4	4419.6	4418.9	0.8	2.6	0.3	-49.4
Fe III	4	4431.0	4430.8	0.9	1.7	0.1	-7.7
He I	14	4471.5	4471.8	0.2	5.1	2.0	21.8
Mg II	4	4481.1	4480.6	0.9	1.5	0.1	-36.8
Si III	2	4567.9	-	-	-	-	-
O II	1	4638.9	4639.1	1.0	2.5	0.1	15.8
C III	1	4650.2	4651.1	0.9	2.0	0.4	37.5
He I		4713.2	4713.7	0.7	2.7	0.4	22.9
H beta		4861.3	4862.1	0.1	4.7	2.1	44.9
He I		4921.9	4922.3	0.4	4.5	1.3	22.4

HD 184279 JD= 46639.932 JD= 46991.482

ELEMENT	MVLT.	λ(LAB)Å	λ(OBS.)Å	Ic	FBWC(Å)	EQWCÅ	RV(km/s)	λ(OBS)Å	Ic	FBWC(Å)	EQW(Å)	RV(km/s)
He I	4	5015.7	5014.9	0.7	3.4	0.6	-43.9	5016.1	0.5	4.1	1.1	26.3
Fe III	5	5127.3	5126.4	0.9	4.5	0.2	-52.7	5127.7	0.9	5.0	0.4	23.0
Fe III	5	5156.0	5155.1	0.9	3.4	0.2	-54.8	5126.7	0.8	3.8	0.4	42.2
He I	11	5875.7	5874.6	0.5	5.8	1.3	-54.2	5876.4	0.1	3.4	1.6	39.1
Na I	1	5890.0	5889.8	0.7	3.0	0.5	-5.5	5889.9	0.6	2.9	0.5	-5.2
Na I	1	5895.9	5895.8	0.7	3.4	0.5	-4.1	5895.6	0.8	2.2	0.3	-17.5
	1	6562.8	6561.7	0.6	3.5	0.7	-53.5	6563.8	0.4	2.2	0.6	45.8
He I	46	6678.2	6676.6	0.8	5.8	0.6	-68.4	6679.0	0.2	3.6	1.5	37.8

III.1.3.HD 183656

Figure III.1.3.1 presents observed H alpha profiles of HD 183656.All of them were double-peak emission with a central absorption.It is clearly seen from the figure that R/V changes occurred in the emission components.Also intensities and radial velocities of the central absorption components were variable.Measured spectral parameters for H alpha are given in Table III.1.3.1. H beta profiles of the HD 183656 are presented in Figure III.1.3.2.The general structure of the profiles were similar to each other; they were composed of a wide stellar component and a narrow central absorption , variable with time. Figures III.1.3.3 to III.1.3.5 present H gamma, H delta and H epsilon profiles respectively, which were similar to H beta in structure and in variation.

HD 183656 presented a rich shell spectrum with a time variation in profiles of the lines.This rich spectrum can be seen through the figures III.1.3.6 to III.1.3.12.The lines which are presented in these figures are listed in figure captions.Table III.1.3.2 presents the measured spectral parameters of the lines of HD 183656.

Now let's give a close look to this part of the spectra.We remark here at JD=584.6 large profile change of Ti II 4300 probably a defect on the spectrogram, because the similar variation cannot be seen on the other lines of the same multiplet.As seen from the figures the shell was always present during the observation period.But it's intensity

slightly diminished at JD=640.9.All the lines exhibited small but systematic variations in the radial velocities and in equivalent widths which we will analyze later.Fe II 4384 at JD=584.6, and at JD=929.6 presented a shell component superimposed a stellar profile. Also Fe II ' 4923 presented notable changes in the half-widths.Profile changes were more evident in the red part of the spectra.,.i.e. Fe II 6330,5169,5018 and Si II 6347.Emission wing at JD=930.6 for Fe II 5018, variable asymmetry for Fe II 4923 were interesting characteristics of this part of the spectra.

Last visible Balmer line was about n=30 and shell effect was seen after n=10.Figure III.1.3.13 gives the plot of the RV measurements versus log (EP+IP) for blue spectra.Between JD=584.6 to 640.9 there was a slight decrease in the RV of Ca II ,metals and H lines although RV of He I increased and was positive. At JD=930.5 the RVs of Ca II lines were sligthly increased, while those of Fe II and H lines were decreased; also He I increased more than its previous value.At JD=989.6 all the lines presented a decrease in their RV including He I.Figure III.1.3.14 presents the same parameters for the red spectra.At JD=640.5 the velocities were negative and 0 and -25 km/s.At JD=930.6 Na I lines and H lines remained at their previous values, while Fe II lines exhibited a slight increase in their RV.At JD=990.5 all the measured RV were diminished from their previous values.Figure III.1.3.15 presents measured relative intensities versus log(EP+IP) for

blue spectra.At JD=640.9 the relative intensities slightly increased for all lines i.e.the central depths of the narrow shell components were decreased, compared with the JD=584.6 with the exception CaII. At JD=930.5 Ca II lines increased in relative intensity,Ti II ,He I, and Fe II lines were decreased although H lines remained unchanged.At JD=989.6 Ca II and H lines showed a big decrease in relative intensities while Si II and He I lines increased slightly.For the red spectra, at JD=930.6 Na I and Si II lines remained about at their previous values, Fe II decreased and H lines were slightly increased compared with JD=640.5.At JD=990.5 Na I and H lines didn't changed but Fe II, and Si II increased (Figure III.1.3.16)

Equivalent widths for the same observation nights for the blue spectra are presented in Figure III.1.3.17.At JD=640.9 H lines were at their maximum values. Then at JD=989.6 while Ca II, H and He I EQWs were decreasing, Ti II remained constant and Fe II slightly increased.At JD=930.5 EQWs of Fe II remained constant although Ca II ,Ti II and He I lines increased substantially, and H increased slightly.For the red part of the spectra EQWs of Na I and Si II remained at their previous values, Fe II increased , H alpha and H beta decreased at JD=930.6 compared with JD=640.5.At JD=990.6, while Na I lines remained constant Fe II ,Si II and H alpha decreased but H beta increased (Figure III.1.3.18).

Figure III.1.3.19 presents plots of RVs of Balmer lines versus n quantum number.At JD=584.6 there was no progression

but at JD=640.9 a slight Balmer progression was observed.At JD=930.5 all of the RVs were negative, specially higher members of the serie were more negative than first members (inverse progression).At JD=989.6 RVs of the Balmer lines were more negative than the previous ones with a slight inverse progression.

Ringuelet and Sahade (1981) had published spectroscopic observations of this star as we mentioned before.We want to compare their observations with ours before concluding the description of the visual spectral results of HD 183656. Shell spectrum which was displayed by HD 183656 in this research was very similar to their observed spectra as richness of the metallic shell lines.One important difference can be noted as we didn't observed any other absorption components rather than the narrow shell components for the H lines (n > 8), Fe II multiplets 38 and 74, Ca II and Na I as their observations indicate.

Ringuelet and Sahade (1981) interpreted the H alpha emission profile of HD 183656 as being composed from two superimposed emission profiles.(1)The wings of the profile (1.0< r <1.25) where r is the relative intensity, could be understood as a flat and very broad emission ,(2) the central part of the profile (1.25< r <1.55) could be interpreted as being the central part of a strong, narrow emission that had an estimated total width of 540 km/s.The ratio of the central intensities of the two emissions that they had described

appeared to be on the order of 1:4.They have concluded that H emission originated in two different layers of the envelope where the "flat broad emission" formed outside the region responsible for the "strong narrow emission". As a reason for this the outer layers of the envelope appeared to be an expanding formation so the center of the narrow emission should be displaced towards the red, relative to the broad feature, as it was observed by them. The same researchers (1984)observed HD 183656 again with similar double-peak absorption components in H lines.

Table and Figure captions.

Figure III.1.3.1.H alpha profiles of HD 183656.Same as Figure III.1.1.1, only difference is every interval on the "y" axis corresponds to 0.2 continuum units.

Figure III.1.3.2.H beta profiles of HD 183656.Same as previous figure.

Figure III.1.3.3.H gamma profiles of HD 183656.Same as previous figure.

Figure III.1.3.4.H delta profiles of HD 183656.Same as previous figure.

Figure III.1.3.5.H epsilon profiles of HD 183656.Same as previous figure.

Figure III.1.3.6.Ti II 4025,4300,4301,4307,4312,4314,Fe II 4303 lines of HD 183656.

Figure III.1.3.7.Si II 4128,4130, Fe II 4173,4178 lines of HD 183656.

Figure III.1.3.8.Ti II 4468,4520,4533,4563,4571,Fe II 4498,4491,4508,4515,4522,4555,4558,4576,4583 ,Cr II 4588 lines of HD 183656.

Figure III.1.3.9.Fe II 4923,4384,Ti II 4395 lines of HD 183656.

Figure III.1.3.10.Ti II 3900,3913, Fe II 3906,Ca II 3933, Fe II 6330, 6347 lines of HD 183656.

Figure III.1.3.11.Fe II 5018,4923 lines of HD 183656.

Figure III.1.3.12.Na I 5890,5895, Fe II 5169,5197 lines of HD 183656.

Figure III.1.3.13.RV's versus log(EP+IP) for blue spectra.Typical log(EP+IP) values for the group of lines are the following:H I=(1.373-1.358), He I=(1.648), Mg II=(1.309), Ti II=(0.305, 0.696-0.733), Ca II=(0.496-0.492), Fe II=(0.901-0.945), Si II=(1.258-1.353), Na I=(0.322-0.320),H alpha=1.346.

Figure III.1.3.14.Same as previous figure for red spectra.

Figure III.1.3.15.Relative intensities versus log(EP+IP) of HD 183656 for blue spectra.

Figure III.1.3.16.Relative intensities versus log(EP+IP) of HD 183656 for red spectra.

Figure III.1.3.17.EQW's versus log(EP+IP) of HD 183656 for blue spectra.

Figure III.1.3.18.Same as previous figure but for red spectra.

Figure III.1.3.19.RV's of Balmer lines versus "n" quantum numbers.

Table III.1.3.1.Measured spectral line parameters of H alpha emission components of HD 183656.

Table III.1.3.2.Measured spectral line parameters of absorption lines of HD 183656.

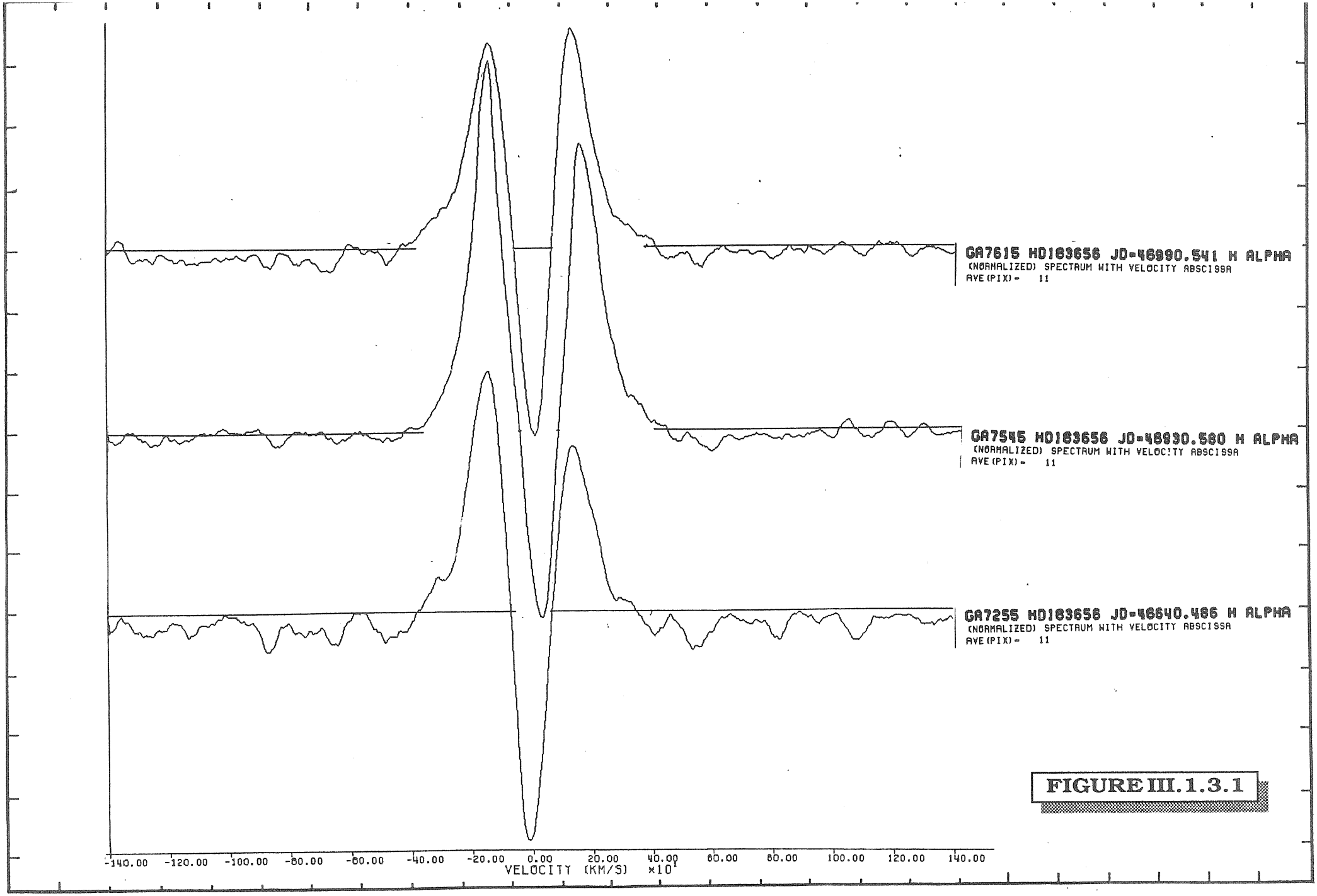

FIGURE III.1.3.1

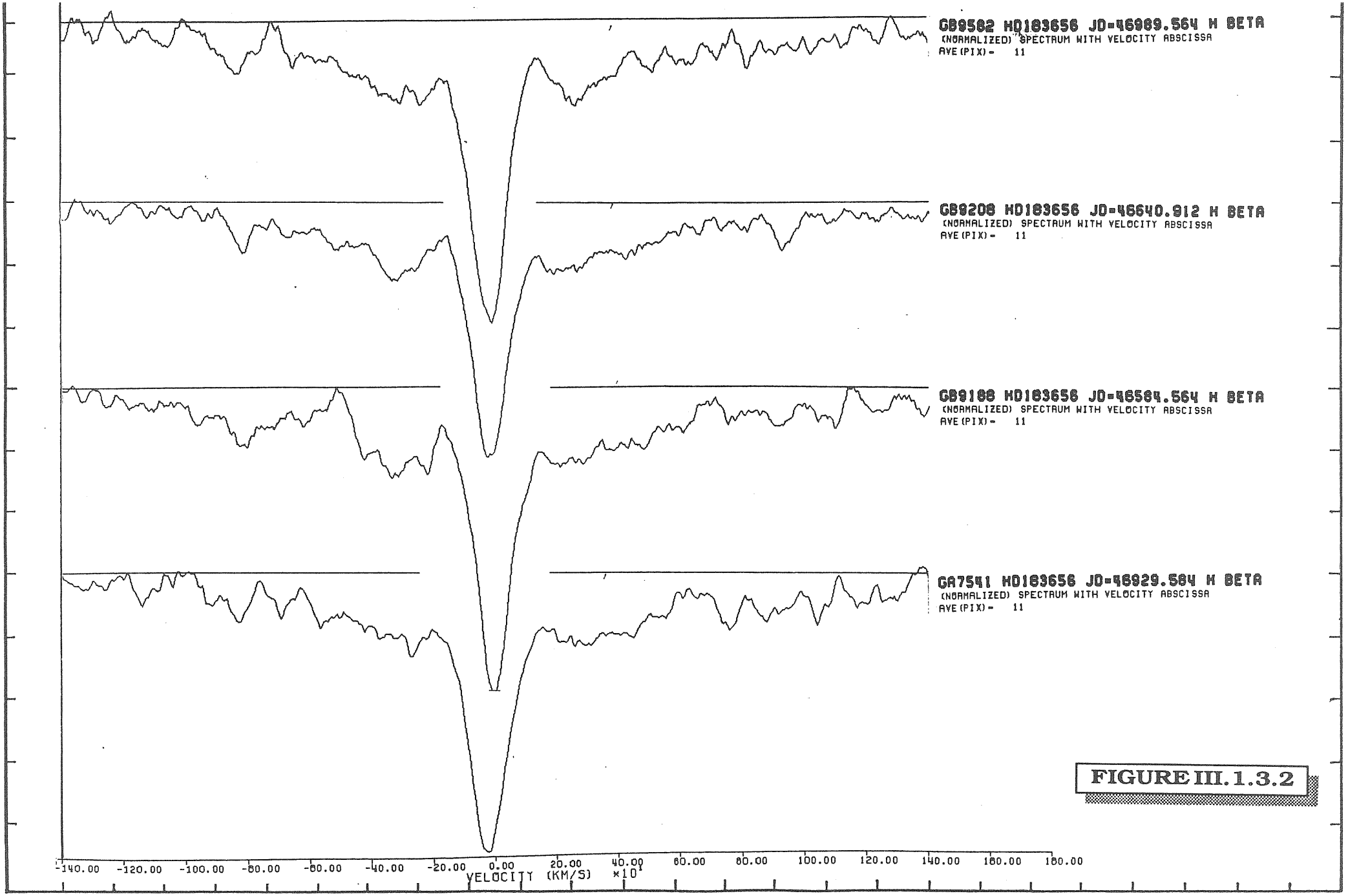

FIGURE III.1.3.2

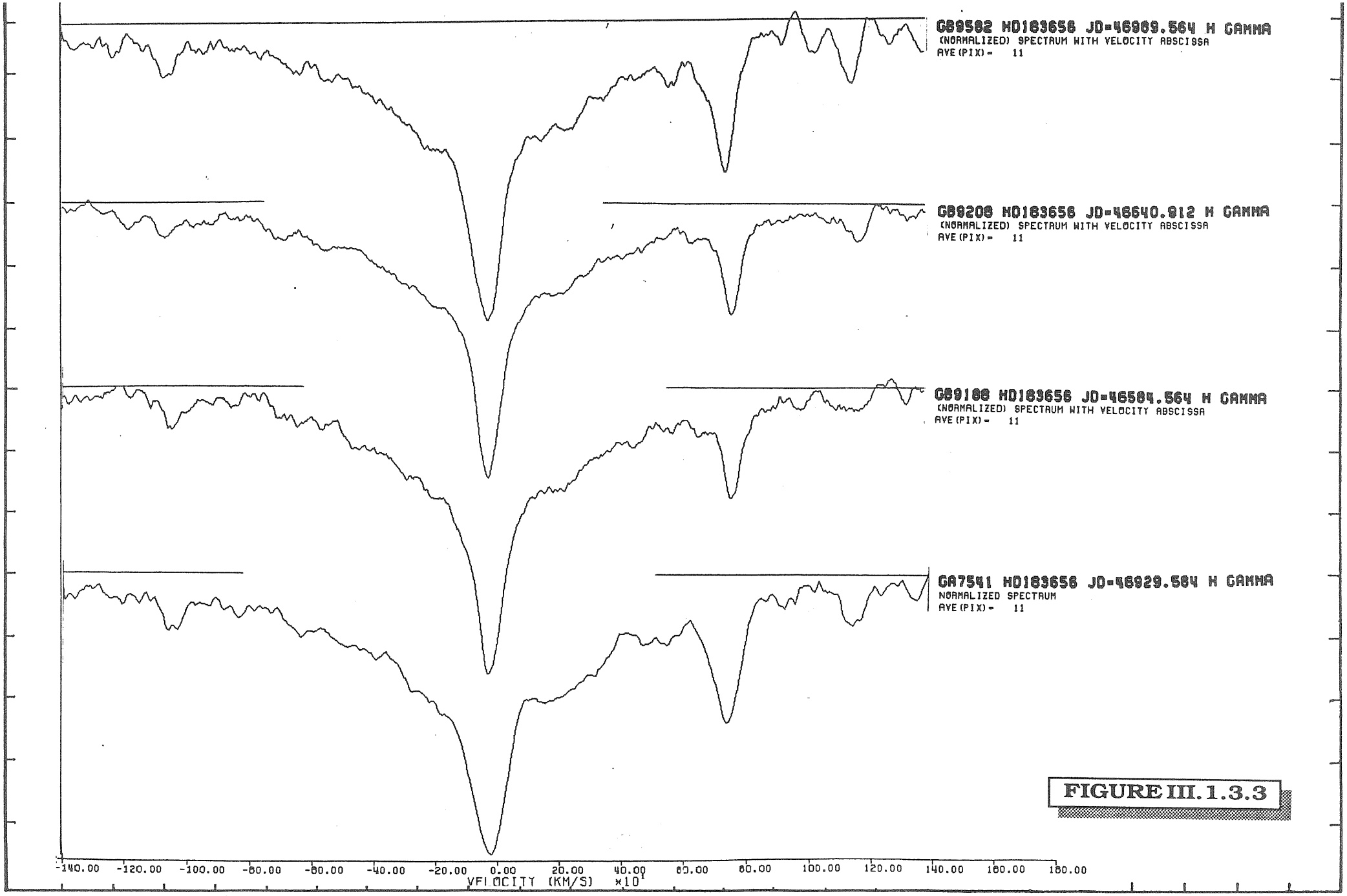

FIGURE III.1.3.3

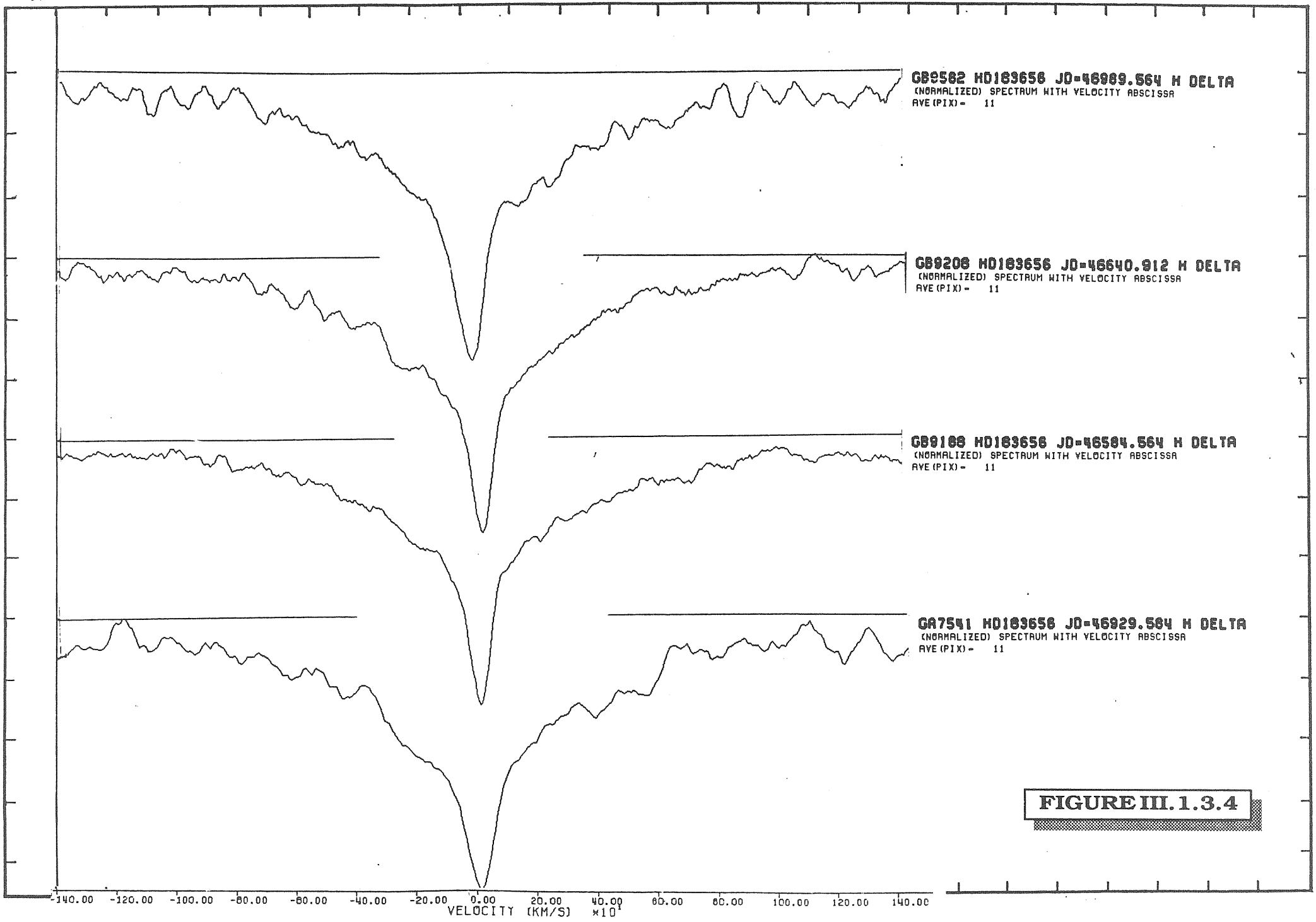

FIGURE III.1.3.4

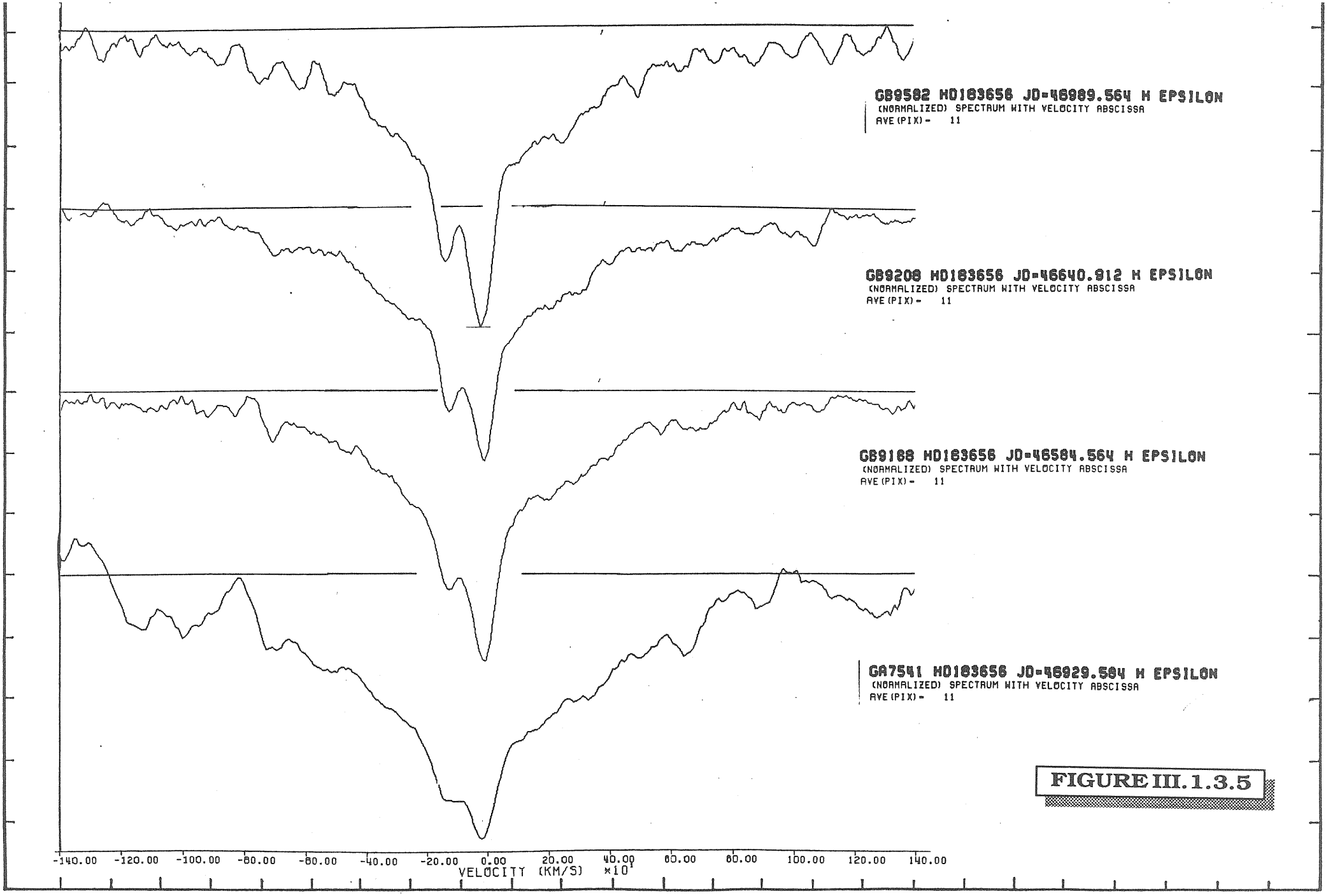

FIGURE III.1.3.5

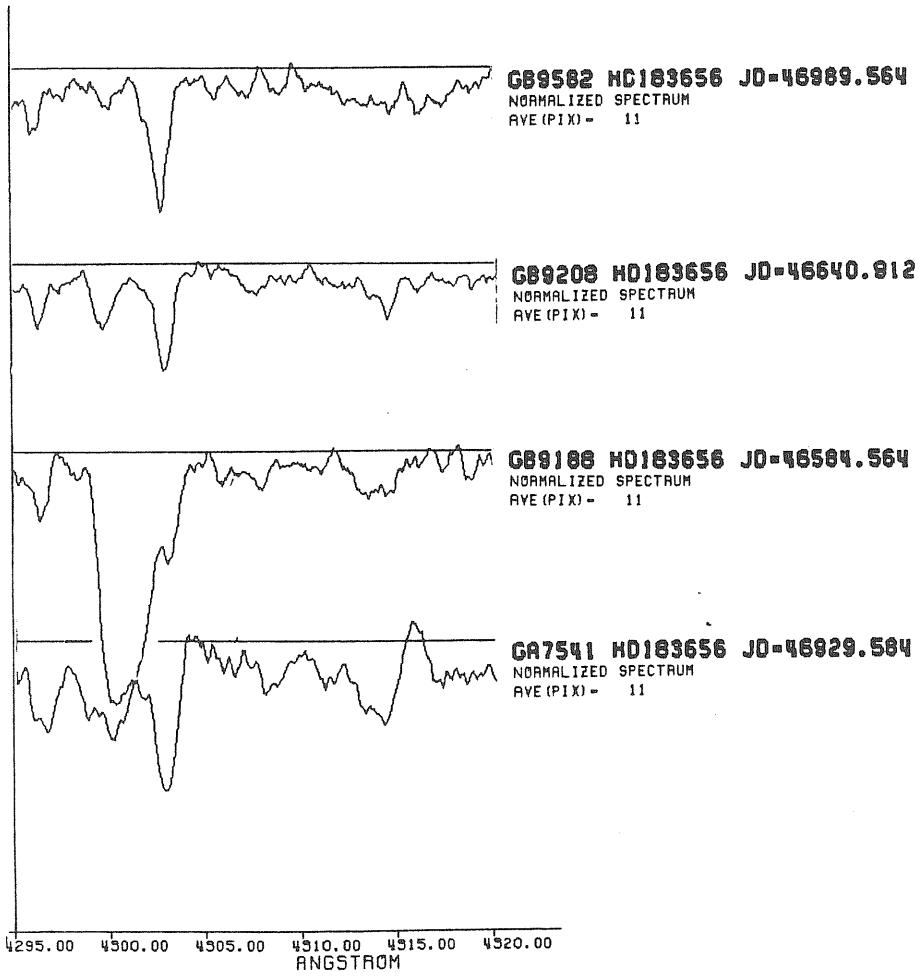

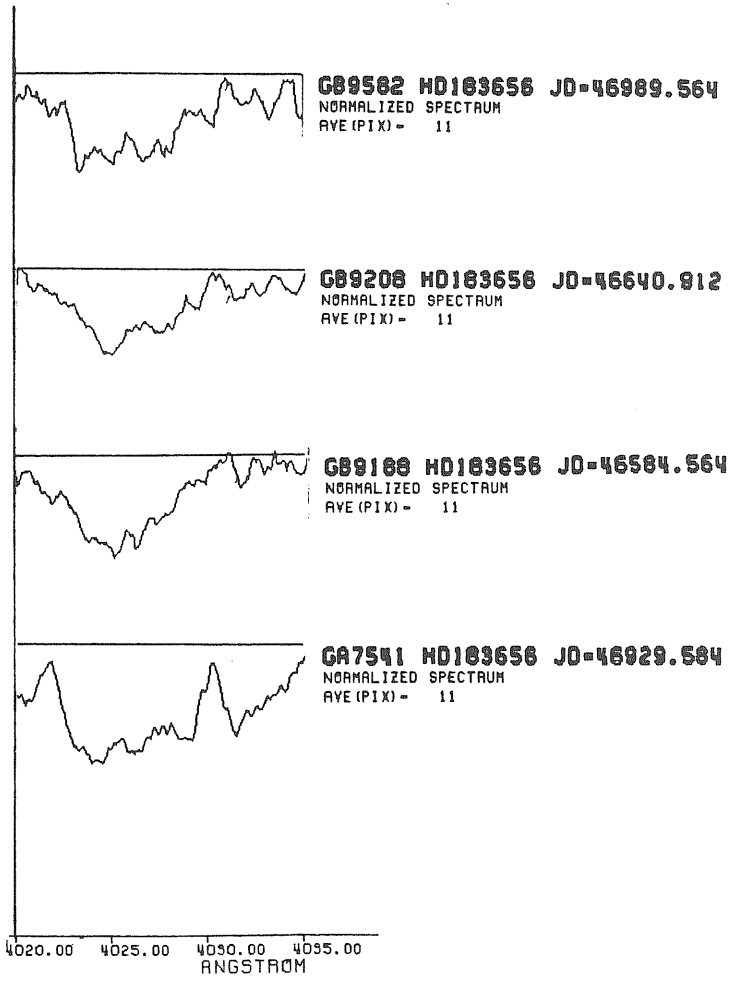

FIGURE III.1.3.6

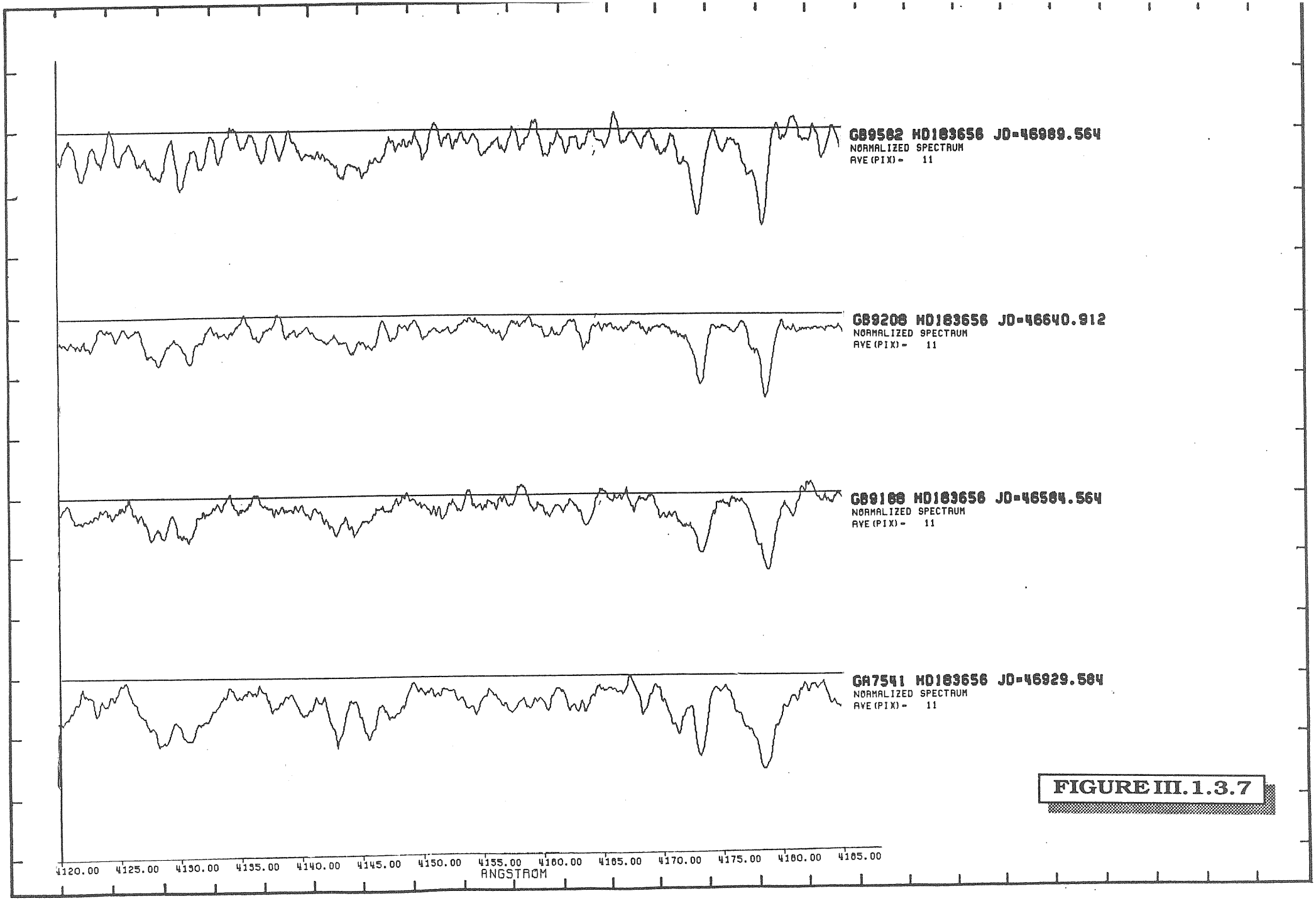

FIGURE III.1.3.7

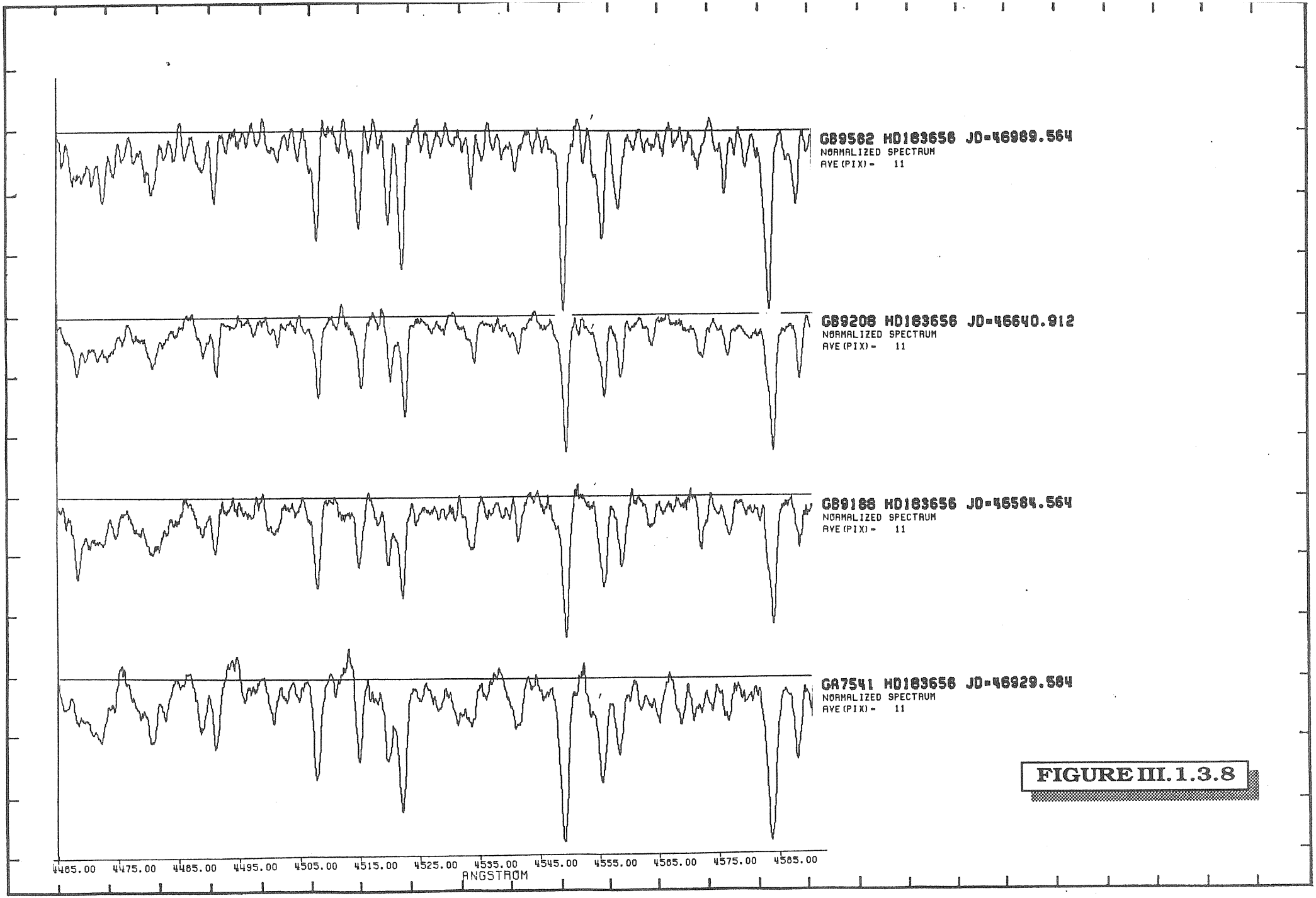

FIGURE III.1.3.8

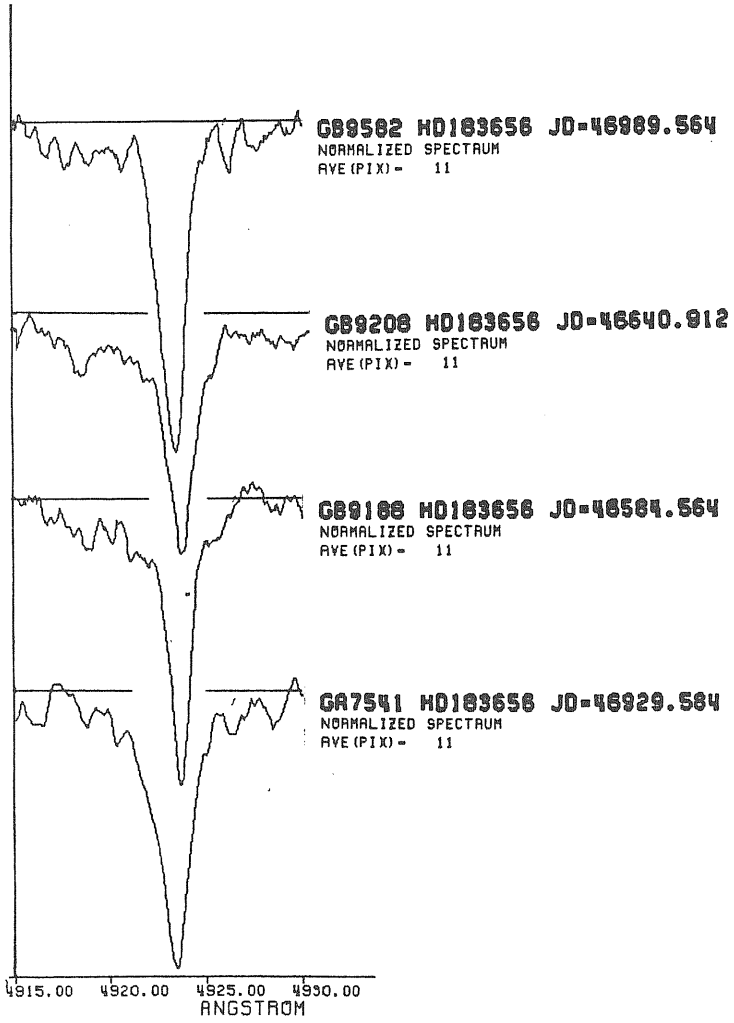

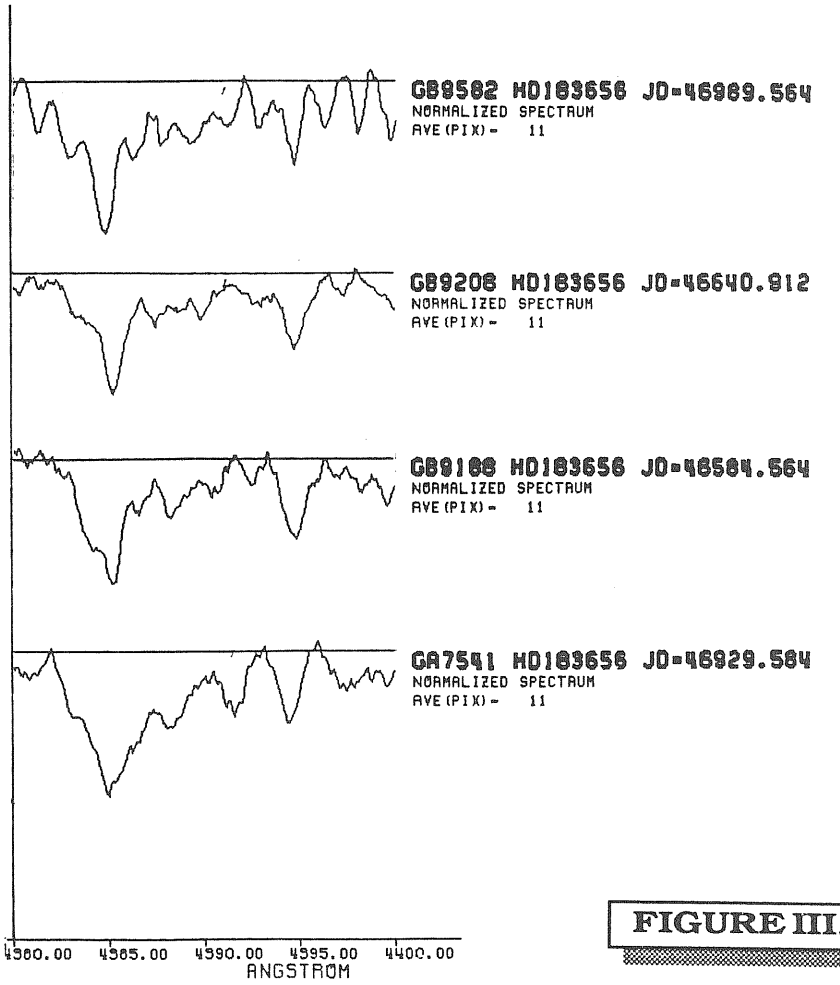

FIGURE III.1.3.9

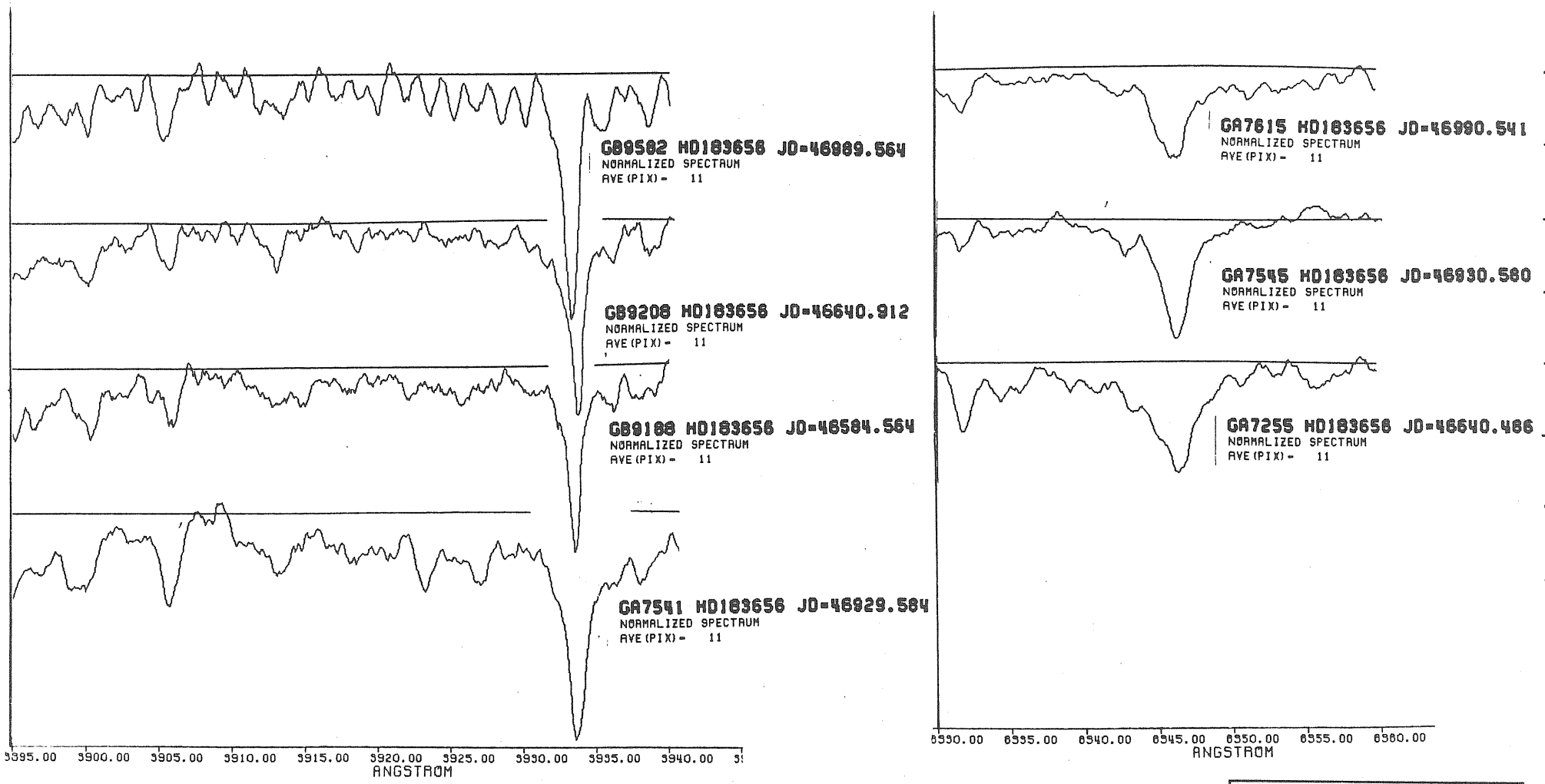

FIGURE III.1.3.10

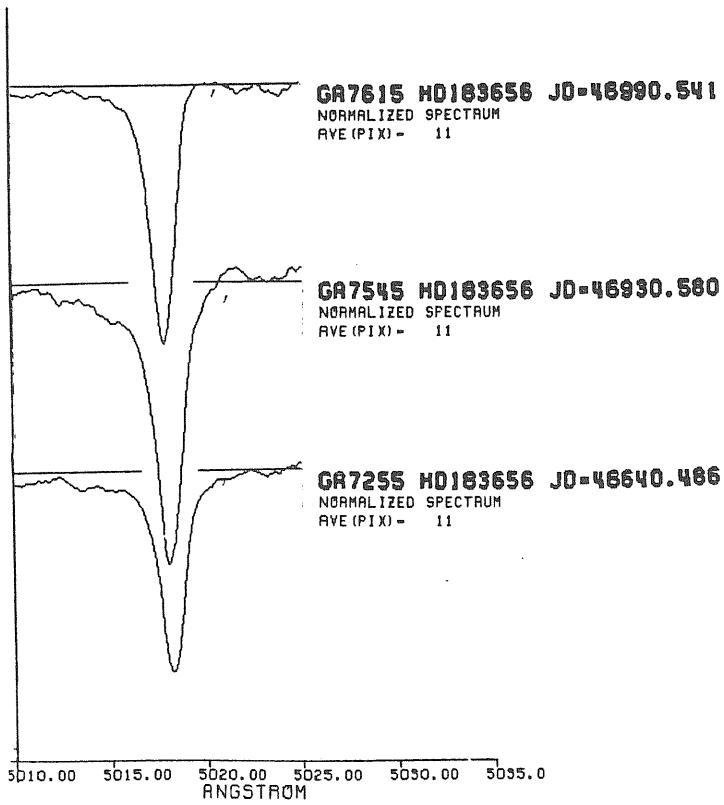

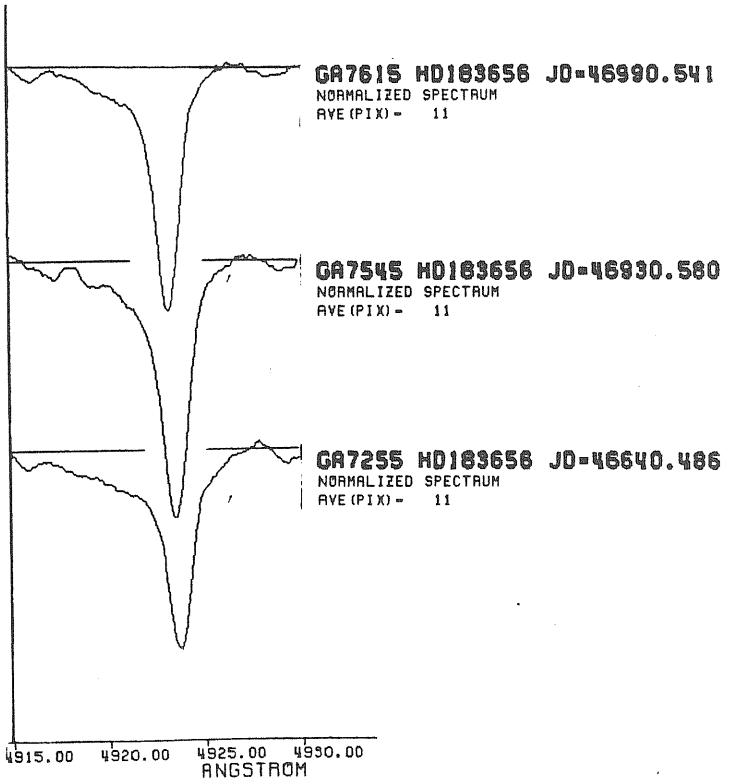

FIGURE III.1.3.11

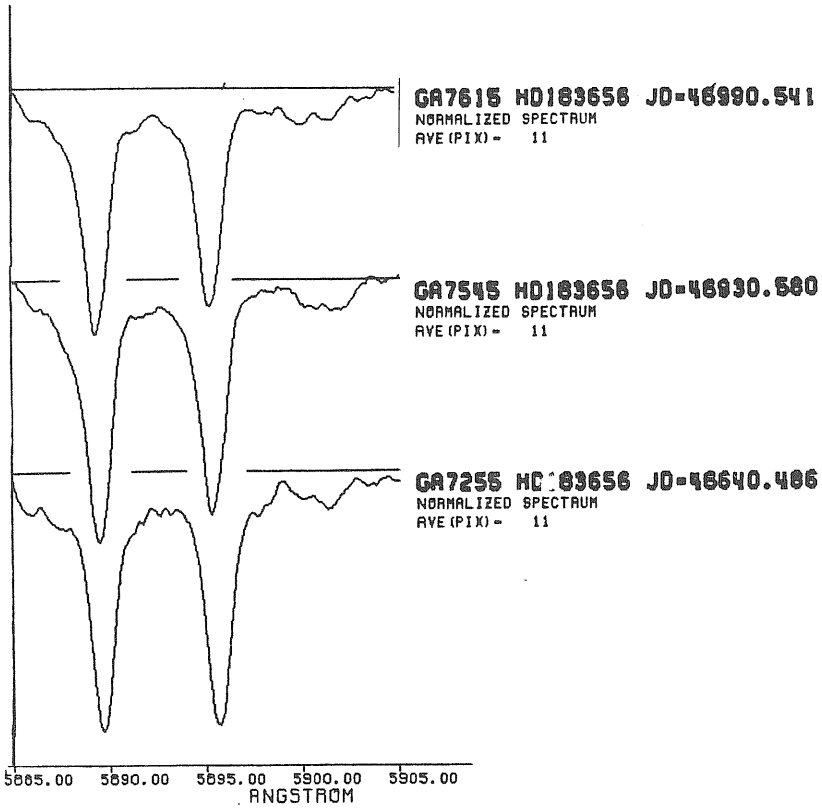

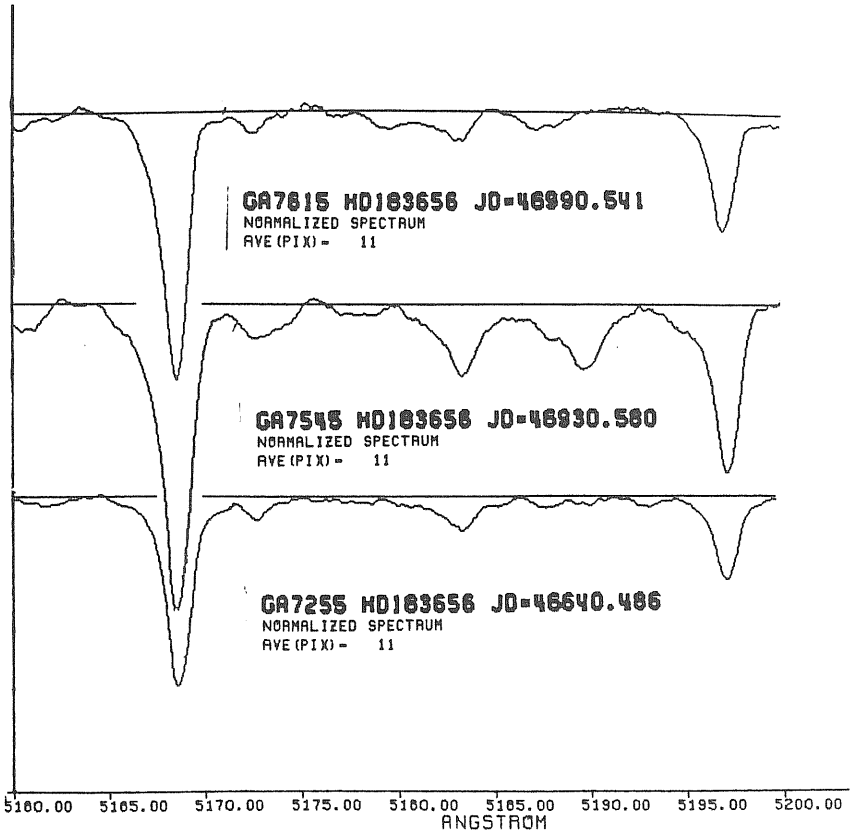

FIGURE III.1.3.12

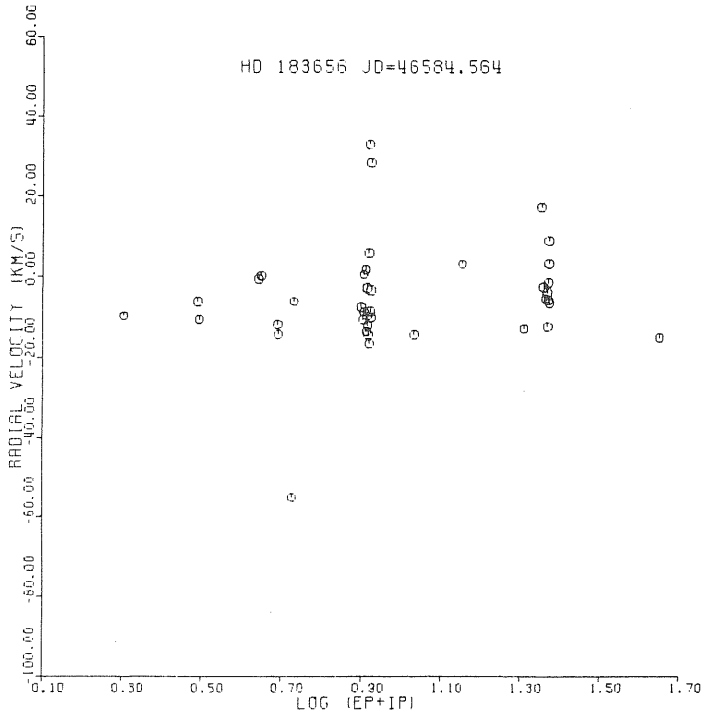

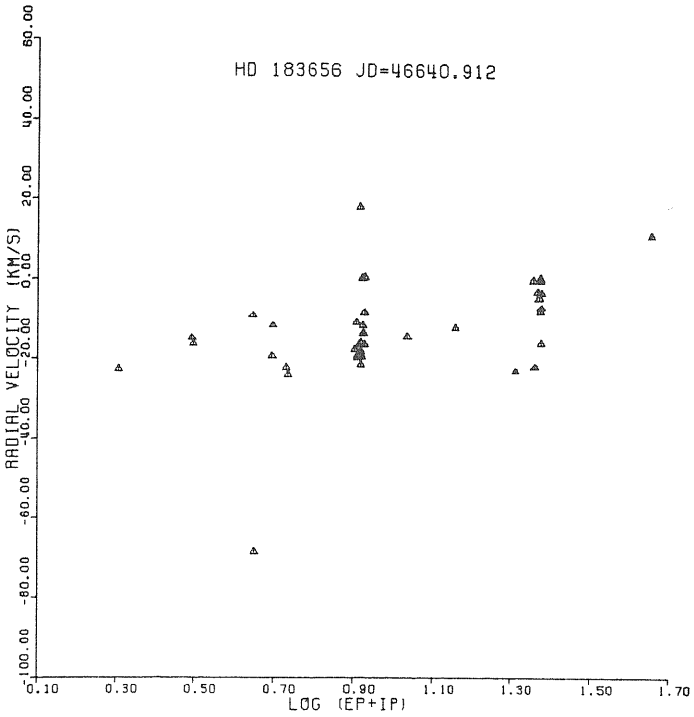

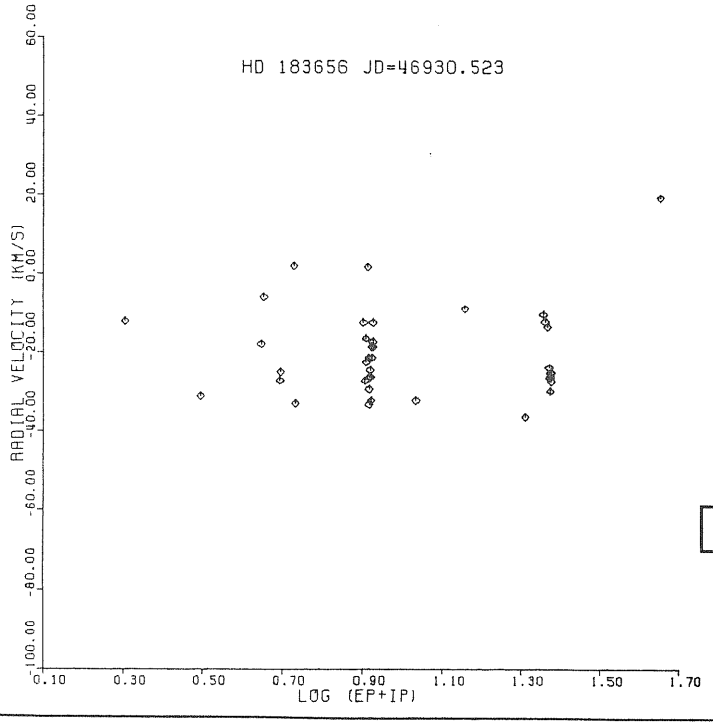

FIGURE III.1.3.13

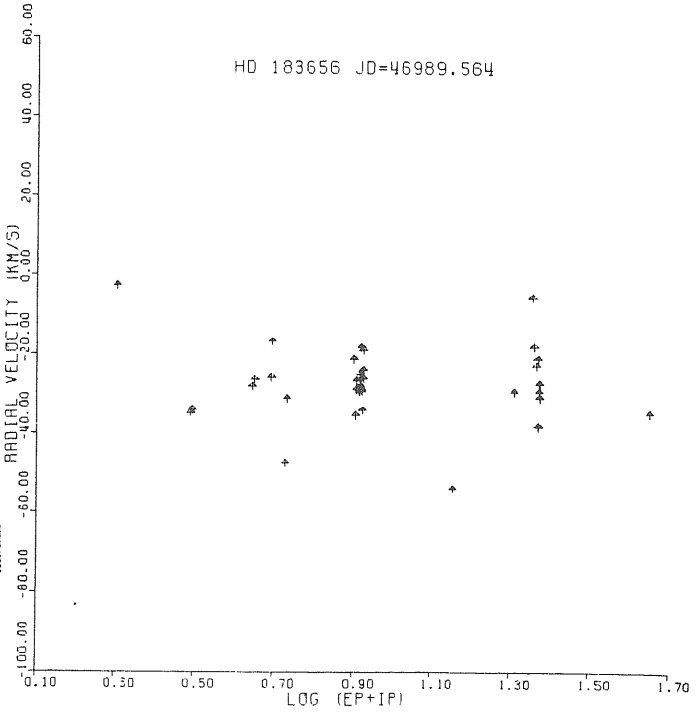

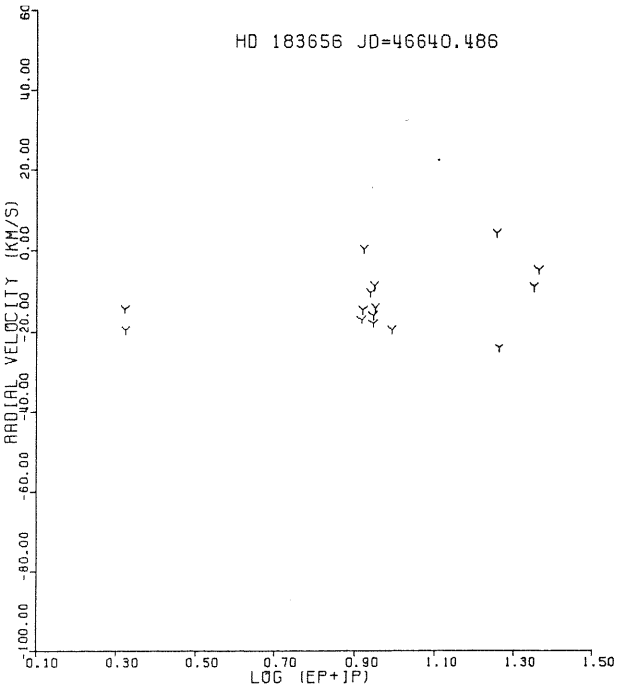

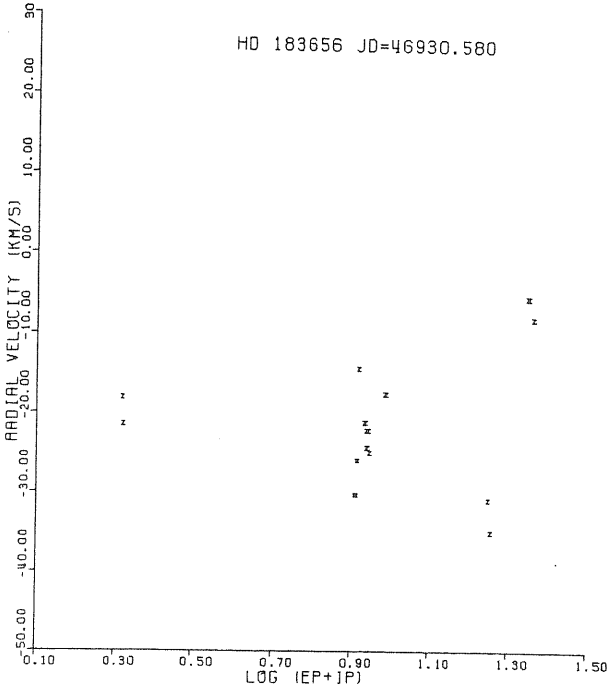

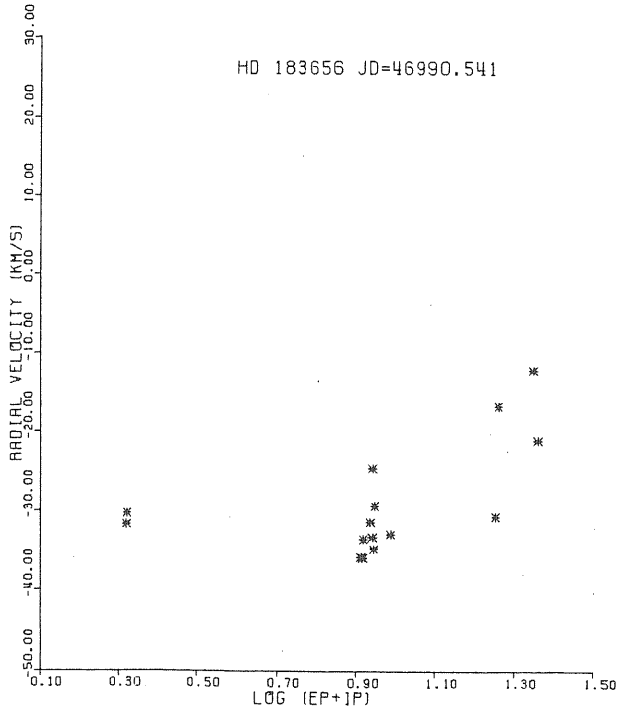

FIGURE III.1.3.14

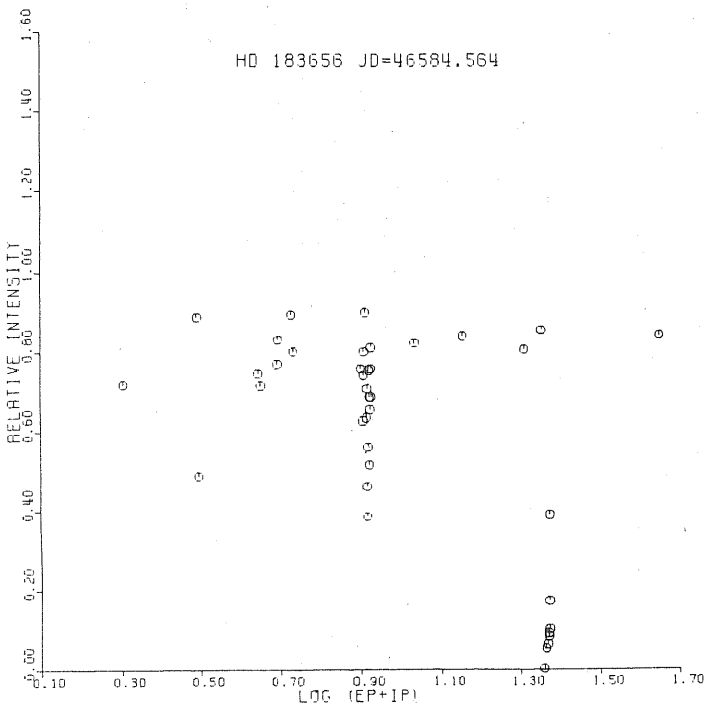

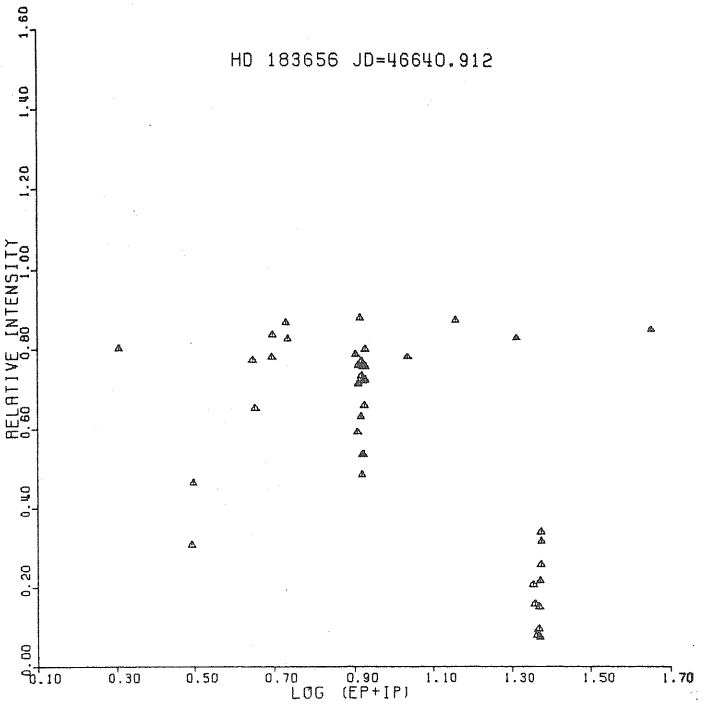

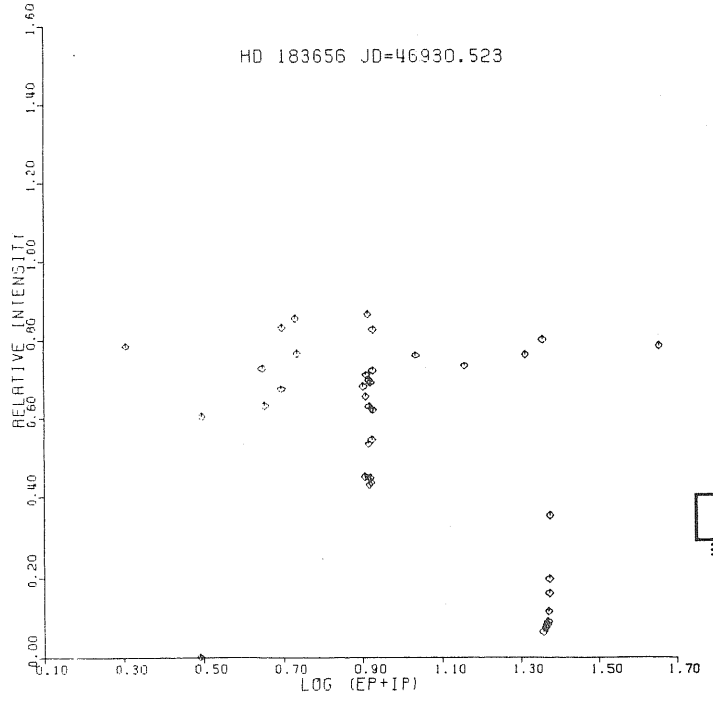

FIGURE III.1.3.15

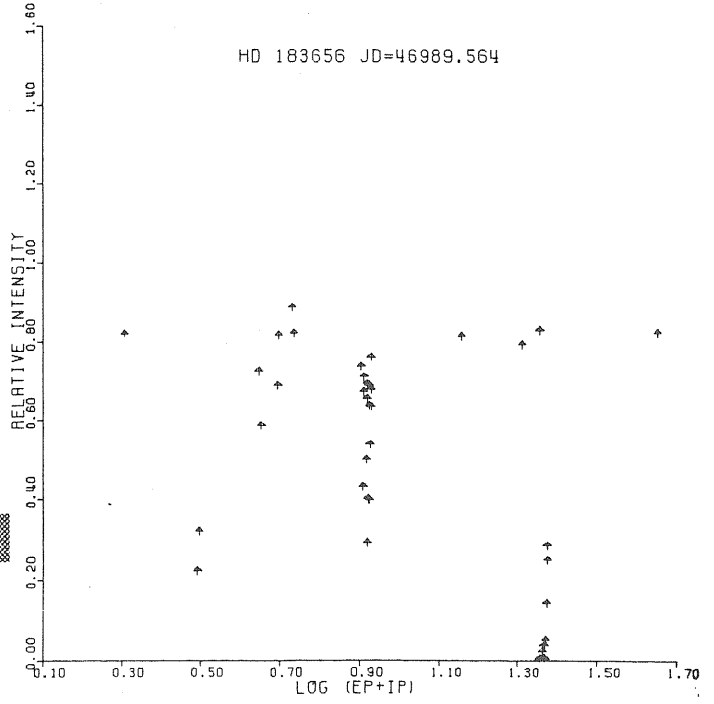

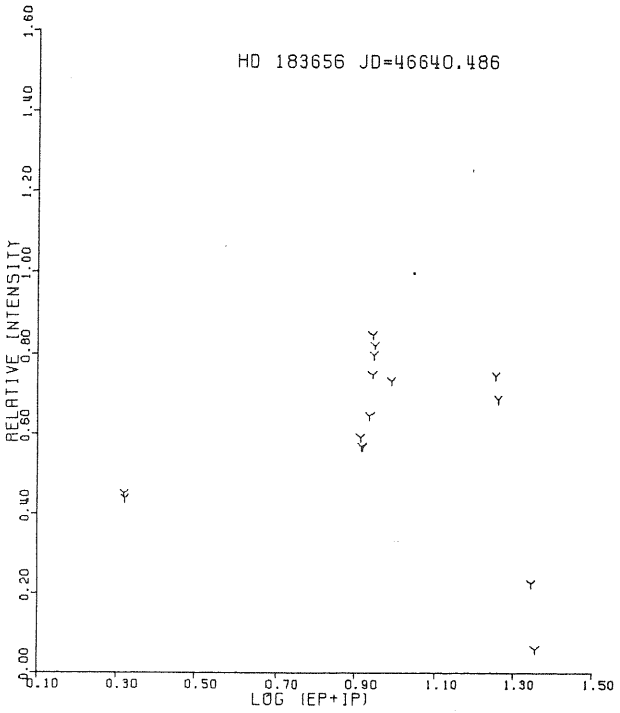

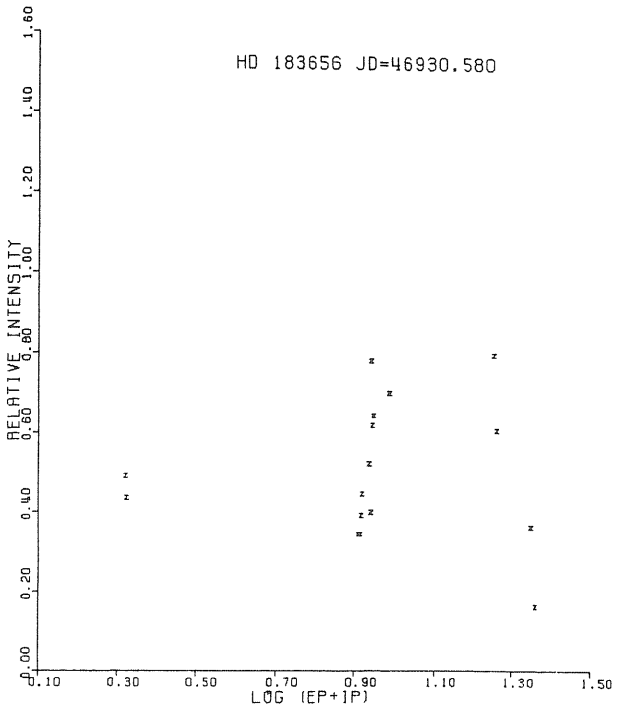

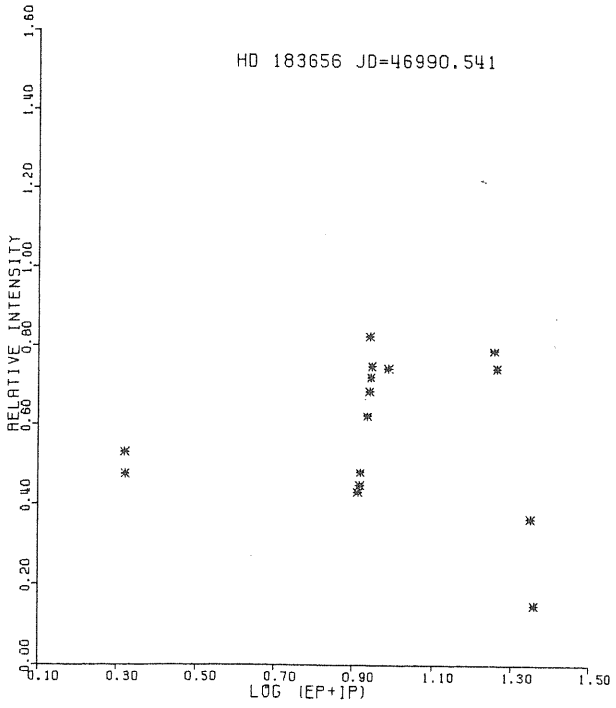

FIGURE III.1.3.16

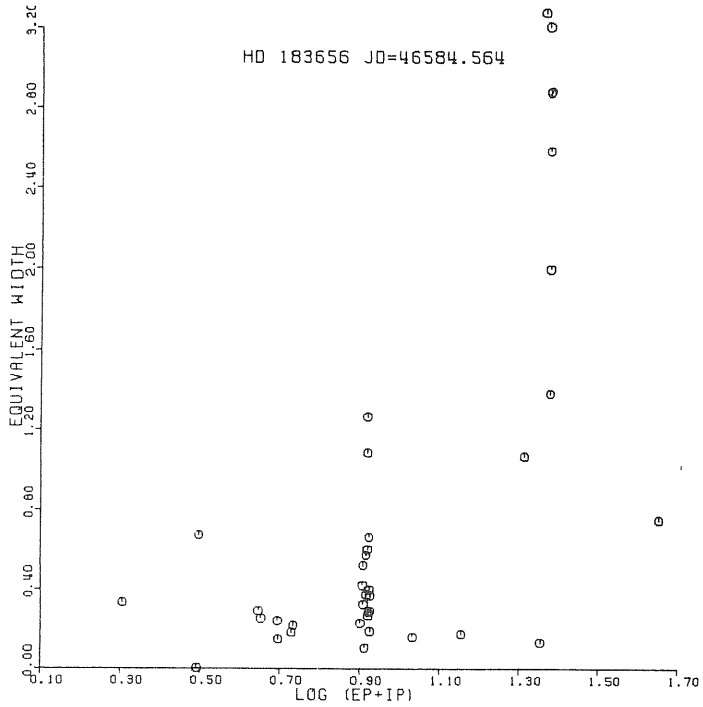

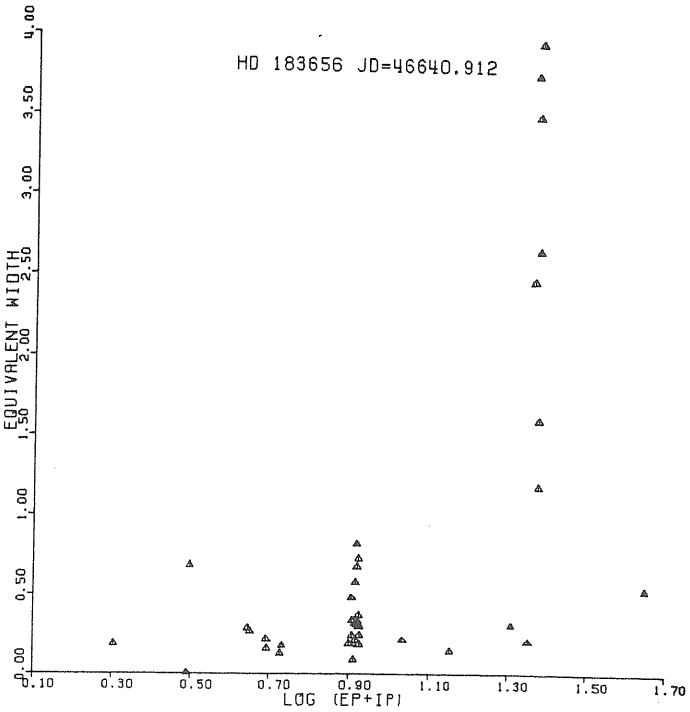

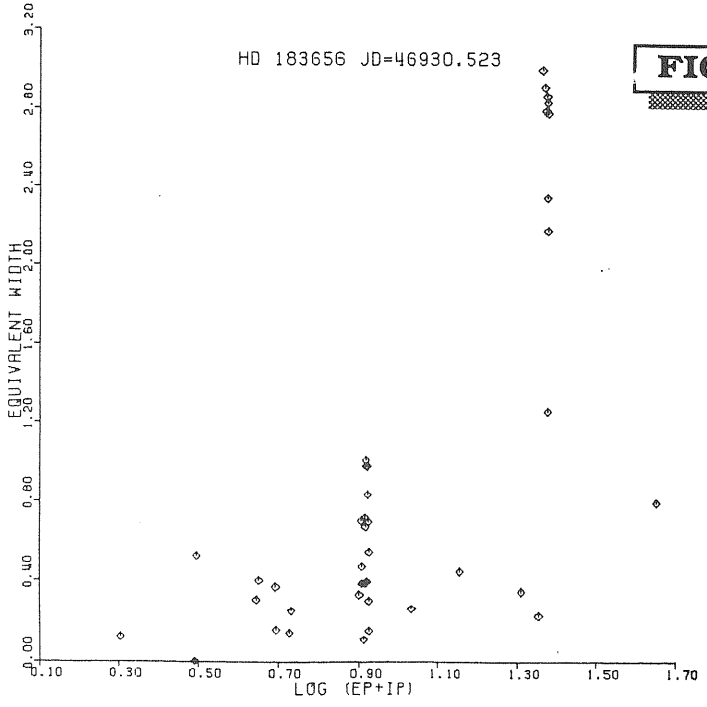

FIGURE III.1.3.17

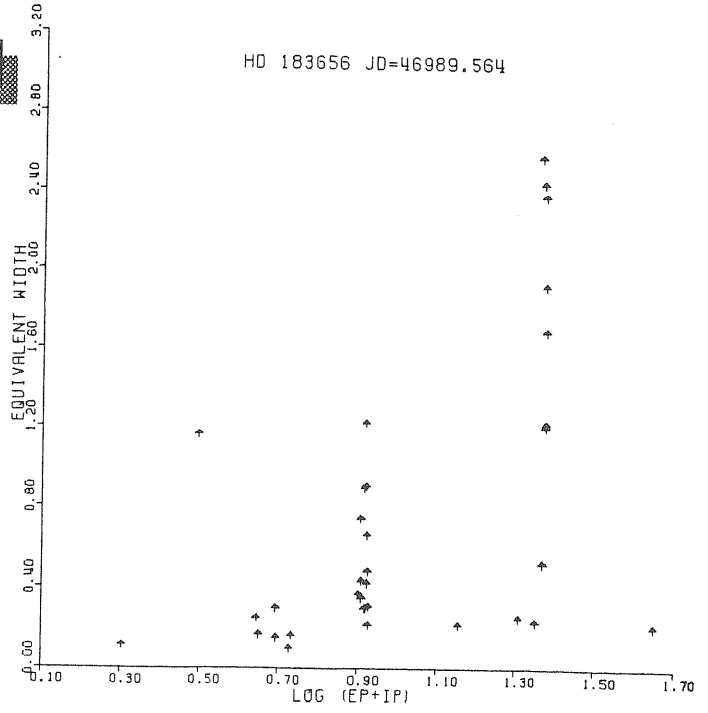

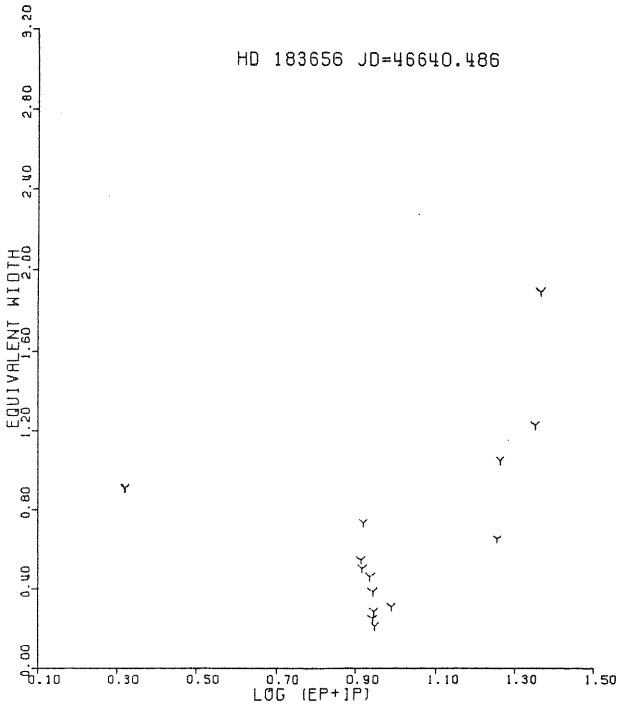

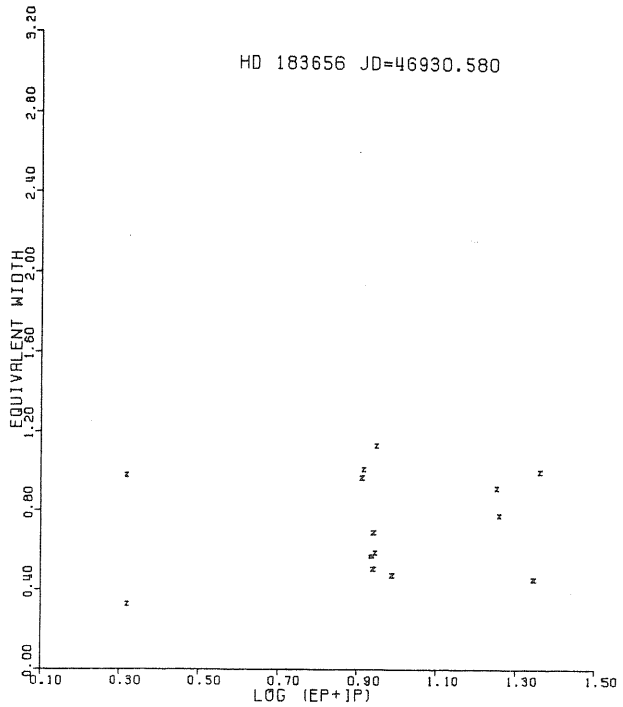

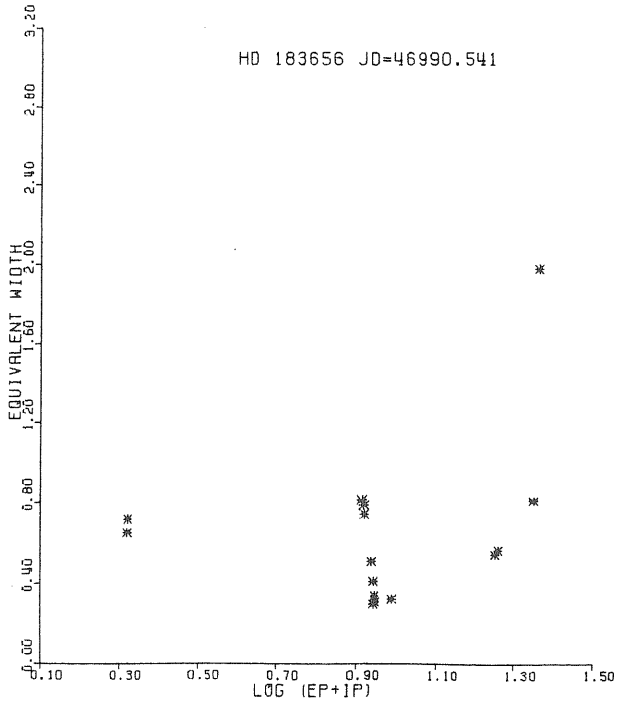

FIGURE III.1.3.18

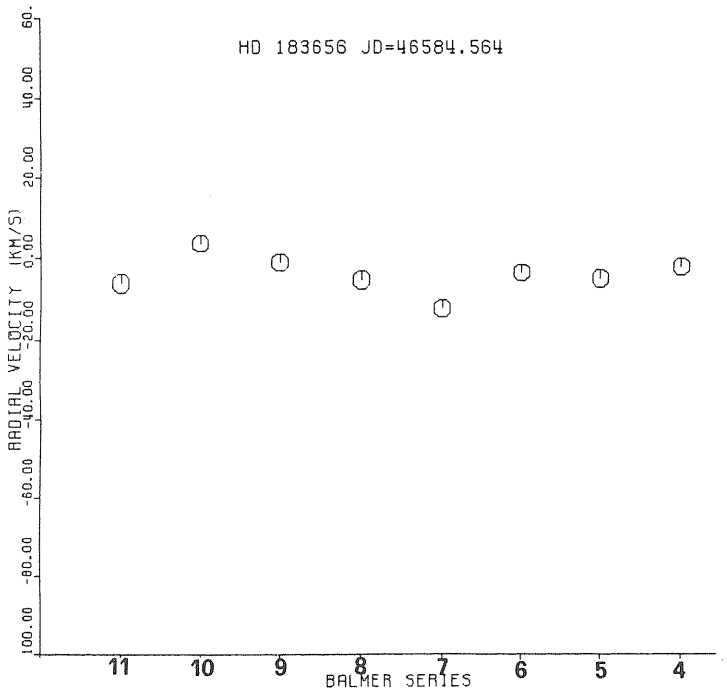

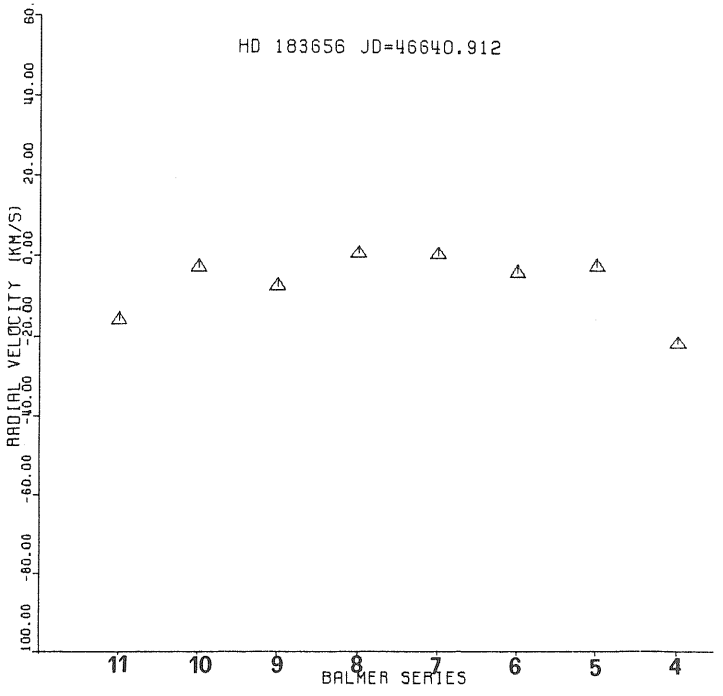

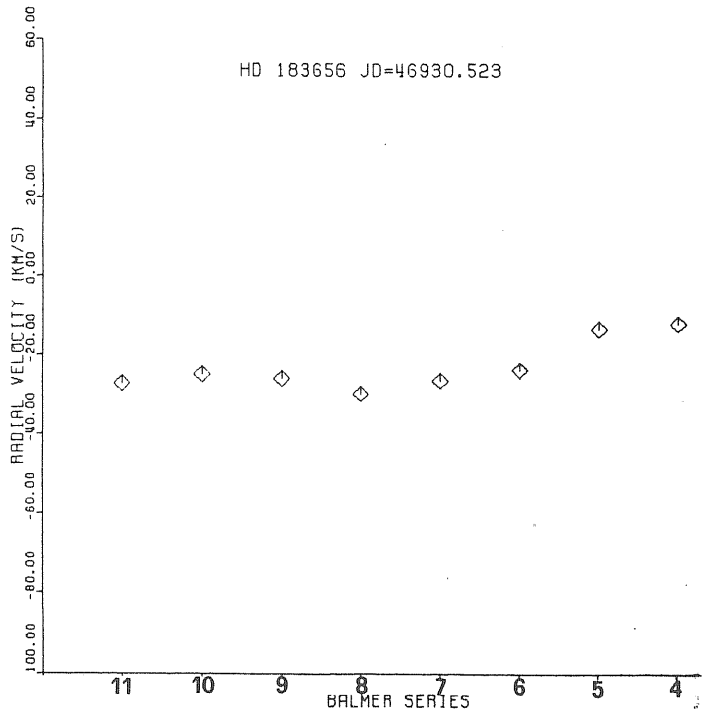

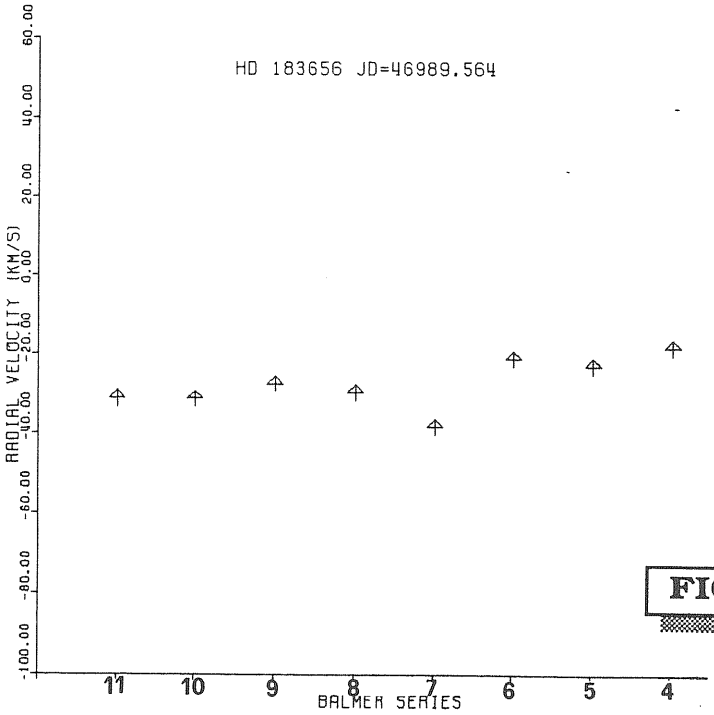

FIGURE III.1.3.19

Table III.1.3.1.Spectral measurements of the H alpha line profiles of HD 183656.

J.D.	OBSERVED WAVELENGTH(A)	EQW (A)	DEPTH	FBWC (A)	HWC(B) (A)	HWC(R) (A)
46640.486	6559.7	2.6	0.8	6.6	4.8	1.8
	6562.5	1.2	-0.8	3.1	1.3	1.9
	6565.6	1.7	0.6	6.1	1.8	4.3
46930.580	6559.9	4.3	1.2	7.0	4.8	2.2
	6562.9	1.1	-0.6	3.3	1.5	1.8
	6565.8	3.6	0.9	7.6	2.0	5.6
46990.541	6559.6	2.6	0.7	7.7	5.9	1.8
	6562.4	0.8	-0.6	2.7	1.1	1.6
	6565.3	2.8	0.7	7.6	1.7	5.9

NOTE:EQW=Equivalent width,DEPTH=Central intensity of the fitted asymmetric gaussian emission profiles,FBWC=Full band width on the continuum including both emission components of double-peak emission profile,HWC(B)=Half width on the continuum; the total width of the blue emission component on the continuum,HWC(R)=Half width on the continuum;the total width of the red emission component on the continuum.Negative depth values corresponds to the central absorption of the measured double-peak emission profile.

Table III.1.3.2. Measured spectral line parameters of the absorption lines of HD 183656.

HD 183656			JD= 46584.564					JD= 46640.912					JD= 46930.523				
ELEMENT	MULT.	λ(LAB)Å	λ(OBS)Å	Ic	FBWC(Å)	EQW(Å)	RV(km/s)	λ(OBS)Å	Ic	FBWC(Å)	EQW(Å)	RV(km/s)	λ(OBS)Å	Ic	FBWC(Å)	EQW(Å)	RV(km/s)
H 18	4	3691.6	3691.4	0.5	3.3	0.9	-15.0	3691.3	0.3	2.2	0.7	-24.5	3691.3	0.4	3.6	1.0	-24.2
H 17	3	3697.2	3697.1	0.4	3.6	1.2	- 4.5	3697.0	0.4	2.8	0.9	-14.1	3696.8	0.4	2.7	0.8	-30.0
H 16	3	3703.9	3703.8	0.4	3.8	1.2	- 7.3	3703.6	0.4	2.8	0.7	-23.2	3703.5	0.4	2.9	0.8	-32.7
H 15	3	3712.0	3712.0	0.3	4.8	1.7	- 1.0	3711.9	0.2	3.8	1.5	- 4.2	3711.7	0.3	4.7	1.7	-26.4
H 14	3	3721.9	3722.0	0.3	4.4	1.6	1.8	3721.8	0.3	4.1	1.5	-14.1	3721.7	0.3	4.3	1.5	-23.6
H 13	3	3734.4	3734.5	0.2	4.9	1.9	8.1	3734.2	0.3	4.7	1.8	-13.9	3734.0	0.3	5.0	1.8	-26.6
H 12	2	3750.2	3750.2	0.2	4.8	2.0	3.4	3750.1	0.3	4.9	1.6	- 2.9	3749.8	0.2	5.2	2.2	-24.9
Ti II	13	3759.3	3759.3	0.7	1.8	0.3	0.2	3758.4	0.7	1.5	0.3	-68.6	3759.2	0.6	2.2	0.4	- 6.0
Ti II	13	3761.3	3761.3	0.8	2.3	0.3	- 0.6	3761.2	0.8	2.5	0.3	- 8.3	3761.1	0.7	2.2	0.3	-17.7
H II	2	3770.6	3770.8	0.1	6.3	2.8	9.0	3770.6	0.2	9.4	4.0	- 6.6	3770.3	0.1	6.9	2.8	-25.3
H 10	2	3797.9	3797.9	0.1	7.4	3.4	- 1.4	3797.8	0.2	5.7	2.2	- 7.6	3797.5	0.1	5.5	2.4	-29.3
H 9	2	3835.4	3835.3	0.1	5.1	2.3	- 1.4	3835.3	0.2	8.5	3.1	- 7.2	3835.1	0.1	7.3	3.3	-22.5
H 8	2	3889.1	3889.0	0.1	5.7	2.6	- 5.5	3889.1	0.1	9.6	4.5	0.6	3888.7	0.1	5.3	2.3	-29.7
Ti II	34	3900.6	3900.5	0.8	2.2	0.2	- 5.9	3900.2	0.8	3.7	0.2	-23.9	3900.1	0.8	2.2	0.3	-32.9
Fe II	173	3906.0	3906.1	0.8	2.0	0.2	3.2	3905.9	0.9	2.2	0.1	-11.9	3905.9	0.7	3.3	0.4	- 8.9
Ti II	34	3913.5	3912.8	0.9	3.4	0.2	-55.1	3913.2	0.9	1.9	0.1	-22.1	3913.5	0.9	2.0	0.1	2.0
Ca II K	1	3933.7	3933.5	0.5	2.6	0.7	-10.3	3933.5	0.5	2.6	0.7	-16.3	3933.2	0.6	2.6	0.5	-31.2
Ca II H	1	3968.5	3968.4	0.9	-	-	- 5.9	3968.2	0.3	-	-	-14.8	-	-	-	-	-
H eps	1	3970.1	3970.2	0.1	7.1	3.2	-12.2	3970.1	0.2	11.2	4.8	0.3	3969.7	0.1	6.3	2.9	-26.4
Ti II	11	4025.1	4025.1	0.8	2.3	0.3	- 2.2	4024.7	0.8	4.9	0.5	-32.1	4024.7	0.7	3.3	0.5	-31.8
H delta	1	4101.7	4101.7	0.1	7.3	3.5	- 3.7	4101.7	0.1	7.6	3.5	- 4.2	4101.4	0.1	6.1	2.8	-23.6
Si II	3	4128.1	4128.6	0.9	1.6	0.1	36.1	4128.2	0.8	2.7	0.2	13.2	4127.5	0.8	2.6	0.2	-38.8
Si II	3	4130.9	4130.9	0.9	1.9	0.2	- 1.5	4130.8	0.8	2.4	0.2	- 7.3	4131.0	0.8	2.1	0.2	18.4
Fe II	27	4173.5	4173.3	0.8	3.3	0.3	- 8.4	4173.2	0.8	2.0	0.2	-19.7	4173.1	0.8	2.7	0.4	-22.5
Fe II	28	4178.9	4178.9	0.7	4.0	0.5	0.6	4178.6	0.7	2.4	0.3	-19.2	4178.6	0.7	2.7	0.5	-16.4
Fe II	27	4233.2	4233.0	0.6	2.3	0.4	-10.4	4233.0	0.6	2.4	0.5	-10.5	4232.8	0.5	2.6	0.7	-27.1
Fe II	27	4303.2	4303.0	0.5	4.7	1.3	- 9.4	4302.9	0.8	1.8	0.2	-15.7	4302.8	0.7	2.6	0.4	-29.4
Fe II	32	4314.3	4314.3	0.9	2.0	0.1	1.7	4314.6	0.9	1.4	0.1	18.1	4314.3	0.9	1.6	0.1	1.7
H gam	1	4340.5	4340.4	0.1	8.5	4.0	- 5.3	4340.4	0.1	8.2	3.8	- 2.6	4340.3	0.1	6.3	2.9	-13.4
Fe II	27	4351.8	4351.6	0.6	3.1	0.6	-13.5	4351.5	0.6	3.1	0.6	-16.2	4351.5	0.5	3.1	0.7	-21.2
Ti II	19	4395.0	4394.8	0.8	1.7	0.2	-14.2	4394.9	0.8	1.9	0.2	-11.5	4394.7	0.8	1.9	0.2	-24.9
Fe II	27	4416.8	4416.9	0.8	2.2	0.3	5.8	4416.8	0.8	2.5	0.3	0.4	4416.4	0.7	2.6	0.4	-26.2
Ti II	31	4468.5	4468.4	0.7	2.4	0.3	- 9.4	4468.2	0.8	1.9	0.2	-22.6	4468.3	0.8	1.1	0.1	-12.0
He I	14	4471.5	4471.3	0.8	9.3	0.8	-14.9	4471.7	0.9	7.3	0.5	11.4	4471.8	0.8	7.4	0.8	19.3
Mg II	4	4481.1	4480.9	0.8	11.0	1.1	-12.6	4480.8	0.8	3.5	0.3	-22.8	4480.6	0.8	2.9	0.4	-36.2
Fe II	37	4491.4	4491.3	0.8	2.0	0.2	- 9.8	4491.4	0.8	1.8	0.2	0.7	4491.2	0.8	1.8	0.2	-12.4
Fe II	38	4508.3	4508.2	0.7	2.4	0.4	- 3.2	4508.0	0.7	2.2	0.3	-16.2	4508.0	0.6	2.9	0.5	-17.2
Fe II	37	4515.3	4515.8	0.8	2.4	0.3	28.4	4515.2	0.8	2.0	0.2	- 8.0	4515.1	0.7	2.2	0.3	-18.5
Ti II	30	4520.4	4520.2	0.8	2.1	0.2	-11.6	4520.1	0.8	1.9	0.2	-19.4	4520.0	0.7	2.3	0.4	-27.1
Fe II	38	4522.6	4522.5	0.7	2.3	0.4	- 8.2	4522.4	0.7	2.2	0.4	-13.5	4522.3	0.6	3.1	0.7	-21.2
Fe II	38	4549.5	4549.2	0.5	0.5	0.7	-16.6	4549.3	0.5	3.1	0.7	-11.4	4549.0	0.4	2.9	0.8	-32.1
Fe II	37	4555.9	4556.4	0.7	1.8	0.3	33.1	4555.7	0.7	2.4	0.3	-13.4	4555.6	0.6	5.2	1.0	-18.6
Fe II	20	4558.6	4558.5	0.8	1.9	0.2	- 7.2	4558.3	0.8	1.8	0.2	-17.5	4558.4	0.7	2.1	0.3	-12.4
Fe II	38	4583.8	4583.6	0.6	2.8	0.6	-14.1	4583.5	0.5	2.9	0.7	-19.3	4583.5	0.5	3.5	1.0	-24.4
Cr II	44	4588.2	4629.3	0.0	6.6	3.3	- 2.4	4588.0	0.8	1.9	0.2	-14.1	4587.7	0.8	2.2	0.3	-32.2
Fe II	37	4629.3	-	-	-	-	-	4629.1	0.7	2.4	0.3	-18.0	4628.8	0.6	3.6	0.7	-33.3
H beta	1	4861.3	-	-	-	-	-	4861.0	0.2	5.9	2.5	-21.7	4861.1	0.1	4.9	2.3	-12.0
Fe II	42	4923.9	4923.7	0.4	3.5	1.1	-11.9	4923.6	0.5	3.2	0.8	-21.5	4923.5	0.4	3.5	1.0	-26.3

Table III.1.3.2.(continued)

HD 183656 JD= 46989.564

ELEMENT	MULT.	λ(LAB)Å	λ(OBS)Å	Ic	FBWC(Å)	EQW(Å)	RV(km/s)
H 18	4	3691.6	3691.2	0.4	2.1	0.7	-27.8
H 17	3	3697.2	3696.7	0.3	3.1	1.0	-36.4
H 16	3	3703.9	3703.5	0.2	2.1	0.8	-32.8
H 15	3	3712.0	3711.7	0.2	4.5	1.7	-21.7
H 14	3	3721.9	3721.6	0.2	3.2	1.3	-28.4
H 13	3	3734.4	3733.9	0.1	4.1	1.8	-39.1
H 12	2	3750.2	3749.8	0.1	3.9	1.7	-31.2
Ti II	13	3759.2	3759.0	0.6	0.8	0.2	-26.4
Ti II	13	3761.3	3761.0	0.7	1.8	0.3	-28.3
H 11	2	3770.6	3770.3	0.3	3.4	1.2	-27.6
H 10	2	3797.9	3797.6	0.1	4.3	2.0	-24.7
H 9	2	3835.4	3835.0	0.1	3.8	1.8	-30.2
H 8	2	3889.1	3888.7	0.1	4.0	1.9	-29.6
Ti II	34	3900.6	3900.1	0.8	1.8	0.2	-31.5
Fe II	173	3906.0	3905.3	0.8	2.3	0.2	-54.1
Ti II	34	3913.5	3912.8	0.8	1.5	0.1	-47.6
Ca II K	1	3933.7	3933.2	0.3	3.4	1.2	-34.2
Ca II H	1	3968.5	3968.0	0.2	-	-	-34.9
H eps	1	3970.1	3969.6	0.0	1.0	0.5	-38.2
Ti II	11	4025.1	4025.2	0.8	4.6	0.5	5.9
H delta	1	4101.7	4025.7	0.8	5.0	0.5	-
Si II	3	4128.	4101.5	0.0	4.9	2.4	-21.0
Si II	3	4130.9	4128.6	0.9	3.3	0.2	37.4
Fe II	27	4173.5	4130.2	0.8	2.3	0.2	-48.6
Fe II	28	4178.9	4163.1	0.7	2.4	0.4	-26.7
Fe II	27	4233.2	4178.5	0.7	2.1	0.3	-29.2
Fe II	27	4303.2	4232.7	0.4	2.6	0.7	-35.5
Fe II	32	4314.3	4302.8	0.7	1.9	0.3	-26.6
H gam	1	4340.5	4340.1	0.0	5.0	2.4	-22.9
Fe II	27	4351.8	4351.3	0.5	3.6	0.9	-29.7
Ti II	19	4395.0	4394.8	0.8	1.6	0.2	-16.9
Fe II	27	4416.8	4416.6	0.7	1.9	0.3	-18.2
Ti II	31	4468.5	4467.7	0.8	1.2	0.1	-52.9
He I	14	4471.5	4471.0	0.8	2.3	0.2	-34.7
Mg II	4	4481.1	4480.7	0.8	2.4	0.3	-29.7
Fe II	37	4491.4	4491.1	0.8	1.8	0.2	-19.0
Fe II	38	4508.3	4507.9	0.6	1.7	0.3	-24.1
Fe II	37	4515.3	4514.9	0.7	1.9	0.3	-26.3
Ti II	30	4520.4	4520.0	0.7	1.9	0.3	-25.9
Fe II	38	4522.6	4522.1	0.5	2.1	0.5	-34.3
Fe II	38	4549.5	4549.0	0.4	2.2	0.7	-29.5
Fe II	37	4555.9	4555.5	0.6	2.3	0.4	-29.0
Fe II	20	4558.6	4558.3	0.7	2.8	0.4	-21.5
Fe II	38	4583.8	4583.4	0.4	3.0	0.9	-28.3
Cr II	44	4588.2	-	-	-	-	-
Fe II	37	4629.3	4628.9	0.7	1.7	0.3	-29.4
H beta	1	4861.3	4861.0	0.0	5.2	2.6	-18.1
Fe II	42	4923.9	4923.5	0.3	3.5	1.2	-25.1

Table III.1.3.2.(continued)

HD 183656			JD= 46640.486					JD= 46930.580					JD= 46990.541				
ELEMENT	MULT.	λ(LAB)Å	λ(OBS.)Å	Ic	FBWC(Å)	EQW(Å)	(RV(km/s)	λ(OBS)Å	Ic	FBWC(Å)	EQW(Å)	RV(km/s)	λ(OBS)Å	Ic	FBWC(Å)	EQW(Å)	RV(km/s)
H beta	1	4861.3	4861.3	0.1	4.0	1.9	-4.8	4861.2	0.2	4.6	1.9	-7.8	4861.0	0.2	4.7	2.0	-21.1
Fe II	42	4923.9	4923.9	0.6	3.4	0.7	0.4	4923.7	0.5	3.7	1.0	-14.3	4923.4	0.5	1.5	0.7	-33.6
Fe II	42	5018.4	5018.2	0.6	2.3	0.5	-14.2	5018.0	0.4	3.2	1.0	-25.9	5017.8	0.5	2.9	0.8	-36.0
Fe II	42	5169.0	5168.8	0.6	2.7	0.5	-16.5	5168.5	0.3	3.5	1.1	-30.2	5168.4	0.4	2.9	0.8	-35.9
Fe II	49	5197.6	5197.3	0.8	2.4	0.2	-13.6	5197.1	0.6	3.3	0.6	-24.9	5197.1	0.8	2.4	0.3	-29.4
Fe II	49	5234.6	5234.5	0.8	2.8	0.3	-8.6	5234.2	0.6	2.7	0.5	-22.1	5234.0	0.7	2.4	0.3	-34.9
Fe II	49	5276.0	5275.7	0.8	3.1	0.4	-17.5	5275.6	0.4	2.9	0.6	-24.2	5275.4	0.7	2.6	0.4	-33.4
Fe II	49	5316.6	5316.4	0.7	2.6	0.5	-10.0	5316.2	0.5	2.9	0.7	-21.1	5316.1	0.6	2.7	0.5	-31.5
Fe II	48	5362.9	5362.6	0.9	3.3	0.3	-15.4	5362.5	0.8	3.0	0.3	-22.0	5362.4	0.8	3.4	0.3	-24.6
Na I	1	5890.0	5889.6	0.4	3.3	0.9	-19.5	5889.5	0.4	3.5	1.0	-21.5	5889.4	0.5	2.8	0.7	-30.3
Na I	1	5895.9	5895.7	0.5	3.3	0.9	-14.1	5895.6	0.5	3.1	0.8	-18.1	5895.3	0.5	2.8	0.7	-31.7
Au I	1	6278.3	6277.6	0.7	6.8	0.9	-35.0	6278.1	0.8	4.8	0.6	-8.7	6277.6	0.8	4.0	0.3	-31.6
Fe II	199	6332.0	6331.8	0.8	1.3	0.1	-6.0	6331.5	0.9	2.4	0.1	-22.7	6331.9	0.9	3.3	0.2	- 5.9
Si II	2	6347.1	6346.6	0.7	6.7	1.1	-23.8	6346.4	0.6	4.7	0.9	-34.9	6346.7	0.7	4.4	0.6	-16.7
Si II	2	6371.4	6371.5	0.8	5.1	0.7	4.3	6370.7	0.8	4.7	0.5	-30.8	6370.7	0.7	5.1	0.5	-30.7
Fe II	74	6456.4	6456.0	0.7	2.3	0.3	-19.3	6456.0	0.7	3.0	0.5	-17.4	6455.7	0.7	2.5	0.3	-33.0

III.1.4.HD 193182

This star exhibited very similar spectra to HD 183656 in many aspects. Figure III.1.4.1 presents observed H alpha profiles.All of them were double-peak emission components with a central absorption.At JD=646.4 V emission was slightly deeper than the R one (Depth(V)=1.3, Depth(R)=1.2),but FBWC of R component was more wider than V and also equivalent width was bigger (FBWC(V)=5.8 A, FBWC(R)=7.2 A ,EQW(V)=3.8 A, EQW(R)=4.3).Central absorption depth was 0.4, EQW=0.3 A and RV=-24.7 km/s.At JD=995.4 both emission wings increased in intensity, and the central depth of the central absorption component decreased.Measured spectral parameters for H alpha were followings:For the V emission component; Depth=1.8 , FBWC=1,8 A, EQW=7.6 A; for the R emission component, Depth=1.6 , FBWC=8.2 A, EQW=6.5; and for the central absorption component, Depth=0.6 , FBWC=1.2 A, EQW=0.4 A, RV=-22.9 km/s.So there was an evident V/R variation just like HD 183656, only H alpha emission of this star was more stronger.

Figure III.1.4.2 presents the observed H beta profiles.Wide stellar profile was filled -in with emission, also a strong shell component was observed for all the profiles.V wings of the shell components presented a faint emission and intensity variation although there were no significant V/R variations.Measured spectral parameters of H beta and all other lines are given in Table III.1.4.1.Figure III.1.4.3 presents the H gamma profiles of HD 193182.A wide

stellar component was very evident.On the wings of the central absorption components a weak emission was present, in H beta the R component was more stronger than the V component.The measured spectral parameters of the shell component presented slight variations. Figures III.1.4.4 and III.1.4.5 presents H delta and H epsilon profiles. These profiles were similar to H gamma but there were no trace of emission.From these last four figures we see that at JD=929.6 shell component widened substantially.

The very rich shell spectra of the HD 193182 is presented through Figures III.1.4.6 to III.1.4.13, for the blue part of the spectra; and through Figures III.1.4.14 to III.1.4.16 for the red.Spectral lines in the presented regions are listed in figure captions and Table III.1.4.1. At the blue part of the spectra some variations in line profiles were observed. At JD=929.6 all the shell components were widened in a same manner as the first Balmer lines but the central depths were didn't changed a appreciably. On the same night a big contribution from stellar component observed for Ca II 3933 profile and H beta presented maximum FBWC for the shell component and emission was fainter than in the other two spectra. Fe II 4923 presented a P Cygni profile at JD=929.6 and 990.4.At JD=929.6 the shell component was more than at the other dates. In the red part of the spectra profile variations were much more significant as compared with the blue region.Si II lines exhibited a strong profile

variation.Some Fe II lines also displayed double-peak emission components, and some other presented a notable asymmetry.Na I line 5889 presented a asymmetric stellar component at JD=646.4.Lastly we can note that Balmer seris were visible up to n=37 and shell was evident after n=12, but at JD=929.6 the shell effect was not present.

Now we would like to discuss the plots of spectral parameters versus log(EP+IP).Figure III.1.4.17 presents the measured radial velocities which changed very little at JD=929.6 compared with JD=646.0.He I line RVs increased while Cr II decreased and the rest of the lines remained constant. Similarly at JD=990.4, only He I and Cr II exhibited a small increase while the other lines had about their previous RV values.For the red spectra, Figure III.1.4.18, if we compare JD=995.4 with JD=646.425 Na I and Fe II lines didn't changed, Ti II and Si II slightly, H alpha and He I substantially increased while H beta decreased.In any case all these variations were very small in comparison with other program stars.

Figure III.1.4.19 presents relative intensities of the shell components versus log(EP+IP) for blue part of the spectra.At JD=929.6 Ca II, Ti II lines slightly decreased, He I increased while Fe II, Cr II and H lines remained approximately same compared with JD=646.0.At JD=990.4 Ca II ,He I remained constant ,Fe II, Cr II and H lines decreased while Ti II and Si II increased.For the red part of the

spectra, JD=995.4 compared with JD=646.4 Na I, Ti II, Si II decreased H and He I increased while Fe II remained same (Figure III.1.4.20). Probably variations most clearly could be seen in equivalent widths.For the blue spectra comparin JD=646.0 with JD=929.6 all the EQWs were substantially increased.At the JD=990.4 except Fe II lines which were remained at their previous values, all the other lines decreased in EQWs (Figure III.1.4.21).For the red part of the spectra, Figure III.1.4.22 we see a similar drop at the values of EQWs for all elements except few lines of Ti II and He I at JD=995.438 compared with JD=646.4.

Figure III.1.4.22 presents the radial velocities of the Balmer lines plotted versus n quantum number.It is interesting to note there were no Balmer progression in any of the observation nights.As we rewieved the available biblography, HD 193182 was not analysed in details.Our data show that this star is one of the few of this class with very stable optical shell features.

Table and Figure captions.

Figure III.1.4.1.H alpha profiles of HD 193182.Same as figure III.1.1.1.

Figure III.1.4.2.H beta profiles of HD 193182.Same as previous figure but every interval on the "y" axis corresponds to 0.2 continuum units.

Figure III.1.4.3.H gamma profiles of HD 193182.Same as previous figure.

Figure III.1.4.4.H delta profiles of HD 193182.Same as previous figure.

Figure III.1.4.5.H epsilon profiles of HD 193182.Same as previous figure.

Figure III.1.4.6.Ti II 3900,3913, Fe II 3913, Ca II 3933 lines of HD 193182.

Figure III.1.4.7.Fe II 4024, Si II 4128,4130 lines of HD 193182.

Figure III.1.4.8.Fe II 4173,4178,4233 lines of HD 193182.

Figure III.1.4.9.Ti II 4374,4395,4399,4468, He I 4471, Mg I 4481 lines of HD 193182.

Figure III.1.4.10.Fe II 4508,4515,4522, Ti II 4520,4533 lines of HD 193182.

Figure III.1.4.11.Fe II 4549,4555,4558, Ti II 4563,4571 lines of HD 193182.

Figure III.1.4.12.Fe II 4629,4635,4923,Cr II 4618,4634 lines of HD 193182.

Figure III.1.4.13.Fe II 5018,4923 lines of HD 193182.

Figure III.1.4.14.Fe II 5169,5197,5234, Ti II 5183,5188,5226 lines of HD 193182.

Figure III.1.4.15.Fe II 5275,5318,5362, Na I 5890,5895, Si II 6347, 6371 lines of HD 193182.

Figure III.1.4.16.RV's versus log(EP+IP) of HD 193182 for blue spectra.Log (EP+IP) values are same as figure III.1.3.13.

Figure III.1.4.17.Same as previous figure for red spectra.

Figure III.1.4.18.Relative intensities versus log(EP+IP) of HD 193182 for blue spectra.

Figure III.1.4.19.Same as previous figure for red spectra.

Figure III.1.4.20.EQW's versus log(EP+IP) of HD 193182 for blue spectra.

Figure III.1.4.21.Same as previous figure for red spectra.

Figure III.1.4.22.RV's of the Balmer lines versus "n" quantum numbers for HD 193182.

Table III.1.4.1.Measured spectral line parameters of HD 193182.

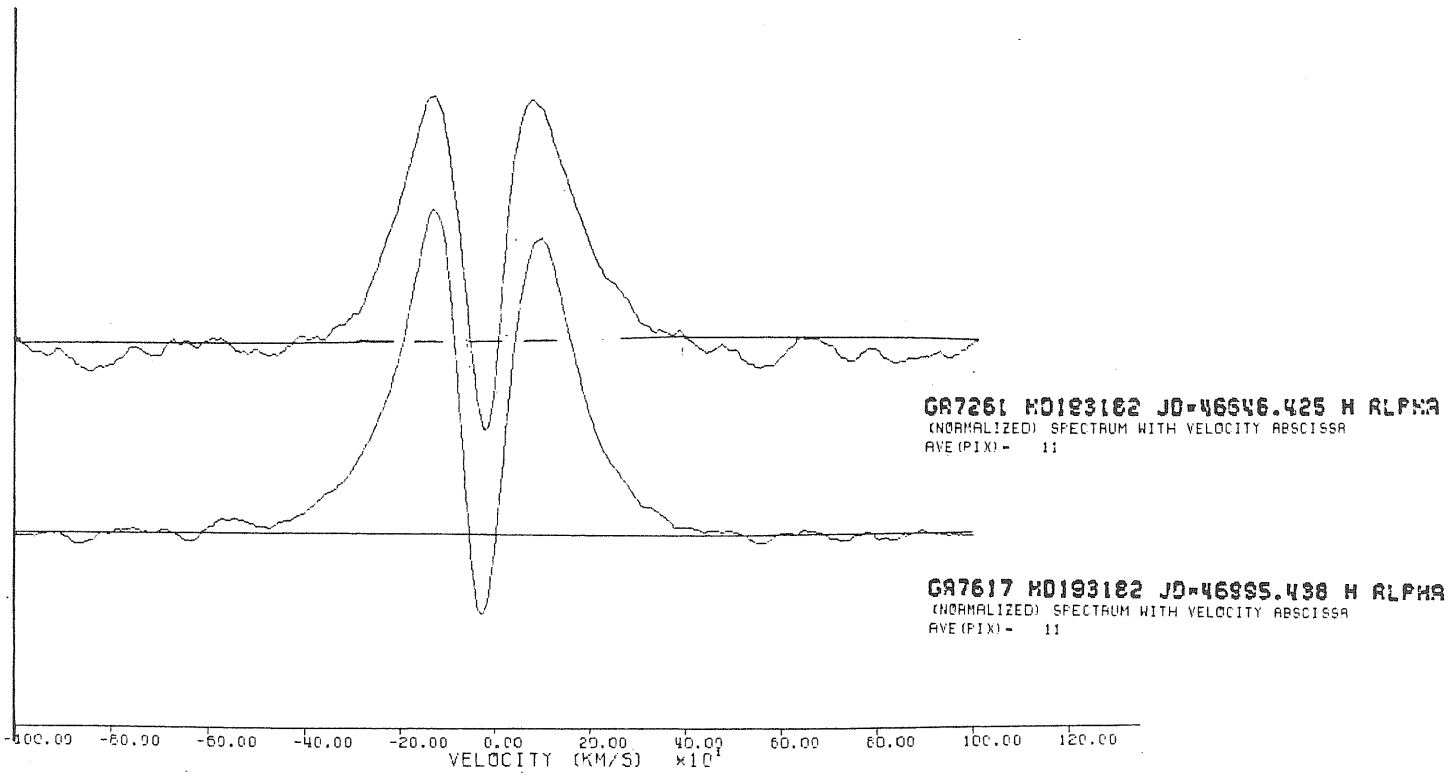

FIGURE III.1.4.1

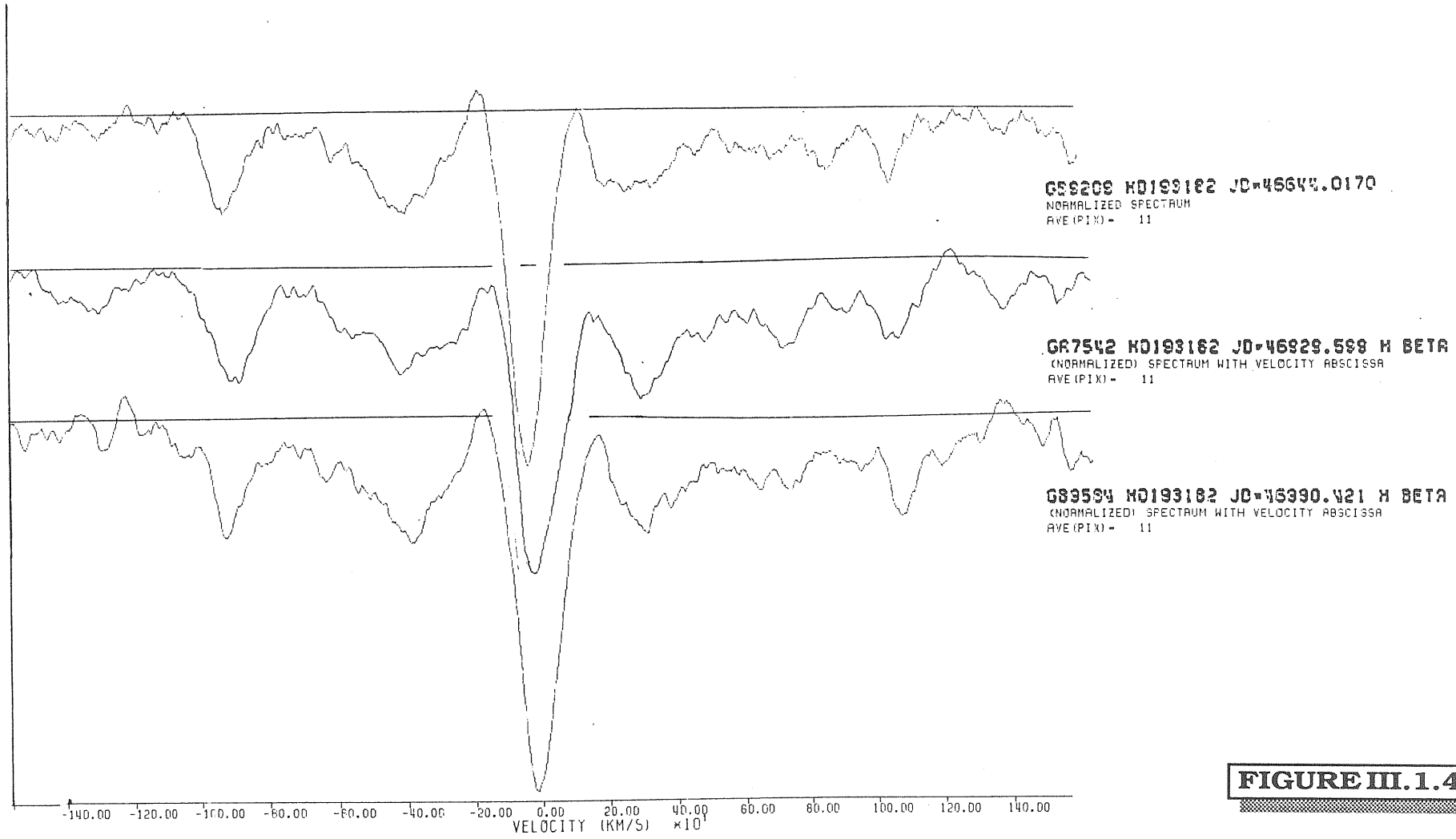

FIGURE III.1.4.2

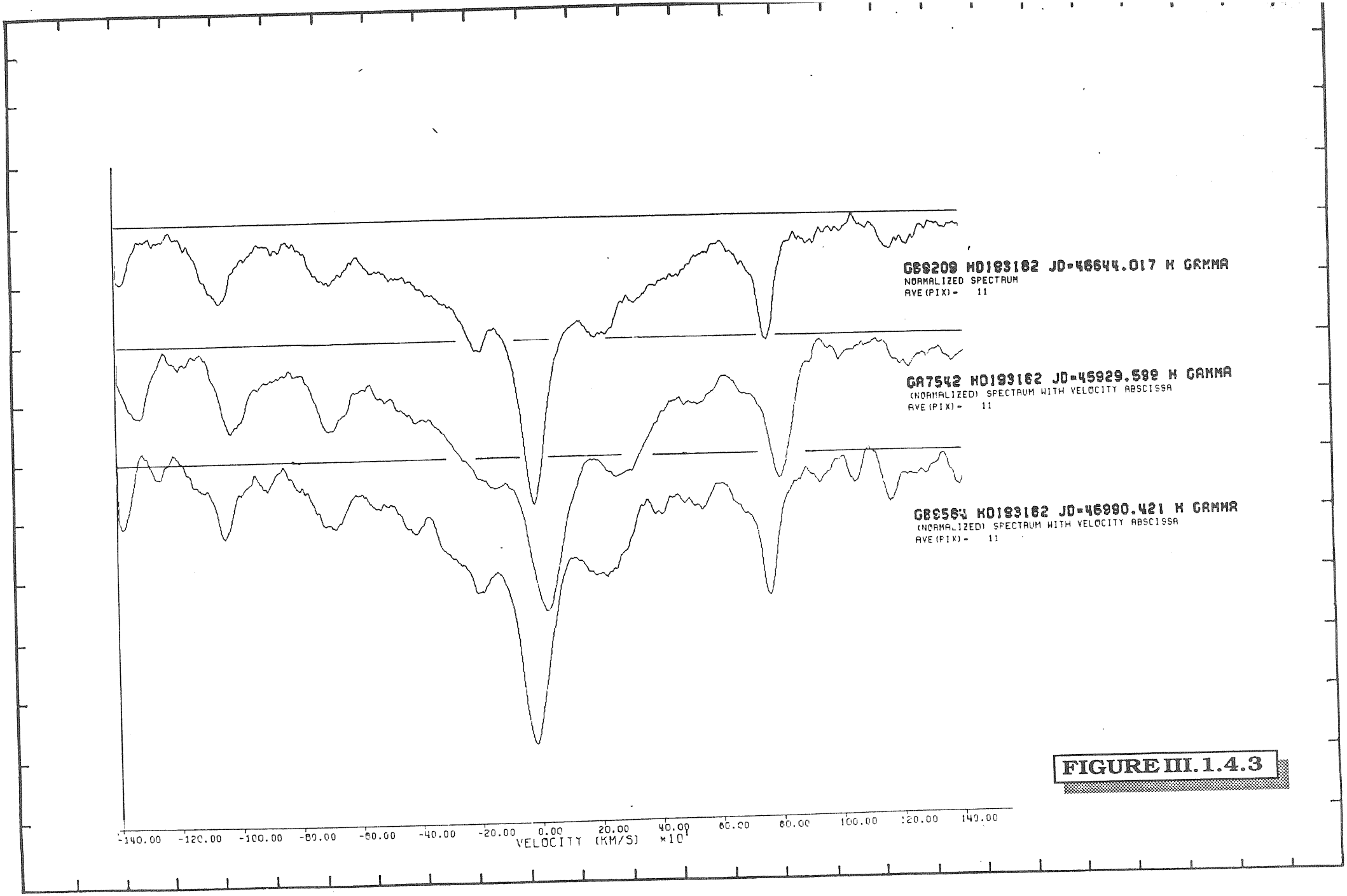

FIGURE III.1.4.3

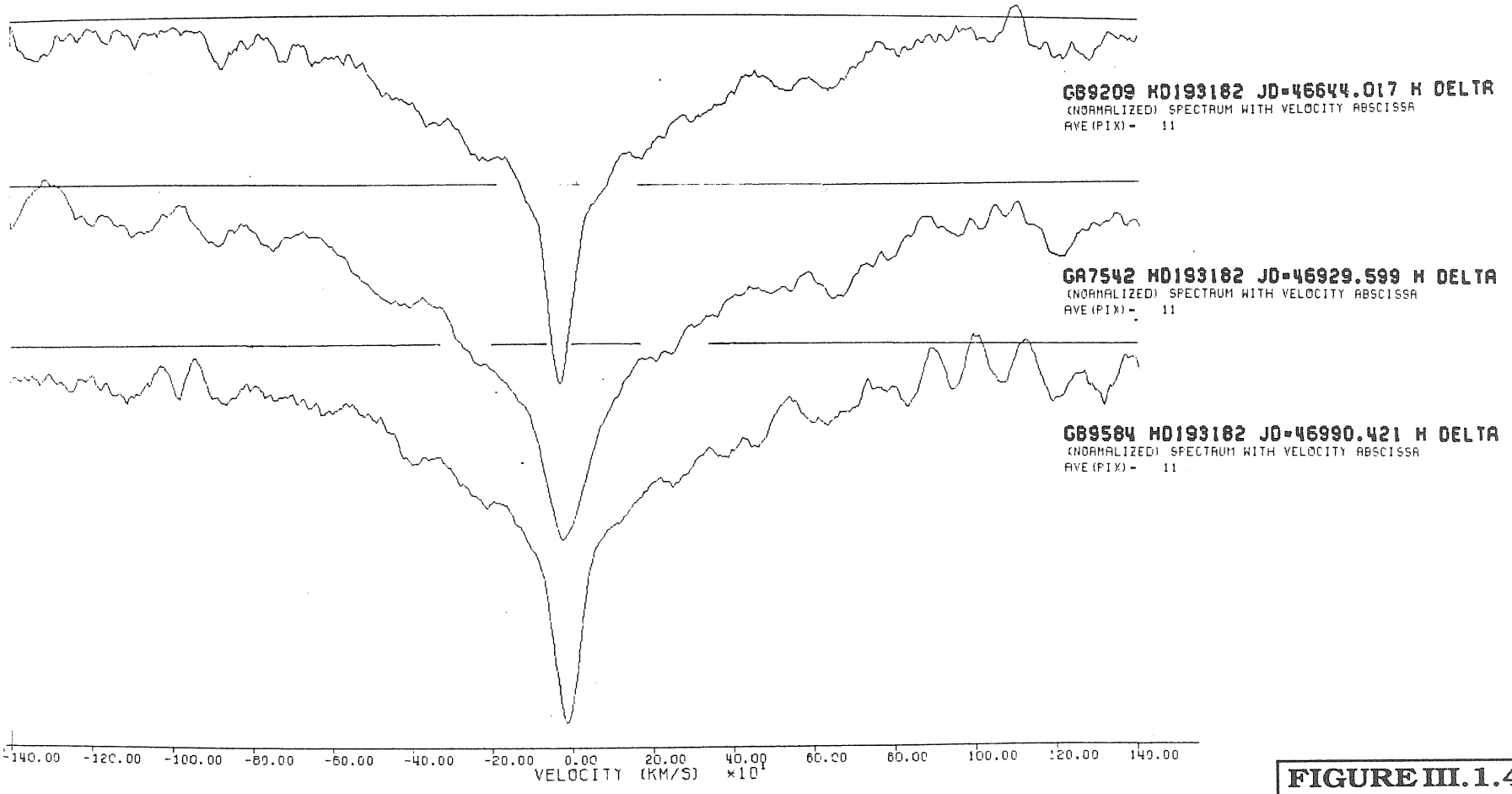

FIGURE III.1.4.4

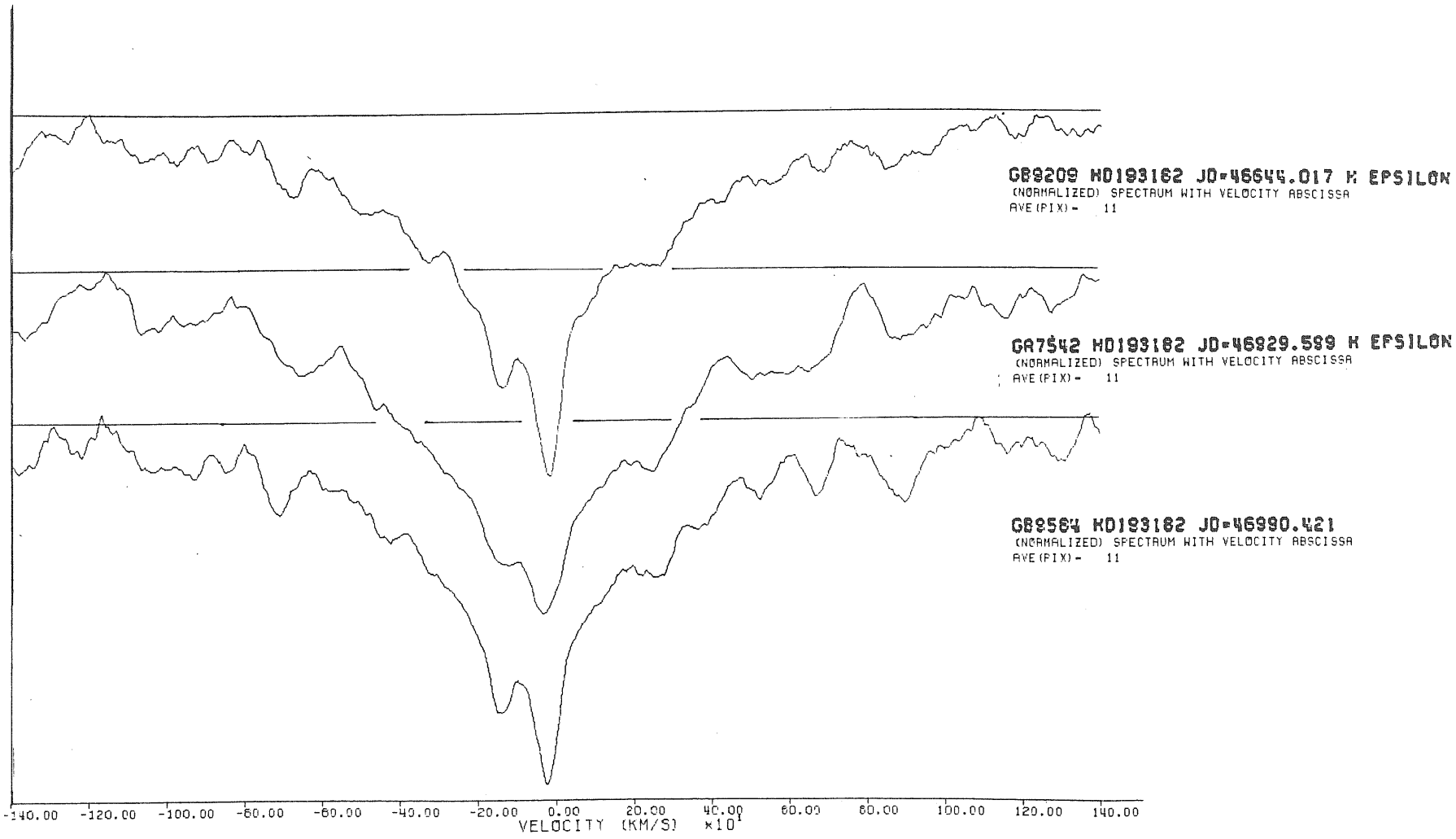

FIGURE III.1.4.5

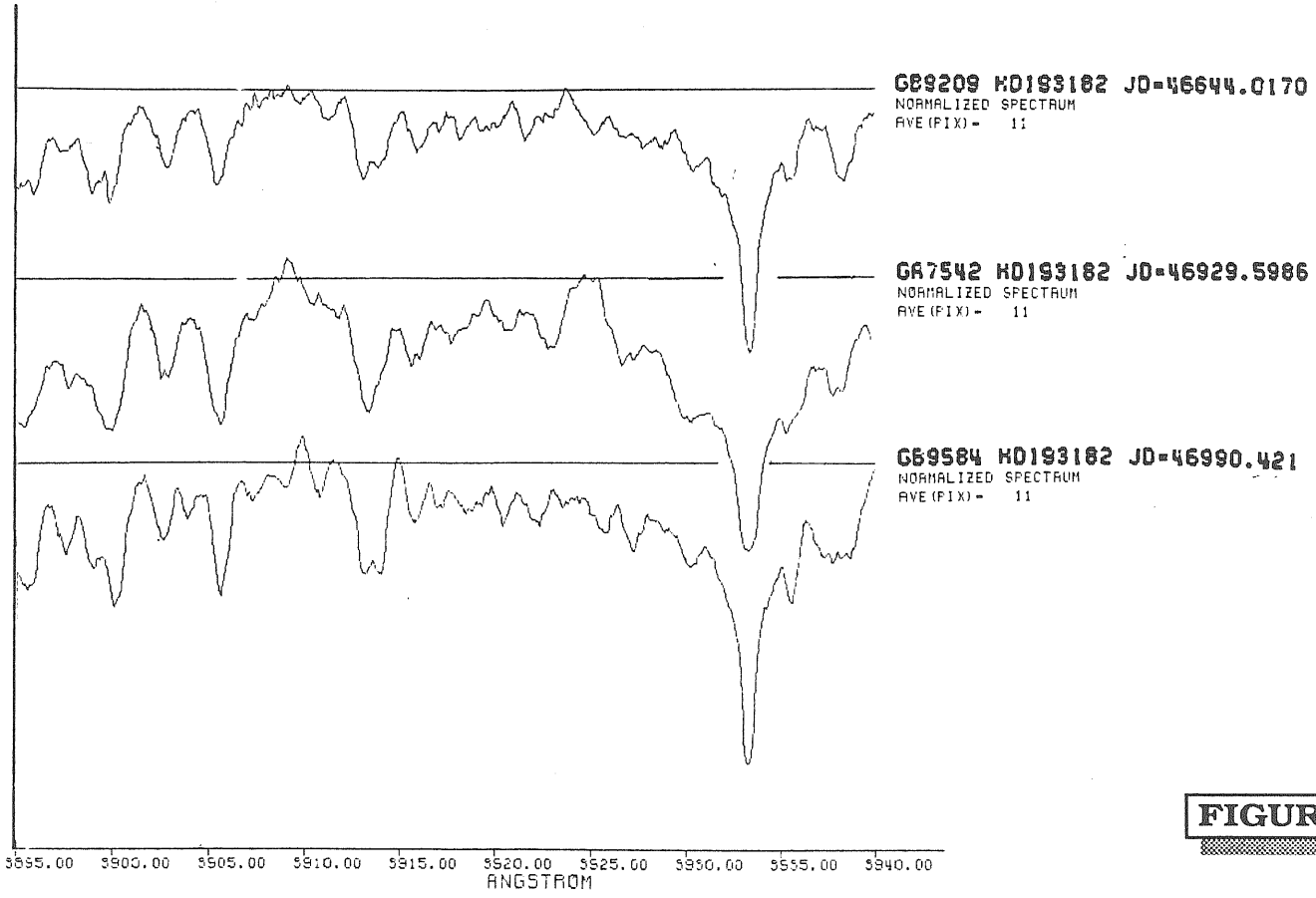

FIGURE III.1.4.6

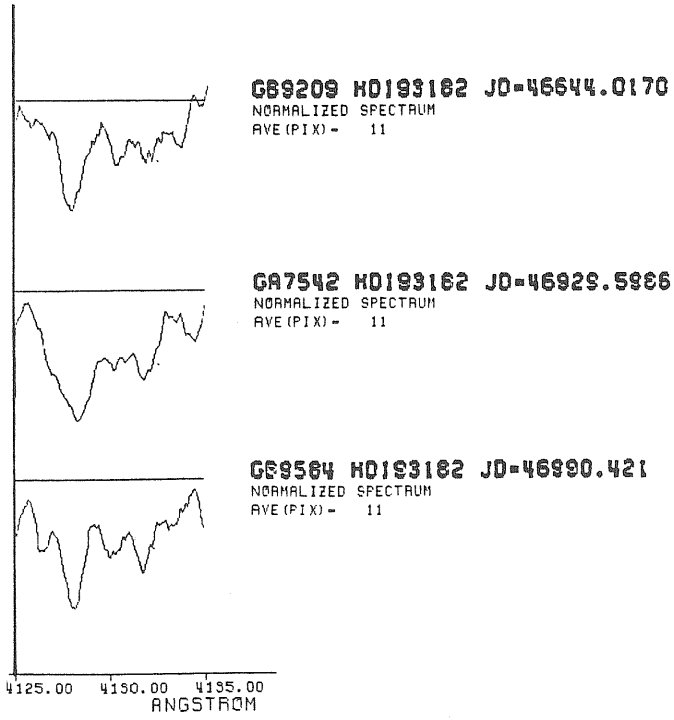

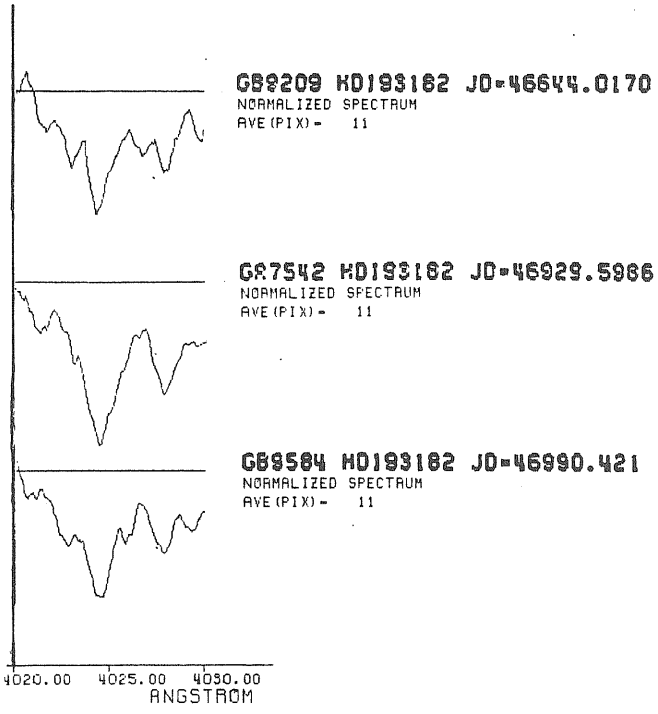

FIGURE III.1.4.7

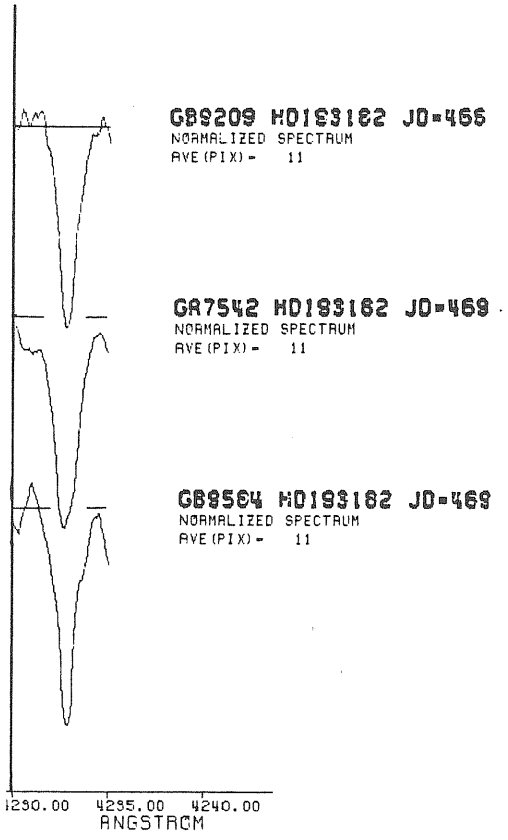

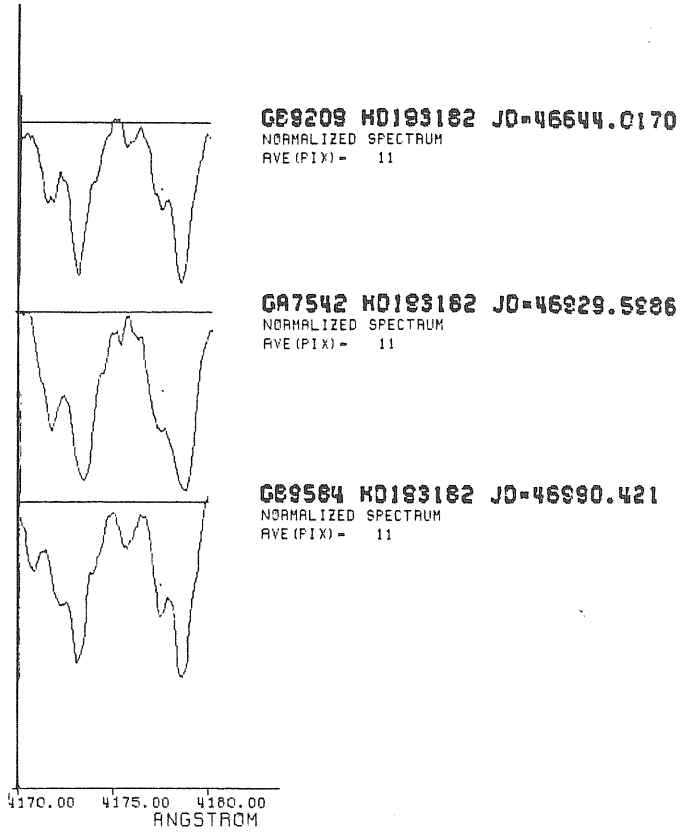

FIGURE III.1.4.8

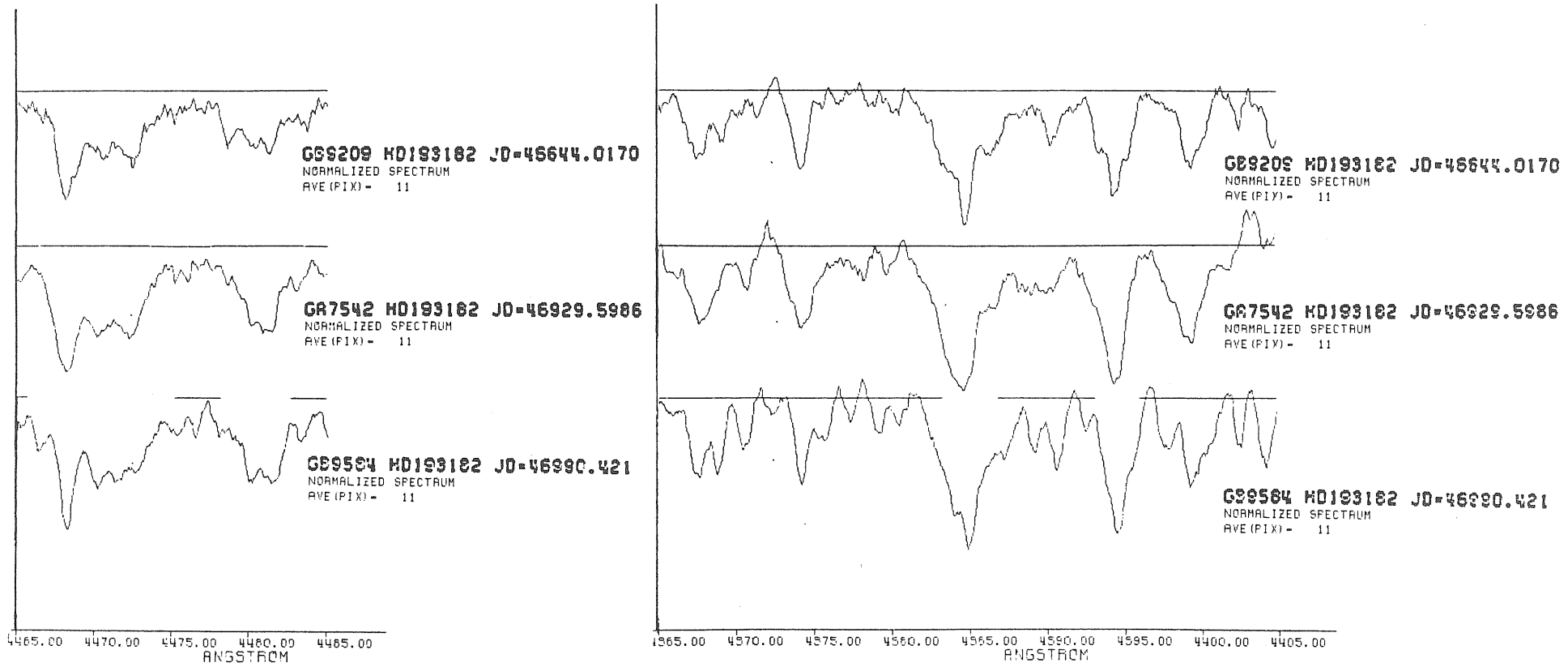

FIGURE III.1.4.9

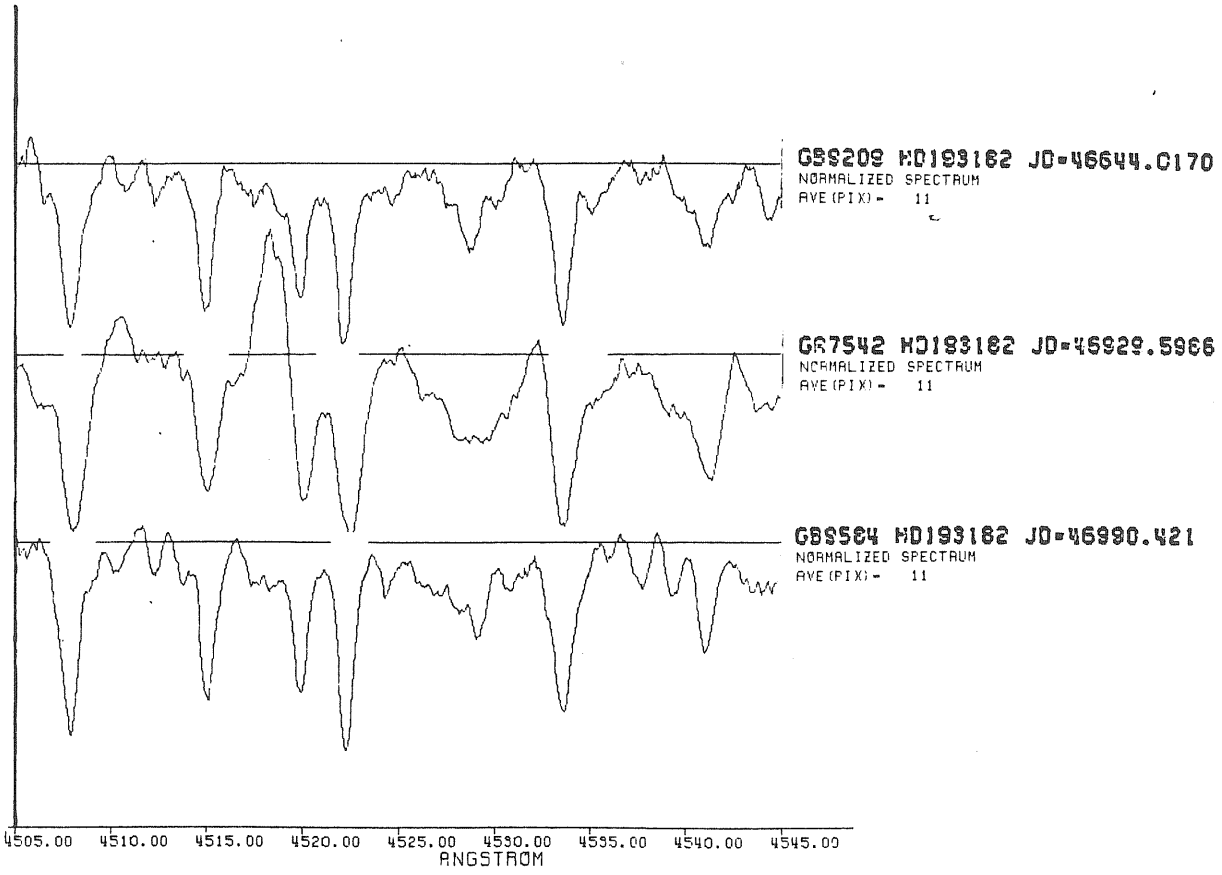

FIGURE III.1.4.10

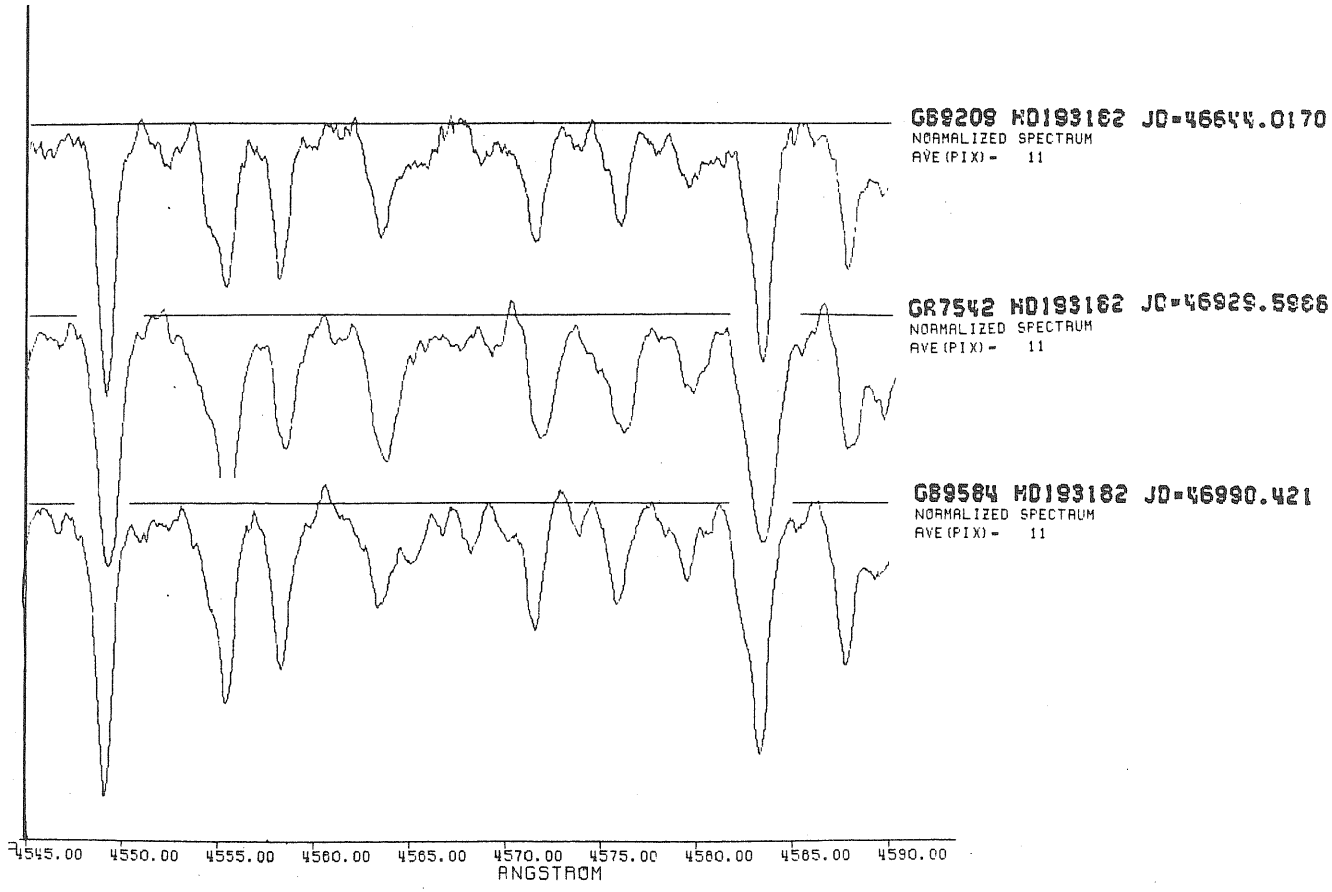

FIGURE III.1.4.11

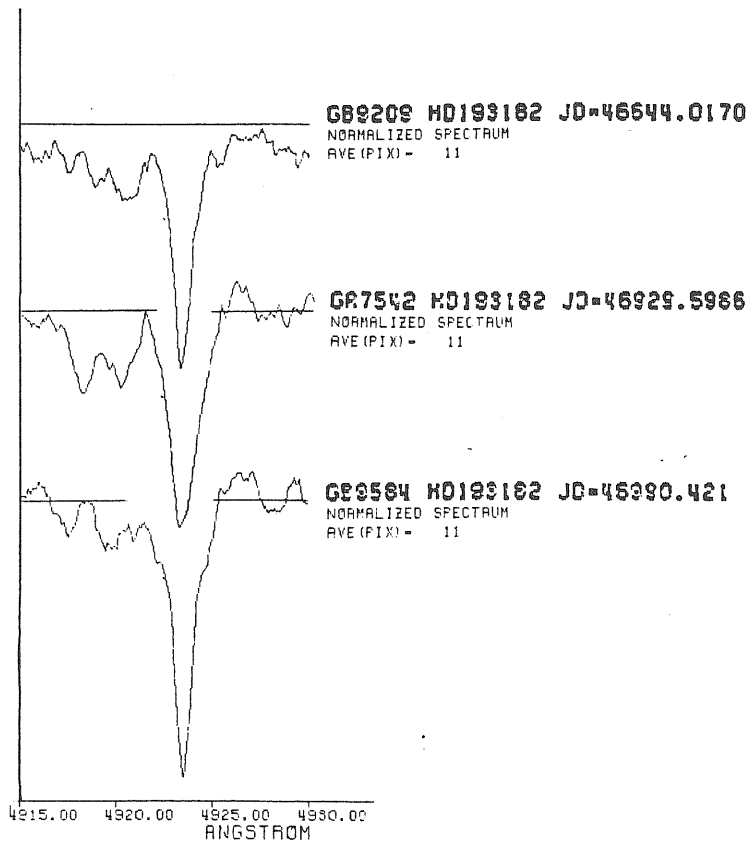

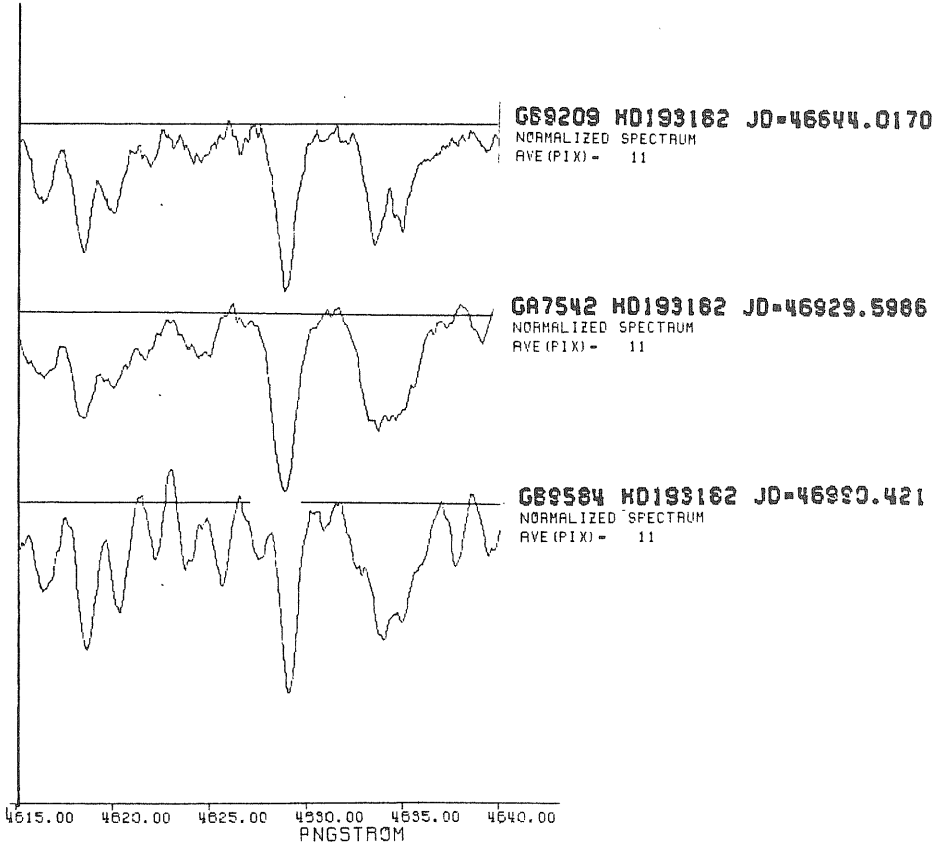

FIGURE III.1.4.12

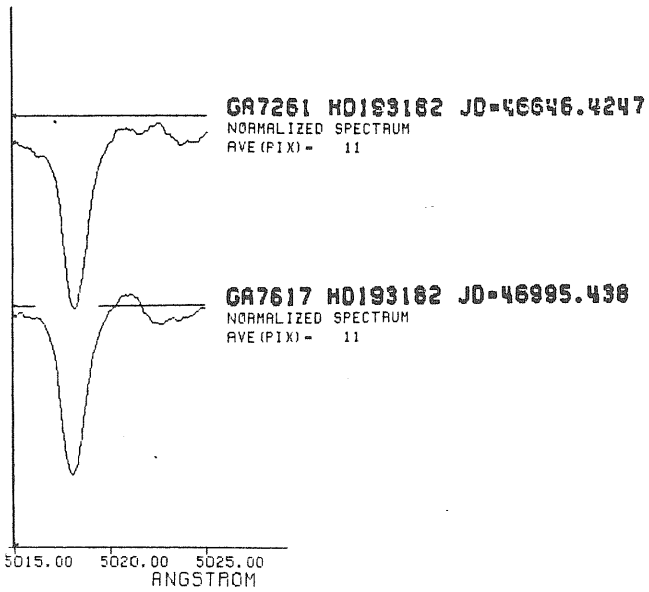

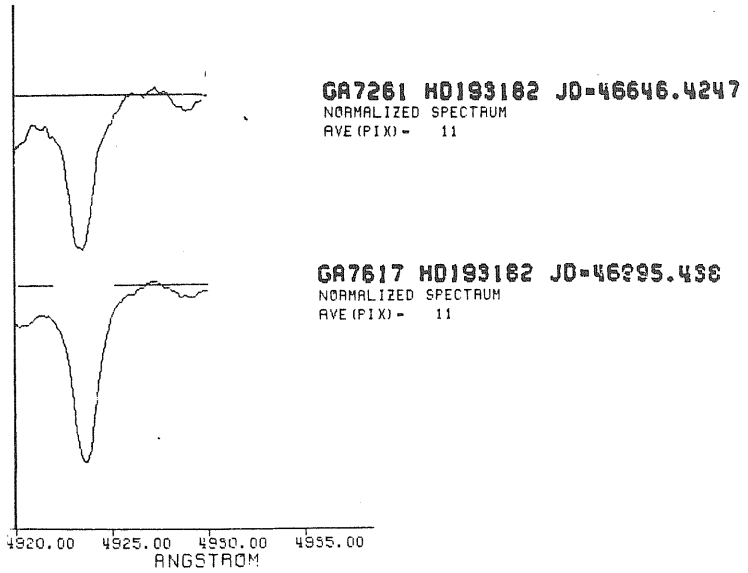

FIGURE III.1.4.13

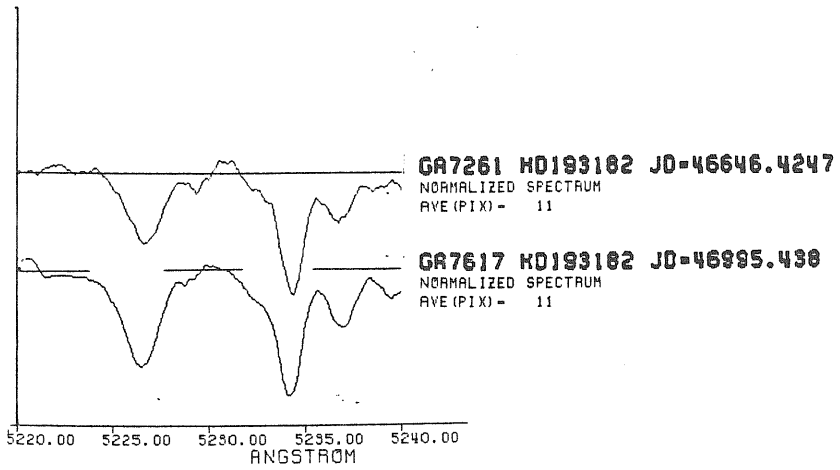

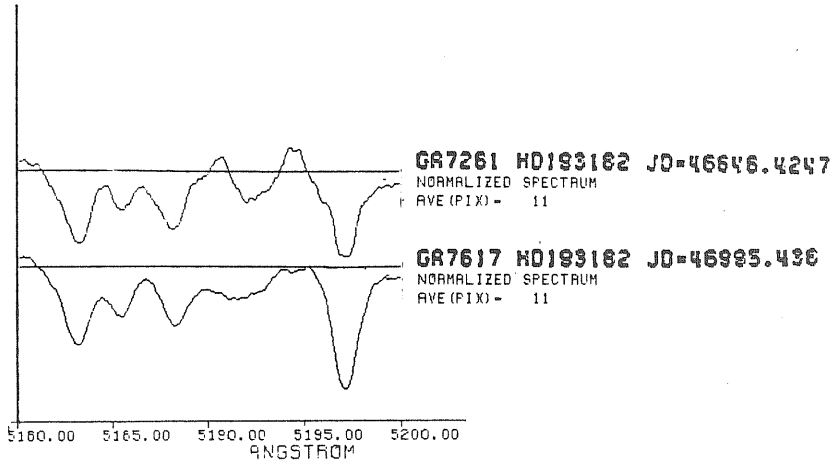

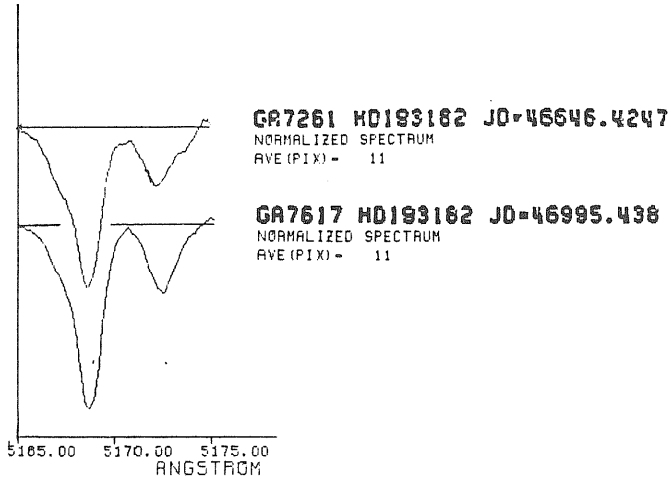

FIGURE III.1.4.14

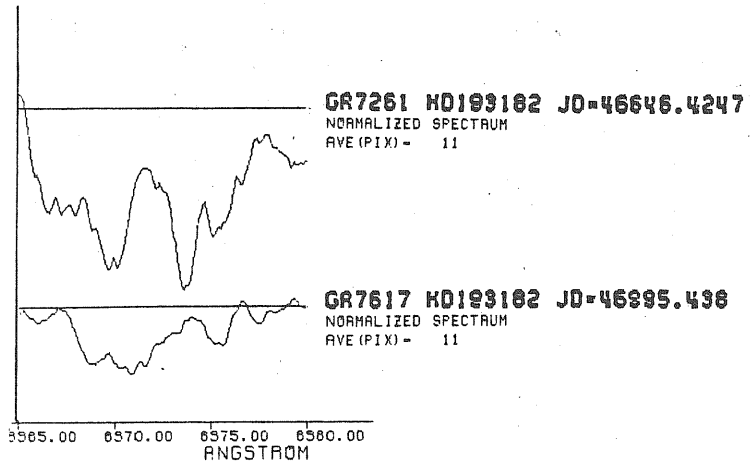

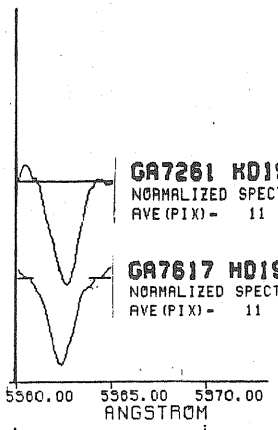

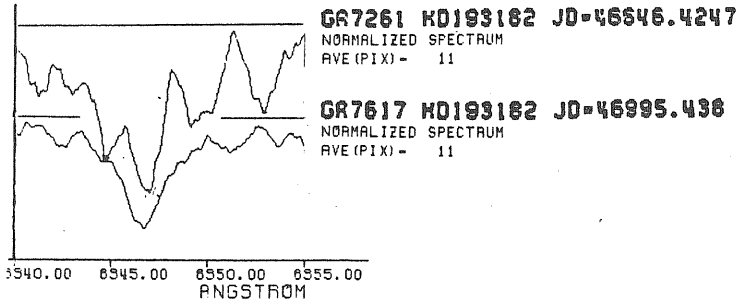

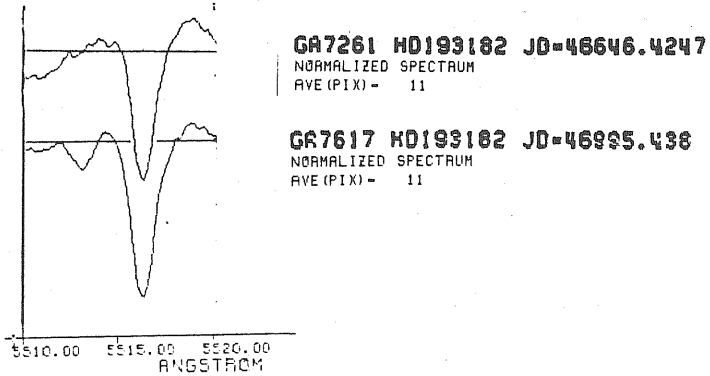

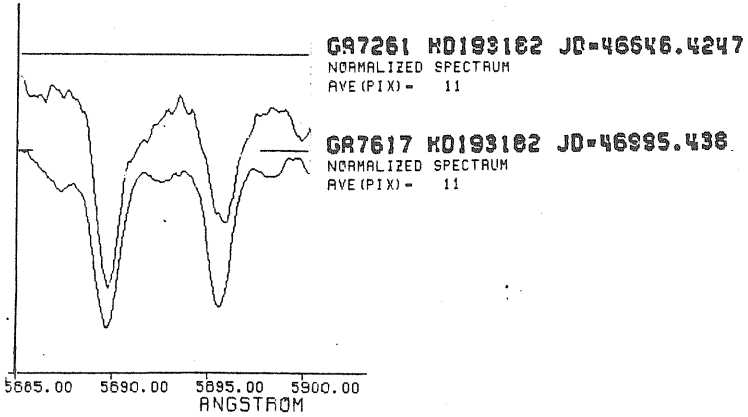

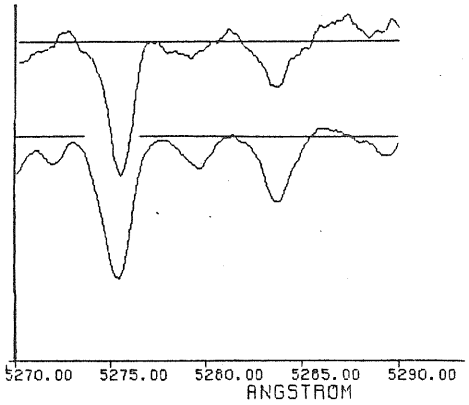

GA7261 HD193182 JD=46646.4247
NORMALIZED SPECTRUM
AVE(PIX)= 11

GA7617 HD193182 JD=46995.438
NORMALIZED SPECTRUM
AVE(PIX)= 11

FIGURE III.1.4.15

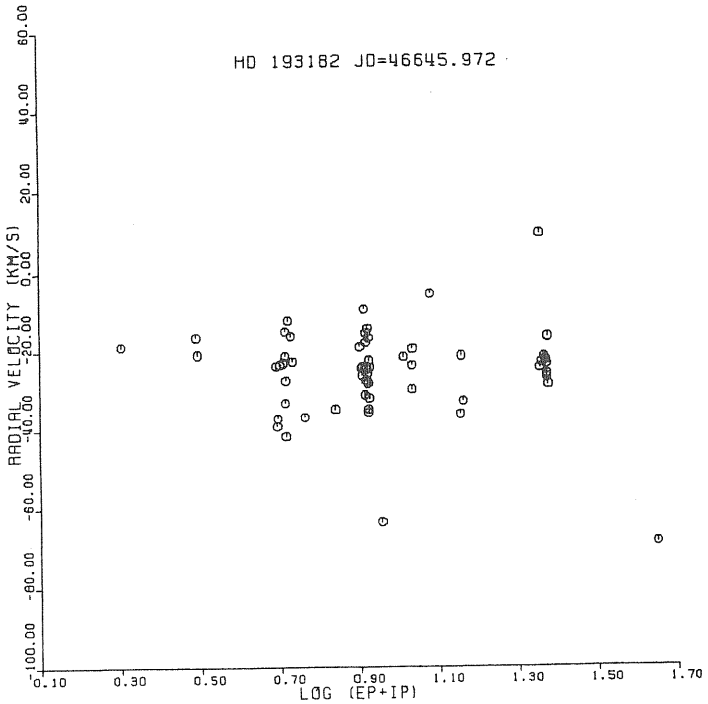

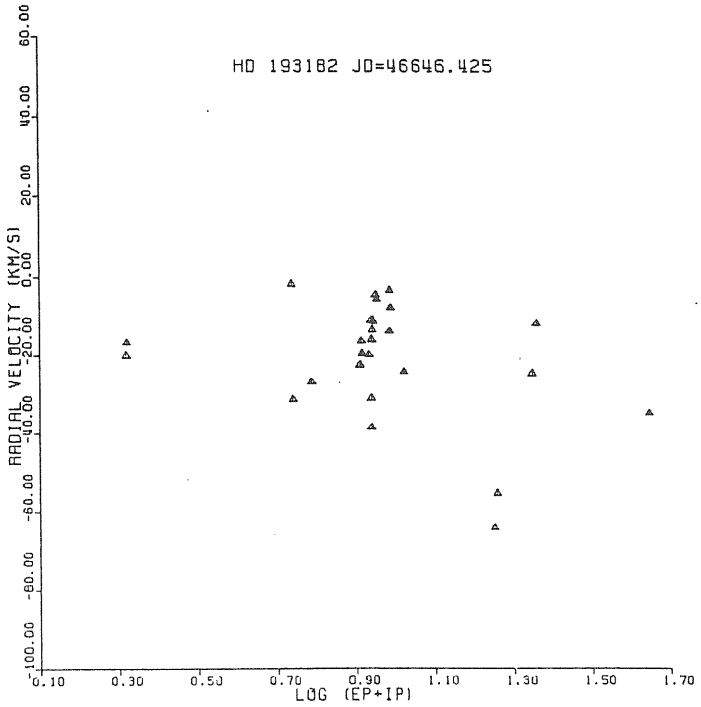

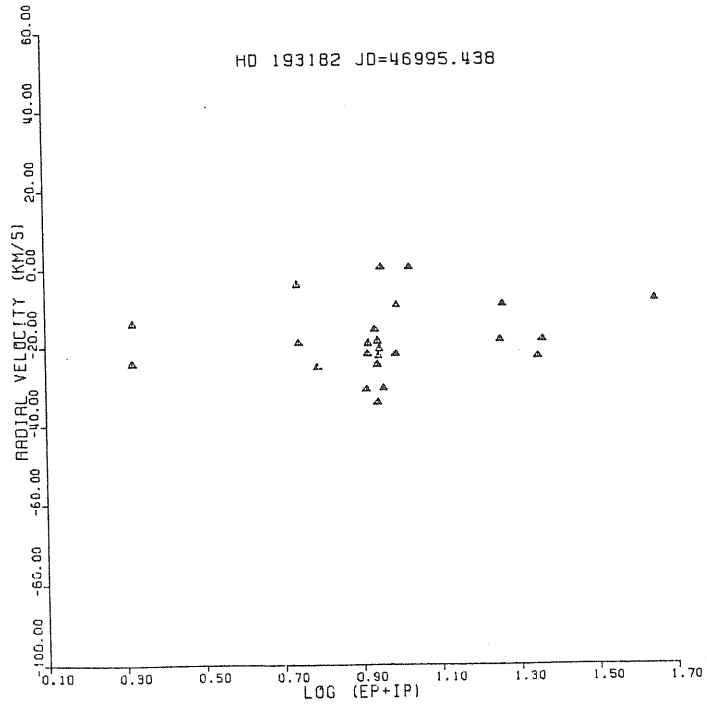

FIGURE III.1.4.16

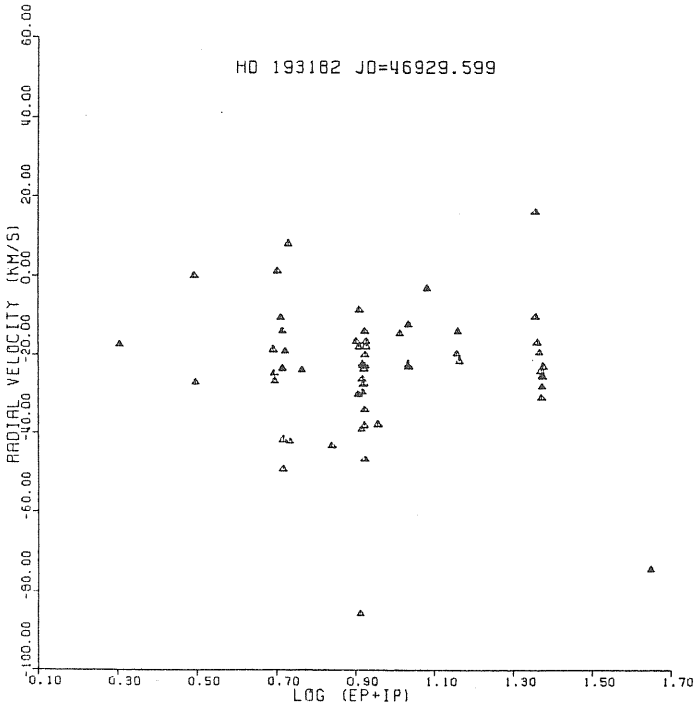

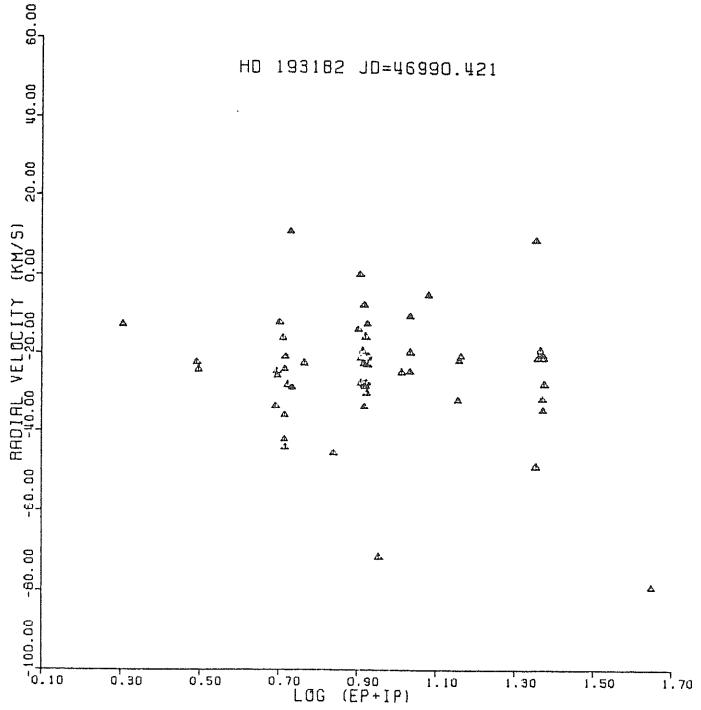

FIGURE III.1.4.17

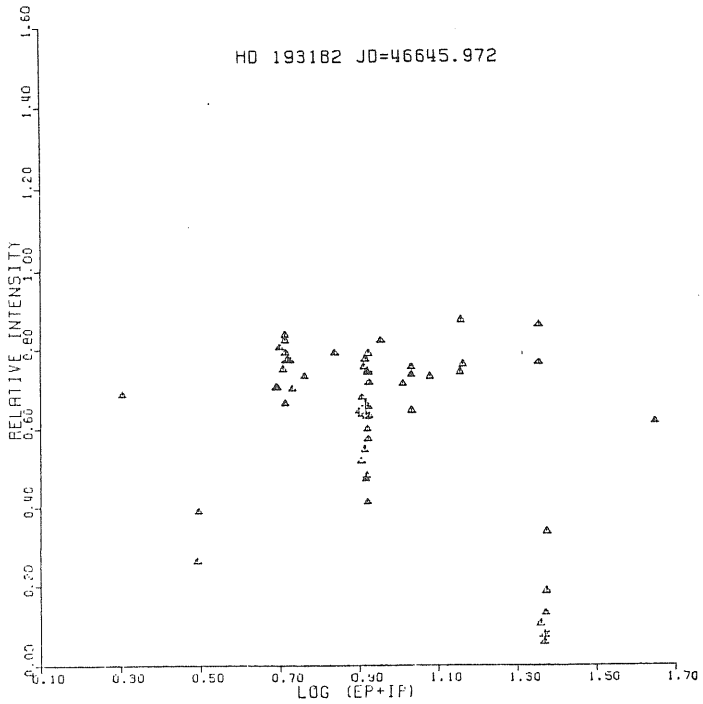

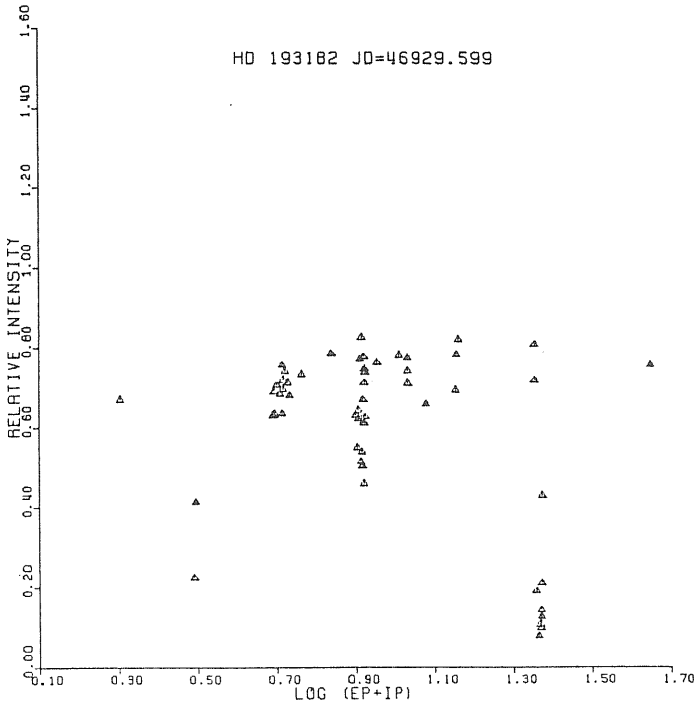

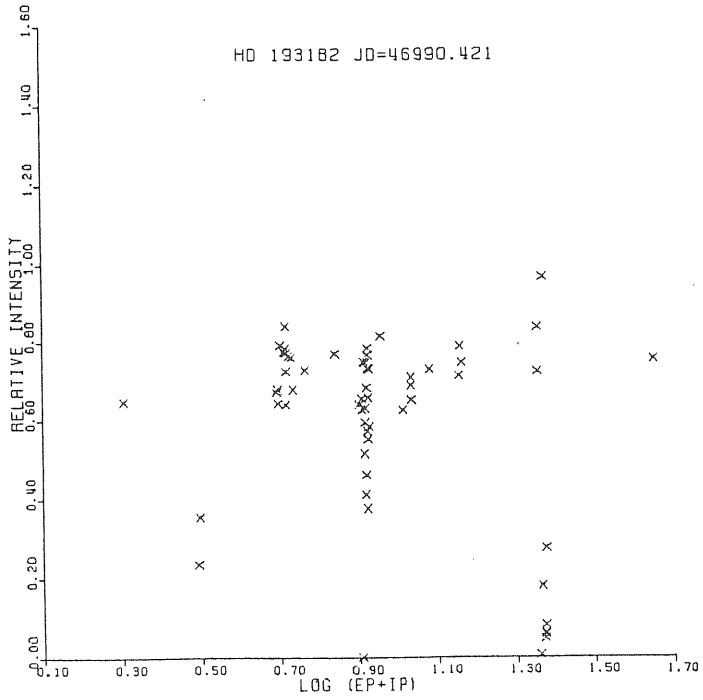

FIGURE III.1.4.18

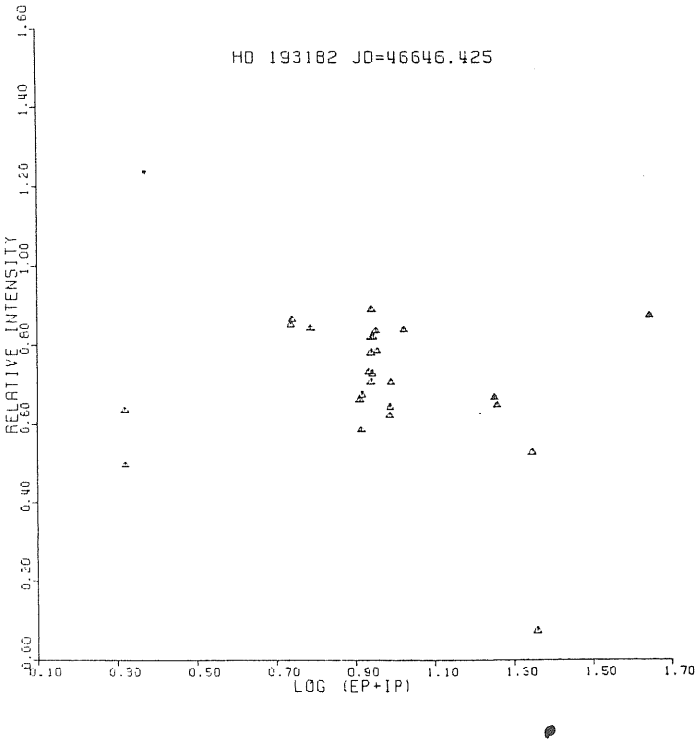

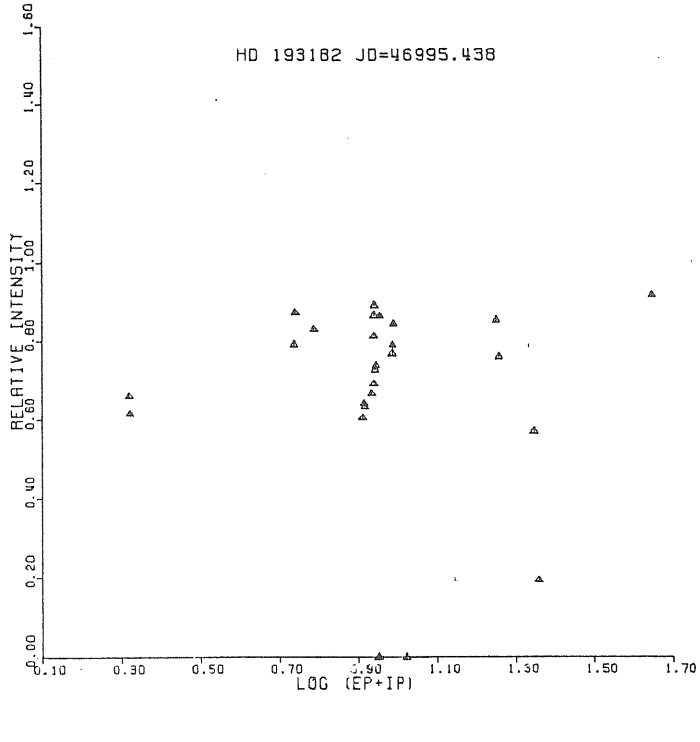

FIGURE III.1.4.19

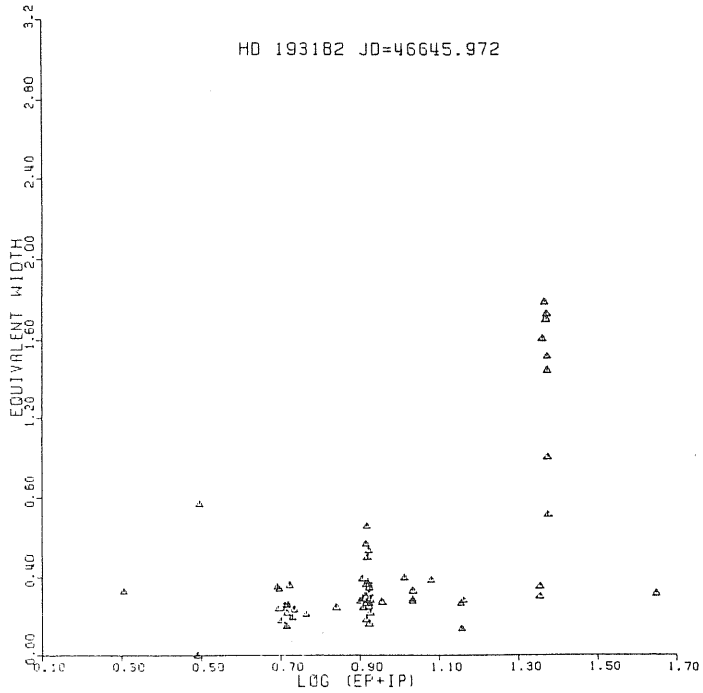

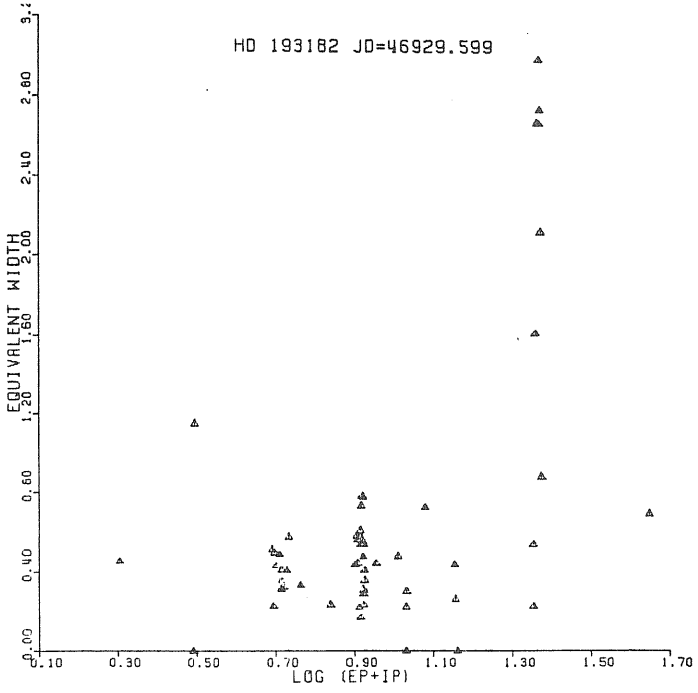

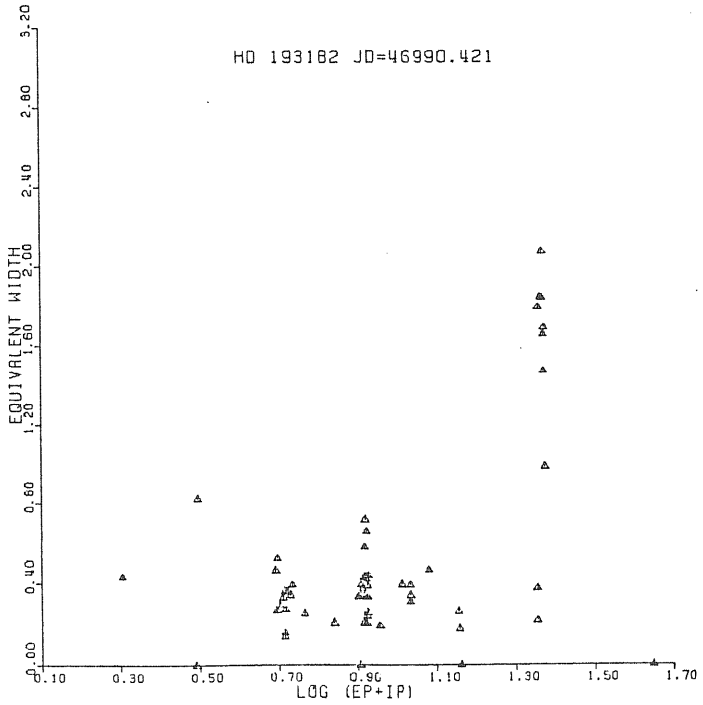

FIGURE III.1.4.20

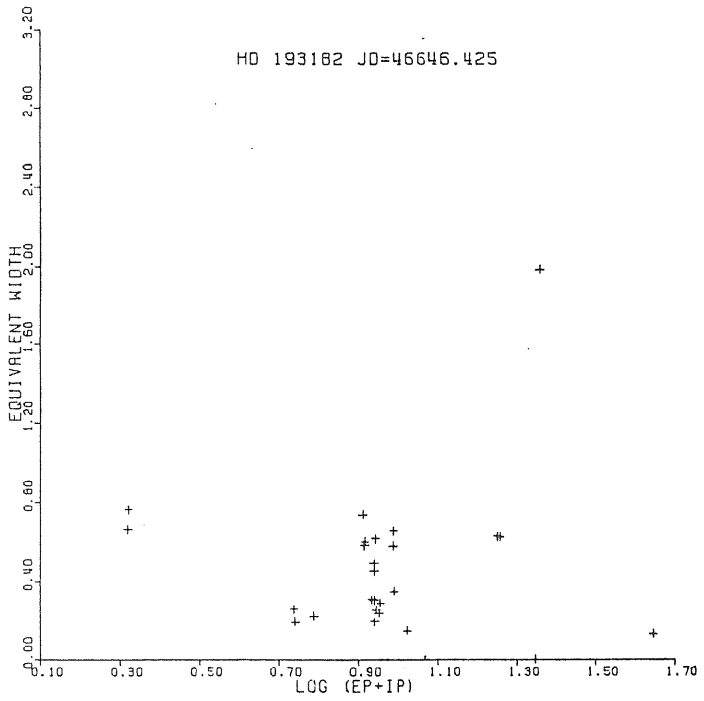

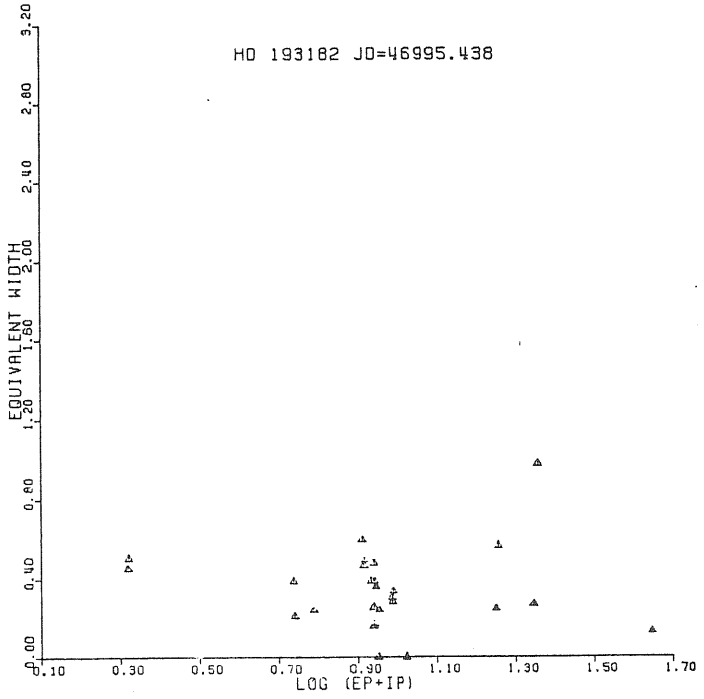

FIGURE III.1.4.21

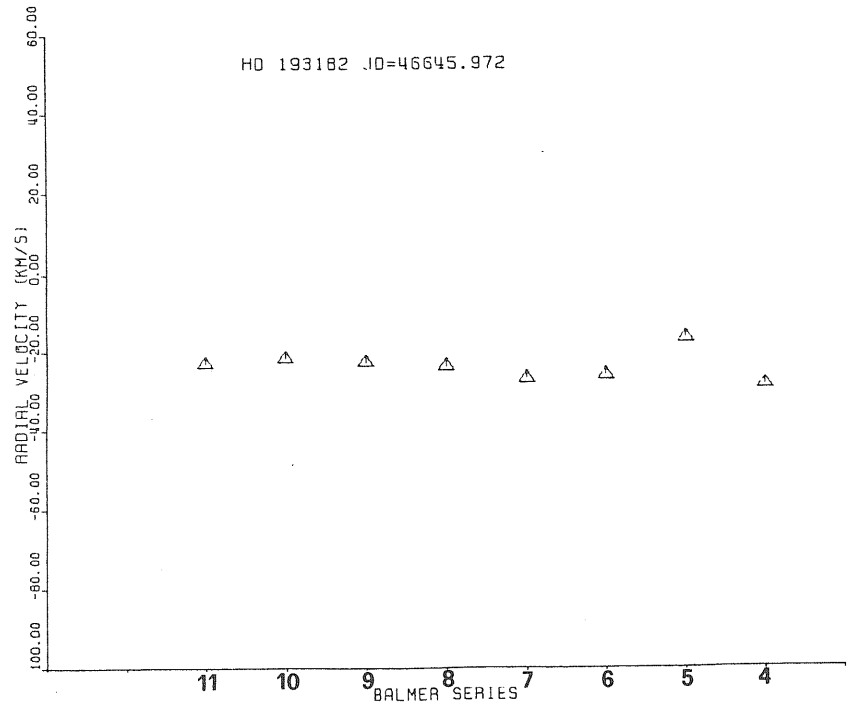

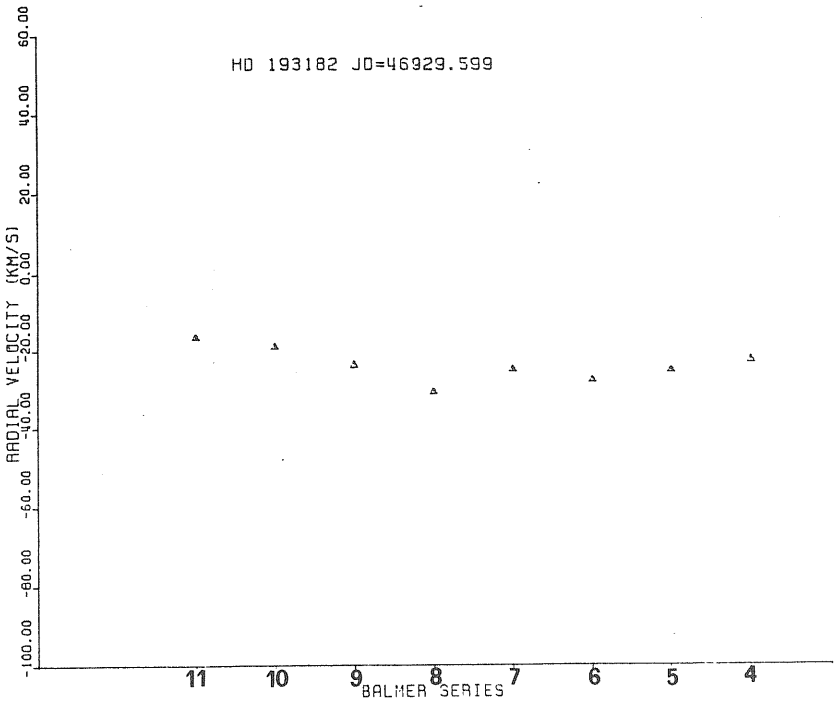

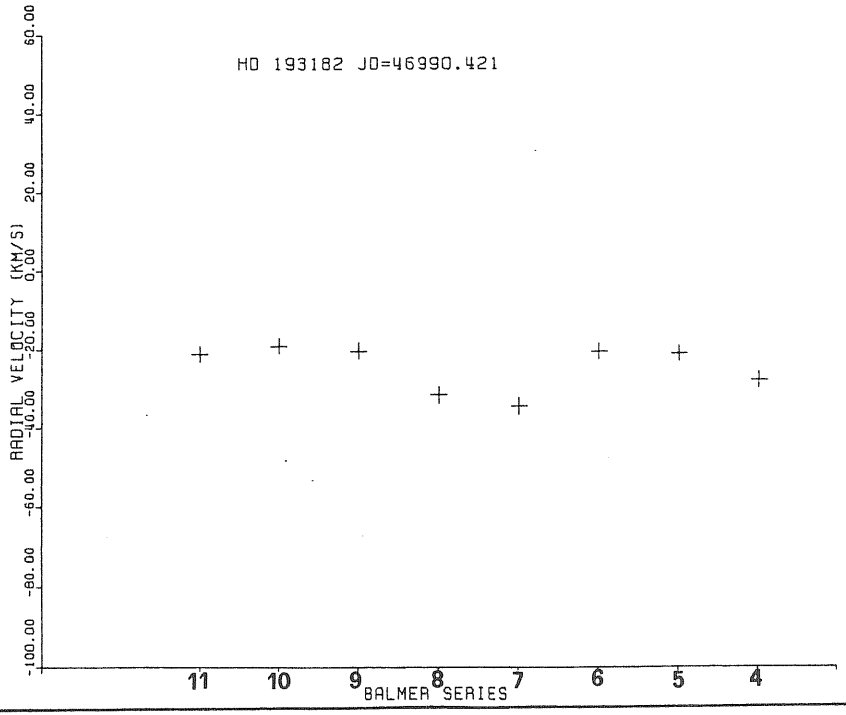

FIGURE III.1.4.22

Table III.1.4.1. Measured spectral line parameters of the absorption lines of HD 193182

HD 193182			JD= 46645.972					JD= 46929.599					JD= 46990.421				
ELEMENT	MULT.	λ(LAB)Å	λ(OBS)Å	Ic	FBWC	EQW(Å)	RV(km/s)	λ(OBS)Å	Ic	FBWC	EQW(Å)	RV(km/s)	λ(OBS)	Ic	FBWC(Å)	EQW(Å)	RV(km/s)
H 21	4	3679.4	3679.1	0.4	1.5	0.4	-21.0	3679.2	0.5	2.5	0.7	-13.0	3679.1	0.4	2.3	0.7	-19.2
H 20	4	3682.8	3682.5	0.6	1.6	0.4	-24.5	3682.5	0.6	2.2	0.5	-29.2	3682.4	0.4	1.7	0.5	-31.4
H 19	4	3686.8	3686.6	0.5	1.7	0.4	-19.4	3686.5	0.5	2.3	0.6	-26.3	3686.6	0.3	2.3	0.8	-21.7
H 18	4	3691.8	3691.1	0.4	1.6	0.5	-56.6	3691.2	0.5	2.7	0.7	-50.1	3691.2	0.3	2.4	0.9	-48.8
H 17	3	3697.2	3696.8	0.3	1.8	0.6	-30.0	3697.0	0.3	2.8	1.0	-15.7	3696.9	0.3	3.0	1.0	-25.1
H 16	3	3703.9	3703.6	0.1	1.9	0.8	-24.8	3703.7	0.4	2.7	0.8	-10.5	3703.5	0.3	3.3	1.2	-27.2
H 15	3	3712.0	3711.7	0.4	2.1	0.7	-26.4	3711.8	0.4	3.9	1.2	-16.9	3711.7	0.2	4.5	1.8	-25.9
H 14	3	3721.9	3721.7	0.2	2.0	0.8	-23.8	3721.7	0.4	3.8	1.2	-18.9	3721.6	0.1	2.3	1.0	-30.2
H 13	3	3734.4	3734.1	0.2	2.3	0.9	-23.5	3734.1	0.3	4.1	1.4	-23.3	3734.1	0.1	2.4	1.0	-20.1
H 12	2	3750.2	3749.9	0.2	2.6	1.0	-17.0	3749.8	0.2	4.3	1.7	-27.0	3749.9	0.1	3.7	1.7	-21.0
H 11	2	3770.6	3770.4	0.2	2.3	1.0	-16.0	3770.3	0.2	6.4	2.5	-23.6	3770.4	0.1	3.7	1.7	-21.2
H 10	2	3797.9	3797.6	0.2	3.5	1.4	-21.6	3797.6	0.2	5.8	2.4	-27.7	3797.6	0.1	3.8	1.8	-22.3
H 9	2	3835.4	3835.0	0.1	3.2	1.5	-30.2	3835.0	0.1	6.9	3.0	-28.1	3835.2	0.1	3.6	1.5	-18.5
H 8	2	3889.1	3888.7	0.1	3.1	1.5	-26.7	3888.7	0.1	7.6	3.3	-25.2	3888.6	0.1	3.1	1.5	-34.4
Ti II	34	3900.6	3900.3	0.7	1.6	0.2	-22.5	3900.0	0.7	3.6	0.6	-42.0	3900.2	0.7	2.4	0.4	-28.8
Fe II	173	3906.0	3905.6	0.7	2.1	0.3	-36.0	3905.8	0.7	2.9	0.4	-19.4	3905.6	0.7	1.9	0.3	-31.9
Ti II	34	3913.5	3913.3	0.8	1.7	0.2	-16.1	3913.6	0.7	2.9	0.4	8.1	3913.6	0.8	2.9	0.3	10.8
Ca II K	1	3933.7	3933.4	0.4	2.4	0.8	-20.7	3933.3	0.4	3.9	1.2	-26.7	3933.4	0.4	2.6	0.8	-24.1
Ca II H	1	3968.5	3968.3	0.3	-	-	-16.3	3968.5	0.2	-	-	0.1	3968.2	0.2	-	-	-22.3
H eps	1	3970.1	3969.8	0.1	3.8	1.7	-23.4	3969.7	0.1	5.9	2.7	-30.8	3969.7	0.1	4.3	2.1	-31.6
Cr II	183	4012.5	4012.2	0.9	2.2	0.1	-21.3	4012.3	0.8	2.5	0.3	-13.8	4012.2	0.8	1.6	0.2	-21.7
Fe II	127	4024.6	4024.5	0.7	2.9	0.4	- 5.6	4024.5	0.7	4.2	0.7	- 3.1	4024.5	0.7	3.4	0.5	- 5.1
H delt	1	4101.7	4101.4	0.1	3.6	1.7	-22.4	4101.4	0.1	6.7	3.0	-23.8	4101.5	1.0	3.8	1.8	-20.3
Si II	3	4128.1	4128.2	0.8	3.0	0.4	- 8.9	4128.3	0.7	3.8	0.5	-16.1	4128.2	0.7	2.7	0.4	- 8.9
Si II	3	4130.9	4130.6	0.9	2.6	0.3	-24.3	4130.8	0.8	2.4	0.2	-10.1	4130.2	0.8	2.6	0.2	-48.7
Fe II	27	4173.5	4173.1	0.7	1.5	0.3	-23.9	4173.3	0.6	2.6	0.5	- 8.5	4173.7	0.7	2.0	0.4	-27.5
Fe II	28	4178.9	4178.5	0.6	1.6	0.3	-26.2	4178.6	0.6	3.0	0.6	-17.7	4178.6	0.6	2.1	0.4	-21.0
Fe II	27	4233.2	4232.8	0.5	1.6	0.4	-24.4	4232.8	0.6	2.6	0.6	-29.9	-	-	-	-	
Ti II	41	4290.2	4289.6	0.8	2.3	0.3	-41.6	4289.6	0.7	2.9	0.4	-41.6	4289.6	0.7	2.0	0.3	-44.1
Ti II	20	4294.1	4293.8	0.8	1.8	0.2	-23.5	4294.1	0.7	2.9	0.4	1.2	4293.9	0.8	2.8	0.3	-12.2
Fe II	28	4296.6	4296.3	0.8	1.6	0.2	-17.7	4296.2	0.8	2.0	0.2	-25.9	4296.5	0.8	1.7	0.2	- 7.5
Fe II	27	4303.2	4302.8	0.7	1.6	0.3	-23.9	4302.8	0.6	3.1	0.6	-29.4	4302.8	0.6	2.3	0.4	-27.8
Ti II	41	4307.9	4307.7	0.8	2.7	0.2	-14.9	4307.6	0.8	2.7	0.3	-23.1	4307.3	0.8	1.8	0.1	-42.1
Fe II	32	4314.3	4314.2	0.8	2.5	0.3	- 9.3	4313.1	0.8	2.0	0.2	-85.4	4314.0	0.8	2.9	0.4	-19.3
Ti II	11	4321.0	4320.5	0.8	1.7	0.2	-33.0	4320.8	0.8	2.6	0.3	-13.9	4320.5	0.8	1.5	0.2	-35.8
Mn II	6	4325.1	4325.0	0.8	2.1	0.3	- 6.9	4325.2	0.7	2.2	0.3	4.2	4325.4	0.7	2.2	0.3	18.3
Ti II	41	4330.7	4330.3	0.8	2.4	0.3	-27.4	4330.0	0.7	2.7	0.4	-49.1	4330.4	0.8	3.1	0.4	-20.9
H gamma	1	4340.5	4340.2	0.1	3.9	1.8	-21.6	4340.2	0.1	5.8	2.7	-19.1	4340.2	0.2	4.5	1.8	-19.0
Fe II	27	4351.8	4351.3	0.5	2.5	0.6	-31.1	4351.2	0.5	2.5	0.6	-38.9	4351.4	0.5	1.8	0.4	-22.5
Ti II	93	4374.9	4374.3	0.8	2.4	0.3	-34.8	4374.2	0.8	2.2	0.2	-43.1	4374.2	0.8	1.8	0.2	-45.4

Table III.1.4.1.(continued)

HD 193182			JD= 46645.972					JD= 46929.599					JD= 46990.421				
ELEMENT	MULT.	λ(LAB)A°	λ(OBS)A°	Ic	FBWC(Å)	EQWC(Å)	RV(km/s)	λ(OBS)A°	Ic	FBWC(Å)	EQW(Å)	RV(km/s)	λ(OBS)A°	Ic	FBWC(Å)	EQW(Å)	RV(km/s)
Ti II	19	4395.0	4394.5	0.7	2.3	0.3	-36.9	4394.6	0.6	2.7	0.5	-26.4	4394.7	0.6	2.9	0.5	-25.6
Ti II	51	4399.8	4399.6	0.8	3.2	0.4	-12.2	4399.5	0.7	2.5	0.3	-18.9	4399.4	0.8	3.1	0.4	-28.0
Fe II	27	4416.8	4416.6	0.6	2.1	0.4	-14.3	4416.5	0.7	3.4	0.6	-23.4	4416.6	0.6	2.3	0.4	-15.6
Ti II	19	4443.8	4443.5	0.7	2.4	0.4	-23.8	4443.5	0.6	2.8	0.5	-18.4	4443.3	0.7	2.9	0.5	-33.6
Ti II	31	4468.5	4468.2	0.7	2.1	0.3	-18.7	4468.2	0.7	2.8	0.5	-17.2	4468.3	0.7	2.5	0.4	-12.7
He II	14	4471.5	4470.5	0.6	1.7	0.3	-68.9	4470.4	0.8	5.7	0.7	-74.3	4470.3	0.8	-	-	-78.9
Mg II	4	4481.1	4480.4	0.8	2.6	0.2	-48.1	4480.7	0.8	5.7	0.6	-27.0	4480.2	0.8	3.1	0.4	-64.1
Fe II	37	4489.2	4488.7	0.8	1.6	0.2	-34.7	4488.5	0.7	2.2	0.3	-46.6	4488.7	0.7	2.5	0.3	-30.2
Fe II	37	4491.4	4491.0	0.7	1.6	0.2	-24.2	4491.1	0.7	2.8	0.4	-17.6	4491.1	0.7	1.9	0.3	-20.5
Fe II	38	4508.3	4507.8	0.6	1.6	0.3	-31.9	4508.0	0.6	2.2	0.4	-16.2	4507.9	0.6	2.1	0.4	-22.9
Fe II	37	4515.3	4515.0	0.7	1.6	0.3	-22.4	4515.0	0.8	1.9	0.2	-22.4	4515.2	0.7	1.6	0.3	-12.4
Ti II	30	4520.4	4519.8	0.7	1.6	0.2	-38.9	4520.0	0.7	1.5	0.2	-24.6	4520.0	0.7	1.7	0.3	-24.6
Fe II	38	4522.6	4522.1	0.6	1.6	0.4	-35.6	4522.3	0.6	2.8	0.5	-19.7	4522.3	0.6	1.7	0.4	-22.4
Ti II	50	4534.0	4533.7	0.7	1.6	0.3	-21.1	4533.6	0.6	1.0	0.4	-27.3	4533.6	0.6	2.0	0.4	-23.9
Fe II	38	4549.5	4549.1	0.4	1.8	0.5	-25.7	4549.1	0.5	2.8	0.8	-24.9	4549.0	0.4	2.1	0.7	-28.6
Fe II	37	4555.9	4555.5	0.6	1.8	0.4	-27.7	4555.3	0.6	2.5	0.5	-37.9	4555.5	0.6	2.0	0.4	-27.5
Fe II	20	4558.6	4558.3	0.6	1.6	0.3	-18.8	4558.3	0.6	2.4	0.4	-16.4	4558.4	0.6	1.9	0.3	-13.9
Ti II	50	4563.8	4563.4	0.8	2.1	0.3	-23.0	4563.6	0.7	3.1	0.5	-10.4	4563.5	0.8	2.9	0.3	-15.9
Ti II	82	4572.0	4571.4	0.7	1.6	0.2	-36.7	4571.6	0.7	2.5	0.3	-23.7	4571.6	0.7	1.9	0.3	-22.4
Fe II	38	4576.3	4575.9	0.7	2.5	0.3	-28.2	4576.1	0.8	2.3	0.3	-13.8	4576.0	0.8	2.2	0.2	-21.2
Fe II	38	4583.8	4583.5	0.5	1.9	0.5	-24.5	4583.4	0.5	3.2	0.8	-27.3	4583.4	0.5	2.7	0.7	-28.4
Cr II	44	4588.2	4587.9	0.7	1.9	0.3	-19.4	4587.9	0.7	2.1	0.3	-22.8	4587.9	0.7	2.0	0.3	-19.6
Cr II	44	4618.8	4618.4	0.7	2.1	0.3	-29.8	4618.5	0.8	2.0	0.2	-22.1	4618.5	0.7	2.0	0.3	-24.4
Fe II	37	4629.3	4629.1	0.6	2.0	0.4	-15.4	4629.0	0.6	2.9	0.5	-22.0	4629.0	0.6	1.7	0.3	-22.4
Cr II	44	4634.1	4633.8	0.8	2.4	0.3	-23.6	4633.9	0.7	-	-	-12.2	4634.0	0.7	2.7	0.4	-10.5
Fe II	186	4635.3	4634.8	0.8	2.4	0.3	-32.7	4635.0	0.8	-	-	-21.2	4635.0	0.8	-	-	-20.6
Fe II	43	4731.4	4731.2	0.8	2.0	0.3	-16.7	4730.9	0.8	2.9	0.3	-33.9	4731.0	0.8	1.8	0.2	-27.3
Fe II	50	4780.6	4779.6	0.8	3.1	0.3	-63.5	4780.0	0.8	3.8	0.4	-37.7	4779.5	0.8	2.1	0.2	-71.5
Cr II	30	4824.1	4823.8	0.7	2.8	0.4	-21.5	4823.9	0.8	4.4	0.5	-14.4	4823.7	0.6	2.1	0.4	-24.7
H beta	1	4861.3	4861.0	0.1	3.6	1.6	-23.0	4861.1	0.2	4.0	1.6	-16.6	4860.9	0.0	3.6	1.8	-20.9
Fe II	42	4923.9	4423.5	0.5	2.5	0.7	-27.5	4923.6	0.5	3.2	0.8	-22.4	4923.4	0.4	2.0	0.6	-33.6

Table III.1.4.1.(continued)

HD 193182			JD= 46646.425					JD= 46995.438				
ELEMENT	MULT.	λ(LAB)Å	λ(OBS)Å	Ic	FBWC(Å)	EQW(Å)	RV(km/s)	λ(OBS)Å	Ic	FBWC(Å)	EQW(Å)	RV(km/s)
H beta	1	4861.3	4861.1	0.1	4.2	2.0	-11.9	4861.0	0.2	2.4	1.0	-18.6
Fe II	42	4923.9	4923.6	0.7	3.7	0.6	-19.4	4923.6	0.6	2.7	0.5	-19.3
Fe II	42	5018.4	5018.2	0.6	2.8	0.6	-16.3	5018.1	0.6	2.6	0.5	-21.9
Fe II	42	5169.0	5168.6	0.7	4.4	0.7	-22.4	5168.5	0.6	3.0	0.6	-30.9
Ti II	86	5183.7	5183.3	0.8	2.8	0.2	-26.8	5183.3	0.8	2.9	0.2	-25.3
Ti II	70	5188.7	5188.2	0.9	2.9	0.2	-31.2	5188.4	0.9	3.3	0.2	-19.1
Fe II	49	5197.6	5197.4	0.8	2.9	0.3	-11.1	5197.2	0.7	2.8	0.4	-20.7
Ti II	70	5226.5	5226.5	0.9	3.5	0.3	- 1.8	5226.5	0.8	3.8	0.4	- 4.3
Fe II	49	5234.6	5234.4	0.7	4.6	0.6	-13.4	5234.2	0.7	2.8	0.4	-22.5
Fe II	49	5254.9	5254.6	0.9	3.6	0.2	-15.9	5254.6	0.9	3.1	0.2	-18.7
Fe II	49	5276.0	5275.5	0.7	3.4	0.5	-30.9	5275.6	0.7	3.1	0.5	-24.9
Fe II	49	5316.6	5316.3	0.7	2.3	0.3	-19.8	5316.3	0.7	2.3	0.4	-15.7
Fe II	48	5262.9	5362.7	0.8	2.8	0.3	-10.9	5362.4	0.8	2.7	0.3	-24.6
Cr II	50	5508.6	5508.2	0.8	1.9	0.2	-24.3	-	-	-	-	-
Fe II	55	5534.9	5534.2	0.8	2.5	0.5	-38.4	5534.2	0.9	2.3	0.2	-34.3
Fe II	57	5627.5	5627.4	0.8	2.9	0.2	- 4.4	-	-	-		
Fe II	57	5657.9	5657.8	0.8	2.7	0.3	- 5.5	5657.3	0.9	3.6	0.2	-30.8
Na I	1	5890.0	5889.6	0.5	3.0	0.8	-16.6	5889.7	0.6	2.7	0.5	-13.9
Na I	1	5895.9	5895.5	0.6	3.7	0.7	-19.9	5895.5	0.7	2.7	0.5	-24.1
Fe II	74	6147.7	6147.6	0.7	2.4	0.4	- 7.9	6147.5	0.9	4.3	0.3	- 9.5
Fe II	74	6247.6	6247.5	0.6	3.7	0.7	- 3.3	6247.1	0.8	2.7	0.3	-22.0
Si II	2	6347.1	6345.9	0.6	3.6	0.6	-55.2	6346.9	0.8	4.7	0.6	- 9.6
Si II	2	6371.4	6370.0	0.7	3.8	0.6	-64.0	6371.0	0.9	3.4	0.3	-18.6
Fe II	74	6456.4	6456.1	0.6	3.1	0.6	-13.7	6455.9	0.8	2.7	0.3	-22.1
H alpha	1	6562.8	6562.3	0.5	-	-	-24.7	6562.3	0.6	1.2	0.3	-22.9
He I	46	6678.2	6577.4	0.9	2.2	0.1	-34.7	6678.0	0.9	3.1	0.1	- 8.5

III.1.5.HD 200775

We present four H alpha profiles of HD 200775 in Figure III.1.5.1.As seen from the figure, during the observation period H alpha profiles exhibited a variable strong blue-dominated emission, except one night accompanied with central absorption components or depressions (it is difficult to decide).Measured spectral line parameters of the H alpha emission components are presented in Table III.1.5.1.One interesting feature was that the total width of the emission profiles (V+R) remained approximately the same, although the profile changed its shape substantially during the observation period.The wings of the emission features extend from -750 km/s to 500 km/s. From the profiles and their measurements we see blue-dominated emission which in the frame of the rotating disk can only be interpreted as an inflow of matter.

Figure III.1.5.2 presents the H beta profiles of the star,observed approximately the same time with the H alpha profiles.Profiles were composed of a double-peak emission with a central depression.Probably self absorption components were also present and blending with classical Be double-peak central depression which we described in the beginning of this chapter.The intensity and equivalent widths of the emission wings and central component were variable.Measured spectral parameters for H beta are listed in Table III.1.5.2.Also Table III.1.6.3 presents the same data for all the other lines.H beta line profiles are also blue-dominated like H alpha.

H gamma, delta and epsilon profiles also exhibited profile variations. Profiles are composed of a central absorption superimposed on a wide stellar component.Both wings of the central absorption components presented emission features from H gamma to H epsilon with a decreasing intensity (Figures III.1.5.3 to III.1.5.5).At JD=647.6 H gamma exhibited a symmetric double emission peak at the wings of the central absorption component.During the other observing nights it faded away.

Also for the rest of the spectral features, such as [Fe II] emission lines, Ca II and He I lines HD 200775 exhibited notable variations.Figures III.1.5.6 to III.1.5.11 present them.Selected lines are listed in figure captions.In Figure III.1.5.6 we see an evident double-peak absorption components for the higher members of the Balmer series of H.Also He I 4471 line exhibited an interesting sequences of the profile variation.For example at JD=647.6 the profile was without a shell component with several blue shifted components, at JD=715.4 a shell component appeared , later both shell and stellar components increased in central depth without any other components, lastly at JD=987.5 the blue shifted components appeared again.

Now let's give a look to the diagrams constructed with spectral measurements versus log (EP+IP) of each line.Figure III.1.5.12 presents this for RVs.At JD=715.5 compared with JD=647.6 we see small but evident changes in the RVs. While

Fe II, [Fe II], He I and C II were increasing slightly H and Ca II lines decreased in RVs.At JD=931.5 Ca II, H ,He I lines remained the same, although Fe II, [Fe II] lines decreased, and C II lines increased.Lastly at JD=987.5 Ca II, H increased while the rest of the lines remained at their previous values. In this plot we didn't included the double components of H and He I lines which could cause a big confusion.If we include them we can give as conclusion that HD 200775 had a very complex radial velocity structure which was not easy to model.Similarly relative intensities and EQWs presented very little variation (Figures III.1.5.13 and III.1.5.14).We must remark here that the measurements of the spectral parameters of this star were very difficult because of the observed multi components in the lines which can be easily seen from the figures mentioned above.So the measured calmness of the envelope of HD 200775 is illusary, because the observed higher members of H and He lines suggest a variable multi-component velocity field for the envelope of this star.Figure III.1.5.15 presents RVs of the Balmer lines versus quantum numbers.At JD=642.6 and JD=715.5 HD 200775 presented an inverse Balmer progression and had more negative values without any progression at JD=931.5 and JD=987.5. From the figure one can easily see how the very simple RV behavior of the HD 200775 can substantially change if we plot only several of the observed secondary components with the main components (JD=987.1).

HD 200775 is one of the hottest and brightest Herbig Ae and Be stars.Our particular interest was to give a contribution to the few detailed spectroscopic analysis and compare this probably very young object with conventional or classic Be stars.As we outlined in the second chapter Baschek et al. (1982) performed a comparative study of this star, the comparison of our data with theirs and Viotti's (1969) are given in Tables III.1.5.4 and III.1.5.5.Total EQWs measured by Baschek et al(1982) were much more larger than our measurements for H alpha and beta emission components but [Fe II] EQWs were approximately similar.In the case of absorption spectra we see the EQWs are similar.But in our measurements at JD=931.5 EQWs are larger than the others except for two lines.

Table and Figure captions.

Figure III.1.5.1.H alpha profiles of HD 200775, same as figure III.1.1.1 but every interval on the "y" axis corresponds to 1.0 continuum units.

Figure III.1.5.2.H beta profiles of HD 200775, same as figure III.1.1.2.

Figure III.1.5.3.H gamma profiles of HD 200775,same as previous figure.

Figure III.1.5.4.H delta profiles of HD 200775,same as previous figure.

Figure III.1.5.5.H epsilon profiles of HD 200775,same as previous figure.

Figure III.1.5.6.Selected Hydrogen Balmer lines (H9-H13) of HD 200775.

Figure III.1.5.7.H 8, He I 3926, Ca II 3933, lines of HD 200775.

Figure III.1.5.8.He I 4009,4026, C II 4265, [Fe II] 4287 lines of HD 200775.

Figure III.1.5.9.He I 4387, [Fe II] 4413,4416, Mg II 4481, He I 4471 lines of HD 200775.

Figure III.1.5.10.Fe II 4582,4923, He I 4921 lines of HD 200775.

Figure III.1.5.11.RV's versus log(EP+IP) of HD200775 for blue spectra.Log (EP+IP) values same as HD 22192 for line groups, except for [Fe II]=(0.442-0.471).

Figure III.1.5.12.Relative intensities versus log(EP+IP)

of HD 200775 for blue spectra.

Figure III.1.5.13.EQW's versus log(EP+IP) of HD 200775 for blue spectra.

RV's of the Balmer lines versus "n" quantum numbers for HD 200775.

Table III.1.5.1.Spectral measurements of H alpha emission lines of HD 200775.

Table III.1.5.2.Spectral measurements of H beta emission lines of HD 200775.

Table III.1.5.3.Spectral line measurements of the HD 200775.

Table III.1.5.4.Comparison of our spectral line measurements with Baschek et al.(1982) and Viotti(1969).

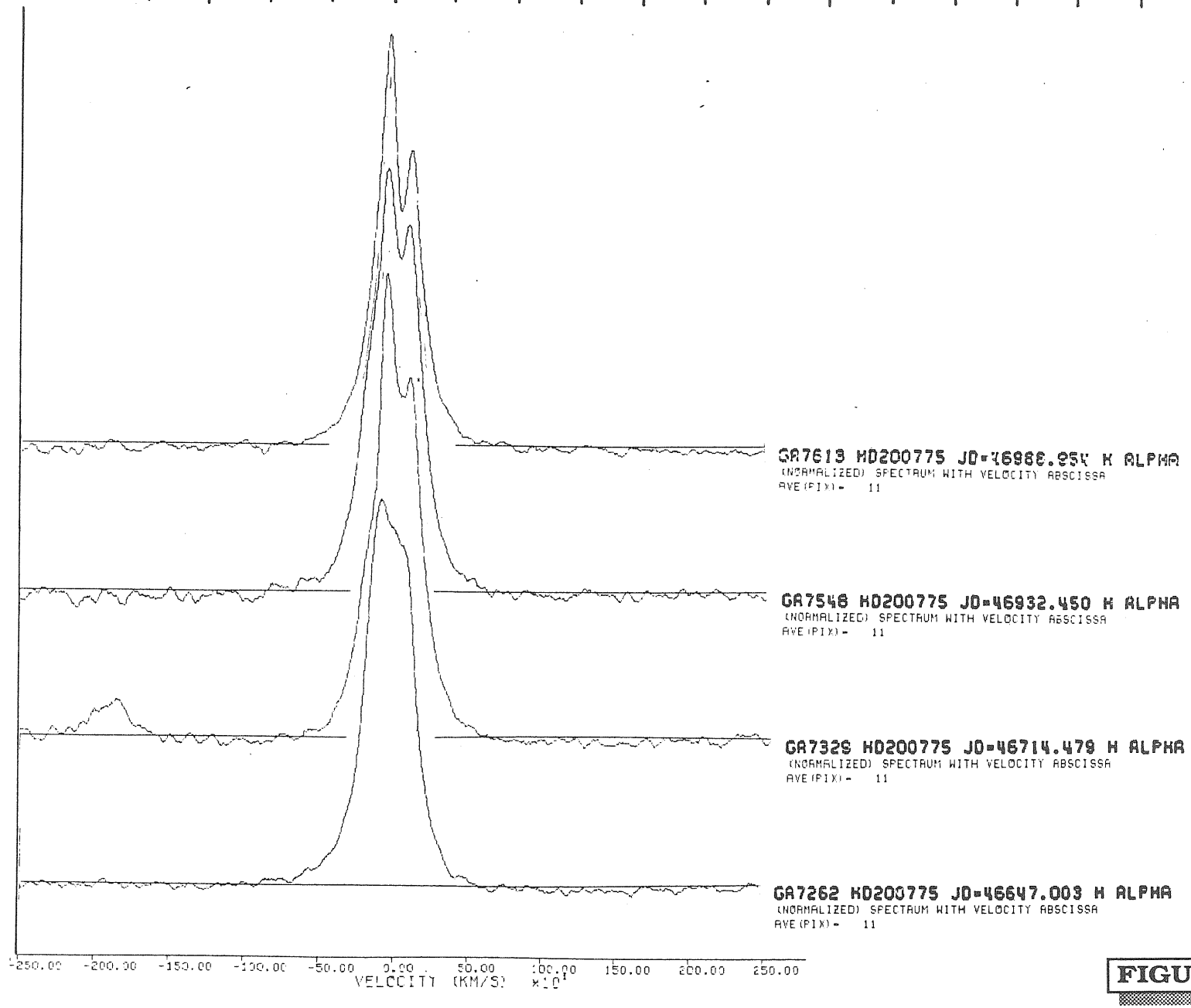

FIGURE III.1.5.1

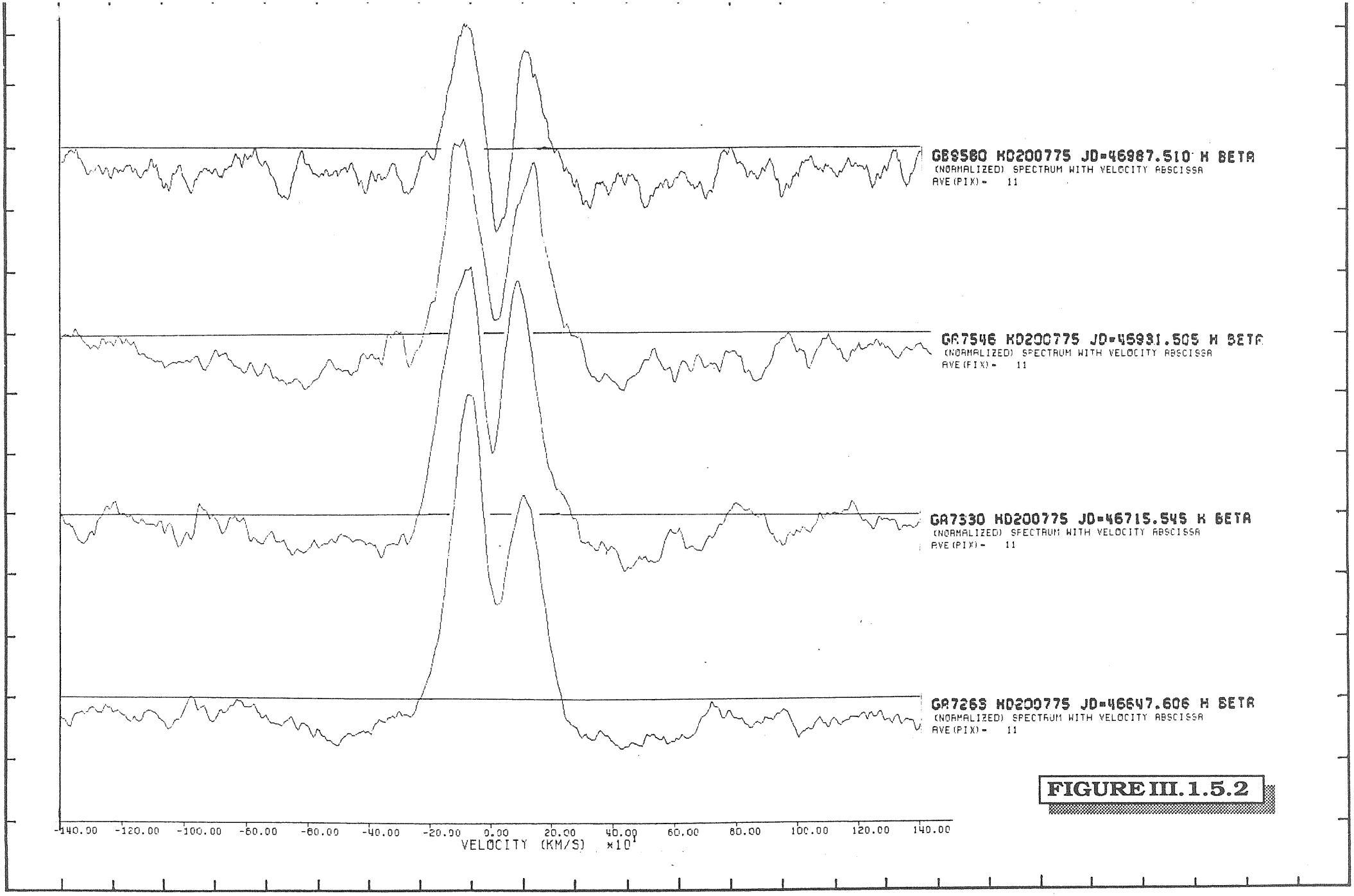

FIGURE III.1.5.2

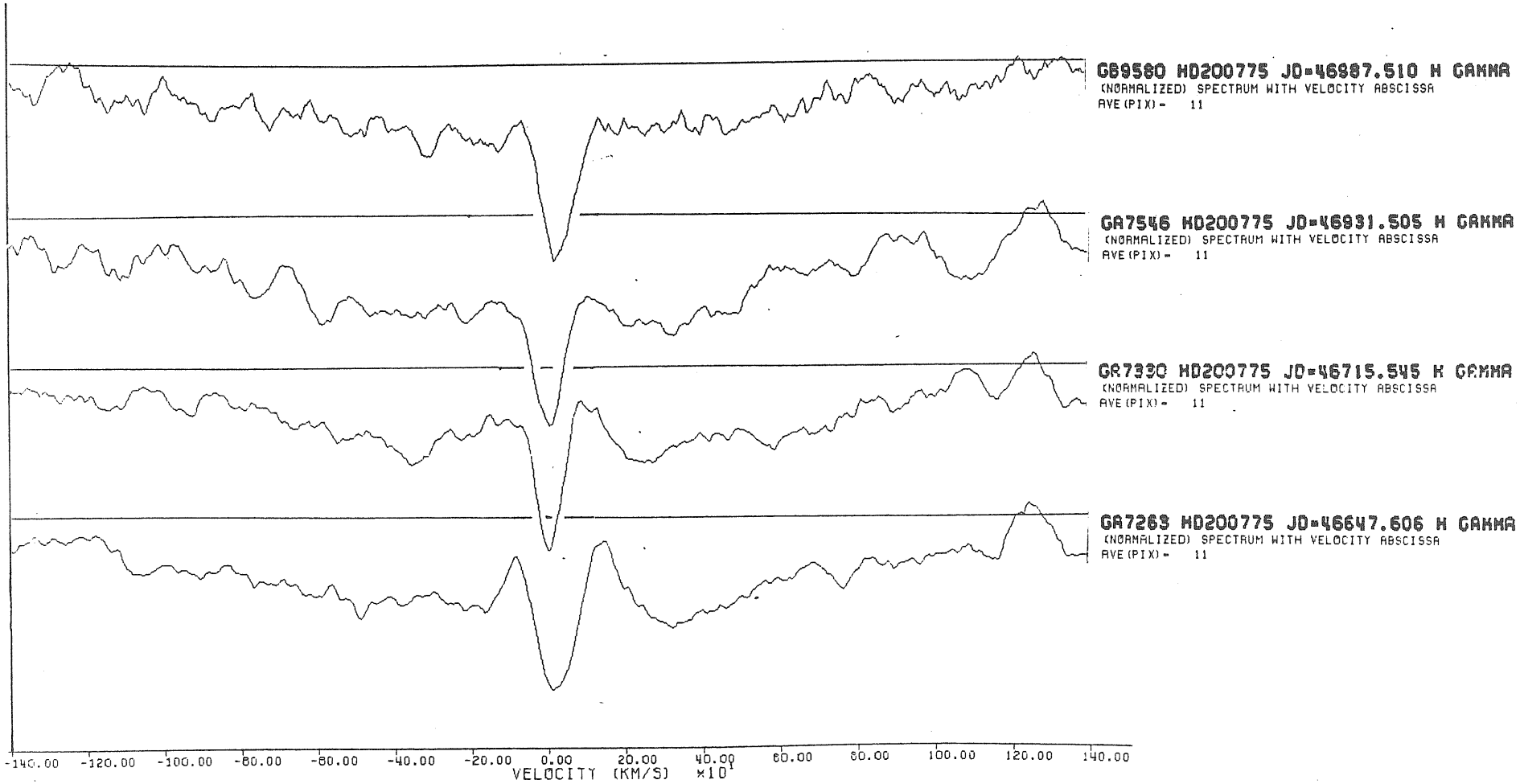

FIGURE III.1.5.3

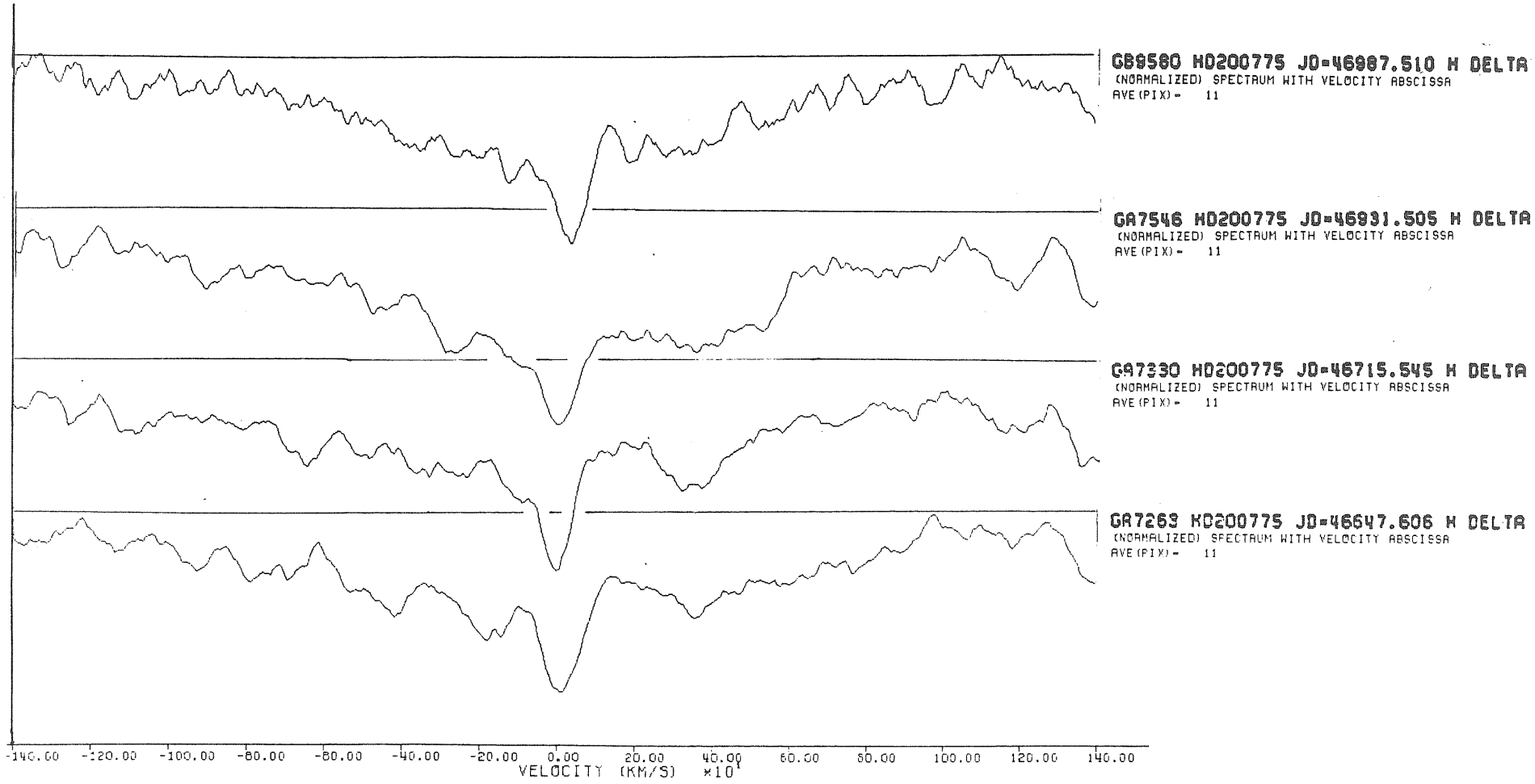

FIGURE III.1.5.4

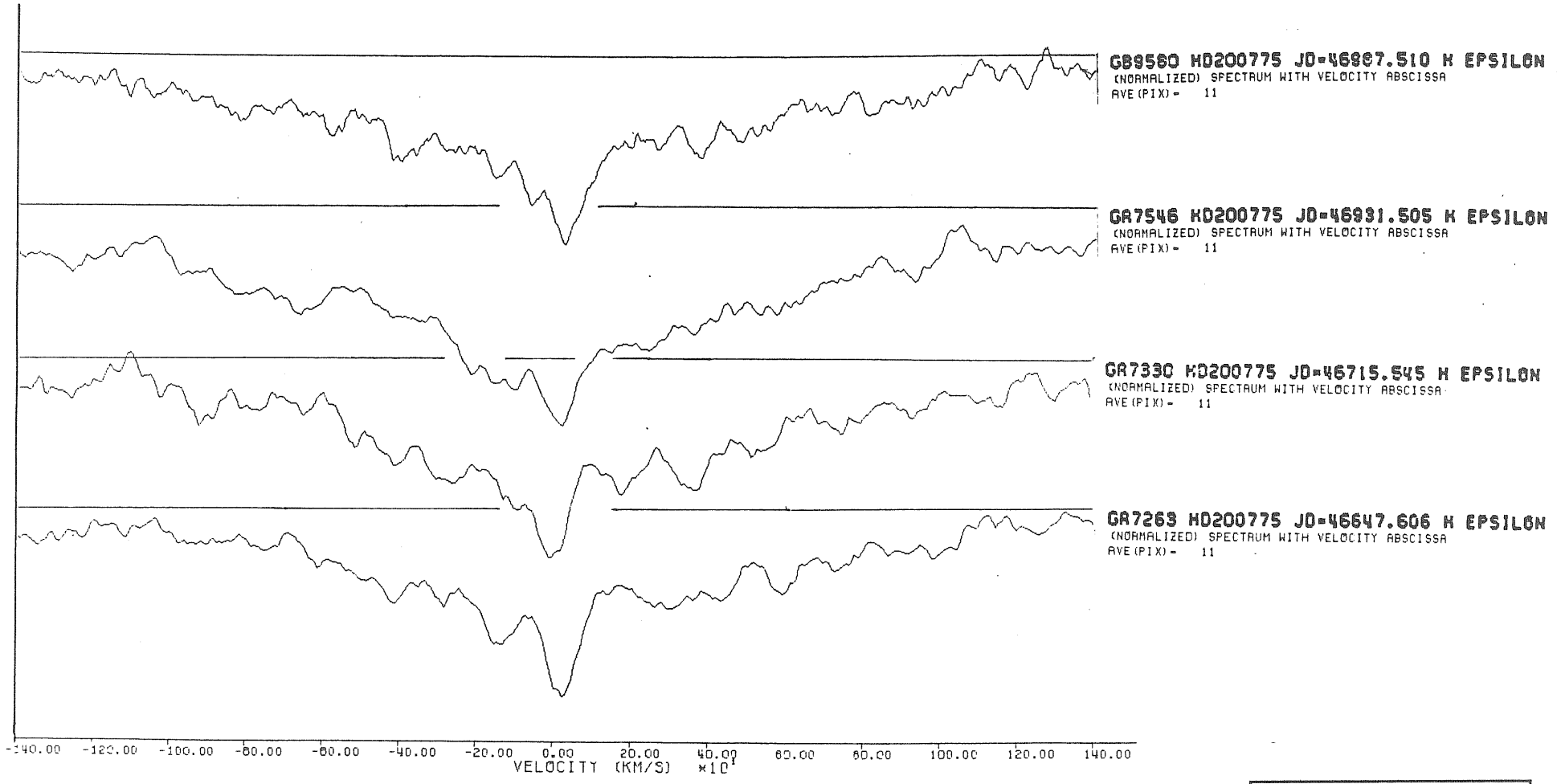

FIGURE III.1.5.5

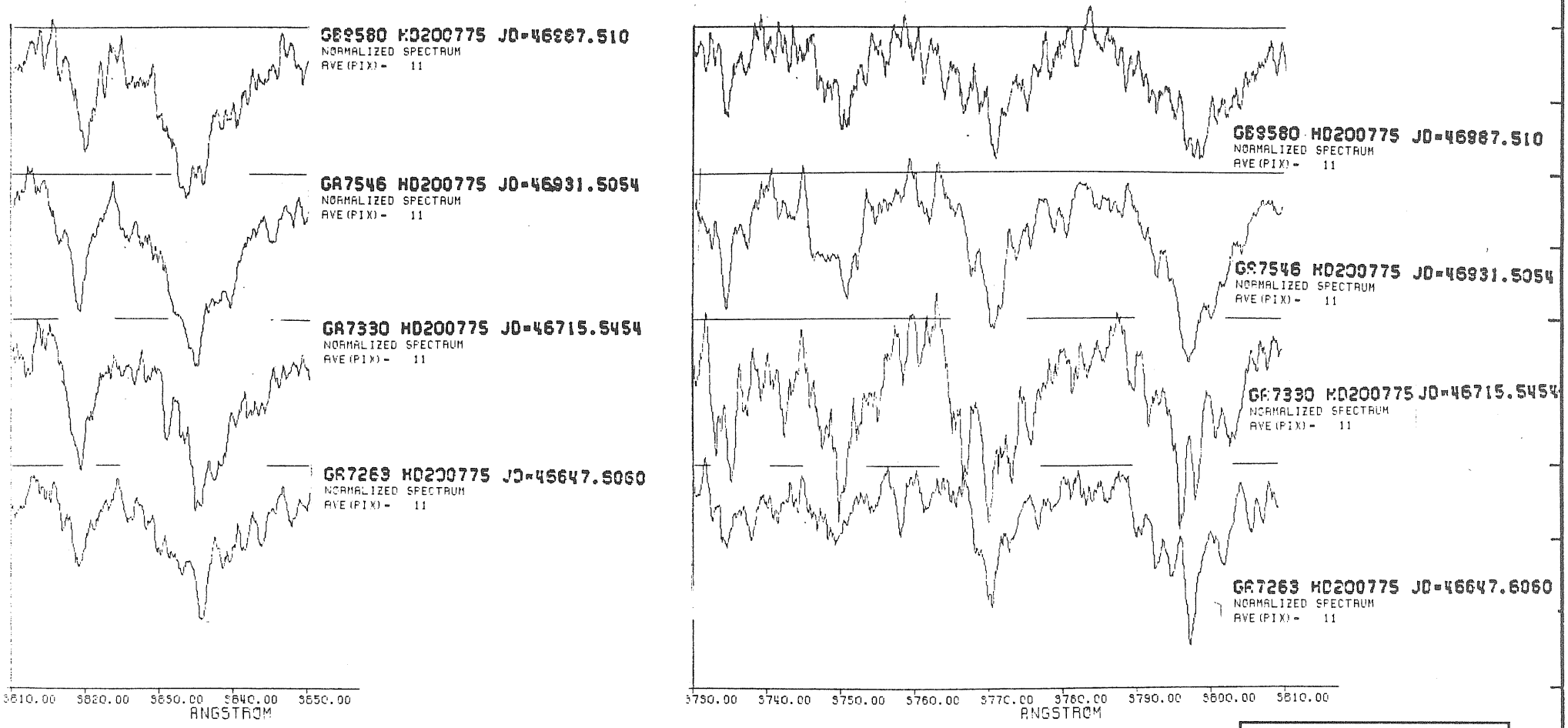

FIGURE III.1.5.6

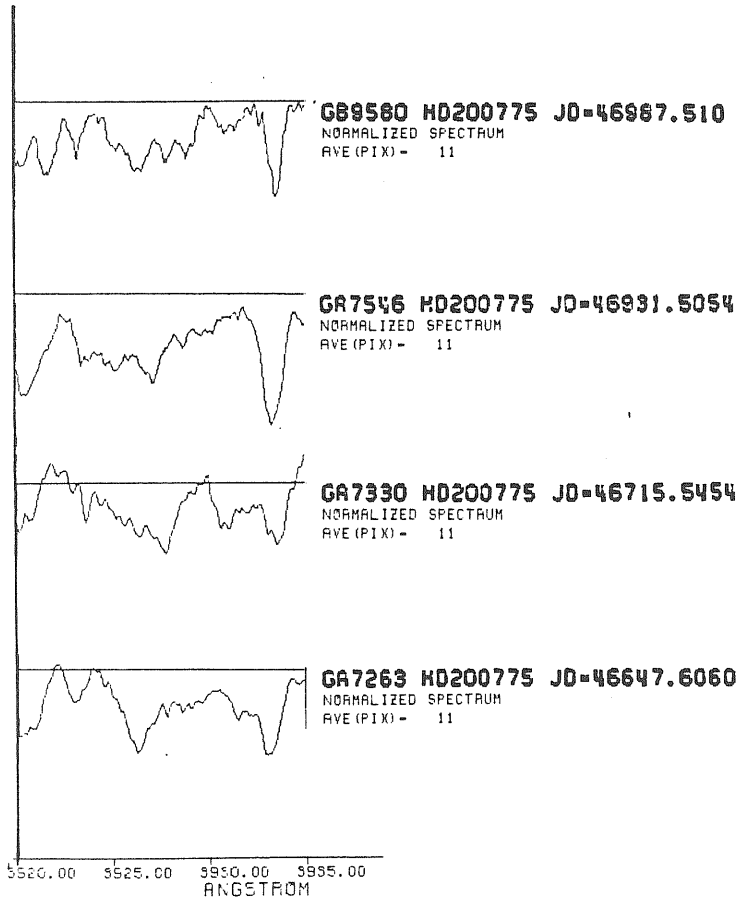

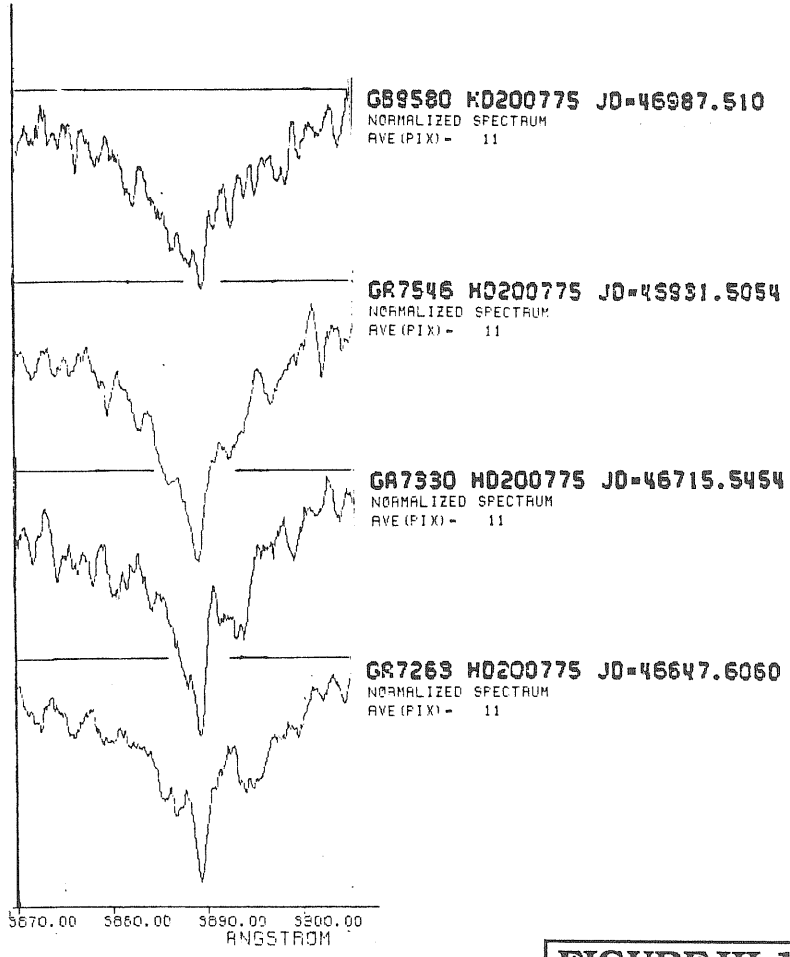

FIGURE III.1.5.7

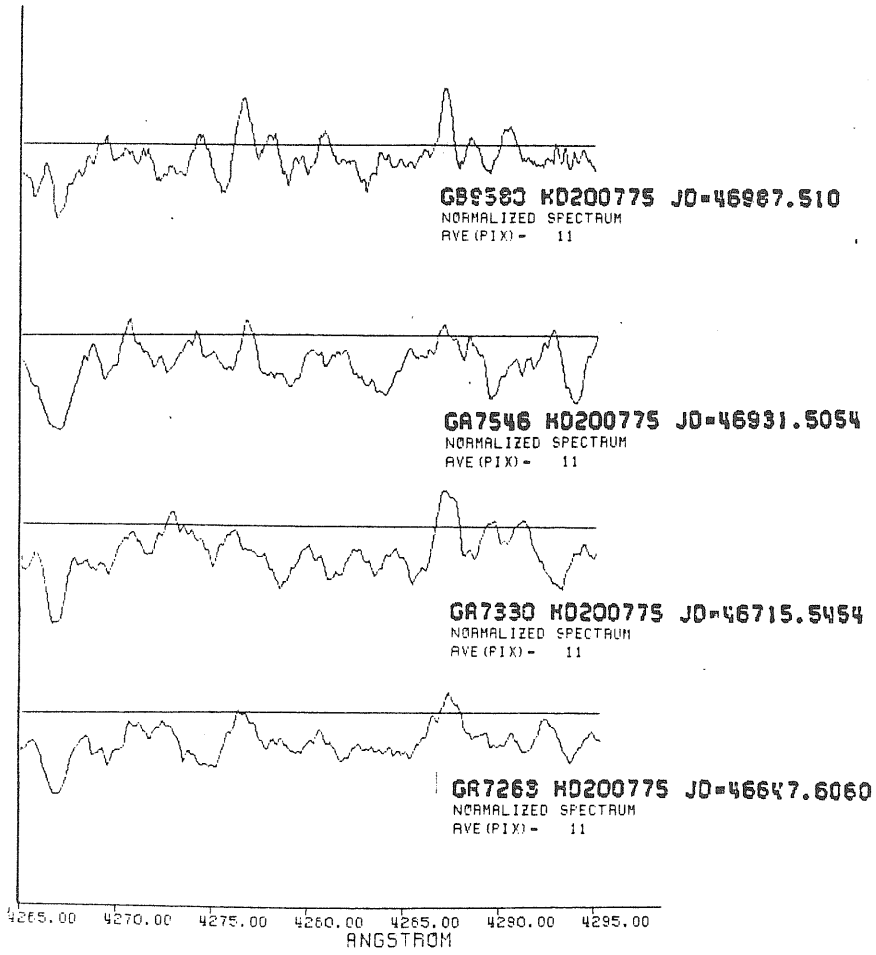

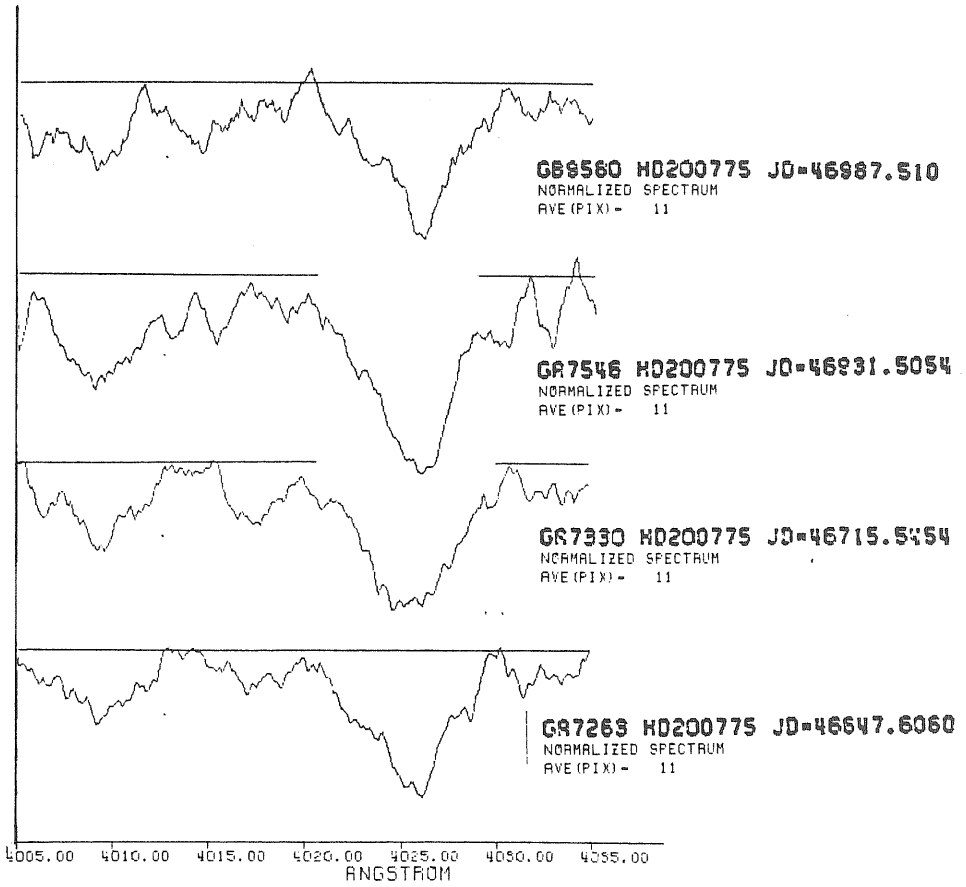

FIGURE III.1.5.8

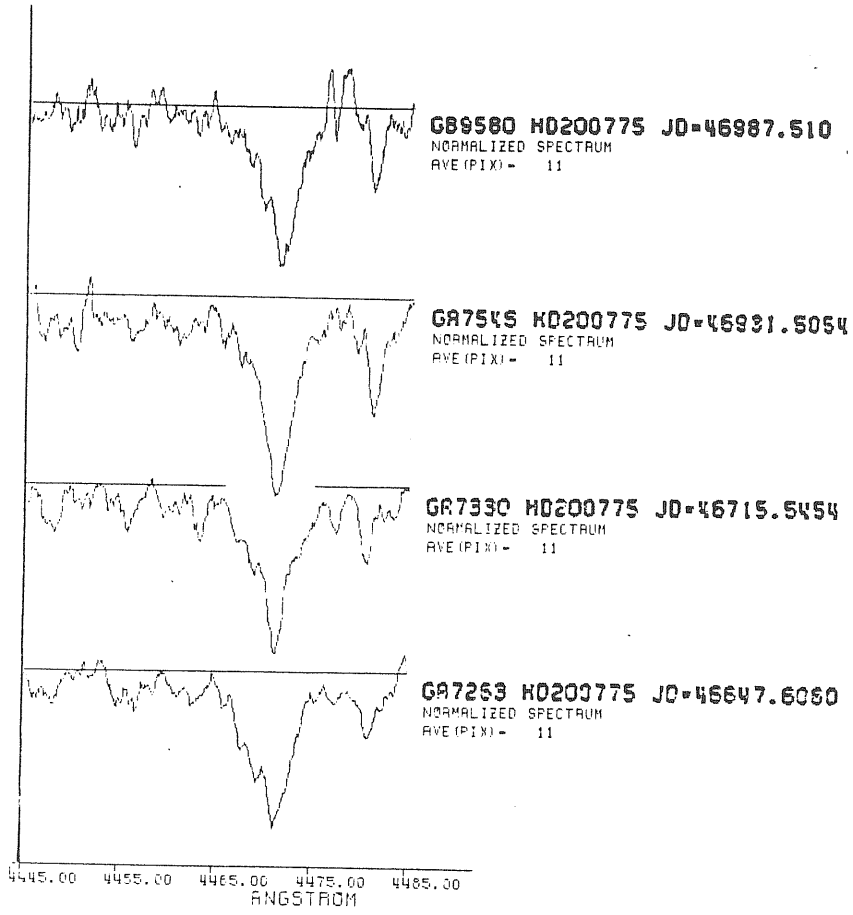

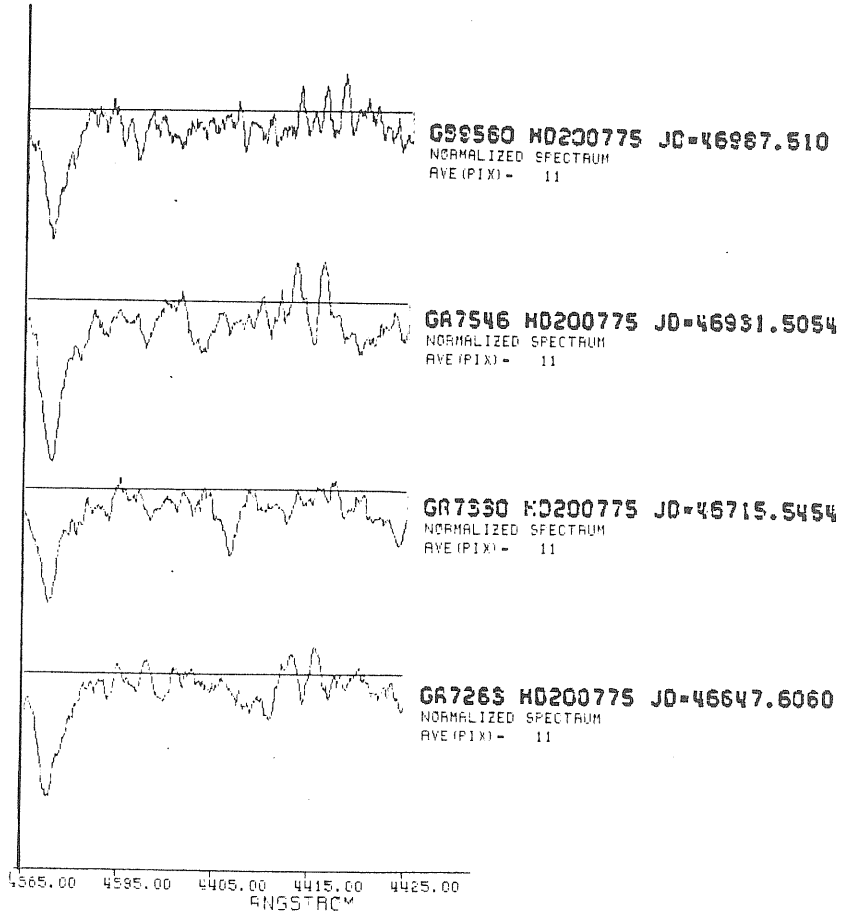

FIGURE III.1.5.9

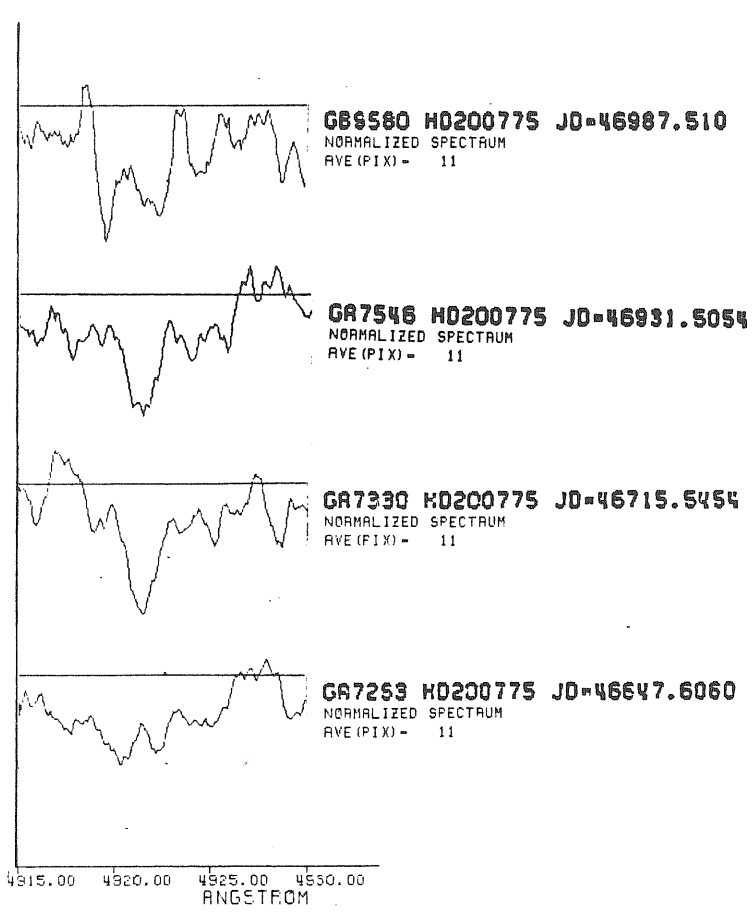

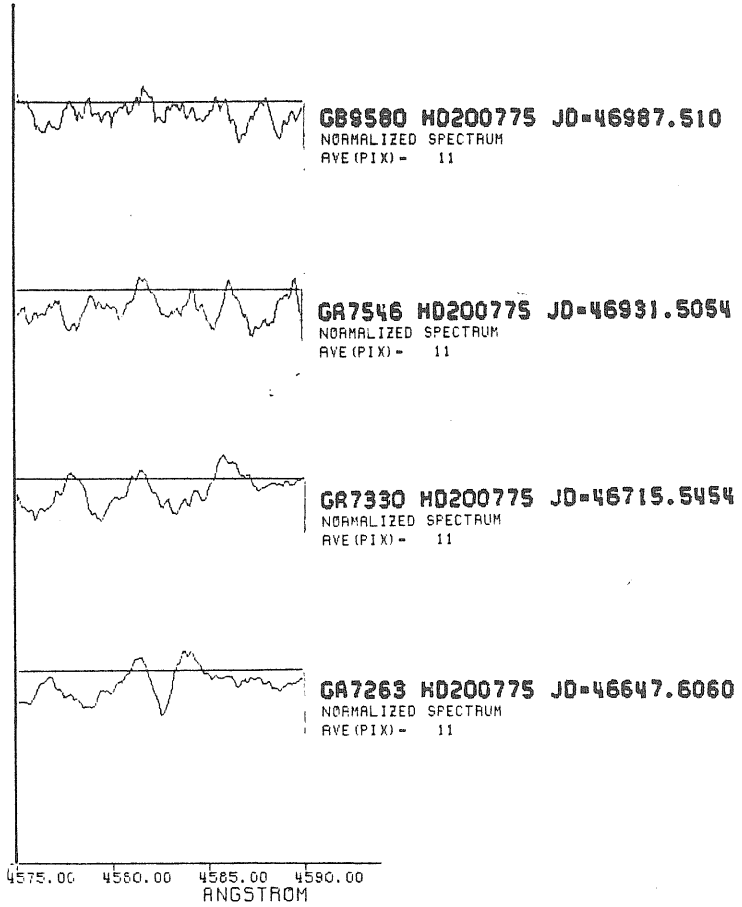

FIGURE III.1.5.10

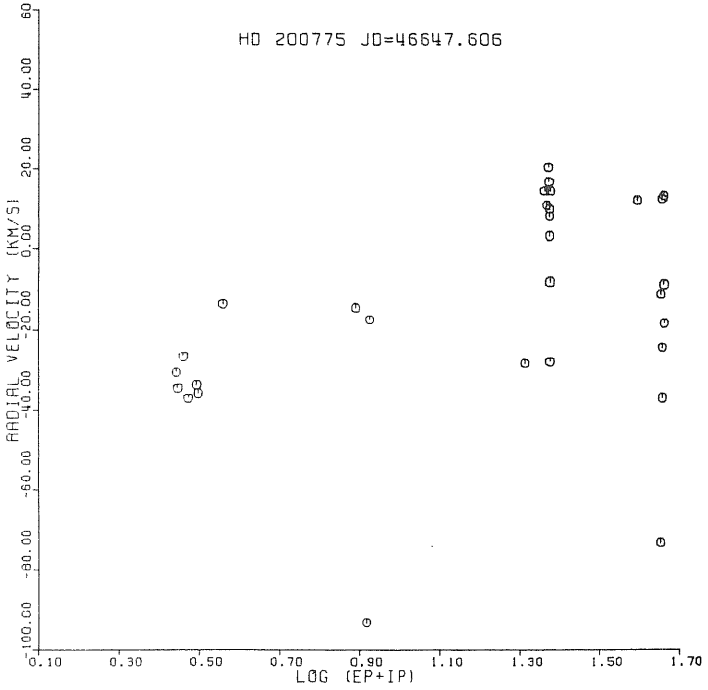

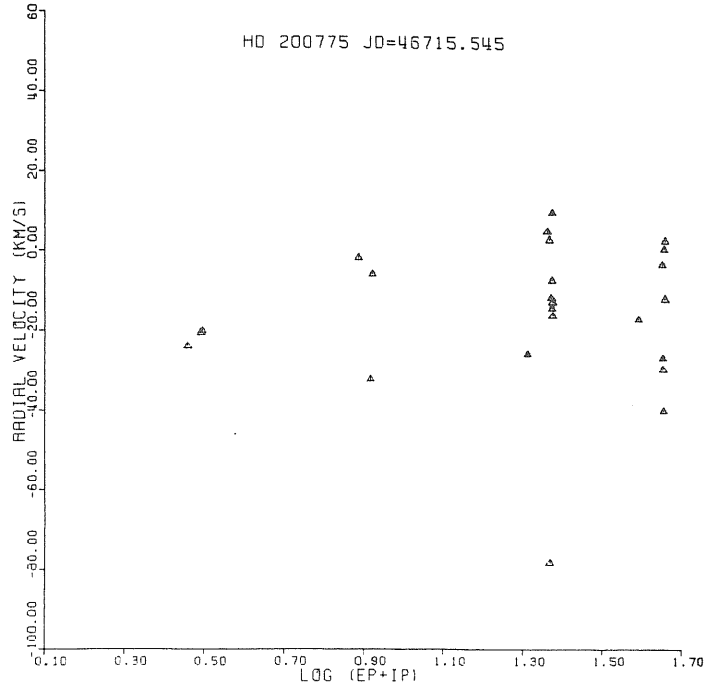

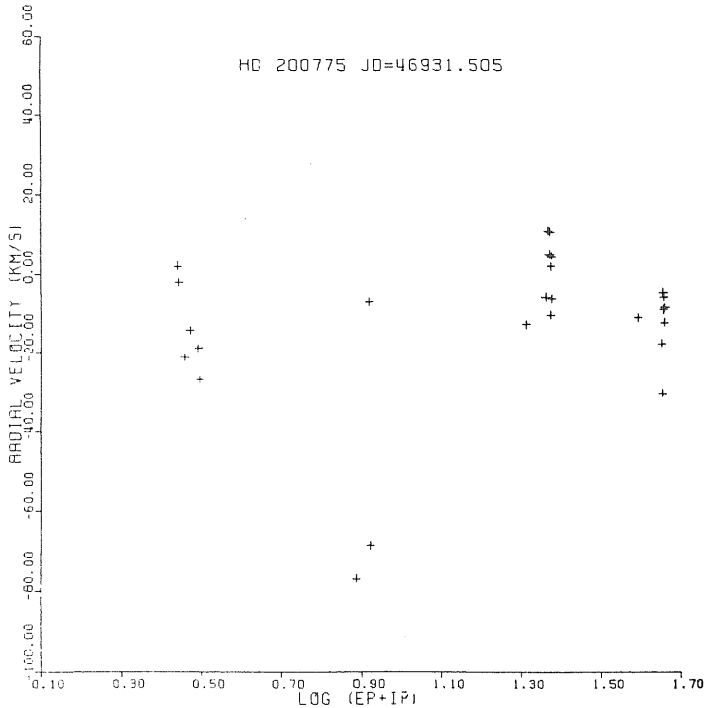

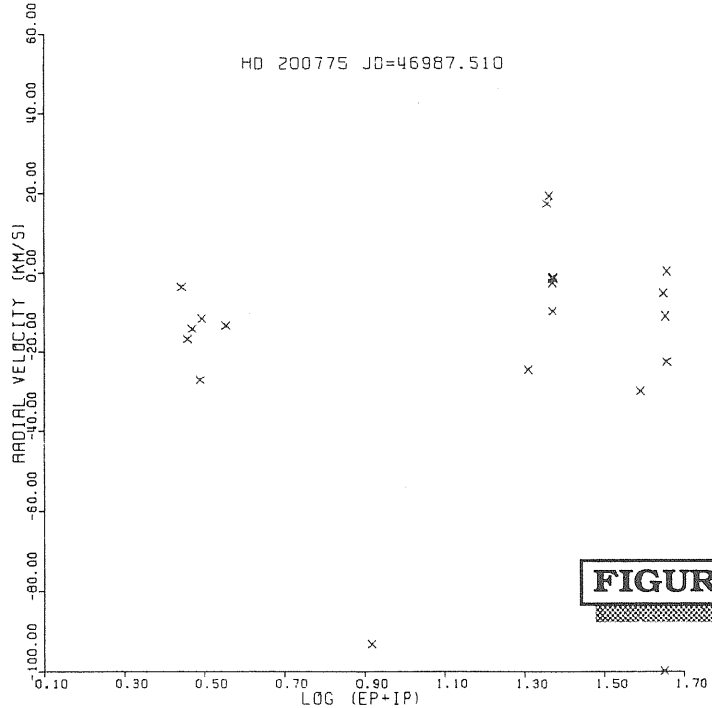

FIGURE III.1.5.11

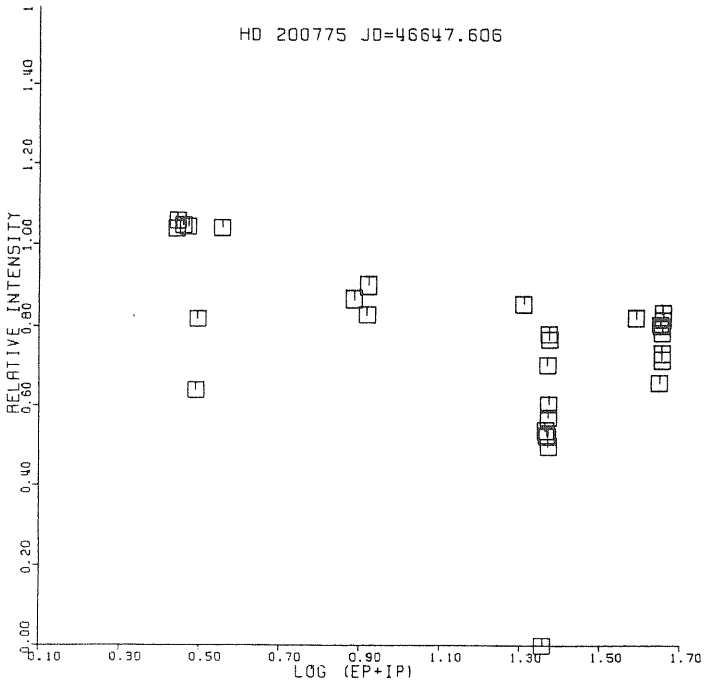

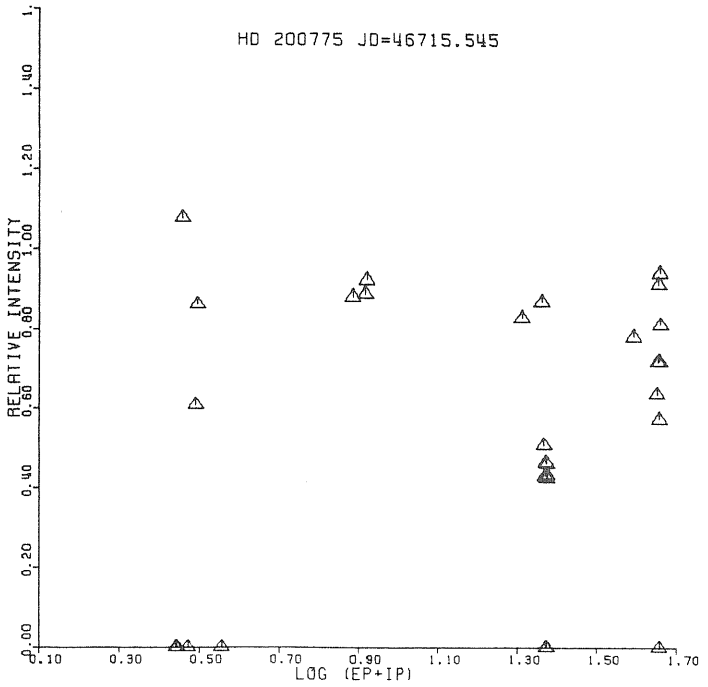

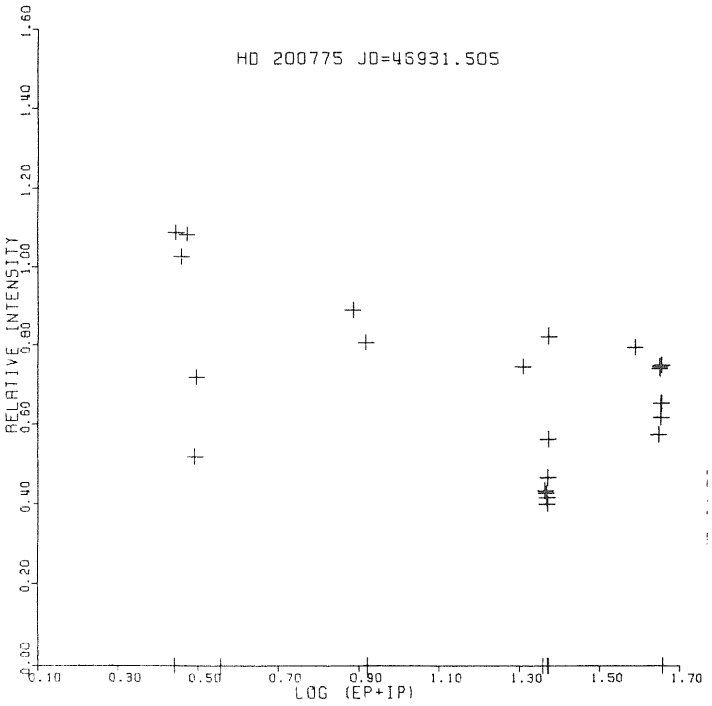

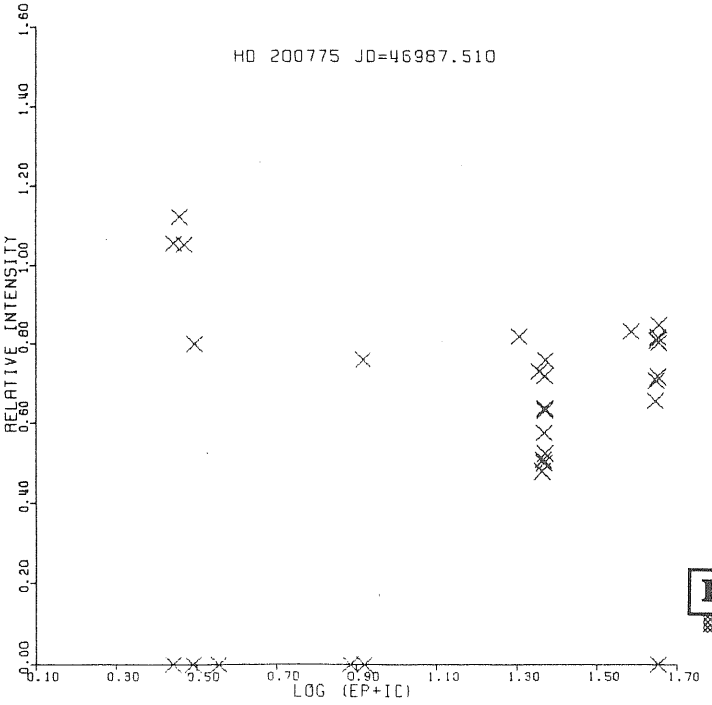

FIGURE III.1.5.12

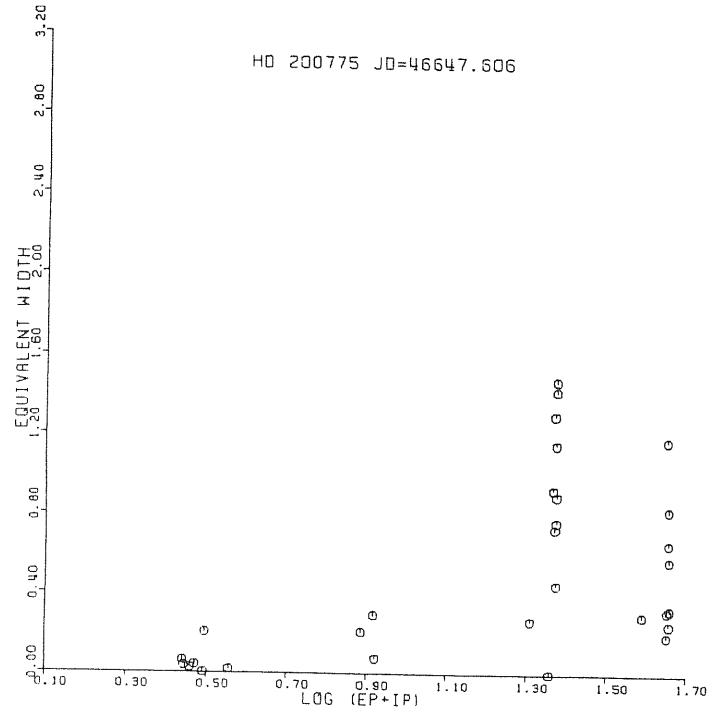

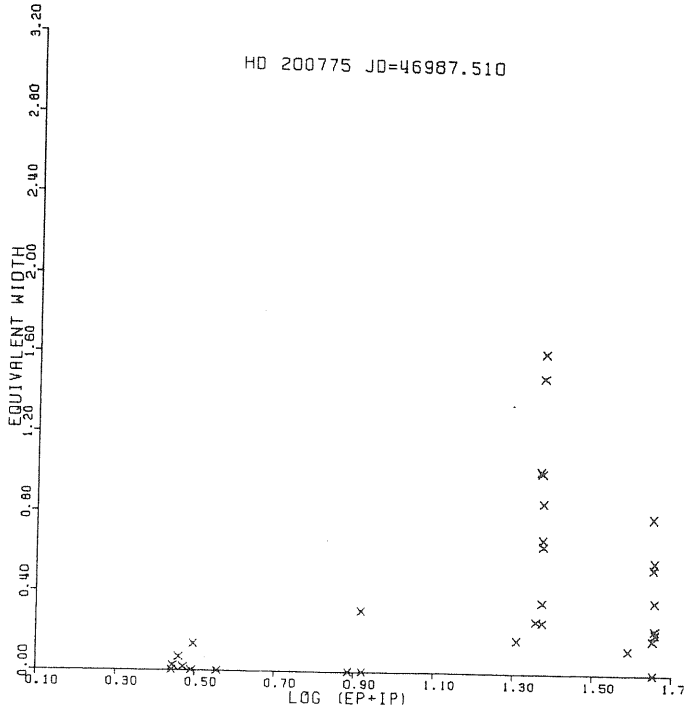

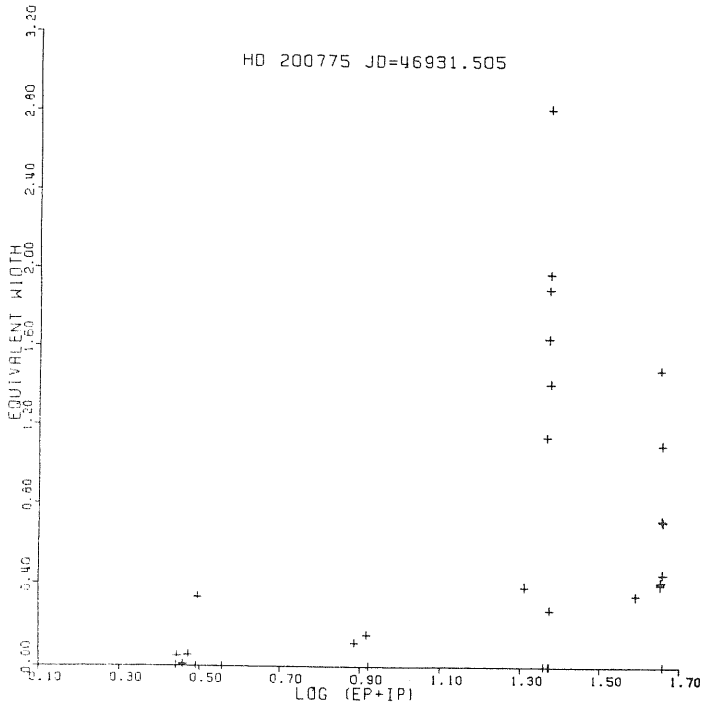

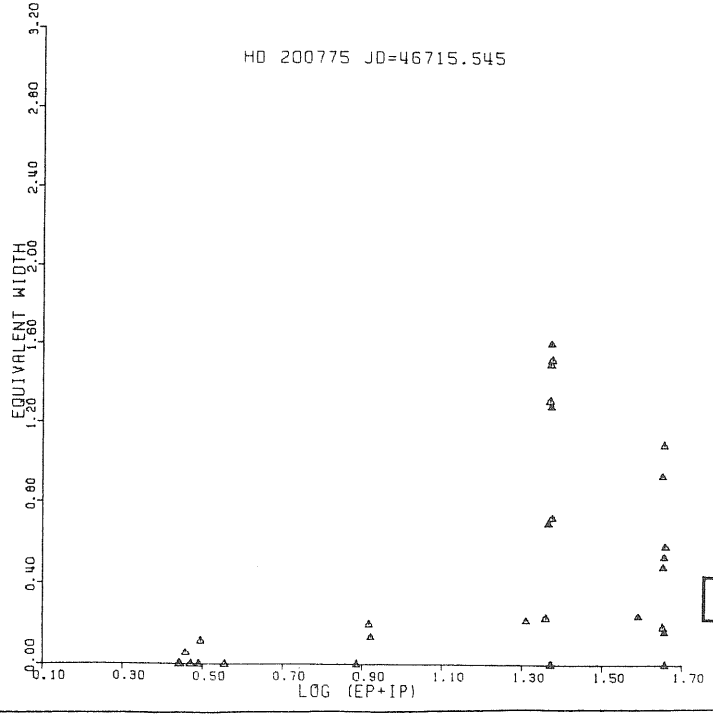

FIGURE III.1.5.13

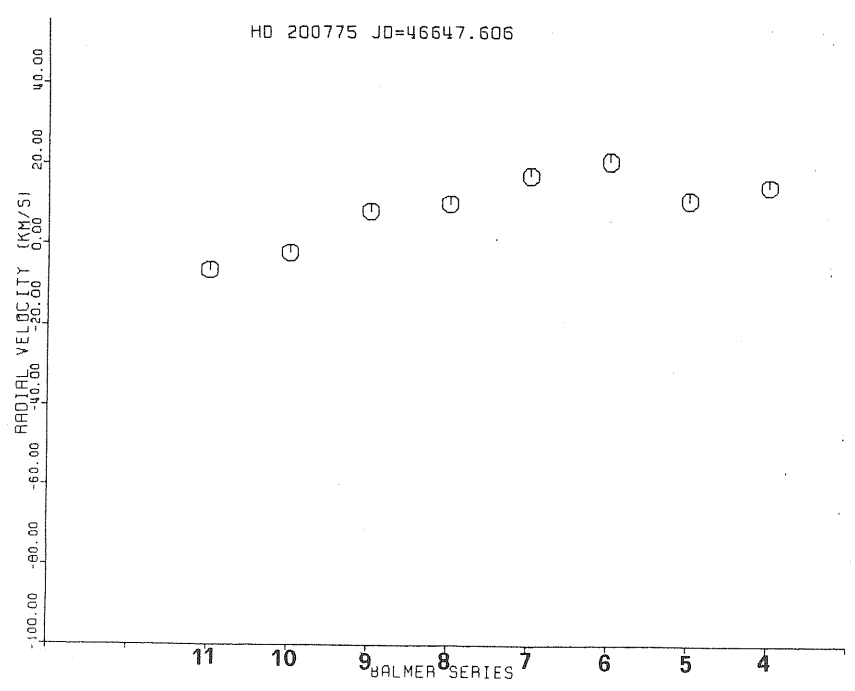

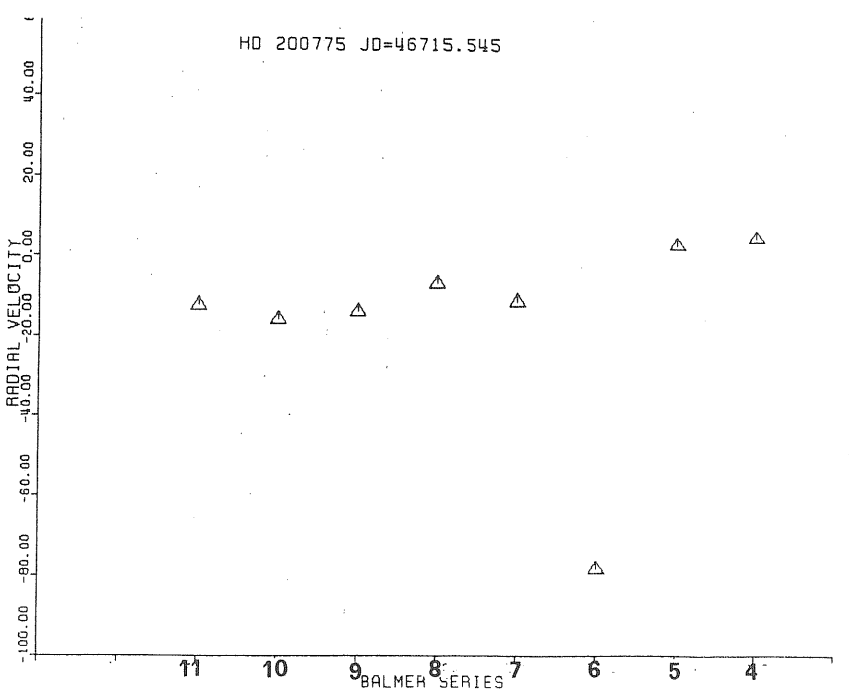

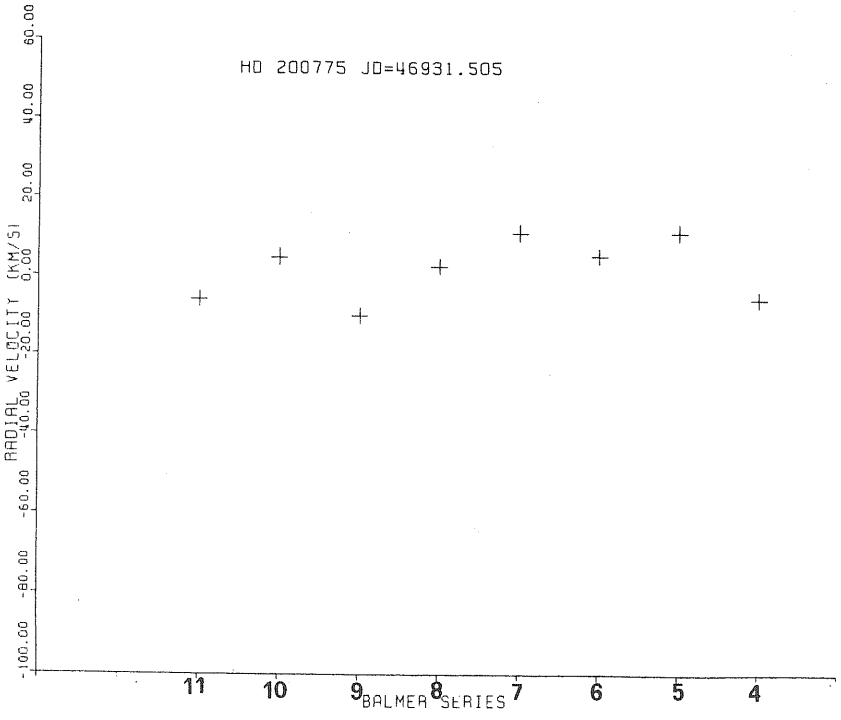

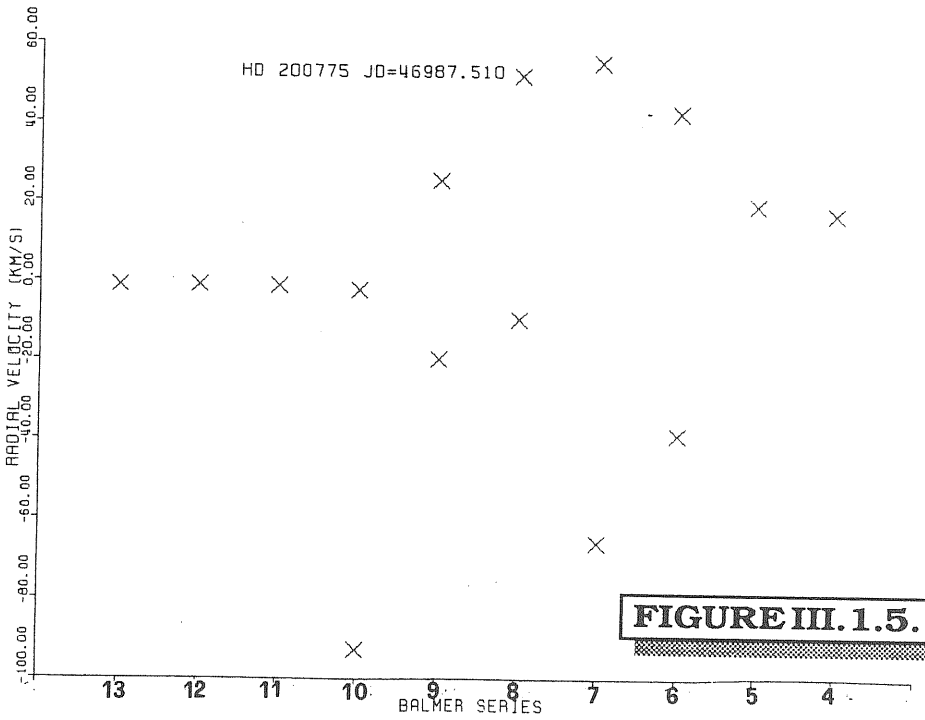

FIGURE III.1.5.14

Table III.1.5.1. Spectral measurements of the H alpha emission components of HD 200775.

J.D.	OBSERVED WAVELENGTH(A)	EQW (A)	DEPTH	FBWC (A)
46647.003	6561.8	62.2	5.4	23.2
46714.479	6561.5	40.9	5.8	14.2
	6564.9	27.4	4.5	12.2
46932.450	6561.5	41.2	6.4	12.9
	6564.5	27.2	4.5	12.1
46988.954	6561.3	32.2	4.5	14.3
	6564.9	25.7	4.3	11.9

NOTE:EQW=Equivalent width,DEPTH=Central intensity of the fitted asymmetric gaussian emission profiles,FBWC=Full band width on the continuum including both emission components of double-peak emission profile.Depth values are corresponding to single and double-peak emission component's central intensities in units of continuum.

Table III.1.5.3. Measured spectral line parameters of the absorption lines of HD 200775.

HD 200775			JD= 46647.606					JD= 46715.545					JD= 46931.505				
ELEMENT	MULT.	λ(LAB)Å	λ(OBS)Å	Ic	FBWC(Å)	EQW(Å)	RV(km/s)	λ(OBS)Å	Ic	FBWC(Å)	EQW(Å)	RV(km/s)	λ(OBS)Å	Ic	FBWC(Å)	EQW(Å)	RV(km/s)
H 13	3	3734.4	3734.6	0.8	3.9	0.5	14.6	3750.0	0.4	2.6	0.7	-12.3	3734.3	0.8	3.3	0.3	- 6.1
H 12	2	3750.2	3749.8	0.8	8.3	0.9	-27.8	3770.4	0.4	5.3	1.5	-15.8	-	-	-	-	-
H 11	2	3770.6	3770.5	0.6	3.9	0.8	- 8.0	-	-	-	-	-	3770.7	0.6	6.5	1.4	4.5
H 10	2	3797.9	3797.9	0.5	4.6	1.2	3.3	3819.1	0.6	5.2	1.1	-39.7	-	-	-	-	-
HeI	22	3819.6	3819.1	0.7	5.9	0.8	-36.8	3835.2	0.5	4.8	1.3	-13.8	3819.5	0.6	5.8	1.1	- 8.9
H 9	2	3835.4	3835.5	0.6	6.9	1.5	8.2	3889.0	0.4	5.6	1.6	- 7.0	3835.3	0.5	7.4	2.0	-10.3
H 8	2	3889.1	3889.2	0.5	6.0	1.4	10.1	-	-	-	-	-	3889.1	0.4	9.4	2.8	2.1
He I	58	3926.5	3926.3	0.8	3.7	0.3	-18.0	3933.4	0.9	1.7	0.1	-20.1	-	-	-	-	-
Ca II	1	3933.7	3933.2	0.8	2.3	0.2	-35.7	3958.2	0.6	-	-	-20.4	3933.3	0.7	2.4	0.3	-26.7
Ca II	1	3968.5	3968.0	0.6	-	-	-33.6	3969.9	0.5	5.6	1.5	-11.3	3968.2	0.5	-	-	-18.8
H eps	1	3970.7	3970.3	0.7	4.3	0.7	16.9	4009.1	0.8	6.4	0.6	-11.4	3970.2	0.4	6.5	1.9	10.7
He I	55	4009.3	4009.2	0.8	3.1	0.3	- 8.5	4100.7	0.4	4.7	1.3	-78.1	4009.2	0.8	3.7	0.5	- 8.5
H delta	1	4101.7	4102.0	0.5	5.5	1.3	20.6	4120.4	0.9	4.5	0.2	-29.8	4101.8	0.4	5.8	1.7	5.1
He I	16	4120.8	4120.6	0.8	3.3	0.3	-12.7	4143.8	0.9	5.7	0.2	3.0	4120.8	0.8	3.3	0.4	- 4.7
He I	53	4143.8	4143.6	0.8	5.4	0.6	-13.6	4266.8	0.8	2.2	0.2	-16.5	4143.6	0.7	4.2	0.7	-12.2
C II	6	4267.02	4266.9	0.8	3.4	0.3	-12.3	4287.1	1.1	1.4	0.1	-34.1	4266.9	0.8	3.5	0.4	-10.9
[Fe II]	7F	4287.4	4287.0	1.1	1.4	0.0	-29.9	4340.5	0.5	2.8	0.7	-23.9	4287.1	1.0	0.8	0.0	-28.5
H gam	1	4340.5	4340.6	0.5	4.0	0.9	-26.5	-	-	-	-	3.0	4340.6	0.4	4.0	1.1	-21.1
[Fe II]	21F	4358.4	4358.2	1.0	0.9	0.0	11.0	4387.9	0.7	4.4	0.5	-	-	-	-	-	-11.0
He I	51	4387.9	4387.6	0.7	5.0	0.7	-13.3	-	-	-	-	0.9	4387.9	0.7	4.2	0.7	- 5.6
[Fe II]	7F	4413.8	4413.2	1.0	1.9	0.0	-24.3	-	-	-	-	-	4413.6	1.1	1.4	0.1	-14.3
[Fe II]	6F	4416.3	4415.8	1.1	1.3	0.0	-36.8	-	-	-	-	-	4416.2	1.1	1.2	0.1	- 2.2
He I	14	4471.5	4471.3	0.7	6.9	1.2	-34.3	4471.4	0.6	5.2	0.9	- 3.1	4471.2	0.6	7.0	1.5	-17.5
Mg II	4	4481.3	4480.9	0.9	3.9	0.3	-10.8	4480.9	0.8	2.6	0.2	-25.7	4481.1	0.8	3.1	0.4	-12.7
Fe II	37	4582.8	4582.6	0.9	1.6	0.1	-28.3	4582.8	0.9	3.5	0.1	- 5.9	4581.8	-	-	-	-68.5
Fe II	17	4622.4	4622.2	0.9	3.2	0.2	-17.2	4622.4	0.			- 1.8	4621.2	0.9	2.2	0.1	-76.8
[Fe II]	4F	4728.1	4727.6	1.0	3.2	0.1	-14.2	-	-	-	-	-	4728.0	-	-	-	2.0
H beta	1	4861.3	4861.6	-	-	-	-30.4	4861.4	0.9	3.7	0.2	5.1	4861.2	-	-	-	- 5.7
He I	48	4921.9	4920.7	0.8	2.6	0.2	14.6	4921.5	0.7	3.5	0.5	-26.6	4921.4	0.7	3.1	0.4	-30.3
Fe II	42	4923.9	4922.4	0.8	3.2	0.3	-73.2	-	-	-	-	-	4923.8	0.8	1.2	0.2	- 7.0
							-93.2	4923.4	0.9	3.7	0.2	-32.2					

Table III.1.5.3.(continued)

HD 200775 JD= 46987.510

ELEMENT	MULT.	λ(LAB)Å	λ(OBS)Å	Ic	FBWC(Å)	EQW(Å)	RV(km/s)
H 13	3	3734.4	3734.4	0.8	2.2	0.3	-1.4
H 12	2	3750.2	3750.1	0.7	2.6	0.4	-1.3
H 11	2	3770.6	3770.6	0.6	3.5	0.6	-1.6
H 10	2	3797.9	3797.9	0.6	3.7	0.7	-2.8
He I	22	3819.6	-	-	-	-	-
H 9	2	3835.4	-	0.5	6.8	1.6	-
H 8	2	3889.1	3888.9	0.5	4.1	0.9	-10.0
He I	58	3926.5	3926.5	0.9	2.8	0.2	0.2
Ca II	1	3933.7	3933.5	0.8	1.4	0.1	-11.6
Ca III	1	3968.5	3968.1	-	-	-	-27.1
H eps	1	3970.7	-	0.5	6.0	1.5	-
He I	55	4009.3	4009.0	0.8	2.4	0.2	-22.6
H delta	1	4101.7	-	0.5	4.1	1.0	-
He I	16	4120.8	-	0.8	1.8	0.2	-
He I	53	4143.8	-	0.8	4.0	0.4	-
C II	6	4267.3 02	4266.8	0.8	1.5	0.1	-30.0
[Fe II]	7F	4287.4	4287.2	1.1	1.1	0.2	-16.7
H gam	1	4340.5	4340.8	0.5	3.9	1.0	19.2
[Fe II]	21F	4358.4	4358.2	-	-	-	-13.4
He I	51	4387.9	4387.8	0.7	4.0	0.6	-11.1
[Fe II]	7F	4413.8	4413.6	1.1	0.8	0.0	-14.2
[Fe II]	6F	4416.3	4416.2	1.1	1.0	0.0	-3.7
He I	14	4471.5	4471.4	0.7	4.6	0.8	-5.4
Mg II	4	4481.3	4481.0	0.8	1.8	0.2	-24.5
Fe II	37	4582.8	-	-	-	-	-
Fe II	17	4622.4	-	-	-	-	-
[Fe II]	4F	4728.1	-	-	-	-	-
H beta	1	4861.3	4861.6	0.7	-	-	17.2
He I	48	4921.9	4919.6	0.7	3.7	0.5	-142.6
Fe II	42	4923.9	4922.4	0.8	2.6	0.3	-93.2

Table III.1.5.3. Comparison of the measured EQW's of HD 200775 with other researchers.

Line	Baschek et al.(1982) (A)	This research J.D.=2446000+ (A)			
		647.0	714.5	932.5	989.0
H alpha	100.0	62.2	68.3	68.4	57.9
		647.6	715.5	931.5	987.5
H beta	6.0	4.5	4.0	1.1	1.1
[Fe II] 4287.4	0.05	0.03	0.05	0.01	0.07
4358.4	<0.03	0.02	-	-	-
4413.8	0.05	0.04	-	0.06	0.02
4416.3	<0.05	0.04	-	0.05	0.03

	Viotti (1969) (mA)	Baschek et al. (1982) (mA)	647.6	715.5	931.5	987.5
He I 4009.2	380	320	251	585	457	228
4120.9	160	240	319	186	419	179
4143.7	550	510	572	160	719	369
4387.9	700	640	658	533	728	569
4471.3	1160	1260	1177	939	1492	795
4921.9	600	-	194	483	405	537
C II 4267.1	370	200	293	239	353	124
SiII 4130.8	100	70	-	-	-	-
MgII 4481.2	200	170	269	218	390	171
CaII 3933.7	100	240	205	113	339	135

III.2.The UV spectra

Recently UV observations of the Be stars revealed very important facts, which can be outlined as follows:

i)Superionized lines such as O VI, N V and C IV whose ionization degree requires much higher temperatures than expected at the effective temperatures of these stars under conditions of radiative equilibrium, are observed in the UV spectra of Be stars.This suggests a nonradiative energy source to explain their formation.

ii)These superionized lines are generally blue shifted- in some cases up to -3000 km/s i.e. at values which exceed the escape velocity at the surface of the star.This proves the existence of a mass flux.

iii)Another observed fact is that the intensities, profiles and blue shifts of these lines can be substantially different for two Be stars of the same spectral type and luminosity class.So the velocity and density distributions in the superionized region can be different for two stars characterized by the same values of Te and effective gravity.This result points out that there is a certain individuality for each star.

iv)The time variability of the blue shifts, intensities and profiles of superionized lines suggest that even for a single star at different epochs, there are very important changes of the physical conditions of the outer layers.

The resonance lines of superionized elements in the hot

stars exhibit a great variety of profiles, which can be roughly classified into three types (Doazan,1982):

1]Direct P Cygni profiles, with an emission component having little or no displacement and a blue shifted absorption component,

2]Blue shifted absorption profiles without an emission component,

3]An asymmetric absorption profile, with little or no displacement of the absorption minumum, exhibiting an extended wing toward shorter wavelengths.

Among these profiles, only type 2] constitutes direct evidence of mass loss when the radial velocity of the center of the absorption line is greater than the escape velocity of the star.In the other two cases their interpretation is model dependent.

The UV spectra of some Be/shell stars exhibit deep, sharp absorption lines similar to the shell lines observed in the visible and arising from atoms that have a degree of ionization or excitation comparable to or smaller than that of the photosphere.The principal lines observed are those of doubly ionized metals such as Fe III, Cr III and Ti III, and singly ionized metals, especially Fe II.The resonance lines of Al III, Al II and Mg II are often very strong.The simultaneous presence of elements in several states of ionization also indicates large variations in the degree of ionization in the envelope of the star.The Mg II doublet near 2800 angstrom

exhibits emission wings in some Be/shell stars.These lines are also very important to study mass flux from Be stars (Morgan et al.,1977).

By keeping in mind these introductory remarks about UV spectra of Be stars we analysed the resonance lines of the program stars.Table III.2.1 presents the list of them with the exception of Fe III (UV34) and some other secondly ionized ion lines which are only measured in HD 184279.

III.2.1.HD 22192(Psi Per)

Psi Per is one of the most well studied Be star in the UV region among the program stars.We give a short description of the UV spectra of this star:

Si IV lines were asymmetric and blue shifted.The two spectra presented in Figure III.2.1.a,b show very evident profile variations.The second spectrum presents a blue shifted component (-171 km/s) blended possibly with Fe III. C IV lines (Figure III.2.1.c) were aymmetric and blue shifted like the Si IV lines; profile variations and a blue shifted secondary component (-138 km/s) were observed.

The resonance lines of Al III and the Fe III(UV34) lines were strong, blue shifted and highly asymmetric in both of our spectra (Figure III.2.1.d,e,f).Mg II lines exhibited double-peak emission and a strong unshifted absorption component.We have detected slight but evident R/V variations in the emission components (Figure III.2.1.g).

Si II(UV2,3) lines were very strong and composed of a sharp interstellar component superimposed on a symmetric stellar one.The blue shifted sharp components are probably arising from a circumstellar envelope(CSE), with an average radial velocity of about -30 km/s.

Several ground level low ionization lines symmetric and unshifted were observed.They are probably of interstellar origin; they are:C II(UV1), Al II(UV1) (-only in the first spectrum it shows a CSE blue shifted component with a radial

velocity of -31 km/s like Si II lines), O I(UV2), C I(UV2) and Si II(1).

In the long wavelength range only the lines of Fe II multiplets 1,2,3 and Mg I 2852.1 formed in interstellar matter were present and their profiles were narrow and unshifted.Measured values of the selected lines are presented Table III.2.2.

III.2.2.HD 184279

This interesting Be star has been studied very little in the UV region up to now.So we want to describe it's UV spectra in detail.

Silicon: This element appeared in several ionization levels.Si II lines were mainly interstellar, very sharp, narrow and unshifted.Lines of the Si II multiplets (2,3) presented secondary blue shifted components probably originated in the CSE with average radial velocity of about -30 km/s.Average edge velocity for these multiplet lines is about -200 km/s, and there were no visible variation in the line profiles.Si II 1526 and 1538 are composed of sharp interstellar features superimposed on wide symmetric components; the average blue edge velocity for this wide component was about -800 km/s.The lines of Si III multiplets (4,9,10) were strong, symmetric and slightly blue shifted with a radial velocity of about -35 km/s.Si III 1417 also presented a wide component with the blue edge velocity of -277 km/s.Lastly Si IV lines were strong and asymmetric towards the

blue edge.There were no significant time variation for Si IV lines in our spectra.Figure III.2.2.a,b presents Si IV line profiles.

Carbon: The lines of C I multiplets(2,4) were very sharp, unshifted and mainly interstellar.Similarly C II multiplet 1 lines were strong, slightly asymmetric and unshifted.The line profiles of this multiplet presented a variation between two spectra taken with two months interval.C IV lines were strong and highly asymmetric towards blue.Line profiles exhibited time variation (Figure III.2.2.c).

Aluminium: Al II 1670.8 was sharp, unshifted and exhibited a line profile with blue edge velocities -224.5 km/s and -176 km/s respectively with two months interval.Al III lines 1855,1863 were asymmetric, strong and blended with Fe III (Figure III.2.2.d).

Iron: Iron is the dominant element in the UV spectra of HD 184279.Almost all of it is in the second ionization level.The lines of UV multiplets (48), (51-53), (57-62), (66-67), (71), (77), (94-97), (100), (101), (103), (108), (134) and (186) were identified.Among these multiplets only few of the lines were blue shifted.Fe II was present with only few unshifted interstellar lines.We measured wind sensible (Viotti et al.,1987) Fe III multiplet (34) lines in order to check the time variablity.Our measurements revealed that there was a small but evident variation.None of the iron lines presented a trace of emission in our spectra.Figure

III.2.2.e,f presents Fe III (UV34) lines.

Magnesium: Mg I 2852 was present, unshifted with a narrow profile. Mg II 2795,2802 lines were strong, unshifted and variable.There were no emission components in the Mg II lines which are presented in Figure III.2.2.g.

Sulphur: S II 1251,1253 lines were sharp, strong and unshifted.

Cromium: Cr III lines of multiplets (4),(9),(37),(40),(70) and (71) are identified.None of these lines were blue shifted; only there was a slight variation in the average blue edge velocities.

O I 1302 was sharp, narrow and unshifted.

Several lines of metallic ions were present:Ni II 1370,1709,Ni III 1692,1698, were identified blended with Mn II 1692 and Co III 1697 respectively.Between the wvelength interval 1714 angs. to 1808 angs. the lines of Ni III multiplets (14),(15),(29),(30), Co III multiplets (21), (22), (27),(42), (47),(57),(172), Mn II multiplets (13),(100), and Zr III multiplet (5) were present and none of the lines of these multiplets were blue shifted. Table III.2.2.3 presents the measured values of the selected lines.

III.2.3.HD 183656

Up to now only one research dealing with the first observed UV spectra of this star has been published (Ringuelet et al.,1984).So our data are important for comparing UV characteristics of this interesting Be/shell star with early

observations.

Si IV lines which are presented in the Figure III.2.3.a,b are heavily blended with firstly and secondly ionized metals.However we can see that Si IV present unshifted symmetric profiles.Comparing our spectra with Ringuelet et al.(1984), there are some profile variations which seems related with the blending metals but not Si IV.

Like the Si IV lines ,the C IV lines were also blended and probably observed variations in the line profiles have the same origin (Figure III.2.3.c).However C IV line centers were blue shifted and there was a slight variation in the center and blue edge velocities.Comparing our spectra with Ringuelet et al., (1984) we see that the line profiles are similar and suggest no significant time variation.

HD 183656 displayed slightly blue shifted strong and asymmetric Al III (UV1) lines in our spectra.Other metallic lines such as Fe II, Si II and Cr II were present in the same region.Some profile variations are observed for these neighbouring metallic lines ; also Al III (UV1) lines may present some variations although not very evident.Fe III (UV34) lines are slightly blue shifted (about few km/s), strong and symmetric.Again slight profile variations are seen for the neighbouring metallic lines, but not for Fe III (UV34) lines (Figure III.2.3.e,f).In the spectrum analysed by Ringuelet et al.,(1984) Fe III displayed line profiles which are similar to those of the Fe II lines.Fe II presented the

richest spectrum of all ions, and all lines of Fe II displayed fairly strong narrow and symmetric profiles, closely similar to our spectra.

From our measurements ,we see that Fe II (UV1,2,3) lines were blue shifted and their blue edge velocities are comparable with those of Fe III lines. The lines of Si II (UV1,2,3) and Al II (UV1) lines were similarly symmetric, all of them were unshifted, with about 200 km/s HWBC.There were no time variation in the profiles and radial velocities of these lines.

The Mg II (UV1) lines were blue shifted strong and asymmetric.Probably there was a contribution from a stellar and IS component (Figure III.2.3.g).Measured values of the selected lines are presented in Table III.2.4.

III.2.4.HD 193182

This star has never been analysed in the UV range.We present four short wavelength and one long wavelength spectra of HD 193182 taken at approximately three year interval.

The presence of Si IV and C IV ions is very doubtful.If these lines are present their equivalent widths must be smaller than 0.1 angstrom (Figure III.2.4.a,b,c).As we see from the same figure UV spectra of HD 193182 presented many metallic shell lines of first and second ionization levels. Lines are very narrow and sharp like those in the optical spectra of the star. It is evidently seen that the shell became more strong in spectra taken in 1982.

Al III (UV1) lines were strong and blue shifted.They presented a variation in the line centers (Figure III.2.4.d).Fe III (UV34) lines were similar to Al III lines; strong, symmetric and blueshifted, but they did not present profile variations (Figure III.2.4.e,f).

Mg II (UV1) lines (Figure III.2.4.g) are composed of wide components on which sharp blue shifted components were superimposed and blended with many metallic lines specially Fe II.

Our radial velocity measurements revealed that HD 193182 had higher radial velocities with the strengthening of the shell.Measured central and edge velocities of Al III, Fe III and Fe II lines are similar although Si II, C II and Al II differed substantially.Table III.2.5 presents measured values of the selected lines.

III.2.5.HD 200775

We present two short wavelength and two long wavelength spectra of this Herbig Be star, which has not been studied in detail.Firstly Baratta et al. (1987) remarked the presence of the double-peak metallic lines in its spectrum.

HD 200775 presented complex line profiles for Si IV (Figure III.2.5.a,b). The whole line profiles could be divided into three main components.Line profiles were asymmetric and presented blue shifted narrow components.Profile variations are evident.The same figure shows the profile variations for neighbouring metallic lines

specially for Fe III where both spectra were taken at the same day with only three hours of interval.

Similar multiple profile structure was present for the C IV lines, which are asymmetric and shortward winged.The short time-scale profile variation was much more evident in the C IV lines than in the Si IV lines.The average measured blue edge velocity for the C IV lines was about 400 km/s (Figure III.2.5.c).

Al III (UV1) and Fe III (UV34) lines also presented strong, blue shifted secondary components; the main components were also blue shifted.Measured blue edge velocities were similar for these two ions, but Al III lines were more asymmetric than Fe III lines.Mg II (UV1) lines , which are presented in Figure III.2.5.f were composed of double peak absorbtion components accompanied with an emission profile at the red edge of the unshifted absorbtion components.These emission wing components presented inflexions on the flanks of the profiles which were variable.

The lines of Si II multiples (UV1,2,3), C II (UV1) and Al II (UV1) were composed of strong, symmetric and unshifted lines.Some lines of these multiplets also presented CSE components with radial velocities of about 30 km/s.Also Al II 1670 line presented a wide component with blue edge velocity about -246 km/s.It is interesting to remark that the center of this wide component was blue shifted of about -160 km/s.Table III.2.6 presents the measured values of the selected lines.

Table and Figure captions.

Table III.2.1.Measured UV lines of program lines.Some secondly ionized .i+19;multiplets are not added .i.e. Fe III(34), Cr III, N III etc.

Figure III.2.1.Selected UV line profiles of HD 22192.

Table III.2.2.UV spectral measurements of HD 22192.

Figure III.2.2.Selected UV line profiles of HD 184279.

Table III.2.3.UV spectral measurements of HD 184279.

Figure III.2.3.Selected UV line profiles of HD 183656.

Table III.2.4.UV spectral measurements of HD 183656.

Figure III.2.4.Selected UV line profiles of HD 193182.

Table III.2.5.UV spectral measurements of HD 193182.

Figure III.2.5.Selected UV line profiles of HD 200775.

Table III.2.6.UV spectral measurements of HD 200775.

Table III.2.1.Measured UV lines of program stars.

Ion	Mult.	Wavelength	EP (1/cm)
Si II	3	1304.372	0.00
		1309.277	287.32
C II	1	1334.532	0.00
		1335.663	63.42
		1335.708	63.42
Si IV	1	1393.755	0.00
		1402.770	0.00
Si II	2	1526.708	0.00
		1533.432	287.32
C IV	1	1548.185	0.00
		1550.774	0.00
Al II	2	1670.787	0.00
Si II	1	1808.012	0.00
		1816.928	287.32
		1817.451	287.32
Al III	1	1854.716	0.00
		1862.790	0.00
Fe II	3	2327.391	667.64
		2332.798	384.77
		2338.005	862.63
		2343.495	0.00
		2344.278	977.03
		2348.300	667.64
		2359.111	862.63
		2364.825	384.77
		2380.757	667.64
Fe II	2	2366.864	0.00
		2373.733	0.00
		2382.034	0.00
		2383.060	384.77
		2388.629	384.77
		2395.416	667.64
		2395.627	384.77
		2399.237	667.64
		2404.430	662.64
		2404.882	667.64
		2406.660	862.63
		2410.521	862.63
		2411.062	977.03
		2413.308	977.03
Fe II	3	2585.876	0.00
		2598.369	384.77
		2599.395	0.00
		2607.086	667.64
		2611.873	384.77
		2613.820	862.63
		2617.618	667.64
		2620.408	862.63
		2621.669	977.03
		2625.664	384.77
		2628.291	977.03
		2631.045	862.63
		2631.321	667.64
Mg II	1	2795.523	0.00
		2802.698	0.00

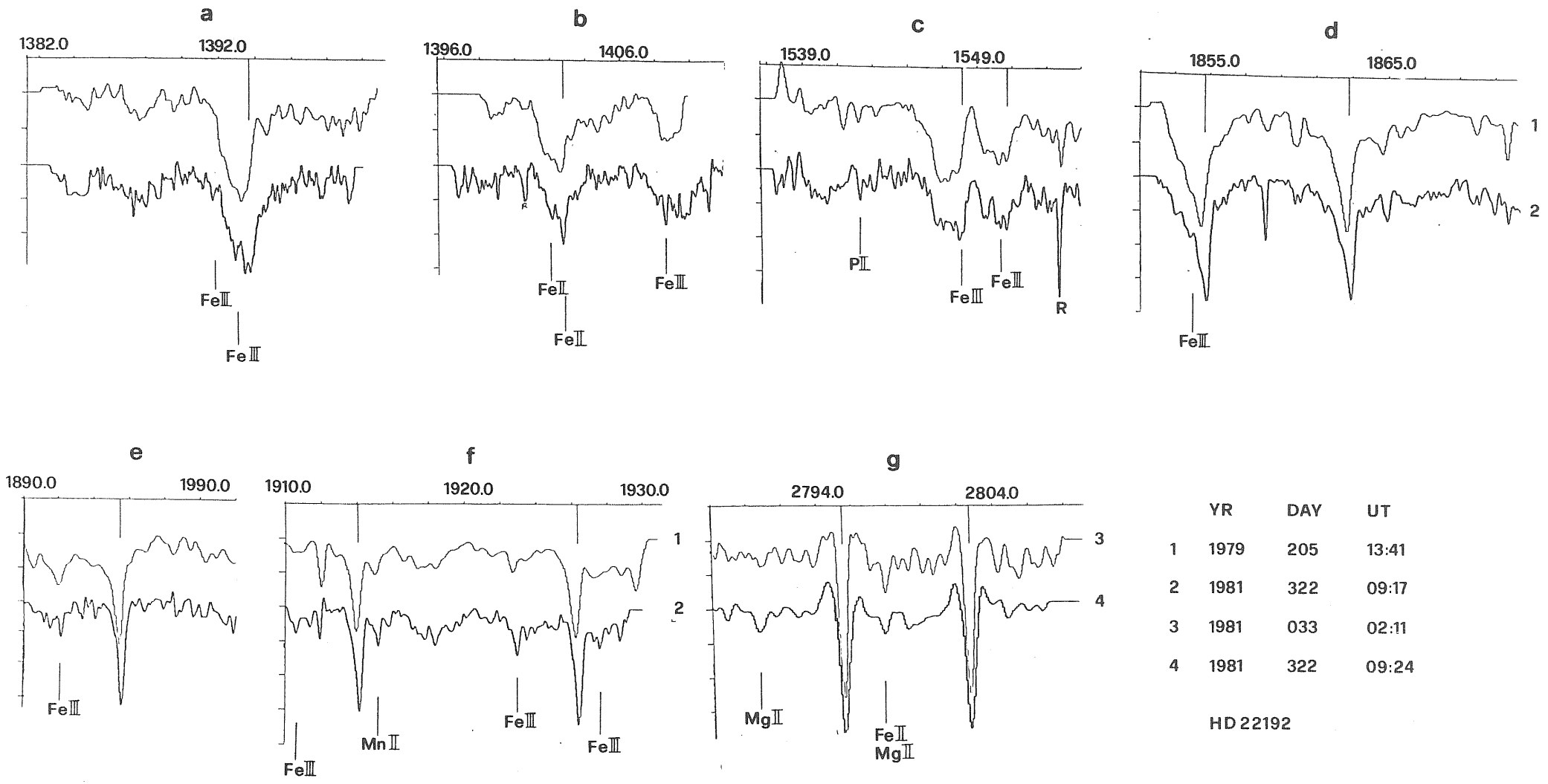

	YR	DAY	UT
1	1979	205	13:41
2	1981	322	09:17
3	1981	033	02:11
4	1981	322	09:24

HD 22192

FIGURE III.2.1

Table III.2.2.UV spectral measurements of HD 22192.

Element	Multip.	Vc	Vedg	EQW	FBWC	R/V	Remarks
Si IV	1	-48.0	-380.7	1.0	2.3	0.84	1
		-64.9	-328.4	0.9	2.3	0.86	2
C IV	1	-46.0	-397.0	0.7	2.1	0.73	1
		-37.0	-380.2	0.8	2.1	0.88	2
Al III	1	-26.6	-154.0	0.7	1.1	0.43	1
		-20.7	- 97.5	0.6	0.9	0.73	2
Fe III	34	-15.4	- 65.0	0.3	0.5	0.53	1
		- 5.6	- 49.0	0.3	0.4	0.80	2
Mg II	1						

line	Vc	Vedg	EQW	DEPTH	FBWC	R/V	Remarks
2795.5	-102.9	-130.9	0.08	0.15	0.5	0.83	3
	- 6.1	- 28.5	0.46	-0.94	0.5	1.20	
	93.0	97.9	0.01	0.07	0.1	1.06	
2802.7	-106.1	-124.5	0.08	0.21	0.4	1.06	3
	- 5.4	- 31.6	0.47	-0.89	0.5	1.04	
	39.6	65.9	0.07	0.16	0.4	1.28	
2795.5	- 49.9	- 68.5	0.05	0.16	0.3	0.60	4
	- 6.7	- 33.5	0.54	-1.04	0.5	0.90	
	35.4	63.9	0.05	0.17	0.3	1.09	
2802.7	- 84.1	-104.7	0.08	0.16	0.5	1.36	4
	- 10.7	- 32.9	0.47	0.97	0.5	1.17	
	102.9	117.1	0.01	0.02	0.2	0.73	

Element	Mult.	Vc	Vedg	Vedg(*)	Remarks
Si II	3	unsh.	-264.4	-415.6	1
		unsh.	-205.7	-421.9	2
C II	1	unsh.	-384.8	-	1
		unsh.	-436.4	-	2
Si II	2	unsh.	-	-	1
		unsh.	-	-	2
Al II	1	- 31.3	-122.3	-217.3	1
		unsh.	- 89.5	-217.4	2
O I	1	unsh.	-	-	1
		unsh.	-	-	2
C I	1	unsh.	-	-	1
		unsh.	-	-	2

Notes:Vc=Central velocity,Vedg= Edge velocity measured from the blue edge of the fitted gaussian line (km/s),FBWC=Full band width on the continuum (km/s),Vedg(*)=Edge velocity measured from the wide stellar component (km/s),R/V=Ratio of the red and blue wings on the continuum.Depth=Central depth of the fitted line,positive values corresponds to emission in continuum units.

Remarks:

	YR	DAY	U.T.
1]	1979	205	13:41
2]	1981	322	09:17
3]	1981	033	02:11
4]	1981	322	09:24

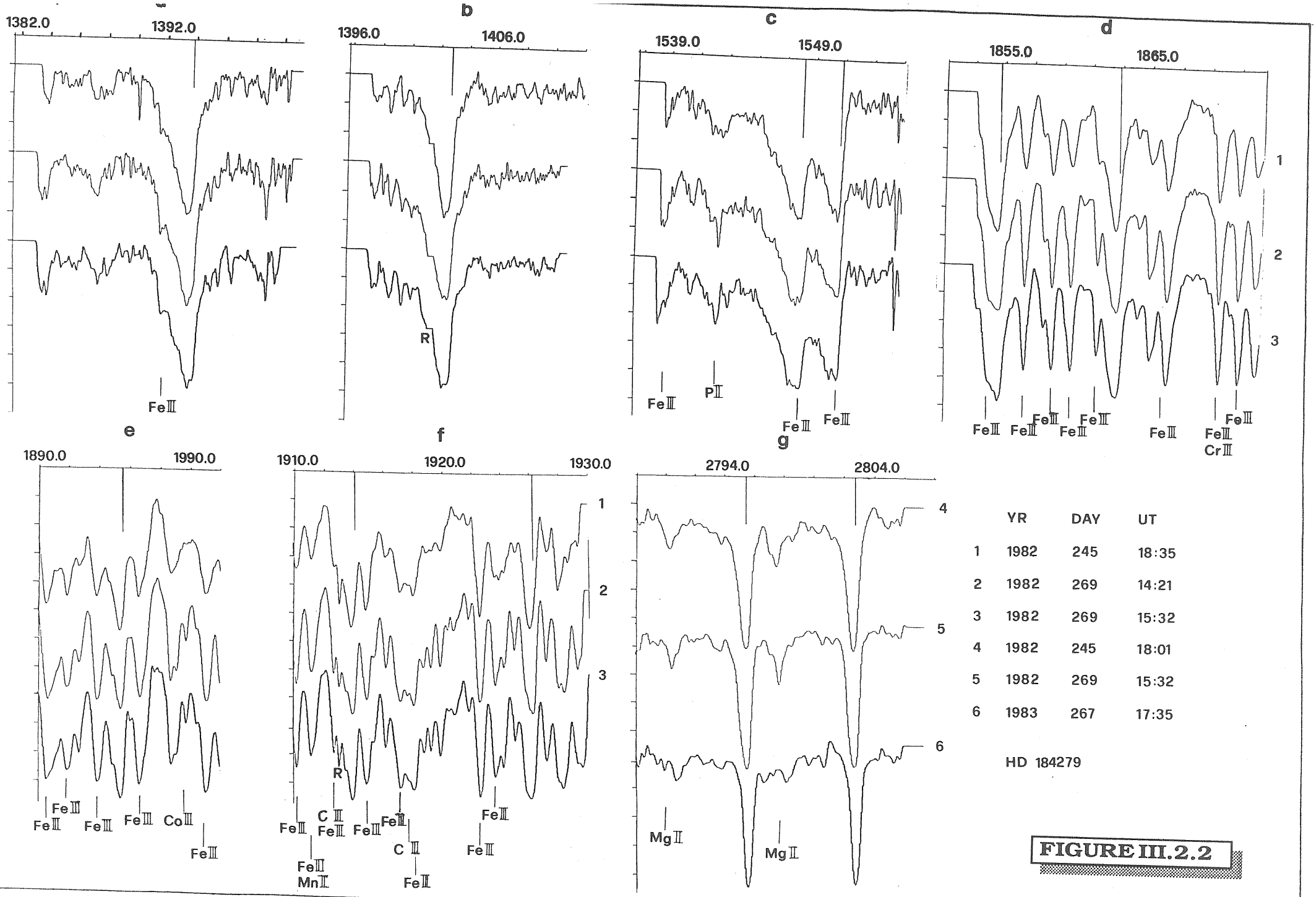

	YR	DAY	UT
1	1982	245	18:35
2	1982	269	14:21
3	1982	269	15:32
4	1982	245	18:01
5	1982	269	15:32
6	1983	267	17:35

HD 184279

FIGURE III.2.2

Table III.2.3.UV spectral measurements of HD 184279.

Element	Multip.	Vc	Vedg	EQW	FBWC	R/V	Remarks
Si IV	1	-18.5	-675.3	2.9	4.3	0.61	1
		-21.4	-507.9	2.6	3.1	0.65	2
		-30.2	-479.3	2.5	2.9	0.72	3
C IV	1	-17.6	-598.4	2.1	3.8	0.58	1
		-15.1	-518.2	2.2	3.8	0.59	2
		-18.0	-490.2	1.8	2.5	0.59	3
Al III	1	-14.2	-246.7	1.5	1.8	0.71	1
		unsh.	-195.6	1.6	1.9	0.83	2
		unsh.	-180.1	1.6	1.8	0.83	3
Fe III	34	-14.8	-116.4	0.9	1.0	0.55	1
		unsh.	- 89.1	0.9	0.9	0.59	2
		unsh.	- 92.2	0.9	1.0	0.60	3
Mg II	1	unsh.	- 60.3	1.0	0.9	0.55	4
		unsh.	- 61.7	1.1	0.9	0.74	5
		unsh.	- 37.2	0.8	0.7	1.20	6

Element	Mult.	Vedg	Remarks
Si III	-	-277.1	1,7
		-199.0	2,7
Ni III	-	-170.5	1,7
		-137.4	2,7
Co III	-	-181.2	1,7
		-132.4	2,7
Cr III	-	-210.1	1,7
		-182.2	2,7
Si II	3	-202.1	1
		-182.2	2
C II	1	-383.3	1
		-355.4	2
Si II	2	-248.6	1
		-187.7	2
Al II	1	-224.5	1
		-176.2	2
He II (Ba. alph.)		-405.9	1
		-365.8	2

Notes:Vc=Central velocity,Vedg= Edge velocity measured from the blue edge of the fitted gaussian line (km/s),FBWC=Full band width on the continuum (km/s),R/V=Ratio of the red and blue wings on the continuum.

Remarks:

	YR	DAY	U.T.
1]	1982	245	18:35
2]	1982	269	14:21
3]	1982	269	15:32
4]	1982	245	18:01
5]	1982	269	15:32
6]	1983	167	17:35

7]Averaged over al multiplets.

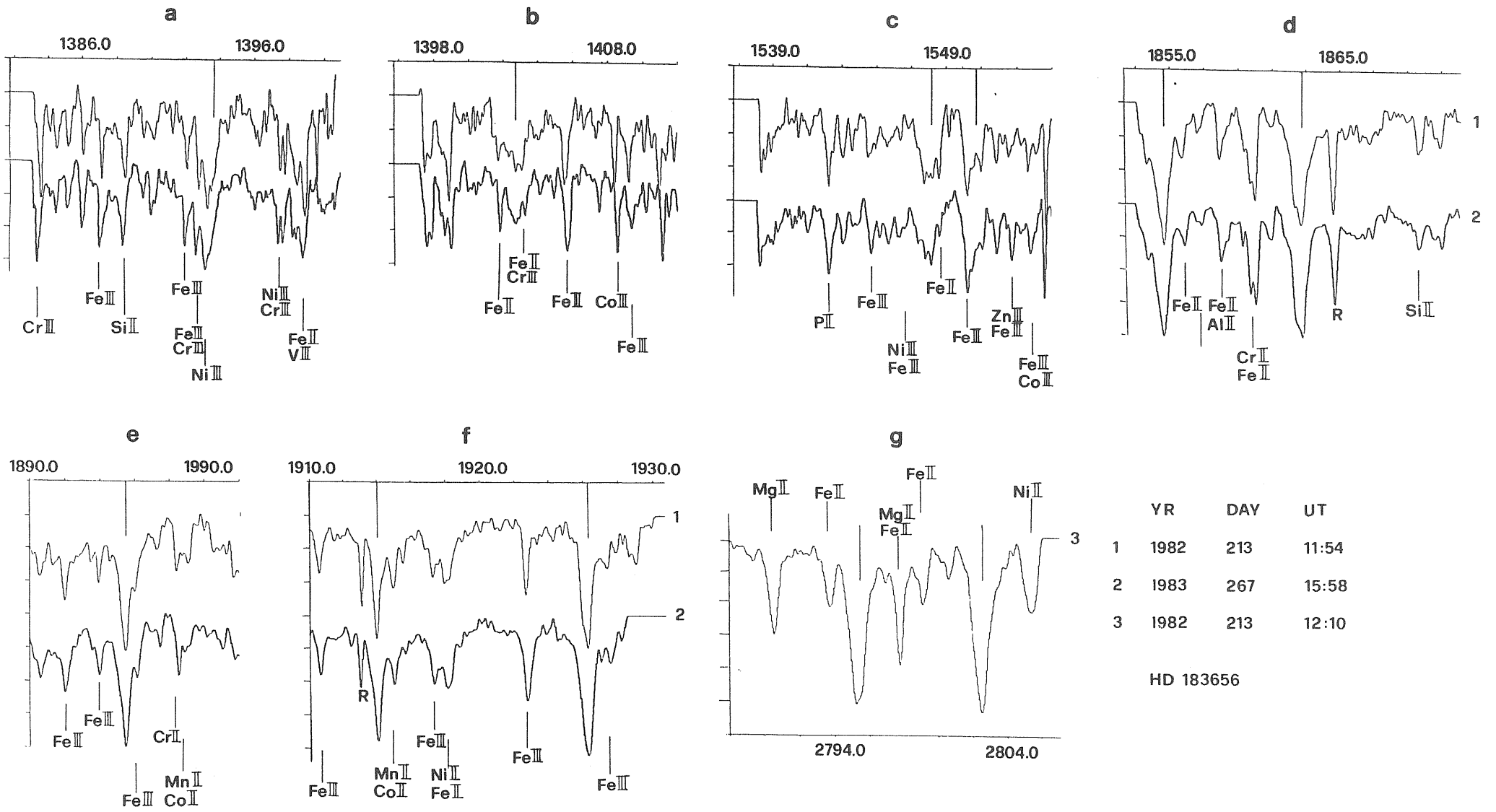

	YR	DAY	UT
1	1982	213	11:54
2	1983	267	15:58
3	1982	213	12:10

HD 183656

FIGURE III.2.3

Table III.2.4.UV spectral measurements of HD 183656.

Element	Multip.	Vc	Vedg	EQW	FBWC	R/V	Remarks
Si IV	1	unsh.	-114.8	0.6	0.9	0.95	1
		unsh	-136.1	0.6	1.1	0.85	2
C IV	1	-29.7	- 71.3	0.2	0.4	0.89	1
		-35.3	- 87.9	0.2	0.4	0.89	2
Al III	1	-18.6	-111.6	0.6	0.8	0.62	1
		-10.9	-114.4	0.6	0.8	0.60	2
Fe III	34	- 4.2	- 48.5	0.4	0.6	0.93	1
		- 7.9	- 48.4	0.4	0.6	0.88	2
Mg II	1	- 30.8	- 86.6	1.2	1.2	0.89	3

Element	Mult.	Vc	Vedg	Remarks
Si II	3	unsh.	-202.3	1
		unsh.	-229.8	2
C II	1	unsh.	-281.6	1
		unsh.	-284.3	2
Si II	2	- 22.1	-211.9	1
		unsh.	-207.8	2
Al II	1	unsh.	-188.5	1
		unsh.	-185.8	2
He II (Ba. alph.)		- 64.4	-	1
		- 62.4	-	2
O I	2	- 14.0	-	1
		- 11.5	-	2
P II	1	- 15.1	-	1
		unsh.	-	2
C I	3	unsh.	-	1
		unsh.	-	2
C I	2	-	-	1
		- 22.1	-	2
Si II	1	- 10.9	-	1
		- 7.7	-	2
Fe II	3	- 17.4	- 52.5	3
Fe II	2	- 19.4	- 68.3	3
Fe II	1	- 15.4	- 53.8	3

Notes:Vc=Central velocity,Vedg= Edge velocity measured from the blue edge of the fitted gaussian line (km/s),FBWC=Full band width on the continuum (km/s),R/V=Ratio of the red and blue wings on the continuum.

Remarks:

	YR	DAY	U.T.
1]	1982	213	11:54
2]	1983	267	15:58
3]	1982	213	12:10

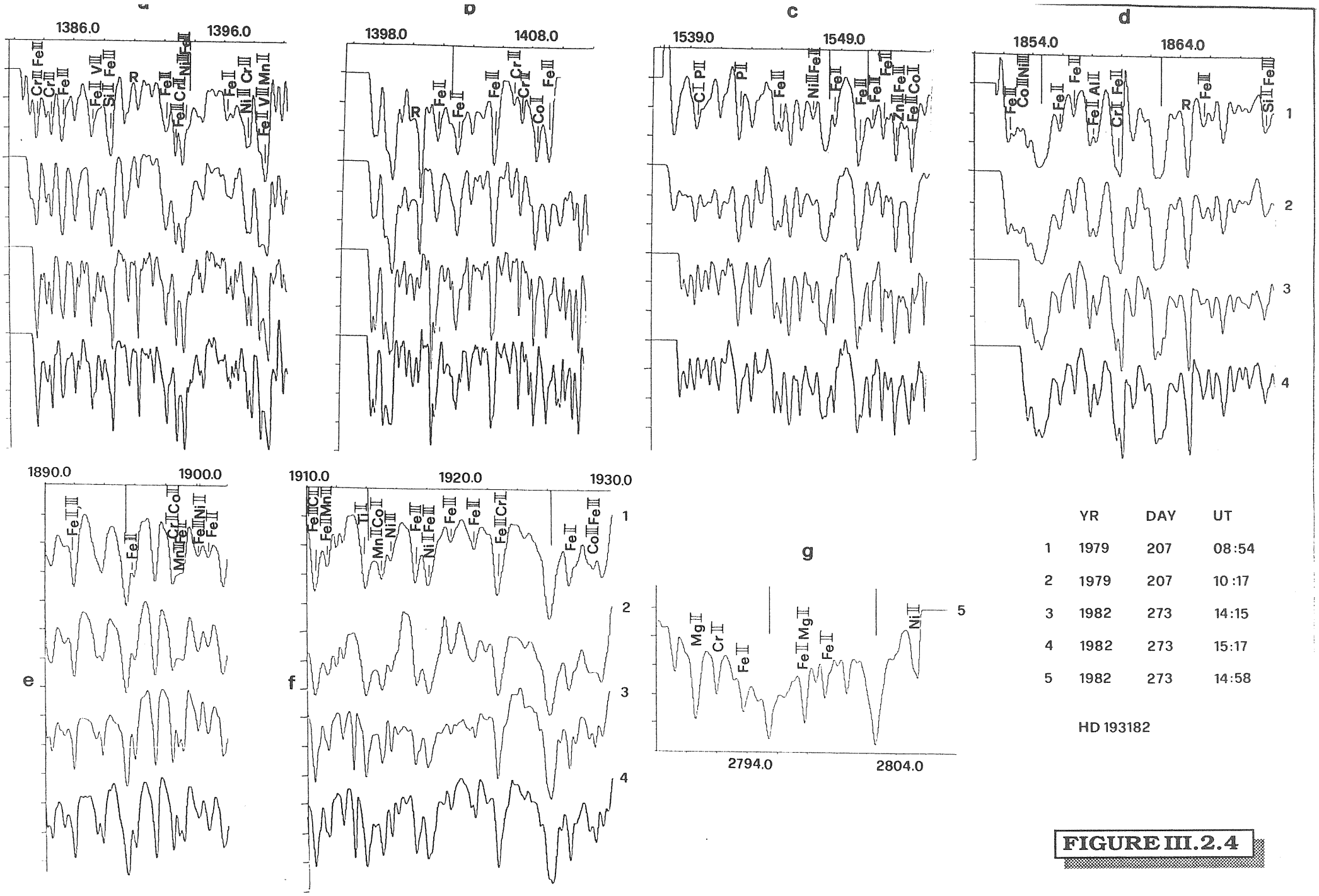

	YR	DAY	UT
1	1979	207	08:54
2	1979	207	10:17
3	1982	273	14:15
4	1982	273	15:17
5	1982	273	14:58

HD 193182

FIGURE III.2.4

Table III.2.5.UV spectral measurements of HD 193182.

Element	Multip.	Vc	Vedg	EQW	FBWC	R/V	Remarks
Al III	1	-24.6	-113.9	0.9	1.2	0.89	1
		-24.7	-121.1	0.7	1.1	0.90	2
		-42.8	-105.7	0.6	1.0	0.80	3
		-35.8	- 95.6	0.8	1.1	0.83	4
Fe III	34	-21.5	- 76.7	0.4	0.6	0.93	1
		-19.5	- 75.5	0.5	0.7	0.97	2
		-14.5	- 71.9	0.4	0.7	0.77	3
		-16.9	- 70.9	0.4	0.7	0.80	4
Mg II	1	- 14.8	-134.6	1.2	2.4	0.95	5

Element	Mult.	Vc	Vedg	Remarks
Si II	3	unsh.	-301.8	1
		- 29.3	-285.6	3
C II	1	unsh.	-307.6	1
		-24.7	-336.5	3
Si II	2	- 27.8	-303.1	1
		- 41.6	-306.7	3
Al II	1	unsh.	-309.3	1
		- 22.4	-281.6	3
He II (Ba. alph.)		- 68.7	-	1
		- 75.4	-	3
O I	2	- 24.9	-	1
		unsh.	-	3
P II	1	- 19.7	-	1
		- 23.4	-	3
C I	3	- 24.1	-	1
		- 30.6	-	3
C I	2	- 15.4	-	1
		- 18.2	-	3
Si II	1	- 21.4	-	1
		- 23.9	-	3
Fe II	3	- 11.7	-110.4	5
Fe II	2	- 11.1	-116.9	5
Fe II	1	- 8.4	-103.6	5

Notes:Vc=Central velocity,Vedg= Edge velocity measured from the blue edge of the fitted gaussian line (km/s),FBWC=Full band width on the continuum (km/s),R/V=Ratio of the red and blue wings on the continuum.

Remarks:

	YR	DAY	U.T.
1]	1979	207	08:32
2]	1979	207	09:47
3]	1982	272	13:50
4]	1982	272	15:17
5]	1982	272	14:46

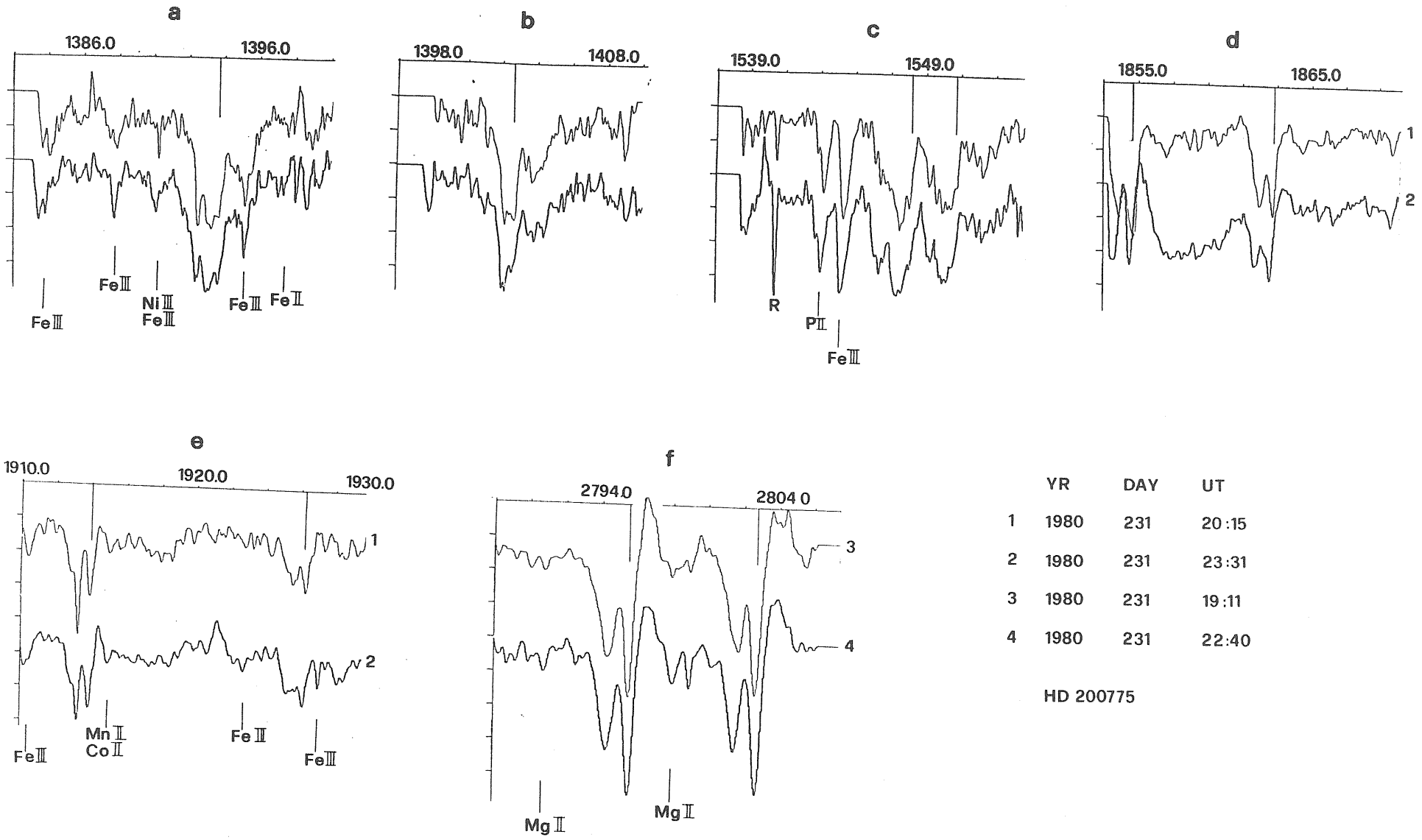

	YR	DAY	UT
1	1980	231	20:15
2	1980	231	23:31
3	1980	231	19:11
4	1980	231	22:40

HD 200775

FIGURE III.2.5

Table III.2.6.UV spectral measurements of HD 200775.

Elem.	Mul.	Vc	Vedg	Vc1	Vedg1	Vc2	Vedg2	EQW	FBWC	R/V	Rem.
Si IV	1	- 3.9	- 36.3	- 93.6	-173.3	-204.5	-290.6	1.2	1.5	0.80	1
		-14.2	- 83.7	-146.6	-201.9	-209.4	-290.5	1.2	1.7	0.90	2
C IV	1	-82.9	-159.1	-180.2	-290.3	-349.5	-391.7	1.2	2.3	0.72	1
		-	-	-125.4	-246.6	-338.9	-418.0	1.3	2.2	0.78	2
Al III	1	-11.4	- 66.4	-142.9	-220.4	-	-	0.7	1.2	0.65	1
		-23.3	- 54.2	-177.1	-198.5	-	-	0.5	0.9	0.72	2
Fe III	34	-10.7	- 39.3	-146.9	-186.2	-	-	0.4	1.2	0.97	1
		-18.9	- 43.3	-147.4	-169.9	-	-	0.5	1.4	1.00	2

Mg II 1

line	Vc	Vedg	EQW	DEPTH	FBWC	R/V	Remarks
2795.5	-133.5	-182.6	0.6	-0.6	1.0	1.00	3
	unsh.	- 26.9	0.6	-1.0	0.5	0.90	
	113.5	157.6	0.3	0.3	0.8	1.00	
2802.7	-129.2	-173.2	0.5	-0.6	0.8	0.90	3
	unsh.	- 36.2	0.6	-1.0	0.4	0.80	
	120.6	156.1	0.2	0.2	0.7	0.80	
2795.5	-132.9	-182.9	0.6	-0.6	1.0	1.00	4
	unsh.	- 27.9	0.6	-1.0	0.6	0.70	
	117.8	158.5	0.3	0.3	0.8	0.90	
2802.7	-126.9	-176.7	0.5	-0.5	0.8	0.80	4
	unsh.	- 32.9	0.6	-1.0	0.6	0.60	
	122.3	155.9	0.2	0.2	0.7	0.80	

Table III.2.6(Continued)

Element	Mult.	Vc	Vedg	V(*)	Remarks
Si II	3	unsh.	-195.0	-	1
		unsh.	-226.8	-	2
C II	1	unsh.	-263.0	- 30.7	1
		unsh.	-258.0	- 36.1	2
Si II	2	unsh.	-117.2	- 29.7	1
		unsh.	- 90.1	- 29.8	2
Al II	1	unsh.	-	- 17.9	1
		-163.9	-253.5	-	1,5
		unsh.	-	- 17.9	2
		-158.0	-238.6	-	2,5
Si II	1	unsh.	-	-	1
		unsh.	-	-	2
O I	1	unsh.	-	-	1
		unsh.	-	-	2
C I	2	unsh.	-	-	1
		unsh.	-	-	2
C I	3	- 20.1	-	-	1
		- 51.2	-	-	2
Fe II	3	unsh.	- 52.7	-	3
		unsh.	- 44.6	-	4
Fe II	2	unsh.	- 39.7	-	3
		unsh.	- 42.6	-	4
Fe II	1	unsh.	- 55.0	-	3
		unsh.	- 57.2	-	4

Notes:Vc=Central velocity,Vedg= Edge velocity measured from the blue edge of the fitted gaussian line (km/s),FBWC=Full band width on the continuum (km/s),V(*)=Radial velocity measured from the circumstellar component(km/s),R/V=Ratio of the red and blue wings on the continuum.Depth=Central depth of the fitted line,positive values corresponds to emission in continuum units.

Remarks:

	YR	DAY	U.T.
1]	1980	231	19:45
2]	1980	231	23:15
3]	1980	231	18:41
4]	1980	231	22:10

5]Al II 1671 presented a wide probably stellar component.

IV.SUMMARY OF THE OBSERVATIONS, INTERPRETATION AND CONCLUSION

IV.1.Results obtained from optical spectra

IV.1.1.Effective temperatures, gravities and spectral types.

As we stated in the previous chapters there are strong discrepancies between different determinations of the effective temperatures, gravity and spectral type estimates of these variable objects.So these values must be redetermined by every researcher as frequent as possible in order in order to compare them with the previous values.For determining effective temperatures and gravities of these stars we fitted the wings of H gamma and H delta lines with the theoretical profiles of Kurucz et al.(1974) models and compared the observed He I 4471 line strength with the theoretical ones.Our estimated values are presented in the fourth and fifth columns of Table IV.1.Figure IV.1 presents the observed and theoretical profiles for the program stars.From Table IV.1 we see that the effective temperatures for HD 183656 and HD 193182 are higher than the values which their spectral types predict; i.e.HD 193182 B8-A0 predicted Teff.=10000 K; HD 183656 B8 predicted Teff.=11000 K (Allen 1973).Oppositely for HD 184279 and HD 200775 estimated values are slightly lower than those expected from the spectral type.Only HD 22192 is in accordance with it's spectral type.This method which we used normally predicts slightly higher values (Underhill 1982), but

discrepancies for HD 183656 and HD 193182 are more higher than the expected 1000 K difference.Similarly for HD 184279 and HD 200775 the Teff lower, which suggests : i]temperature changes in the atmospheres of these stars, ii]wrong determination of the spectral types, iii]another light source disturbing the estimates of the spectral types and/or effective temperatures.Our estimated gravity values revealed that only one of our program stars-HD 184279 is a main sequence star, the others are slightly above the main sequence.

IV.1.2.Emission and shell spectra of the program stars.

Radial velocity and equivalent width measurements of HD 22192 revealed a small but evident radial movement in the envelope, probably including regions near the central object.An important remark is that this star presented V/R variability within 50 days interval for H beta line profile.

During the observational period HD 184279 exhibited two distinct phases: Be and Be/shell episode.Be phase is characterized by a P Cygni profile at H beta and blue shifted line centers suggesting an expansion in the envelope.Shell episode is characterized by a double peak emission with a central absorption having a positive radial velocity for H alpha and other lines, and a strong increase in the central depths of the hidrogen lines.The quasi-period suggested by Ballerau and Hubert-Delplace (1982),-4 years- is not consistent with our data, where a phase change occured in approximately 0.94 years.At JD=989.5 H I (n>6) and He I lines

exhibited double peak absorption components.Specially H delta line presented a form similar to that observed by Ballerau and Chauville (1987).Inflexions seen in the flanks of H alpha emission components at JD=991.5 and radial velocity measurements confirm a multi-component structure in the envelope of HD 184279.

Similarly to HD 184279, spectra of HD 183656 show multi-structure components of H alpha and radial velocity variations of the lines.Furthermore we observed stronger (nearly 30%) emission components than Rinquelet and Sahade (1981,1984) however the inflexions on the flanks at about the same relative intensity.This indicates that the multi-component shell is variable with time in dimensions and/or in density.Moreover the H alpha profile obtained on JD=930.6 presented narrower wings.This is another important sign for the suggested variation.H alpha and H beta emission components exhibited V/R variations within about 60 days. HD 183656 didn't displayed double-peak absorption components as Ringuelet and Sahade (1981,1984) reported.Probably HD 183656 presents a time variation for these double-peak absorption components. According to our equivalent width measurements HD 183656 presented a strong shell at JD=640.9, approximately 56 days after JD=584.6 which coincides with the V/R variation time interval.H alpha,H beta and the shell episode reached their maximum at JD=989.6.

HD 193182 presented H alpha profiles very similar to HD

183656, i.e. again a sign of multi-component structure in the envelope of the star.This star also presented V/R changes for the emission components but the physical and geometrical changes in the shell seem much smaller than HD 183656.

HD 200775 presented a very strong and variable H alpha emission.According to the observed H alpha depressions this line seems to be originated in a very compact region, which confirms the data by Baschek et al. (1982).H alpha and H beta profiles were blue dominated double-peak emission profiles, except on JD=647.0 when a single emission being observed.[Fe II] lines could be observed clearly and exhibited time variation which suggests the presence of variable low density regions.Higher members of the H Balmer lines (n>5) and He I lines exhibited multi-absorption components which suggests several distinct velocity fields although the main components of the same lines presented a simple velocity progression.

The theoretical consideration of the radiation field of extended atmospheres of Be stars developed by Miyamoto(1949,1952), Kogure(1959,1961) and Pottasch(1961) called the static atmosphere theory. We adopted Kogure's (1977) model of formation of shell lines in the Balmer series of the shell stars in order to present more clear physical and geometrical picture of the emission and shell spectra of the program stars; because this model predicts static envelope model and we have very small Balmer progressions and generally inverse Balmer progressions.In this method the expression for

the line profiles is given by taking into account the existence of a large scale velocity field due to differential rotation and/or other causes.When no appreciable Balmer progression appears the problem is simplified and we can specify an envelope by two kinds of parameters: the fractional area β of the stellar disk which is screened by the envelope and the mean optical thickness τ (H_α) of the envelope in the H alpha line.The formulation and the method of Kogure (1977) is described briefly in the in the appendix 2.Kogure (1975,1977,1978) applied this method to Pleione, HD 21750, HD 22192, ϕ Per, ζ Tau, β Mon A, ε Cap, and EW Lac.For each of these stars the values of and (H_α) are estimated based on the measurements of the radial velocities and central intensities of shell lines.His results show that the envelope can be well specified either by a single set of β and τ (H_α) (the single layer approximation), or by two sets of them (the double-layer approximation).The equatorial radii, electron densities and masses of the envelopes of these stars are estimated under the assumption of rotational broadening and the equator-on model.Kogure(1978) compared his results with the current models of the CSE' s of Be stars derived from IR and polarization data.The agreement is satisfactory in general.

As a first look to this method one can think that more than one combination of β and τ(H_α) can represent the CSE of a given star although there is an important observational

constraint which fixes these values to only one model which is the last principal quantum number n of the observed Balmer lines.This should be a measure of the development of the envelopes of shell stars.In this consideration, the value of n is principally determined by the product $\beta\tau(H_\alpha)$; which must be in accordance with the last observed Balmer line.In Table IV.1 , seventh and eighth columns present our estimated values of β and $\tau(H_\alpha)$, column nine gives the calculated last Balmer line and the last column presents the observed one.Kogure (1978) suggested that developed shells have log $\tau(H_\alpha)$ about 3.2-3.6, and weak shells have log $\tau(H_\alpha)$ of about 2.0-2.3.Comparing our program with his research we see that only HD 183656 and HD 193182 have developed shells.HD 22192 presented weaker shell than that observed by him. HD 184279 developed a "shell episode" within one year and HD 200775 presented relatively high $\tau(H_\alpha)$ values, had a "shell episode" like HD 184279.

Following Kogure (1978) we assume that the circular velocity Vc(R) at the distance R in the envelope can be expressed by

$$Vc=V(*)\ (R/R(*))^{j}\qquad\text{.....(IV.1)}$$

where V(*) is the stellar rotational velocity at the equator and R(*) the stellar radius.The value j represents the law of rotation inside the envelope in the following manner:

j=1, rotation with the conservation of momentum;

j=1/2, rotation with the law of Keplerian motion.

So if we assume the pure rotational broadening of shell absorption lines, we can estimate the equatorial radius of the absorption envelope from the measurement of the widths of shell lines:

Let R(a) be the equatorial radius and v (n) be the half width of the H(n) line (km/s), then we have

$$R(n)=R(*)[V(*)\sin i/\ v\ (n)]^{\frac{1}{1+j}} \quad \text{.....IV.2}$$

where V(*)sini and R(*) denote the projected rotational velocity and the stellar radius respectively.In deriving the extension of the outer envelope with the equation (IV.2) we first notice that the number of shell lines visible in the Balmer series is a measurement of the development of the outer envelope and the central intensity of shell lines for the highest members usually falls in the range of 0.75-0.85 as residual intensity, irrespective of the epoch of observation.In addition, the line widths decrease with the quantum number n. These facts enable us to expect that the values of R(a)/R(*) deduced from the mean half widths of the first members (such as H delta,gamma) should represent the outer extension of the absorption region.It should be mentioned that i]these values yield the equatorial extension of the absorption region, as long as the inclination angle i is closer to 90^{o} and ii]the values of R(a)/R(*) in Table IV.2a,b should be read as the lower boundaries of the actual equatorial extension at the respective epoch of observation, because several broadening mechanisms other than rotation are

$$\beta = (2\theta + \sin 2\theta)/\pi \quad \text{.....IV.6}$$

where $\sin\theta = H/R(*)$. It may be reasonable to suppose that layer1 with a larger optical thickness is the layer concentrating toward the equatorial plane where as layer2 with a smaller optical thickness is the one extending vertically from the equatorial plane on both sides of layer1. In other words, for the double layer approximation, the model disk is divided into two layers: layers1 and 2 of heights H(1) and H(2), respectively with the total height H=H(1)-H(2), and symmetrically with respect to the equatorial plane. Then the mass of the envelope relative to the solar mass is given by;

$$M_{gas}/M_{\odot} = 2.49*10^{-24}[R(*)/R(\odot)]^3\,[(R(a)/R(*))^2-1]\sum_i H_i\,\langle N_{e_i}\rangle/R(*) \quad \text{....IV.7}$$

where i denotes the layer i and R(⊙) is the solar radius. In deriving the numerical factor the abundance of 10% helium in the number density and the complete ionization of hydrogen atoms are assumed. In the single layer approximation, the summation over i is not needed. In the numerical calculation the effective temperatures are the one's which we summarized in the first part of this chapter while the electron temperature is assumed equal 10000 K. The numerical value of $B_{2c} I^{*}_{2c}(\nu)$ in equation IV.4 is evaluated from the emergent flux of the model atmospheres given by Kurucz et al.(1974). The stellar radii R(*) are derived from Allen (1973) table by an interpolation. The resultant outer radii R(a) depend on the choice of j with a factor of 1.5,2.0 larger for

the case j=1/2 than for the j=1.The mean electron density <N > is then smaller by a factor of about two in the case of j=1/2 than in the case of j=1.The masses of the envelopes show an increase of only 30% in the case of j=1.

This method is basically relied on the assumption of sole rotational broadening of the shell lines, this assumption holds in the case of very developed shells.But for our program stars,specially HD 184279 and HD 200775, this is a poor approximation.As, if the kinetic temperature in the envelope exceeds 10000 K the thermal broadening may become important, secondly Stark broadening may become important when the mean electron density in the envelope exceeds some critical value. Finally, as for the effect of turbulent broadening, we have no direct evidence suggesting the existence of large scale turbulence for well developed shell stars. Hence we must be cautious for the very active stars such as HD 184279 and HD 200775.In any case we adopted this method because of it's fast and simple approach to modelling Be stars.Table IV.2,a,b presents the values of H /R(*), , R(a)/R(*), R(e)/R(*), $\langle N_2 \rangle$, $\langle N_e \rangle$, and $\mathcal{M}gas/\mathcal{M}(\odot)$ for j=1/2, and j=1 respectively.Figure IV.2 presents the fitted shell models for the program stars.From the table as a whole one can say that the relative sizes of the envelopes, i.e. R(a)/R(*) and H/R(*) is rather similar to each other regardless the development of the envelopes in the stars.The main difference comes from the <N > values;$\langle N_e \rangle = 10^{11}$ cm^{-3} for developed shells, and $\langle N_e \rangle = 10^{10}$ cm^{-3} for

weak shells.

But in our case we have one exception which is HD 200775, probably the method is not applicable for this star, mainly because vsini< 80 km/s and this star is seen almost pole on or with a small i angle which violates one of the most important assumptions of the model.Also besides this, as we stated before, other line broadening mechanisms may probably be effective in this star.

One of the chief indications in the visible spectrum ,that outflow may be occuring in the B type supergiants is the fact that a Balmer progression is, observed for Ia supergiants, i.e. the lines H alpha, H beta and H gamma tend to show more negative radial velocities than do the higher members of the Balmer series. This systematic trend is shown by most of the B supergiants that have been investigated in detail by Hutchings (1976a,1980). Underhill (1982) concluded that the direction of the Balmer progression is never reversed for B supergiants.However our observations confirmed the resarches done by Aydin (1972) for HD 21389 and by Zvereva et al. (1984); and contradicted the above conclusion of Underhill (1982) because these supergiants do have inverse Balmer progressions , like Be stars.However, besides the Balmer progression variations the observed H alpha profiles and their long time scale variations are very similar to those observed in Be stars as it was already stated by Harmenec (1982).As an example H alpha profiles presented in the

appendix I clearly gives us the possibility to see how a disk-like structure can form even in the case of slow rotation i.e. HD 21389 $R(e,H_\alpha)/R(*)=9.4$, HD 199478 $R(e,H_\alpha)/R(*)=2.04$, $R(e,H_\beta)/R(*)=2.66$ (Rosendhal; 1972).Similar conclusion can be obtained easily from radial velocity measurements which reveal a very important fact:Disk-like structures, the only way to understand Be phenomena, are NOT only privilege of Be stars, moreover fast rotation-enhanced stellar mass loss is NOT the only effective parameter generating the Be phenomenon.

IV.2.Results obtained from UV spectra.

IV.2.1,Superionization, stellar winds and mass loss

In the previous chapter (III.2) we dealt with one of the most important astrophysical aspect of the last decades, that is superionized regions surrounding the hot stars, which are revealed by the resonance lines of O VI, N V ,C IV and Si IV.From this point of view this research presented facts which are strongly in favour of variable corona-like superionizing regions.If we give a look at the UV spectra presented in the chapter III.2 and appendix I, although Be stars generally exhibits superionization up to B8-B9 spectral types, we can barely see superionization in the case of HD 183656 and HD 193182 which are hot enough to present this.Besides this, HD 184279 which is the hottest of our program stars exhibits Si IV and C IV profiles comparable to late B supergiants.But immediately we note here a recent research (Grady et al.,1987) which reports that the same star revealed Si IV lines which

were much stronger than ours, with a blue edge velocity exceeding the escape velocity of the star ($\sim$1600km/s)Similarly Snow(1981) reported a wind velocity of 720 km/s for HD 22192.

The general belief is that, although stellar winds itself is a very complicated and multi-face problem; superionization is correlated with the stellar wind and mass loss or vice versa.Hence this research presented observational facts which are strongly in favour of the variable stellar winds and mass loss.Before proceeding further we see that mass loss rates observed from our program stars can feed their envelopes and cause the expectred optical spectral variation.i.e for HD 22192 $\dot{M}_{gas}=5.67*10^{-11}\ M_{\odot}/yr$, and $\dot{M}=2.63*10^{-11}\ M_{\odot}/yr$ (Snow,1981), for HD 183656 $\dot{M}_{gas}=3.63*10^{-11}\ M_{\odot}/yr$, $\dot{M}=2.6*10\ M_{\odot}/yr$ (Slettebak and Carpenter, 1983); where $\dot{M}_{gas}$ is the observed mass variation in the whole envelope and $\dot{M}$ the estimated mass loss from the central object.

The UV spectra of HD 200775 presented the fact that this object and similar ones must be handled alone because of it's amazing complexity in the UV spectra as well as optical.i.e. very short time variation in the line profiles, narrow blue shifted components.

Regarding mass loss , keeping in mind the escape velocities of our program Be stars -at maximum 1000 km/s and at minumum 800 km/s, we have not found any direct evidence of mass loss from them.As we discussed briefly in the beginning

of the chapter III.2 we have indirect evidences which are model dependent, such as asymmetric Si IV, C IV and Al III lines and in the best case P Cygni profiles of Mg II (HD 200775).Our program supergiants gave more direct evidences for mass loss.This is related with their lower surface gravities and lower escape velocities (about 500-600 km/s). We have observed continuous and variable stellar winds in specially Mg II ion for the supergiants.If we add here highly variable envelope structure of HD 21389 -as a reminder C IV sharp emission which was reported by Underhill (1982), we can state that superionization,stellar winds and mass loss are present in these Be supergiants.Looking back to other researchers such as those of Bates et al.(1987) and Praderie et al. (1980) not only our program stars but also α Cyg and β Ori, all presented variable and continuous flow.Regarding the nature of the flow, formation of the disk-like structures in these stars rules out the spherical symmetric homogenous outflow.Also the inverse variation of the blue shifted line component equivalent widths of Mg II with wind velocity shows that after the levitation of the stellar matter from the stellar surface only a small part of it reaches higher velocities, then the biggest part of the material falls down onto the star by having a closed trajectory, depending on the rotational velocity of the star, soon or later.One other remarkable observation was accompaniment of the emission wing with the highest wind velocity as in the Mg II lines of HD 21291 and HD

199478,indicating that mass is probably ejected high in the envelope.

Before closing this part we would like to review briefly other important observational points for the program stars in the UV range.In HD 22192 besides the presence and time variation of the superionized resonance lines of Si IV and C IV , Al III lines also contributed substantially to the wind as indicated by their highly asymmetric profiles.Si II lines revealed CSE components with expandind velocities of about 30 km/s indicating a radial motion.Inversely, Al III and Fe III lines gave no contribution to the wind of HD 184279 although they were quiet strong.Some firstly ionized ion lines i.e.Si II presented sharp components superimposed a wide profile.

In the case of HD 183656 and HD 193182 some contribution from Al III ions, but not from Fe III and Mg II is observed.Also sharp metallic lines in HD 193182 exhibited a strengthening in the shell over three years.For HD 200775 the situation is ,as we said before, very complex with short time variation and observed narrow blue shifted components.Another important remark for this star is that the blue edge velocities of the firstly ionized ions diminished with the increase of the C IV edge velocity.

Besides the above discussion about supergiants we can add the followings: Al III and Fe III lines were strong but gave little contribution to the wind of HD 199478.We have noted some variable inflexions on the weak emission components of Mg

II lines, which reminded us inflexions seen on the wings of H alpha line profiles of Be stars; they can be interpreted as multi structure in the wind. For HD 21291 we observed a relative decrease in the radial velocities of the firstly ionized species, when the wind had it's maximum radial velocity. The same phenomenon was presnet but not so significant in HD 199478. For HD 21389 O I lines were strongly blue shifted and exhibited notable variation.

IV.2.2.Synthetic spectra and possible interpretation of the UV shell lines.

The location of the gas that produces the shell lines is not clear. See for instance narrow lines present in HD 193182.Thomas (1980) argues that there is a low velocity region well beyond the wind where sufficient density builds up to produce the lines.Oppositely Snow et al.(1979) have suggested that the shell lines arise close to the star, in the low velocity region before the wind is strongly accelerated.In this view, the narrowness of the lines is due to the rapidly changing ionization of iron, -so that Fe III exists only in a thin level in the wind- and to the lack of co-rotation by the wind with the stellar rotation.It is fair to say that given the uncertainities in the ionization balance, the possibility cannot be ruled out that the Fe III shell lines form near the base of the wind below the rapid acceleration zone as suggested by Snow et al. (1979).The ionization states of both Si and Fe change very rapidly with height (Kallman 1980), so

the ionization fractions at a given level depend critically on the details of the ionization and recombination rates, many of which are not known accurately.

One objection to this interpretation of the shell lines was raised by Thomas (1980) who argued that the Fe II lines that are seen occasionally rule out any possibility that the lines form close to the star because stellar UV flux should ionize iron at least Fe III.Both Shull (1980) and Kallman (1980) have pointed out however this is not necessarly so, although these are not exact answers to the raised objection.If H I exists in the Fe III region for example ,significant quantities of Fe II may form via exchange reactions.

A different objection was given by Abbott (1981), who pointed out if the lines would form close to the star the co-rotation of the wind could broaden the Fe III lines beyond the 50 km/s widths which are observed.Taking into consideration this last objection we prepared synthetic spectra from Kurucz models using SYNTH procedure of OAT (Castelli et al. 1985).Our aim was two-fold: to see i) how line blending affects superionized lines, and ii) how line profiles are changing with the augmentation of the rotational broadening.(Figures IV.3a,b,c).

From the figures IV.3 we see that i]if the Be stars are fast rotators-it seems most of them so if they are not binary, rotational broadening is so efficient to dominate every other

effect supporting objections raised by Abbot (1980) and Thomas (1980) ii) in the case of 100 and 200 km/s of rotational velocities practically we see only the continuum, because the lines are so widened and merged in the continuum.Actually line widths of these shell lines quite well represented with the rotational broadening less than 50 km/s which is the observed thermal velocities of the gas after decelerating region (Thomas;1980); and this excludes that they are formed at R/R(*)=1.007-1.23.

IV.2.3.UV Continua of the program stars.

Lastly we would like to deal with the UV continua of the program stars, Before proceding further we observe that determination of the UV continua of these stars is inaccurate because of the large line blanketing in the in the UV region.So this part of the discussion is not conclusive.

Although UV continuum observations are undobtfully very important for these objects, namely the only way to see deep in the envelope and central object, so far little theoretical and observational studies done.Doazan (1982) briefly dealed with this subject as follows:We know that the Be stars exhibit an intrinsic reddening in the optical region, which affects the (B-V) index.The existence of this reddening makes it impossible to apply to Be stars the methods of dereddening used for normal B stars.Thus the neglecting these effects leads to an overestimate of the UV flux of the Be stars with respect to that of the B stars; normalizing the fluxes ot the

same V magnitude has the effect of underestimate the UV flux of the Be stars with respect to that of the B stars.We can comment here that probably the determination of the continuum itself introduces larger inaccuracy than the effects of the intrinsic reddening.

For the interstellar extinction correction of the continua we used Nandy et al. (1975) method.Even if we made an overestimation of E(B-V) values because of the intrinsic reddening, K_λ=A/E(B-V) values and determination of the observed corrected fluxes are more important for our aim which is to compare the shape of the continuum, with the Kurucz models. Figure(IV.3 a,b) presents the observed dereddened continua with the LTE model which were determined in the first part of this chapter.Infact we found strong deviations from the LTE continuum shape for all of our program stars, decreasing towards the late spectral types and increasing towards far UV, although near UV fits well in shape.

Lamers and Snow (1978) discussed this problem.The optical depth of the envelopes at the ionization edges of O V, N IV and Si III is of the order of unity.At such an optical depth very large deviations from LTE are to be expected for the radiation in the continuum.Consequently, the assumption of an optically thin envelope in the calculation of the ionization balance is justified except possibly for late B stars.

IV.3.Conclusion

It is almost impossible to interpret all the

observational data presented in this research.But in any case regarding our introductory remarks about Be phenomena we can draw out the following conclusions:

1]In this research we found important clues in favour of Outflow Model(OM).i.e,, variable superionization and mass loss but we must keep in mind that Binary Model(BM) is also very promising for explaining the observed spectra and it's changes.Numerical models for BM is missing.

2]Be phenomenon is not an isolated phenomenon in a definite class of objects but probably it is a common chracteristic of all early spectral type and all luminosity class objects.

3]There is no one single model to explain all the observed phenomena; one or more superimposed causes are needed.

Strategy for the future research can be oulined as follows:The irregular short-time and long-time scale variability of all Be and late-type supergiants reguire that; we observe each object for very long periods (years) regularly in UV and visual regions simultaneously.To build resonable models, it is better to observe few objects for very long periods than many objects episodically.

Table and Figure captions.

Figure IV.1.The Kurucz models selected to fit H gamma and H delta line wings

Table IV.1.The derived fundamental stellar and CSE values for program stars.

Figure IV.2.CSE models for program Be/shell stars.The theoretical curve for each layer is shown with the shifted original points O1,O2 etc. for two different epochs.The upper abscissa gives the positions of Balmer lines,where n is the principal quantum number.

Table IV.2a.Mean electron densities, masses of the envelopes and related parameters when j=1/2.

Table IV.2b.Mean electron densities, masses of the envelopes and related parameters when j=1.

Figure IV.3a,b,c.Synthetic and observed spectra for some selected program stars.Synthetic spectra has been prepared with variable rotational broadening.

Figure IV.4a,b.UV continua of the program Be/shell stars compared with the assigned LTE models.

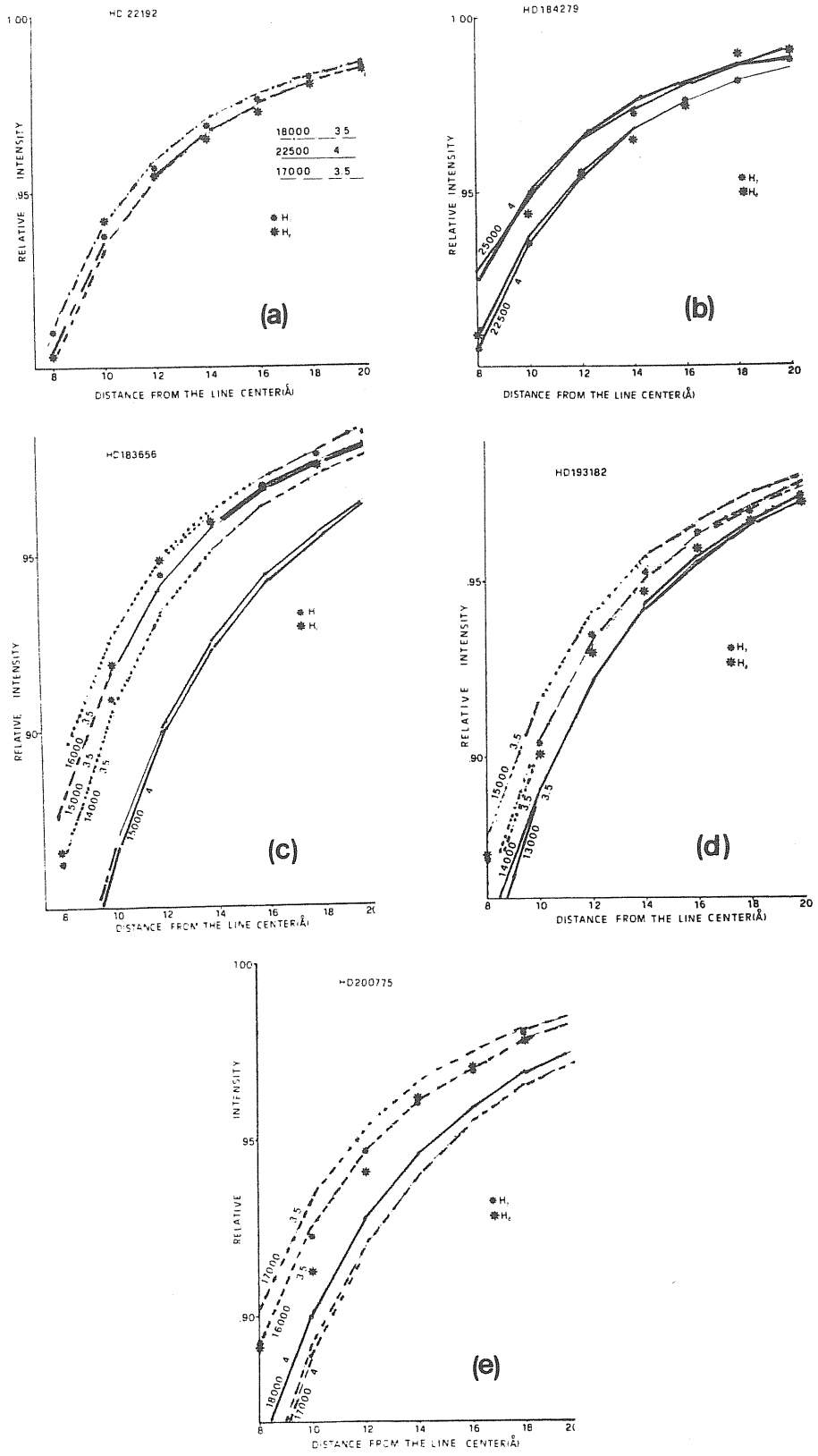
HD 22192
RELATIVE INTENSITY
1.00
.95
18000 3.5
22500 4
17000 3.5
(a)
DISTANCE FROM THE LINE CENTER(Å)
HD184279
25000 4
22500 4
(b)
HD183656
16000 3.5
15000 3.5
14000 3.5
13000 4
(c)
HD193182
15000 3.5
14000 3.5
13000 3.5
(d)
HD200775
17000 3.5
16000 4
18000 4
(e)

FIGURE IV.1

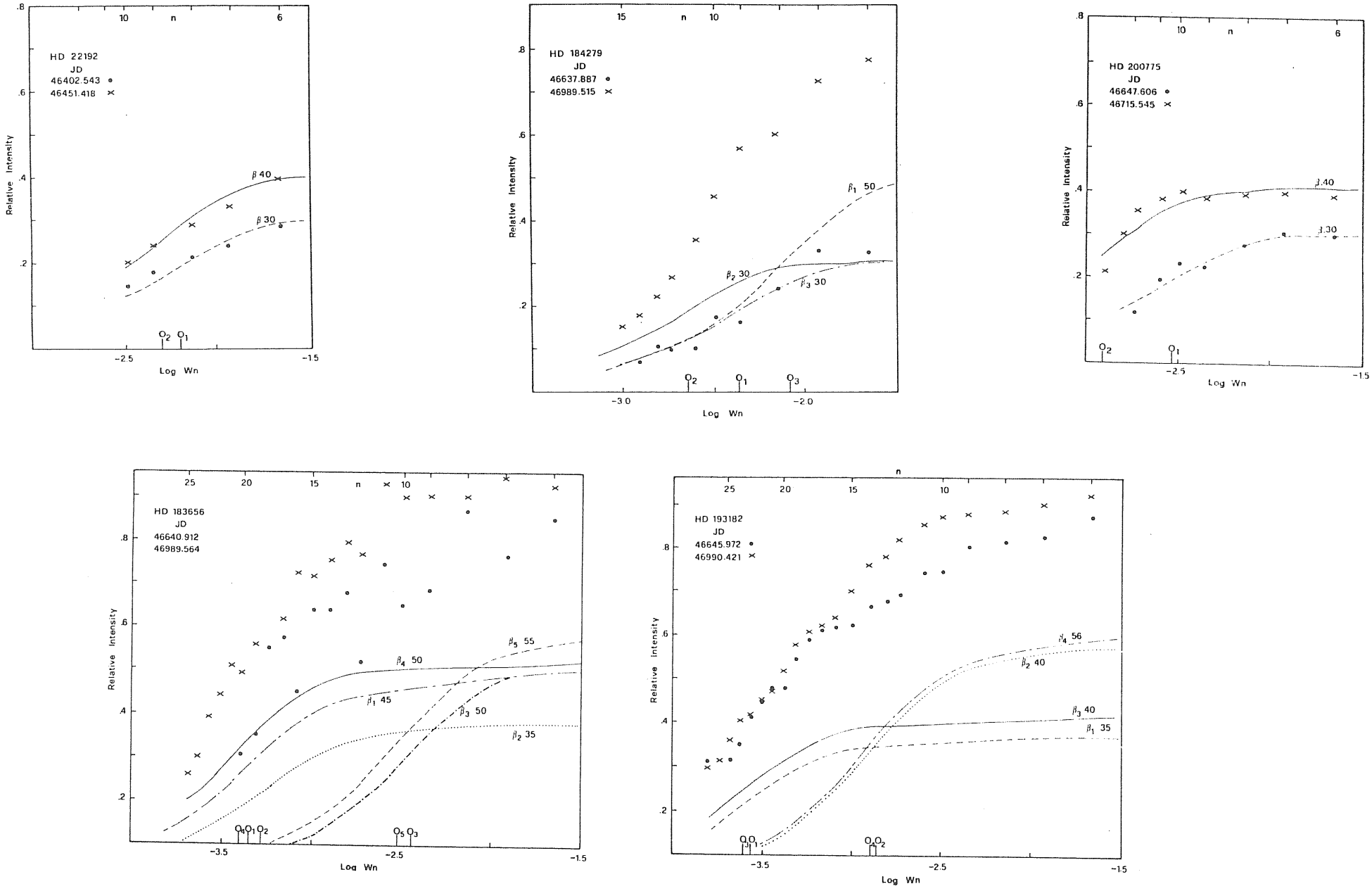
HD 22192
JD
46402.543
46451.418
β 40
β 30
O2 O1
Log Wn
Relative Intensity
HD 184279
JD
46637.887
46989.515
β1 50
β2 30
β3 30
O2 O1 O3
HD 200775
JD
46647.606
46715.545
HD 183656
JD
46640.912
46989.564
β5 55
β4 50
β1 45
β3 50
β2 35
O4 O1 O2
O5 O3
HD 193182
JD
46645.972
46990.421
β4 56
β2 40
β3 40
β1 35
O1 O2

FIGURE IV.2

Table IV.1. Effective temperatures, gravities and shell parameters of program Be stars.

Name	Spectral Type	vsini (km/s)	Teff. (K)	log g	J.D. (2400000+)	β	log $\tau(H_\alpha)$	n (cal.)	n (obs.)
HD 22192	B5(4)	300	16500	3.5	46402.5	0.30	2.20	13	15
					46451.4	0.40	2.31	14	17
HD 184279	B0.5	250	22500	4.0	46637.9	0.30	2.36	13	14
		(second layer)			46989.5	0.30 0.50	2.64 2.08	16	17
HD 183656	B8	180 (second layer)	15000	3.5	46640.9	0.35 0.50	3.32 2.44	30	29
		(second layer)			46989.6	0.50 0.55	3.42 2.52	34	35
HD 193182	B8-9	200 (second layer)	14000	3.5	46646.0	0.35 0.55	3.56 2.86	35	34
		(second layer)			46990.4	0.40 0.56	3.61 2.91	36	37
HD 200775	B3	<80	16000	3.5	46647.6	0.30	2.53	14	12
					46715.6	0.40	2.87	19	17

Table IV. 2. a. Mean electron densities, masses of envelopes and related parameters when j=1/2.

Name	R(*)/Re	J. D	Layer	H/R(*)	R(a)/R(*)	R(e,Hα)/R(*)	$\langle N_2 \rangle$	$\langle N_e \rangle$	$\mathcal{M}_{gas}/\mathcal{M}_\odot$ each layer	TOTAL
HD 22192	4. 27	46402. 5	Single	0. 32	4. 70	2. 98	2. 88(2)*	1. 13(10)		1. 48(-11)
		46451. 4	Single	0. 43	4. 98	–	3. 46(2)	1. 16(10)		2. 31(-11)
HD 184279	7. 41	46637. 9	Single	0. 32	2. 30	1. 54	6. 53(2)	5. 77(10)		8. 03(-11)
		46989. 5	Double	0. 32	2. 66	1. 52	9. 74(2)	6. 09(10)	1. 20(-10)	
				0. 55					2. 06(-10)	3. 26(-10)
HD 183656	3. 63	46640. 9	Double	0. 35	2. 83	1. 18	8. 63(3)	1. 09(11)	3. 18(-11)	
				0. 55					5. 00(-11)	8. 18(-11)
		46989. 6	Double	0. 55	2. 86	1. 17	1. 07(4)	1. 20(11)	5. 64(-11)	
				0. 61					6. 26(-11)	1. 19(-10)
HD 193182	2. 95	46646. 0	Double	0. 38	2. 20	1. 43	2. 81(4)	2. 32(11)	2. 16(-11)	
				0. 61					4. 38(-11)	6. 54(-11)
		46990. 4	Double	0. 43	2. 39	2. 00	2. 75(4)	2. 13(11)	2. 73(-11)	
				0. 63					4. 00(-11)	6. 73(-11)
HD 200775	4. 47	46647. 6	Single	0. 32	1. 22	–	9. 40(3)	3. 20(11)		1. 11(-11)
		46715. 6	Single	0. 43	1. 30	–	1. 05(4)	7. 06(11)		4. 66(-11)

(*)The number in parantheses is the power of 10 by which it is to be multiplied.

Table IV.2.b. Mean electron densities, masses of envelopes and related parameters when γ=1.

Name	R(*)/R$_\odot$	J.D	Layer	H/R(*)	R(a)/R(*)	R(e,H$_\alpha$)/R(*)	$\langle N_i \rangle$	$\langle N_e \rangle$	$\Delta M_{gas}/M_\odot$ each layer	$\Delta M_{gas}/M_\odot$ TOTAL
HD 22192	4.27	46402.5	Single	0.32	3.20	2.27	4.85(2)*	2.15(10)		1.23(-11)
		46451.4	Single	0.43	3.34	–	5.88(2)	2.71(10)		1.92(-11)
HD 184279	7.41	46637.9	Single	0.32	1.87	1.38	9.76(2)	8.67(10)		7.02(-11)
		46989.5	Double	0.32	2.08	1.37	1.50(3)	9.67(10)	1.04(-10)	
				0.55					1.79(-10)	1.83(-10)
HD 183656	3.63	46640.9	Double	0.35	2.18	1.14	1.34(4)	1.76(11)	2.75(-11)	
				0.55					4.33(-11)	7.08(-11)
		46989.6	Double	0.55	2.20	1.13	1.66(4)	1.94(11)	4.87(-11)	
				0.61					5.41(-11)	1.03(-10)
HD 193182	2.95	46646.0	Double	0.38	1.81	1.41	4.18(4)	3.59(11)	1.98(-11)	
				0.61					3.19(-11)	5.17(-11)
		46990.4	Double	0.43	1.92	1.08	4.13(4)	3.34(11)	2.46(-11)	
				0.63					3.61(-11)	6.07(-11)
HD 200775	4.47	46647.6	Single	0.32	1.07	–	2.98(3)	6.98(11)		1.78(-12)
		46715.6	Single	0.43	1.21	–	3.17(4)	5.93(11)		2.63(-11)

(*)The number in parantheses is the power of 10 by which it is to be multiplied

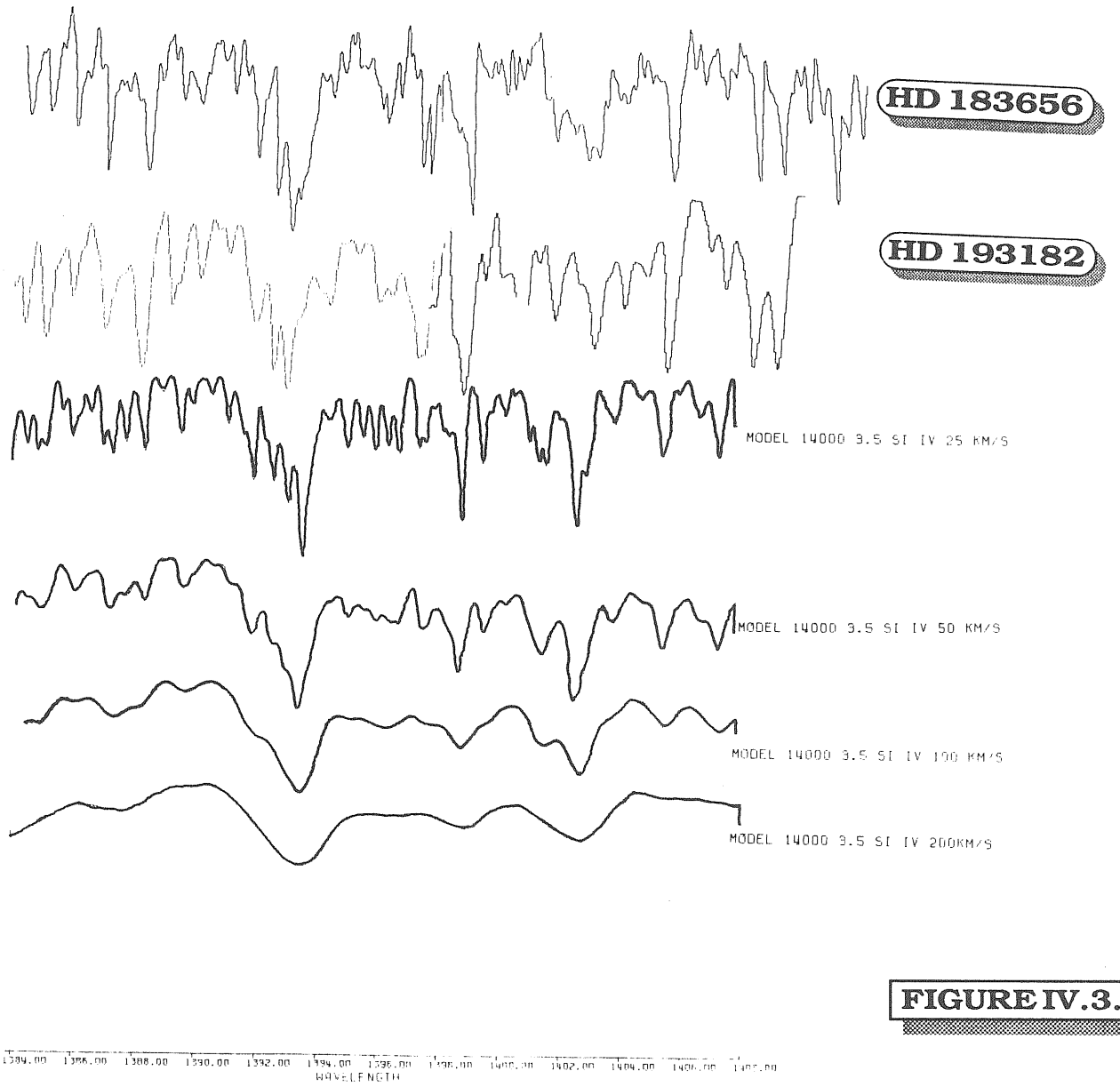
HD 183656
HD 193182
MODEL 14000 3.5 SI IV 25 KM/S
MODEL 14000 3.5 SI IV 50 KM/S
MODEL 14000 3.5 SI IV 100 KM/S
MODEL 14000 3.5 SI IV 200KM/S
1384.00 1386.00 1388.00 1390.00 1392.00 1394.00 1396.00 1398.00 1400.00 1402.00 1404.00 1406.00 1408.00
WAVELENGTH

FIGURE IV.3.a

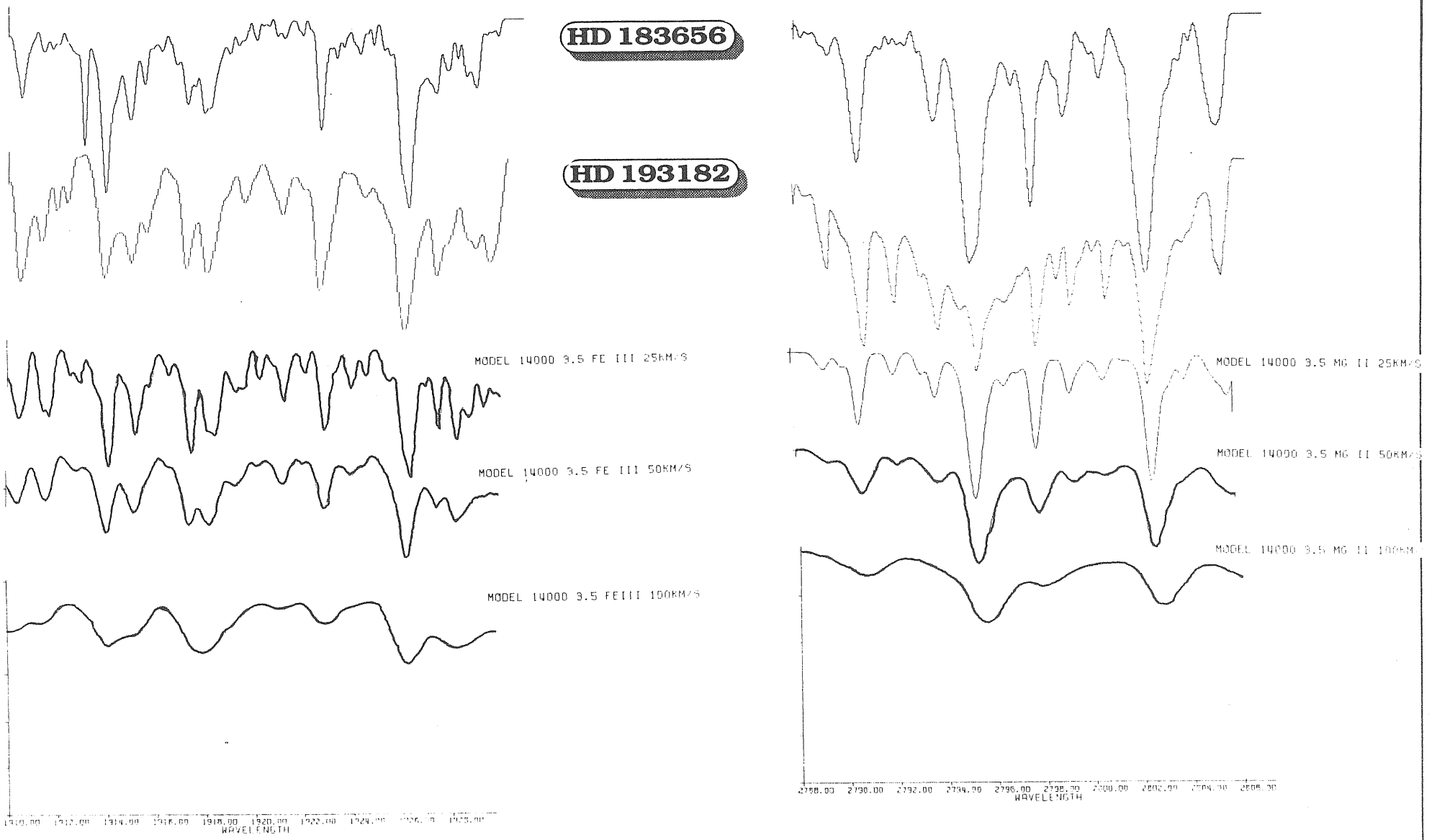
HD 183656
HD 193182
MODEL 14000 3.5 FE III 25KM/S
MODEL 14000 3.5 FE III 50KM/S
MODEL 14000 3.5 FEIII 100KM/S
1910.00 1912.00 1914.00 1916.00 1918.00 1920.00 1922.00 1924.00 1926.00 1928.00
WAVELENGTH
MODEL 14000 3.5 MG II 25KM/S
MODEL 14000 3.5 MG II 50KM/S
MODEL 14000 3.5 MG II 100KM/S
2788.00 2790.00 2792.00 2794.00 2796.00 2798.00 2800.00 2802.00 2804.00 2806.00
WAVELENGTH

FIGURE IV.3.c

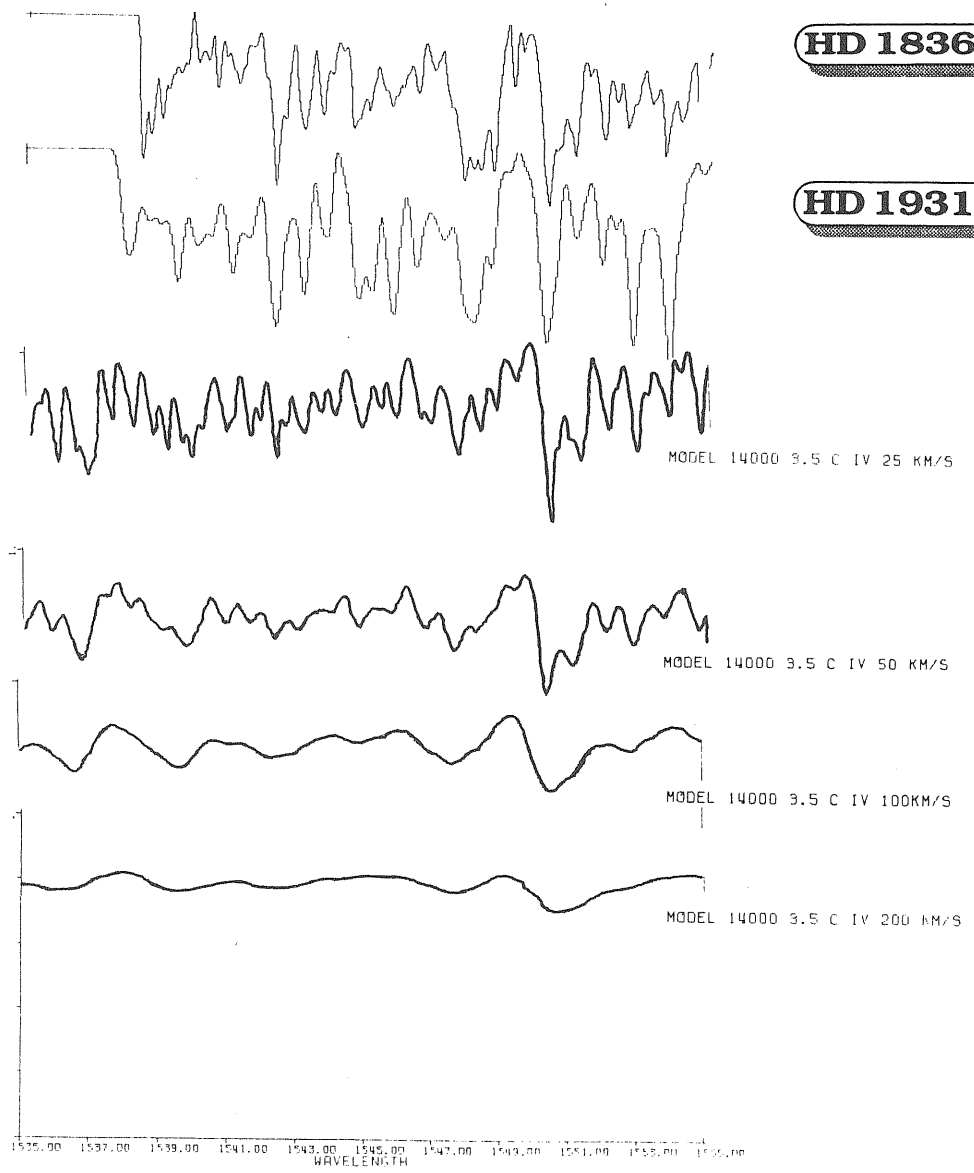
HD 183656
HD 193182
MODEL 14000 3.5 C IV 25 KM/S
MODEL 14000 3.5 C IV 50 KM/S
MODEL 14000 3.5 C IV 100KM/S
MODEL 14000 3.5 C IV 200 KM/S
1535.00 1537.00 1539.00 1541.00 1543.00 1545.00 1547.00 1549.00 1551.00 1553.00 1555.00
WAVELENGTH

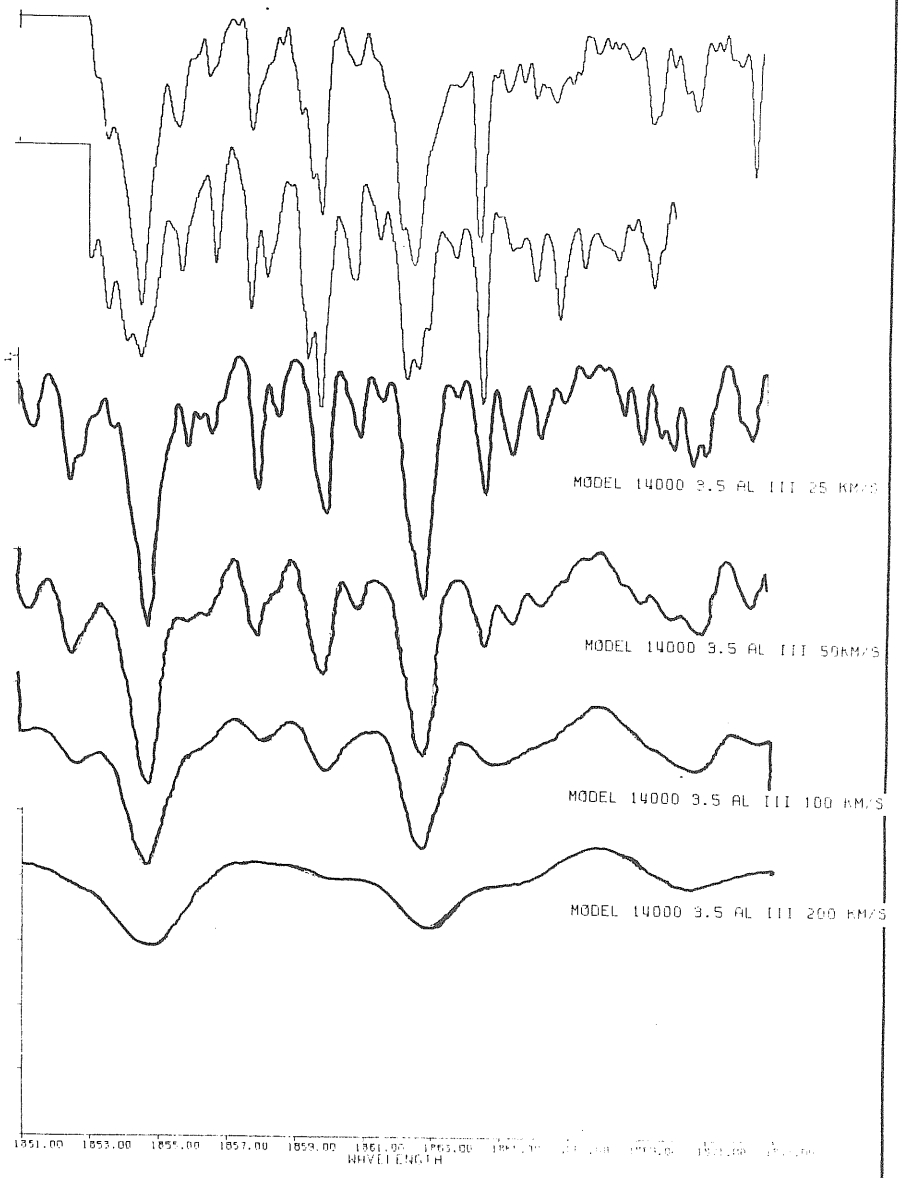
MODEL 14000 3.5 AL III 25 KM/S
MODEL 14000 3.5 AL III 50KM/S
MODEL 14000 3.5 AL III 100 KM/S
MODEL 14000 3.5 AL III 200 KM/S
1851.00 1853.00 1855.00 1857.00 1859.00 1861.00 1863.00
WAVELENGTH

FIGURE IV.3.b

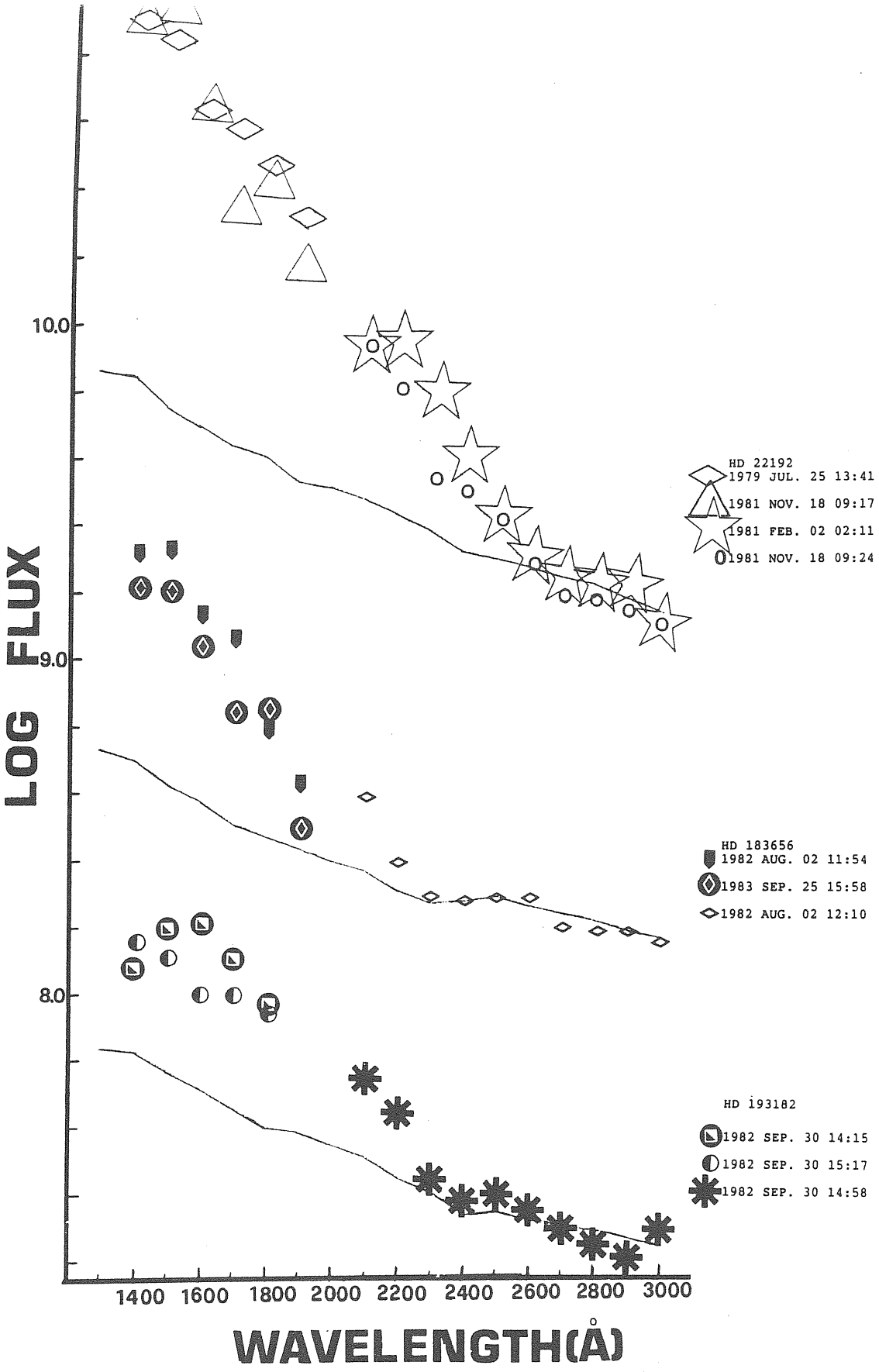
LOG FLUX
10.0
9.0
8.0
1400 1600 1800 2000 2200 2400 2600 2800 3000
WAVELENGTH(Å)
HD 22192
1979 JUL. 25 13:41
1981 NOV. 18 09:17
1981 FEB. 02 02:11
1981 NOV. 18 09:24
HD 183656
1982 AUG. 02 11:54
1983 SEP. 25 15:58
1982 AUG. 02 12:10
HD 193182
1982 SEP. 30 14:15
1982 SEP. 30 15:17
1982 SEP. 30 14:58

FIGURE IV.4.a

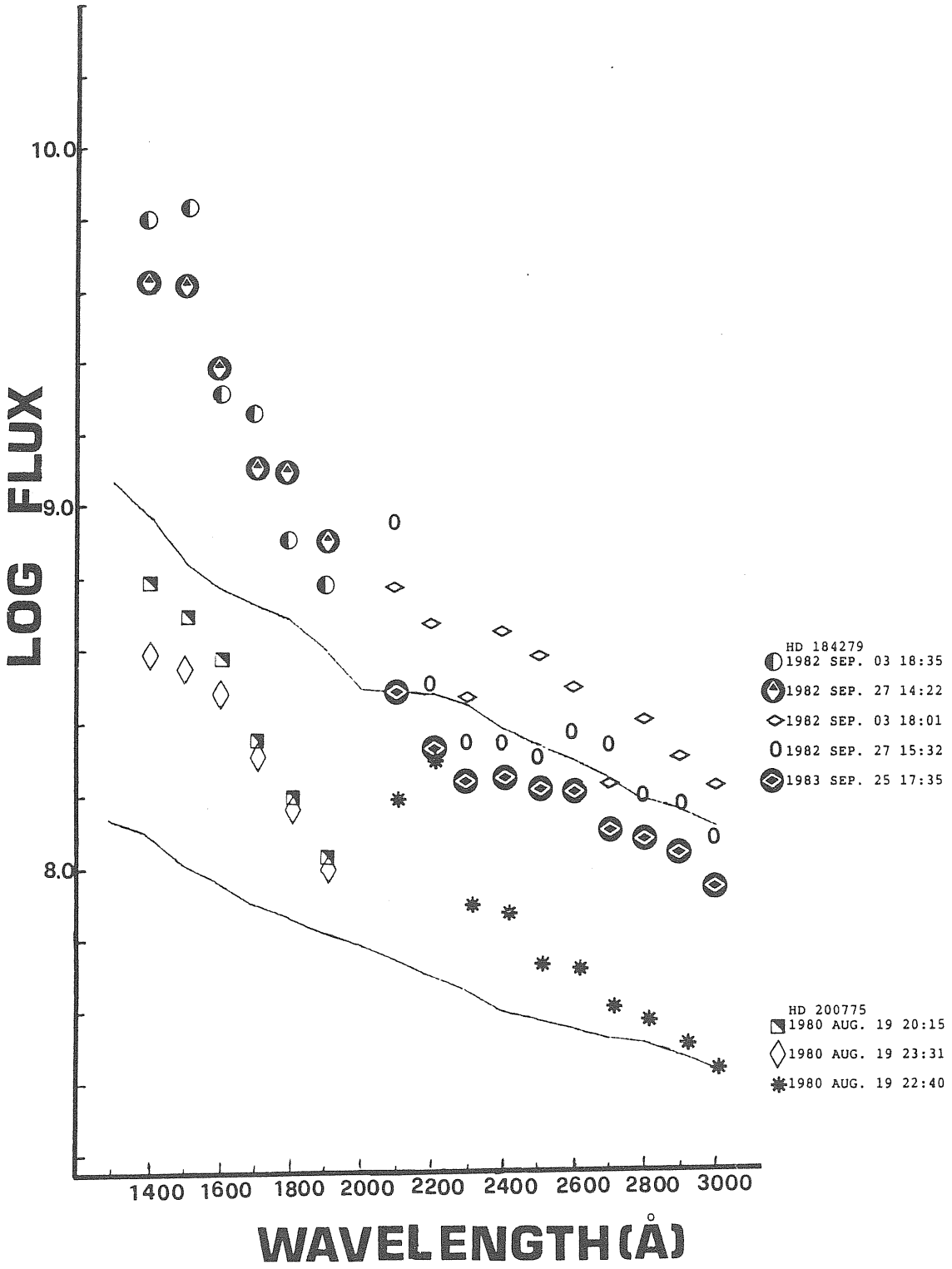
10.0
9.0
8.0
LOG FLUX
1400 1600 1800 2000 2200 2400 2600 2800 3000
WAVELENGTH (Å)
HD 184279
1982 SEP. 03 18:35
1982 SEP. 27 14:22
1982 SEP. 03 18:01
1982 SEP. 27 15:32
1983 SEP. 25 17:35
HD 200775
1980 AUG. 19 20:15
1980 AUG. 19 23:31
1980 AUG. 19 22:40

FIGURE IV.4.b

References

Abt H.A.,1957;Ap. J. 126,183

Abbot D.C.,1981,private comm.(Snow T.P.,1981)

Andrew P.J.,1968;Mon. Not. Roy. Soc. 72,35

Andrillat Y. and Fehrenbach C.H.,1982,A.A. Suppl. 48,93

Allen C.W.,1973;Astrophysical Quantities,London:Athlone Press.

Allochio C.,Morossi C. and Ramella M.,1983;IUEOAT Plotting Procedure,OAT/TRIESTE

Aydin C.,1972;A.A. 19,369

Baliunas S.L., Ciccione M. A. and Guinan E.F.,1975;Pub. Ast. Soc. Pacific,87,969

Ballerau D. and Chauville J.,1987,"Physics of Be stars",eds. A. Sleetbak, T.P. Snow,Cambridge Uni. Press,Cambridge.

Ballerau D. and Hubert-Delplace A.M.,1982;The Be stars,IAU Symp. No=98,171, eds. M. Jaschek- G. Groth,Reidel, Dordrecht

Baratta G.B.,Friedjung M.,Muratorio G. and Viotti R.,1987;"Physics of Be stars",eds. A. Sleetbak, T.P. Snow,Cambridge Uni. Press,Cambridge.

Barker P. K.,1983a;Pub. Ast. Soc. Pasific,95,996

Barsukova E.A.,Lebedeva I.A.Chargeishuili K.B. and Chentsov E.L.,1983; Bull. of Sp Ast. Obs.,North Caucasus 16,34

Baschek B.,Beltrametti M.,Koppen J. and Traving G.,1982;A. A. 105,300

Bates B.,Halliwell D.R. and Brown-Kerr W.,1987;Irish Ast. J.,17,258

Bernacca P.L.,Perinotto M.,1970;Publ. Obs. Padova Asiago,239

Bidelman W.P.,1950;Pub. Ast. Soc. Pasific,62

Cannon C.J. and Thomas R.N.,1977;Ap. J.211,910

Campbell W.N.,1985;Ap. J.,2,177

Castelli F.,1985:Local user note No=6,OAT,Trieste

Castelli F.,Crivellari L. and Magazzu M. ,1986;Local user note No=8,OAT,Trieste

Castle K.G.,1977;Pub. Ast. Soc. Pacific,89

Cester B.,Giuricin G.,Mardirossian F.,Pucillo M.,Castelli F. and Flora U., 1977;A.A. Suppl.,30,1

Curtis R.H.,1923;Pub. Univ. Michigan,VIII,1

Dachs J.,1987;,"Physics of Be stars",eds. A. Sleetbak, T.P. Snow,Cambridge Uni. Press,Cambridge.

Dachs J.,Hanuschik R.,Kaiser D.,.Ballerau D.,Bouchet P.,Kiehling R.,Kozak J., Rudolph R.,Schlosser W.,1986;A. A. Suppl.,63,87

Dachs J.,Hanuschik R.,Kaiser D.,Rohe D.,1986; A. A., 159,276

Davis R.,Strom K.M. and Strom S.E.,1983; Ast.J.,88,1644

Delplace A.M., 1970a, A.A., 7,459

Denizman L. and Hack M.;1988, A. A. Supl. 75,79

Doazan V.,1982; "B stars with and without emission lines",SP-456,NASA

Doazan V.,Selvelli P.,Stalio R.,Thomas R.N.,1980b, Proc. Sec. Eur. IUE-ESA Conf.,Tubingen, pp.145

Doazan V.,Stalio R.,Thomas R.N.,1980c,NASA IUE Sym.,Greenbelt,1980

Doazan V.,Kuhi L.V.,Thomas R.N.,1980a,Ap. J.,235,L17

Ebbets D.,1981;Pub. Ast. Soc. Pacific

Finkenzeller U.,1985;A.A.,151,340

Fontaine G.,Villeneuve B., Landstreet J.D. and Taylor R.H.,1982;Ap. J. Suppl.,49,259

Garrison M.L. and Anderson C.M.,1977,Ap. J., 218,438

Grady C.A.,Bjorkman K.S. and Snow T.P.,1987;Ap. J.,320,376

Gray D.F. and Marlborough J.M.,1974;Ap. J. Suppl.,27,121

Gerasimovic B.P.,1934;Mon. Not. Roy. Ast. Society,94,737

,1935;Observatory,58,115

Gillet D.,Guerin J. and Kohler D.,1986;notice d'utilisation no=2,OHP

Hanuschik R.,1986a,(in press,Dachs J.,1987)

Harper W.E.,1937;Pub. Dom. Ast. Obs.,7,1

Harmanec P.,1982,The Be stars,IAU Symp. No:98,279,,eds. Jaschek M. and Groth H.-G.,Reidel,Dordrecht.

Hirata R. and Kogure T.,1984;Bull. Ast. Soc.

India,12,109

Horn J.,Hudec R. and Koubsky P.,IBVS,2304

Horne K. and Marsh T.R.,1986;Mon. Not. Roy. Ast. Society,218,761

Huang S.,1973a: Ap. J., 183,541

Hubert-Delplace A.M. and Hubert A.,1979; ATLAS, Paris, Meudon Obs.

Hubert-Delplace A.M.,Mon M., Ungerer V., Hirata R., Paterson-Beeckmans F., Hubert H., Baade D.,1983; A.A., 121,174

Hutchings J.B.,1976a;Ap. J. Vol:203,438

Hutchings J.B.,1980;Ap. J. Vol:235,413

Jaschek M., Hubert-Delplace A.M., Hubert H. and Jaschek C., 1980; A. A. Suppl., 42, 103

Kallman T.,1980;Ph. D. Thesis, University of Colorado, Snow T.P.(1981)

Kitchin C.R.,1976;Ast. Spa. Sci., 45,119

Kogure T.,1959;Pub. Ast. Soc. Japan, 11,127 and 278

,1961; " " " " ", 13,335

,1969; A. A., 1, 253

,1977;Pub. Ast. Soc. Japan, 27,165

,1977; " " " " , 29,477

Kogure T., Hirata R.,1982; Bull. Ast. Soc. India., 10, 281

Kogure T., Hirata R. and Asada Y., 1978; Pub. Ast. Soc. Japan,30,385

Koppen J., Finkenzeller U., Mundt R. and Beltrametti M.,

1982; A. A.,112,174

Kriz S., 1976; Bull. Astr. Inst. Czech. ;27, 321

, 1979a; " " " " ;30, 83 and 95

Kriz S. and Harmenec P., 1975; Bull. Astr. Inst. Czech. ;26, 65

Kunacz P.B., 1980; Ap. J., 237, 819

Kurucz R.Z., Peytermann E.,and Avrett E.H., 1974, Line-Blanketed Model Atmospheres for Early type stars(Washington Smithsonian Inst.)

Lamers H.J.G. and Snow T.P., 1978; Ap. J., 219, 504

Lynds C.R., 1959; Ap. J.,130, 577

, 1960; " " ,131,390

Mc Laughlin D.B.,1961; Jou. Roy. Ast. Soc. Canada, 55, 13 and 73

Marlborough J.M. and Snow T.P.,1976; Proc. IAU Symp=70,ed. A. Slettebak, (Dodrecht:Reidel),pp.179

Merrill P.W.,1949; Pub. Ast. Soc. Pacific, 61, 38

,1951; Ap. J., 115, 47

,1952; " " , 116, 501

Merrill P.W. and Burwell C.G., 1933, Ap.J., 78, 87

, 1943, " " , 98, 153

, 1949, " " , 110, 387

, 1950, " " , 112, 72

Miyamoto S., 1949; Jap. J. Ast., 1, 17

, 1952; Pub. Ast. Soc. Japan, 4, 1

Molnar M.R., 1975; Ap. J., 200,106

Morgan T.H., Kondo Y. and Modisette J.L., 1977; Ap. J., 216, 457

Munch D. ,1957;Ap. J., 125,42

Nandy K., Thompson G.I., Jamar C., Monfils A. and Wilson R., 1975; A. A.44, 195

Norris J. and Baschek B., 1970; Ap. J. Suppl., 19, 305

Pasian F.,Rusconi L.,Sedmak G.,1982;Pub. O.A.T. No=806 and 807

Peters G.J., 1976; IAU Symp., 70, pp.401

, 1986; Ap. J. Lett., 301, L61

Plavec M., 1987;"Physics of Be stars",eds. A. Sleetbak, T.P. Snow,Cambridge Uni. Press,Cambridge.

Poeckert R. and Malborough J.M., 1978a; Ap. J., 220, 940

, 1978b; " " Suppl., 38 229

, 1979 ; " " , 233, 259

Polidan R.S., 1976; IAU Symp., 70, pp401

Pollitsch G.F., 1981; A. A. , 97, 175

Pottash S.R., 1961; Ann. d'Ap., 24, 159,

Praderie F., Talavera A., Lamers H.L, 1980; 86,271

Reynolds R.C.,1978; Ap. J. Suppl., 38, 205

Ringuelet A.E. and Sahade J., 1981; Pub. Ast. Soc. Pacific, 93,594

Ringuelet A.e., Sahade J., Rovina M., Fontenla J.M. and Kondo Y., 1984; A. A. 131, 9

Roman N.G. and Morgan W.N., 1950; Ap. J. , 111, 426

Rosendhal J.D., 1970a;Ap. J. ,159,107

, 1972 ;" " ,178,107

, 1973 ;" " ,186,909

Rosendhal J.D. and Wegner G.,1970;Ap. J. Vol:162;547

Rybicki G.B. and Hummer D.G., 1983; Ap. J., 274, 380

Sedmak G., 1987;(private comunication)

Shull J.M., 1980, (private communication,(Snow T.P.,1981)

Slettebak A., 1982; Ap. J. Suppl., 50, 55

Slettebak A. and Carpenter K.G., 1983; Ap. J. Suppl., 53, 89

Slettebak A. and Reynolds R.C., 1978; " " " , 38, 205

Snow T.P., 1981; Ap. J., 251, 139

Snow T.P., Peters G.J. and Mathieu R.D., 1979, Ap. J. Suppl., 39, 359

Sterken C., 1977; A. A. ,57, 361

Sterken C. and Wolf B., 1978; A. A., 70, 641

Strom S.E, Strom K.M. and Yost J., 1972; Ap. J., 173,353

Struve O., 1931a; Ap. J., 74, 225

, 1942 , " " , 95, 134

, 1944 , " " , 99, 205

Struve O and Wurm R., 1938; Ap. J., 88, 84

Swings J. P. and Struve O., 1943; Ap. J., 97, 194

Svolopoulos S.N., 1975; A. A. , 41, 199

Thomas R.N., 1973; A. A., 29, 29

, 1980;(Private communication, Snow T.P.,1981)

Tempesti P. and Patriarca R., 1976; IBVS, 1114

Uesugi A., 1978; Rev. Cat. of Stellar Rot. Velocities.,Kyoto univ.

Underhill A.,1982;B stars with and without emission lines,NASA SP-456

Viotti R., 1969; Mem. S. A. I. T., 40, 75

Viotti R., Altomore A. and Baratta G. B., 1977; 61, 133

Vojkhanaskaya P., 1976; IAU Symp, No=70, pp.237

Wackerling L.R., 1970; Mem. Roy. Ast. Soc., 73, 173

Walker G.A.H., Yang S. and Fahlman G.G, 1980; Pub. Ast. Soc. Pacific, 92, 411

Witt A.N. and Cottriel M.J., 1980; Ap. J., 225, 899

Zvereva E.B.,Zeinalov S.K. and Chentsov E.L.1984;Izves. Spets. Astro. Obs. Vol:18,29

APPENDIX I.Be Supergiant stars

I.Introduction

As it was suggested by several previous investigations (Rosendhal,1970; Aydin, 1972; Zvereva et al., 1984) there is need for continuous observations of early type supergiants for understanding the line variability, the kinematic properties, the large scale and small scale motions in their atmospheres.

The aim of this section is to present the results of the observations of optical and UV spectra for three supergiants which seem to be related to nebulosity and distinguished from other supergiants in having a definite affinity with Be stars.The program stars and their basic data are given in Table 1.It has been noted noted by Zvereva et al. (1984) that two of them,HD 21389 and HD 21291 may be the first samples of late-B and A-type supergiants,which have atmospheres dominated by radial pulsation-type motions.This study includes another object HD 199478, which is similar to the other two.

II.Observations and data analysis

II.1.The Observations

All the program stars have been observed at the Haute-Provence observatory. 30 spectrograms obtained at the Coude spectrograph of the 152 cm telescope at 7 ,12 ,20 A/mm reciprocal dispersions and at the 193 cm telescope at 10.6 A/mm with ISIS(CCD) (Gillet et al.;1986) device, are analyzed.The whole spectral region ranges from 3300 A to 6800 A.Table 2 gives the list of the optical spectra and the dates

of observation for the red and blue plates.Table 9 presents UV data of the program stars.Data processing same as explained in the second chapter, and same lines are being analysed in order to compare with Be stars.

The ISIS (Gillet et al.,1986) image has been processed at the Haute Provence Observatory with IHAP software;then the calibrated and heliocentricly corrected image has been transformed by a special procedure which converts FITS format to standard ELSPEC file(Castelli F. et al.,1986).

III.The Optical Spectra

III.1.Hydrogen lines

The Hydrogen lines of the program stars are sharp with Balmer series visible up to about n=22.Line profiles,radial velocities and equivalent widths are variable for all the program stars.The measured average Balmer discontinuies D for the program stars are the following :for HD199478 D=0.19,for HD 21291 D=0.23,for HD 21389 D=0.27. where

D=(logI[3650(A)+]-logI[3650-]) (1).

The measured radial velocities and average equivalent widths at the corresponding julian date are given in Tables 3a,b,c.Table 4 gives the radial velocities for the H alpha and H beta lines of Hydrogen compared with the radial velocities of the center of mass of the program stars.

III.1.1. HD 199478

The H alpha profile of HD 199478 was first published by Rosendhal(1973).It was a double- peak emission with the

component at the red edge weaker than the blue one with a central absorption at radial velocity +68 km/s.We present four different H alpha profiles.The first two of them which were observed during the same night show variable weak absorption components superimposed on a weak emission with H alpha absorption at the radial velocities +57.7 km/s for the first profile and +63.1 km/s for the second one respectively.(Figure 1a,b). These superimposed weak components were not present on the other two profiles which were observed with one night interval with each other.The emission and the absorption components are stronger,and for these last two profiles H alpha absorption radial velocities are +56.3 km/s and +57.9 km/s.(Figure 1c,d) Unfortunately these absorption components were affected by contribution of the terrestial atmospheric absorption, although their bandwidths on the continuum suggest that the stellar Hydrogen components are also present.

The H beta line profiles and radial velocities show a sequence of variation during the observation period.In the case of HD 199478 the profiles shown in Figure 2a,b,c which were secured on the same night show a contraction phase;the profile given in Figure 2d which was secured four nights later possibly presents the maximum of the contraction.In Figure 2g,h the spectra which were secured with two nights interval represents a passage from contraction to expansion and lastly in Figure 2i,j the profiles indicate expansion.

III.1.2. HD 21291

Two H alpha profiles of this star were analysed by Rosendhal(1973) which the first one was an inverse P Cygni profile, while the second one was an asymmetric absorption profile which was extended towards the blue and a trace of weak emission was present on the red side of the absorption.

Three H alpha profiles of HD 21291 are presented:The first one is an asymmetric,blue shifted absorption profile,radial velocity -33.4 km/s,with a weak emission component on the red edge which is similar to the second profile observed by Rosendhal.The weak equivalent width and the shape of the profile suggest a contribution by the emission component (Figure 3a). The profiles shown in Figure 3b,c were secured with one night interval.The first one shows an asymmetric absorption profile, the second one is more symmetric and both of them have no emission components;the equivalent widths are greater than the first one and the radial velocities are lower(-27.1 km/s and -26.5 km/s respectively).

The H beta line profile and the radial velocity changes during the observational period ,for HD 21291 are given in Figure 4.The profile in Figure 4a was observed during the same night as the H alpha profile in Figure 3a.It is symmetric and has wings up to + 350 km/s and radial velocity of -24.6 km/s;the equivalent width is the smallest among all our observed values.Figure 4b,c presents the profiles secured on the same night, with one night interval with the previous

one;the last two profiles show a notable difference in their shapes and radial velocities,-12.3 km/s and -18.1 km/s respectively. Profiles given in Figure 4 d,e,f,g are taken on the same night, and show the fast variation of the star in expansion phase..

III.1.3. HD 21389

This star is the most extensively studied one among the program stars.The H alpha profiles of this star show a series of variations from pure emission to absorption,or to inverse P Cygni, or to direct P Cygni profiles.Aydin(1972) observed a contraction phase of this star as indicated by the radial velocity progression of the Balmer lines and by the inverse P Cygni profile of H alpha.Later Rosendhal(1973) also analysed the H alpha profiles of HD 21389 and noted a double-peak emission and a superimposed central absorption profile for H alpha.Lastly Zvereva et al.(1984) observed a weak emission on both sides of the H alpha on August 1978 and a P Cygni profile on February 1980.

In this work three H alpha profiles of this star are presented.The first two profiles secured with one night interval show a variable and asymmetric absorption components without any emission feature with radial velocities -54.8 km/s and -46.1 km/s.The third profile shows a double-peak emission with a blue shifted absorption component at -19.3 km/s;it is similar to that observed by E.B. Zvereva et al. on August 1978(Figure 5 a,b,c.).

Similar rapid variations for the H beta profiles are observed for HD 21389. The profiles shown in Figure 6 a,b are observed on the same night;the first profile presents a double-peak asymmetric absorption component, although the second profile looks more symmetric, and the radial velocities -8.1 km/s and -3.4 km/s respectively:a possible contraction phase.Profiles given in Figure 6 c,d,e which were secured on the same night present possibly an atmospheric expansion phase,although Figure 6 f,g which were secured with one night interval,represent a possible contraction phase.Lastly Figure 6 h,i,j;suggest again an expansion.

III.2.The metallic lines

The metallic lines of the program stars also present variable profiles and radial velocities.The average velocity differences between the hydrogen lines (n > 10) and that of the metallic lines are also variable;in some cases there is a notable difference, during some other nights the differences are very small. Differences between the average velocities of Si II and Fe II for the program stars are given in Table 5.It seems that HD 21389 presents a change of the sign of the difference.This change was noted by Aydin (1972),and then by Zvereva et al.(1984).These observations indicate a change of the sign in a short time interval(hours).For HD 199478 and HD 21291 on the contrary all the measured differences were always positive. Some selected metallic line profiles of the program stars are presented as follows:SiII 3853.6,3856.0,3862.5 in

Figures 7a,8a,9a; HeI 4471.4 and MgII 4481.1 in Figures 7b,8b,9b; HeI 4921.9 and FeII 4923.9 in Figures 7c,8c,9c for HD 199478,HD 21291 and HD 21389 respectively.They show the variations clearly. Also the measured wavelengths,equivalent widths,relative depths, bandwidths on the continuum,and halfwidths on the continuum of HeI 4471 and MgII 4481 lines which are sensitive to the rotational broadening are given in Table 6.These values confirm the vsini values given in Table 1 showing that HD 199478 is a fast rotator than the other two.Figure 10 present the measured radial velocities of the absorption cores of the lines versus optical depth, for HD 199478, HD 21291 and HD 21389 respectively.These diagrams have been prepared in order to display the differential line shift pattern and compare them with Zvereva et al.(1984). So we combined lines with similar formation depths into groups.These optical depth values (Zvereva et al. ;1984) were calculated on the basis of a plane parallel atmospheric models containing macroturbulence.Typical values of the assigned optical depths are given in Table 7.

III.3.The interstellar lines

These stars are closely associated with nebulosities.Hence the interstellar Ca II and Na I lines are sharp and strong.All the program stars presented also evidence for shell components as seen in Beta Ori (Barsukova et al.,1983) but it was difficult to measure them with the available dispersions.Only one spectrogram of HD 199478

secured with the highest dispersion (7 A/mm) shows clearly an extended blue flank for the Ca II K line up to -102 km/s ,and also there is another component with velocity +39.1 km/s.For the same star Na I D lines also show a component at radial velocity +43.5 km/s.According to Munch(1957) HD 21291 had a very weak component at Na I 5890 line, with radial velocity -35 km/s that was not possible to detect with our available data.The unidentified interstellar features such as λ 5780,5797 and 6614 are observed in all the program stars. Their equivalent widths,relative depths and bandwidths on the continuum are given in Table 8.

Table 1.Basic data for the program supergiants.

Table 2.Available visual data for program supergiants.

Table 3.Measured radial velocities and equivalent widths for program supergiants.

Figure 1.H alpha profiles of HD 199478.X axis gives the relative radial velocity with heliocentric correction and Y axis gives the relative intensity.Solid lines are continuum and each level corresponds to 0.1 difference in relative intensity.JD=2440000+

Figure 2.H beta profiles of HD 199478.Same axis as figure 1,but each level corresponds to 0.2 difference in relative intensity.JD=2440000+

Figure 3.H alpha profiles of HD 21291.Same as figure 1.

Figure 4.H beta profiles of HD 21291.Same as figure 2.

Figure 5.H alpha profiles of HD 21389.Same as figure 1.

Figure 6.H beta profiles of HD 21389.Same as figure 2.

Table 4.Radial velocities of the H alpha and H beta lines relative to the center of mass velocities of the program supergiants.

Table 5.Measured radial velocity differences between the average values of Si II and Fe II values.

Table 6.Observed average spectral parameters of Mg II 4481 and He I 4471 lines.

Figure 7.Some selected lines of HD 199478.X axis gives heliocentricly corrected wavelengths in Angstrom.Each level corresponds to 0.2 difference in relative intensity and

continua are marked with a solid line.JD=2440000+ a)SiII 3853.6,3856.0,3862.5,b)HeI 4471.4 and MgII 4481.1,c)HeI 4921.9 and FeII 4923.9.

Figure 8.Some selected lines for HD 21291.Same as figure 7.

Figure 9.Some selected lines for HD 21389.Same as figure 7.

Table 7.Assigned optical depths for line and line groups.

Figure 10.Measured radial velocities versus log optical depth for HD 199478, HD 21291 and HD 21389.

Table 8.Observed quantities of the unidentified interstellar features.

Table 1. Basic data for the program stars.

	HD 199478	HD21291	HD21389
Spect. Type	B8 Ia	B9 Ia	A0 Ia
V(mag.)	5.69	4.23	4.58
B-V(mag.)	0.46	0.41	0.57
r(kpc.)	1.84	1.03	1.00
R(kpc.)	10.09	10.83	10.81
Vel.(km/s)	-16.00	-6.80	-6.00
Assoc. or Clust.	NGC 6991	CAM OB1	CAM OB1
vsini(km/s)	49.00	15.00	8.00

where V=Apparent visual magnitude, B-V=Observed B-V colour, r=Distance from the sun, R=Distance from the galactic center, Vel.=Radial velocity of the star, Assoc. or clust.=Stellar assocation or cluster to which the star may belong, Vsini= Measured rotational velocity. Vsini values are taken from following researchs: for HD199478 from Rosendal (1970), for HD 21291 from Bernacca P.L. et al. (1970), and for HD21389 from Aydin C. (1972). Other values are taken from Humpreys (1970).

Table 2. Available visual data for the program stars.

Spectrogram	Emultion	Date (d,m,yr)	UT time	Julian day 2400000+
HD 199478				
(a)	(b)			
GB 338	IIaOch	31/08/1970	20:18	40830.3487
GB 339	IIaOch	31/08/1970	21:12	40830.3862
GB 340	IIaOch	31/08/1970	21:54	40830.4154
GC 23	IIaOch	4/09/1970	22:05	40834.4230
GB 380	IIaF	6/09/1970	23:00	40836.4612
GB 381	IIaF	6/09/1970	24:04	40836.5056
GB 726	IIaOch	10/12/1970	17:38	40931.2344
GB 746	IIaOch	12/12/1970	19:35	40933.3155
GB9062	IIaOch	30/11/1985	19:57	46400.3314
GB9065	IIaOch	2/12/1985	18:58	46402.2903
ISIS(CCD)	-	25/07/1986	21:30	46637.3982
GA7253	IIIaF	27/07/1986	21:53	46639.4141
HD 21291				
GB9064	IIIaF	30/11/1985	22:47	46400.4537
GB9068	IIaOch	2/12/1985	01:57	46401.5856
GB9069	IIaOch	2/12/1985	02:36	46401.6127
GB9397	IIaOch	22/01/1987	17:57	46818.2504
GB9398	IIaOch	22/01/1987	18:25	46818.2698
GB9399	IIaOch	22/01/1987	19:55	46818.3323
GB9403	IIIaF	22/01/1987	25:01	46818.5448
GB9405	IIIaF	23/01/1987	19:00	46819.2941
HD21389				
GB4136	IIaOch	4/09/1977	03:17	43390.6372
GB4137	IIaOch	4/09/1977	03:33	43390.6484
GB4142	098-82	5/09/1977	01:34	43391.5658
GB4143	098-82	5/09/1977	02:08	43391.5894
GB4144	IIaOch	5/09/1977	02:42	43391.6130
GB4145	IIaOch	5/09/1977	03:00	43391.6255
W 7486	IIaOch	8/02/1984	19:53	45739.3298
W 7498	IIaOch	10/02/1984	18:27	45741.2694
GB9116	IIaOch	20/01/1986	20:48	46451.3693
GB9118	IIaOch	20/01/1986	21:30	46451.3984
GB9406	IIIaF	23/01/1987	20:30	46819.3566

(a)The dispersions of the spectra are the followings: GB = 12 Å/mm, GA =20 Å/mm, GC = 7 Å/mm, W= 10 Å/mm, ISIS= 10 Å/mm

(b)Effective Wavelength regions for emultions are the followings: IIaoch 3600-5100 Å, IIIaF and 098-82 4800-6700 Å, for ISIS image centered on H alpha and 50 Å total width of the observational band.

Table 3a. Measured radial velocities and average equivalent widths of HD 199478.

Elem.	Mult.	Wav. Lab. (A)	JULIAN DATE (2440000+) 0830.348	0830.386	0830.415	0834.423	0931.234	0933.316	6400.331	6402.290	Ave Eqw (A)
			Radial velocities (km/s)								
H	18 4	3691.6	- 7.6	-16.8	-35.8	-19.8	-13.4	-23.0	-18.2	-31.0	0.8
H	17 3	3697.2	-35.5	- 4.2	-26.9	-25.2	-18.9	-34.8	-15.7	-23.7	1.2
H	16 3	3703.9	- 8.4	-11.2	-28.0	-	-13.7	-43.9	- 1.0	-10.5	2.1
H	15 3	3712.0	- 5.6	-29.5	-28.0	-29.5	-21.7	- 1.1	-21.7	- 1.1	1.5
H	14 3	3721.9	- 6.2	- 6.8	-31.5	-25.3	-41.0	-26.8	-26.9	-22.1	1.5
H	13 3	3734.4	-20.0	-27.9	-21.9	-21.9	-23.5	-21.9	- 6.1	-12.5	1.8
H	12 2	3750.2	-	-12.9	- 6.1	-31.2	-27.4	-32.7	- 7.6	-20.2	1.7
H	11 2	3770.6	-	- 5.6	-14.5	-23.8	-20.7	-25.4	-20.7	-11.3	1.6
H	10 2	3797.9	-12.2	-28.2	-27.7	-15.3	-15.4	-37.1	- 1.2	-12.2	1.4
He	I bl 22	3819.6	- 1.7	-	-24.5	-32.2	-26.1	-33.8	-10.7	-15.3	0.8
H	9 2	3835.4	- 1.4	-20.3	- 4.2	-30.2	-30.2	-18.0	-13.4	- 7.2	1.5
Si	II 1	3853.7	-36.1	-26.6	-43.5	-45.1	-37.5	-42.0	-28.3	-37.4	0.2
Si	II 1	3856.0	-20.6	-13.9	-27.6	-32.1	-24.6	-30.7	-15.4	-18.4	0.4
Si	II 1	3862.6	-19.4	-28.7	-35.3	-27.7	-35.3	-30.8	-17.1	-18.1	0.4
H	8 2	3889.1	- 8.2	- 2.9	-13.0	-20.6	- 7.0	-26.7	-28.2	-25.2	1.7
C	II 4	3919.0	-32.3	-27.3	-19.3	-28.3	-17.8	-35.8	-	-26.8	0.1
C	II 4	3920.7	-14.3	-26.3	-23.3	-20.0	-23.3	-47.4	-29.3	- 36.8	0.2
Ca	II 1	3933.7	-22.1	-13.9	-20.7	-19.2	-20.7	-22.3	-11.8	-10.3	1.1
He	I 5	3964.7	-21.8	-11.8	-32.8	-44.6	-22.4	-43.2	-46.2	-38.7	0.3
Ca	II 1	3968.5	-13.3	-17.7	-20.7	-22.2	-11.9	-20.7	-13.3	-25.2	0.8
H	Epsl 1	3970.1	- 5.6	- 5.7	-19.0	-33.8	- 8.6	-30.8	-14.5	-35.3	1.4
He	I 55	4009.3	-25.7	-24.8	- 4.7	-29.0	-21.7	-33.4	-12.9	-29.2	0.2
He	I bl 18	4026.3	-26.0	-32.6	-23.5	-35.9	-24.9	-35.2	-36.6	-37.8	0.6
H	Delt 1	4101.7	- 4.0	- 0.3	-10.9	- 9.4	-13.8	-23.8	-22.4	-26.7	1.6
He	I 16	4120.8	- 7.6	- 0.5	-33.5	-26.3	-20.6	-19.1	- 4.9	-10.4	0.2
Si	II 3	4128.1	-35.8	- 7.1	-19.6	-25.3	-26.7	-33.8	-18.2	-15.3	0.4
Si	II 3	4130.9	-11.1	-22.8	-27.2	-30.0	-18.7	-24.3	-22.9	-28.6	0.5
He	I 53	4143.8	-10.9	-15.0	-18.1	-39.3	-32.3	-29.5	-26.6	-37.9	0.4
Fe	II 27	4233.2	-16.0	-29.8	-21.6	-41.0	-45.2	-50.8	-32.5	-29.9	0.3
H	Gamm 1	4340.5	0.4	13.2	-13.4	-22.9	- 3.9	-14.8	-16.1	- 3.6	1.7
Fe	II 27	4351.8	-47.3	-56.7	-45.9	-57.9	-43.1	-57.9	-22.9	-33.7	-
He	I 51	4387.9	-16.8	-30.8	-15.3	-23.3	- 7.2	-23.3	-35.7	-19.2	0.3
He	I 14	4471.5	- 4.2	-30.4	- 5.7	-24.1	-16.2	-21.5	-25.4	-20.2	0.9
Mg	II 4	4481.1	-11.9	-18.0	-25.7	-19.1	- 6.0	-20.5	-25.8	-16.5	1.0
Fe	II 37	4515.3	-	- 7.8	-	-14.4	-	-12.0	- 8.1	-39.4	-
Fe	II 38	4549.5	-29.5	-16.5	-30.9	-43.7	-27.2	-30.9	-32.1	-23.1	0.2
Fe	II 37	4555.9	-20.1	-26.2	-30.2	-34.0	-28.9	-	-21.2	-10.7	-
Fe	II 38	4583.8	-	-23.7	-35.0	-28.4	-15.8	-42.3	-33.5	-26.1	0.2
Fe	II bl 37	4629.3	-29.7	-30.7	-18.0	-	-31.9	-53.4	- 2.2	-21.7	0.1
He	I 12	4713.1	-13.9	-10.5	-11.4	-10.4	-20.4	-20.4	-30.4	-31.6	0.7
S	II 9	4815.5	-32.1	-30.2	-18.7	-	-21.2	-20.2	-38.3	- 7.6	0.2
H	Beta 1	4861.3	15.5	20.7	16.1	23.2	8.7	- 2.2	-20.2	-32.3	1.9
He	I 48	4921.9	-	-18.2	-18.4	-	-22.0	-25.6	-18.4	-22.0	0.6
Fe	II 42	4923.9	-	-17.8	-46.6	-	-13.2	-28.7	-32.2	-23.9	0.7

Table 3a(continued).

Elem.	Mult.	Wav. Lab. (A)	JULIAN DATE (2440000+) 0836.461	0836.506	6639.414	Ave Eqw (A)
			Radial velocities(km/s)			
H Beta	1	4861.3	5.3	9.3	-	-
He I	48	4921.9	-25.2	-22.0	-30.3	-
Fe II	42	4923.9	-13.0	-23.9	-48.7	-
He I	4	5015.7	- 6.7	-16.9	-20.0	0.1
Fe II	42	5018.4	-23.6	-17.8	-18.7	0.1
S II	7	5032.4	-16.9	-	-18.7	0.1
Si II	5	5041.1	-	-40.0	-31.4	0.2
Si II	5	5056.0	- 9.6	- 2.3	-24.4	0.2
Fe II	42	5169.0	-25.0	-16.5	-25.8	0.2
S II	6	5428.6	-21.0	-17.0	-28.7	0.2
S II	6	5432.8	-19.5	-27.3	-41.2	0.1
S II	6	5453.8	-14.8	-29.4	-12.2	0.3
S II	14	5640.0	- 5.4	-13.6	-18.7	0.1
S II	14	5647.0	-22.8	-20.8	-23.6	0.2
N II	3	5666.6	-28.6	-38.9	-13.1	0.1
N II	3	5679.6	- 4.0	- 7.9	-	0.1
Fe II	24	5779.7	-22.9	- 7.4	-	0.2
He I bl	11	5875.7	- 2.9	-10.1	-27.0	0.6
Na I	1	5890.0	-15.3	-17.5	-14.9	0.6
Na I	1	5895.9	-13.7	-12.1	-18.5	0.5
Si II	4	5957.6	-	- 8.0	-49.1	0.1
Si II	2	6347.1	-18.4	-16.3	-27.4	0.6
Si II	2	6371.4	-25.3	-13.2	-20.4	0.4
Ne I	1	6402.2	-18.8	- 7.9	-41.2	0.1
H Alph	1	6562.8	57.7	63.1	57.9	0.1
C II	2	6578.0	-15.0	-26.0	-18.7	0.2
C II	2	6582.9	-34.7	- 9.3	-20.2	0.2
He I	46	6678.2	-15.1	-22.6	-12.2	0.5

Table 3b. Measured radial velocities and average equivalent widths of HD 21291.

Elem.	Mult.	Wav. Lab. (A)	JULIAN DATE (2440000+) 6401.586	6401.613	6818.250	6818.270	6818.323	Ave Eqw (A)
			Radial velocities (km/s)					
H	18 4	3691.6	0.9	- 3.8	- 4.5	-13.4	-18.0	0.8
H	17 3	3697.2	- 1.8	- 6.3	- 4.5	- 4.6	-12.0	1.6
H	16 3	3703.9	- 9.1	- 7.5	- 4.2	-24.5	-18.5	0.8
H	15 3	3712.0	- 7.2	- 8.3	- 1.1	- 1.0	-18.6	0.8
H	14 3	3721.9	- 7.6	-16.0	-28.1	-26.6	-18.3	1.3
H	13 3	3734.4	-14.0	-13.8	-13.2	-14.0	- 9.2	0.9
H	12 2	3750.2	- 4.5	-13.4	- 4.3	-18.2	- 5.7	1.3
H	11 2	3770.6	-11.6	-11.2	- 1.6	-25.3	-31.0	1.3
H	10 2	3797.9	-	- 3.0	-10.6	- 1.9	-38.4	1.0
He	I bl 22	3819.6	-23.0	-19.7	-24.5	-16.7	-22.9	0.2
H	9 2	3835.4	-14.9	- 5.5	-27.9	- 5.3	-16.2	1.2
Si	II 1	3853.7	-14.0	-14.2	-31.4	- 5.4	- 8.1	0.2
Si	II 1	3856.0	- 7.8	-12.7	- 1.3	-16.6	-15.0	0.5
Si	II 1	3862.6	- 2.6	-21.2	- 7.9	-17.0	-13.7	0.3
H	8 2	3889.0	-13.3	-17.4	-32.7	-12.7	-10.0	1.0
C	II 4	3919.0	- 4.3	-	-38.8	-15.8	-17.5	0.1
C	II 4	3920.7	- 3.8	-	- 0.5	-	-23.0	0.1
Ca	II 1	3933.6	- 5.1	-15.3	-17.8	-10.3	-13.3	0.6
He	I 5	3964.7	- 7.3	-25.5	- 8.9	- 4.8	-20.9	0.1
Ca	II 1	3968.5	-11.3	-10.7	-13.1	- 8.5	-16.1	0.5
H Epsl	1	3970.1	- 3.6	- 9.7	-11.6	- 5.6	-17.3	1.0
He	I 55	4009.3	- 0.2	-14.0	- 5.6	-11.2	- 9.7	0.1
He	I bl 18	4026.3	-16.6	- 1.5	-20.2	-14.5	-20.2	0.2
H Delt	1	4101.7	- 2.3	- 1.7	-18.6	-35.0	-19.3	0.9
He	I 16	4120.8	-13.2	-59.1	- 2.5	-14.5	-26.2	0.2
Si	II 3	4128.1	- 5.8	- 1.0	-20.4	- 6.4	- 6.4	0.3
Si	II 3	4130.9	-16.7	-12.7	- 1.6	-18.5	-12.8	0.3
He	I 53	4143.8	- 4.1	- 2.5	-14.9	-14.8	-10.6	0.1
Fe	II 27	4173.5	- 2.3	-	-12.4	-19.5	- 6.7	0.1
Fe	II 28	4178.9	- 7.0	-17.7	- 7.6	-17.6	-12.3	0.2
Fe	II 27	4233.2	-10.4	-20.5	- 9.1	-14.3	-17.2	0.2
Fe	II 27	4303.2	- 5.9	- 7.3	-10.1	-22.2	- 5.9	0.2
H Gamm	1	4340.5	-10.5	- 6.4	- 3.5	-17.1	1.7	1.3
He	I 51	4387.9	- 5.7	-40.3	-10.9	-10.9	-19.1	0.3
He	I 14	4471.5	- 1.2	-46.5	- 1.7	- 5.7	-10.8	0.2
Mg	II 4	4481.1	- 2.1	- 9.6	- 8.3	- 6.2	- 7.3	0.6
Fe	II 37	4515.3	-20.8	-22.6	- 2.9	- 1.7	-	0.4
Fe	II 38	4549.5	- 2.8	- 6.5	-24.2	-21.5	-10.4	0.3
Fe	II 37	4555.9	-13.9	- 8.3	-31.1	-18.3	- 9.4	0.4
Fe	II 38	4583.8	-10.6	- 3.3	-16.9	- 4.2	-18.1	0.2
Fe	II bl 37	4629.3	-14.1	-	-17.8	-25.6	-11.5	0.2
He	I 12	4713.1	-16.7	-	- 7.7	-11.3	- 5.2	0.1
H Beta	1	4861.3	-12.3	-18.1	-20.4	- 3.5	- 7.0	0.9
He	I 48	4921.9	- 3.9	- 5.1	-20.5	-19.4	-22.2	0.2
Fe	II 42	4923.9	-11.5	-12.8	-29.7	-14.3	-24.1	0.9

Table 3b(continued).

Elem.	Mult.	Wav. Lab. (A)	JULIAN DATE (2440000+) 6400.454	6818.545	6819.294	Ave. Eqw (A)
			Radial velocities(km/s)			
H Beta	1	4861.3	-24.6	-16.1	-20.2	-
He I	48	4921.9	-11.1	- 2.7	- 8.6	-
Fe II	42	4923.9	-10.7	-10.7	-10.5	0.3
He I	4	5015.7	- 2.7	- 9.8	- 3.8	0.1
Fe II	42	5018.4	- 8.9	-15.2	- 3.4	0.3
Si II	5	5041.1	-10.3	-15.2	-10.7	0.2
Si II	5	5056.0	- 4.4	- 8.1	- 6.9	0.3
Fe II	42	5169.0	-11.6	-16.3	-10.7	0.4
Fe II	49	5234.6	- 7.3	- 5.0	-14.0	0.2
Fe II	49	5276.0	-11.8	-10.6	-10.8	0.2
Fe II	49	5316.6	-16.5	-12.2	-12.0	0.3
He I bl	11	5875.7	- 0.9	- 4.0	- 1.1	0.3
Na I	1	5890.0	- 8.7	-10.3	- 7.5	0.4
Na I	1	5895.9	- 7.8	- 5.9	-10.9	0.3
Si II	4	5957.6	- 2.0	- 8.0	-11.1	0.1
Si II	2	6347.1	- 1.5	- 9.7	-10.7	0.5
Si II	2	6371.4	- 8.6	-16.7	-11.3	0.4
H Alph	1	6562.8	-33.4	-27.1	-26.5	0.6
C II	2	6578.0	- 9.4	-11.8	- 7.1	0.1
C II	2	6582.9	-13.7	- 8.0	- 3.7	0.1
He I	46	6678.2	-10.9	-10.1	-15.4	0.3

Table 3c. Measured radial velocities and average equivalent widths for HD 21389.

Elem.	Mult.	Wav. Lab. (A)	JULIAN DATE (2440000+) 3390.637	3390.684	3391.613	3391.626	5739.330	5741.270	6451.369	6451.398	Ave Equ (A)
			Radial velocities (km/s)								
H 18	4	3691.6	-34.1	-10.2	- 3.8	-11.8	- 6.9	-26.2	-11.1	-17.6	0.7
H 17	3	3697.2	- 9.3	-31.6	-28.5	-12.6	- 1.3	-12.3	- 9.2	- 8.6	1.2
H 16	3	3703.9	- 5.8	-15.3	-16.0	- 1.9	- 1.0	-24.8	- 5.1	-17.9	0.7
H 15	3	3712.0	- 4.2	-12.1	- 1.0	-20.0	-16.7	-20.1	-14.2	-17.4	1.3
H 14	3	3721.9	-31.5	- 4.7	- 3.1	- 1.6	-47.3	-11.0	- 8.9	- 3.1	1.3
H 13	3	3734.4	- 1.4	- 7.2	- 3.0	- 1.4	-18.8	- 0.2	- 3.5	-20.0	1.0
H 12	2	3750.2	- 1.4	-12.3	- 0.2	- 1.4	- 7.6	- 9.2	-15.0	- 6.5	1.2
H 11	2	3770.6	- 5.1	- 8.2	- 6.6	-22.2	- 1.9	- 9.8	-24.1	- 9.5	1.7
H 10	2	3797.9	- 0.9	- 7.6	- 6.0	- 7.6	-23.1	-15.3	-16.4	-11.4	1.2
He I bl 22		3819.6	-39.5	- 1.4	- 5.6	-48.9	-12.3	- 7.5	-17.1	- 3.6	0.3
H 9	2	3835.4	- 8.5	- 4.2	-10.3	- 6.0	-11.8	-24.1	- 7.8	- 3.5	1.2
Si II	1	3853.7	-28.3	-22.0	-11.5	-13.0	-14.5	-28.3	-15.3	- 5.6	0.3
Si II	1	3856.0	-13.9	-12.3	-10.8	-21.5	-24.5	- 0.8	-11.8	-11.1	0.4
Si II	1	3862.6	-20.1	-17.1	-14.0	-14.1	-21.6	- 7.9	- 7.5	- 6.2	0.4
H 8	2	3889.1	-20.6	-11.5	- 0.6	- 4.8	-11.5	- 5.5	- 7.0	-13.4	1.2
C II	4	3919.0	-28.3	-14.8	-32.8	-	-14.8	-17.5	-25.4	-46.9	0.4
C II	4	3920.7	- 9.8	-	-18.8	-29.3	- 9.8	-29.0	- 5.6	-27.6	-
Ca II	1	3933.7	-13.3	- 7.3	- 8.8	-13.3	- 5.8	- 8.8	- 8.5	-11.6	0.8
He I	5	3964.7	- 4.6	-28.3	-16.3	- 7.6	-15.4	-19.2	-20.9	-40.3	0.2
Ca II	1	3968.5	-16.3	-11.8	- 7.4	-20.7	-19.2	-11.8	-14.0	- 6.1	0.6
H Epsl	1	3970.1	- 5.6	- 5.6	- 5.6	- 6.1	- 5.8	- 6.2	- 8.4	-14.8	1.2
He I	55	4009.3	-29.0	- 7.0	- 7.1	-33.2	- 5.3	- 2.6	- 2.4	- 5.6	0.4
He I bl 18		4026.3	-17.6	-10.3	-17.6	-22.0	-10.3	- 1.5	-15.0	-24.1	0.2
H Delt	1	4101.7	- 8.1	- 2.3	6.3	- 0.9	- 3.4	-12.3	- 1.7	-16.5	1.5
He I	16	4120.8	-19.4	-16.6	-28.8	-10.7	-24.9	-10.7	- 2.2	-12.0	0.1
Si II	3	4128.1	-18.1	-13.8	-12.4	- 5.3	-12.4	- 5.3	- 3.4	- 7.4	0.4
Si II	3	4130.9	-11.6	-17.2	-12.9	-10.1	- 4.4	-10.2	-11.0	- 7.4	0.3
Fe II	27	4173.5	- 6.8	-11.2	- 9.8	- 9.8	-18.3	- 9.8	-18.9	-19.7	0.3
Fe II	28	4178.8	- 7.5	- 6.1	-29.4	- 9.1	- 8.9	- 0.4	- 0.5	-14.5	0.3
Fe II	27	4233.2	- 6.3	-11.9	-14.6	-18.8	-10.4	-18.9	-15.3	-13.2	0.4
Fe II	27	4303.2	-16.9	-17.0	- 7.5	- 8.0	- 6.1	-18.4	- 7.4	-14.3	0.3
H Gamm	1	4340.5	- 5.3	- 1.2	-14.7	-10.5	4.9	-12.9	1.5	-12.2	1.6
He I	51	4387.9	-	- 7.2	-	-20.2	-23.3	- 8.5	-11.1	- 1.9	0.3
He I	14	4471.5	-	- 1.7	- 3.1	- 4.4	-14.9	- 4.4	-10.6	-10.7	0.3
Mg II	4	4481.1	-17.8	- 2.1	- 1.1	- 6.0	- 8.7	- 7.6	- 1.7	- 7.0	0.8
Fe II	37	4515.3	-10.7	-17.2	-19.0	- 5.5	-13.8	- 4.2	- 9.1	-12.7	0.2
Fe II	38	4549.5	- 7.5	-11.4	-19.2	-16.2	-20.4	-17.9	-10.2	-14.7	0.7
Fe II	37	4555.9	-22.5	- 4.4	-14.6	-10.9	-17.4	- 7.2	- 5.1	-15.3	0.3
Fe II	38	4583.8	-26.1	-17.0	-16.3	-10.7	-10.7	- 9.4	-12.8	-12.8	0.4
Fe II bl 37		4629.3	-12.9	- 2.7	-11.6	-19.3	- 7.0	-29.4	-11.2	- 7.6	0.3
H Beta	1	4861.3	- 8.1	- 3.4	- 2.2	- 4.6	-10.7	4.0	3.7	-13.8	1.5
He I	48	4921.9	-38.7	- 5.2	-17.2	- 7.7	-12.4	-	-13.1	- 7.6	0.2
Fe II	42	4923.9	- 2.4	- 8.4	-18.5	- 9.5	-14.3	-	-16.1	- 8.2	0.4

Table 3c(continued).

Elem.	Mult.	Wav. Lab. (A)	JULIAN DATE (2440000+) 3391.566	3391.589	6819.357	Ave Eqw (A)
			Radial velocities(km/s)			
H Beta	1	4861.3	-17.8	-	-13.0	-
He I	48	4921.9	-	-	-13.6	-
Fe II	42	4923.9	- 8.4	-	-10.5	-
He I	4	5015.7	- 3.8	-	-15.5	0.1
Fe II	42	5018.4	-16.0	-	-10.6	0.3
Si II	5	5041.1	-11.5	-	-15.2	0.2
Si II	5	5056.0	-13.4	-	-11.5	0.3
Fe II	42	5169.0	-22.5	-	-12.0	0.4
Fe II	49	5234.6	-22.1	-	-11.9	0.2
Fe II	49	5276.0	-11.5	- 2.8	-10.8	0.2
Fe II	49	5316.6	- 5.0	- 8.9	-12.3	0.3
He I bl	11	5875.7	- 3.2	-10.2	- 5.1	0.3
Na I	1	5890.0	- 5.1	- 9.5	-13.3	0.6
Na I	1	5895.9	- 7.6	- 9.1	- 8.3	0.6
Si II	4	5957.6	-20.4	-15.0	-14.3	0.7
Si II	2	6347.1	- 1.5	-12.6	-13.6	0.7
Si II	2	6371.4	-12.1	-16.0	- 3.0	0.5
H Alph	1	6562.8	-54.8	-46.1	-19.3	0.4
He I	46	6678.2	- 5.6	-12.0	- 8.3	0.3

FIGURE 1

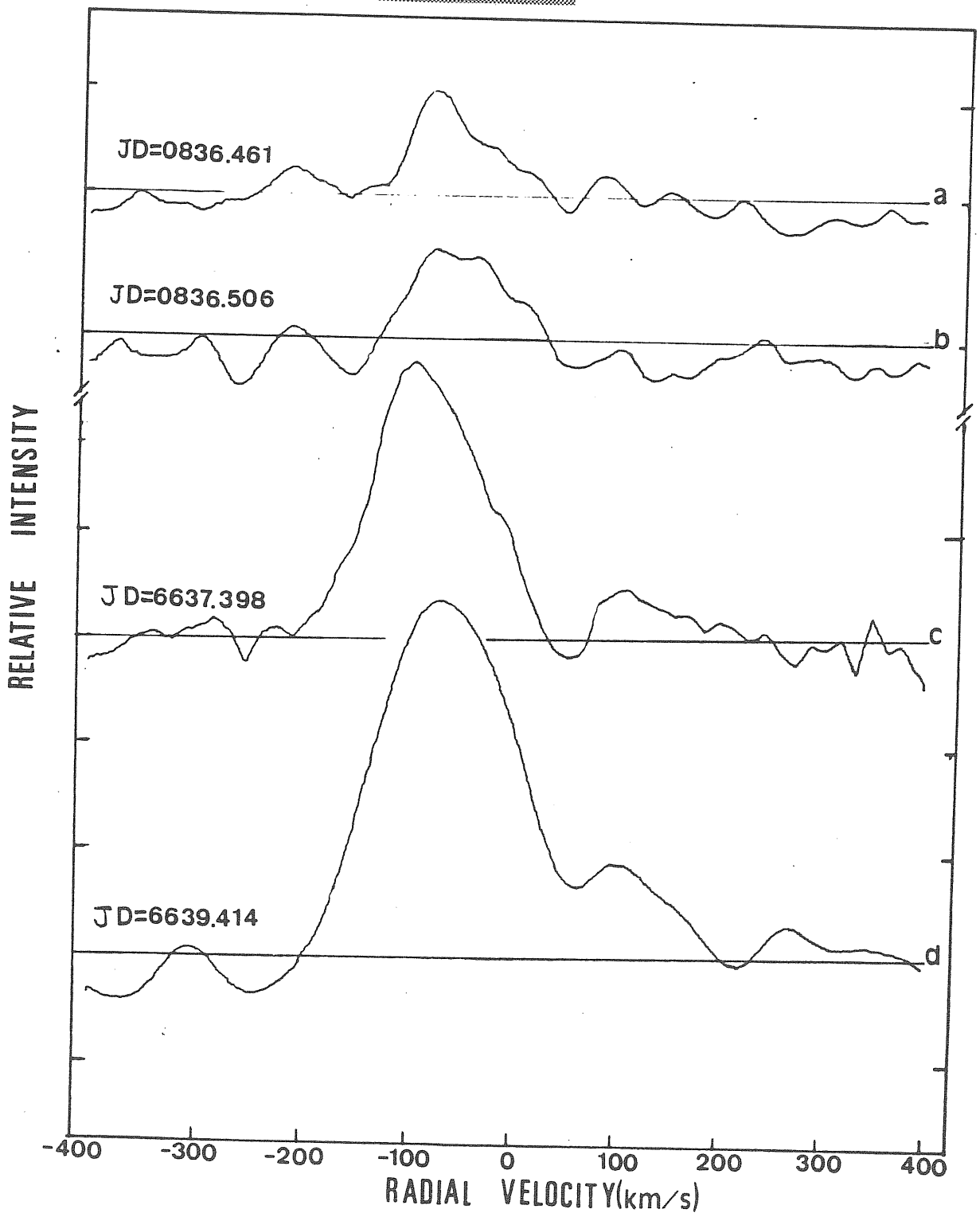
JD=0836.461
a
JD=0836.506
b
JD=6637.398
c
JD=6639.414
d
RELATIVE INTENSITY
-400
-300
-200
-100
0
100
200
300
400
RADIAL VELOCITY(km/s)

FIGURE 2

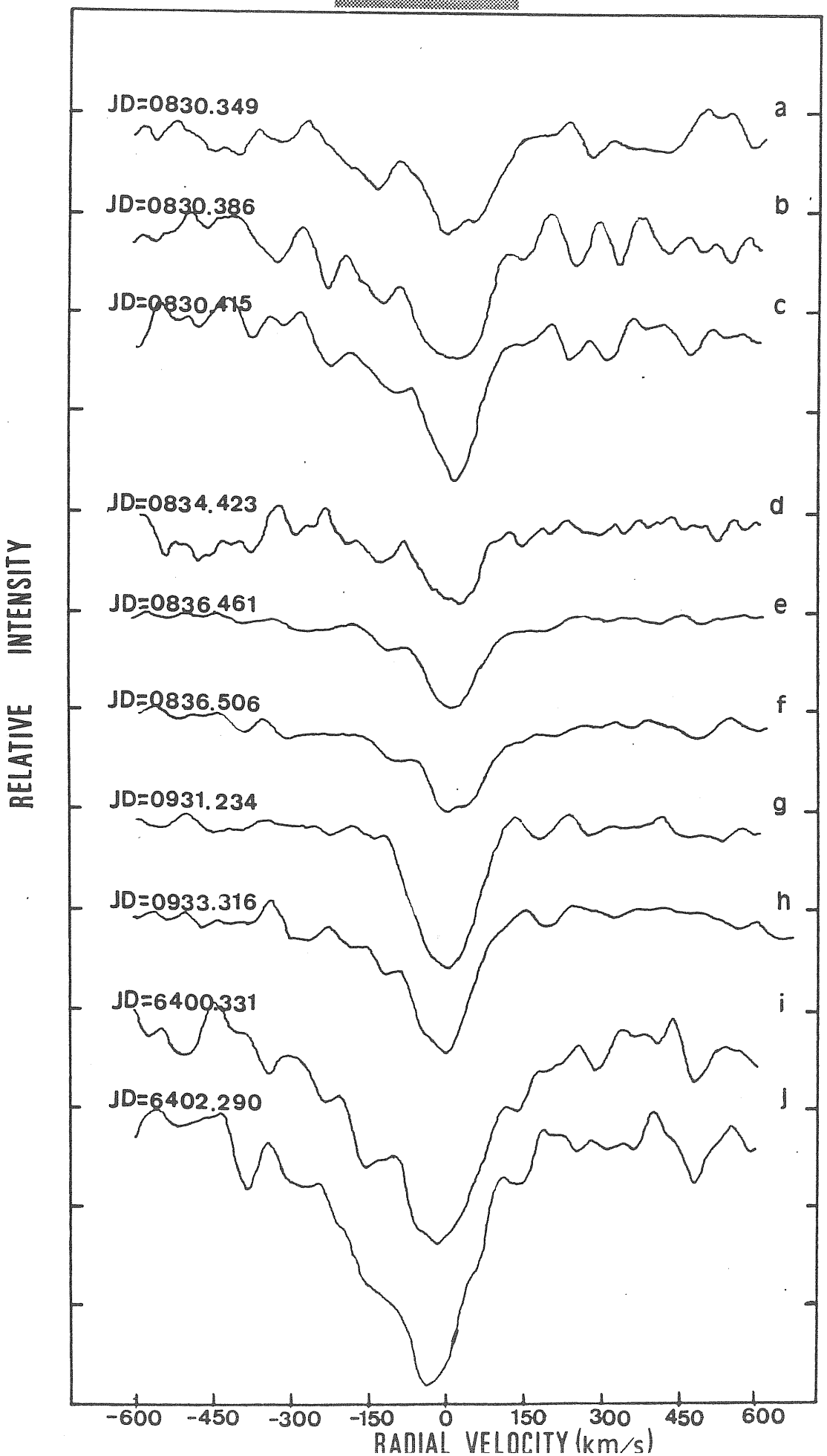
JD=0830.349
a
JD=0830.386
b
JD=0830.415
c
JD=0834.423
d
JD=0836.461
e
JD=0836.506
f
JD=0931.234
g
JD=0933.316
h
JD=6400.331
i
JD=6402.290
j
RELATIVE INTENSITY
-600
-450
-300
-150
0
150
300
450
600
RADIAL VELOCITY (km/s)

FIGURE 3

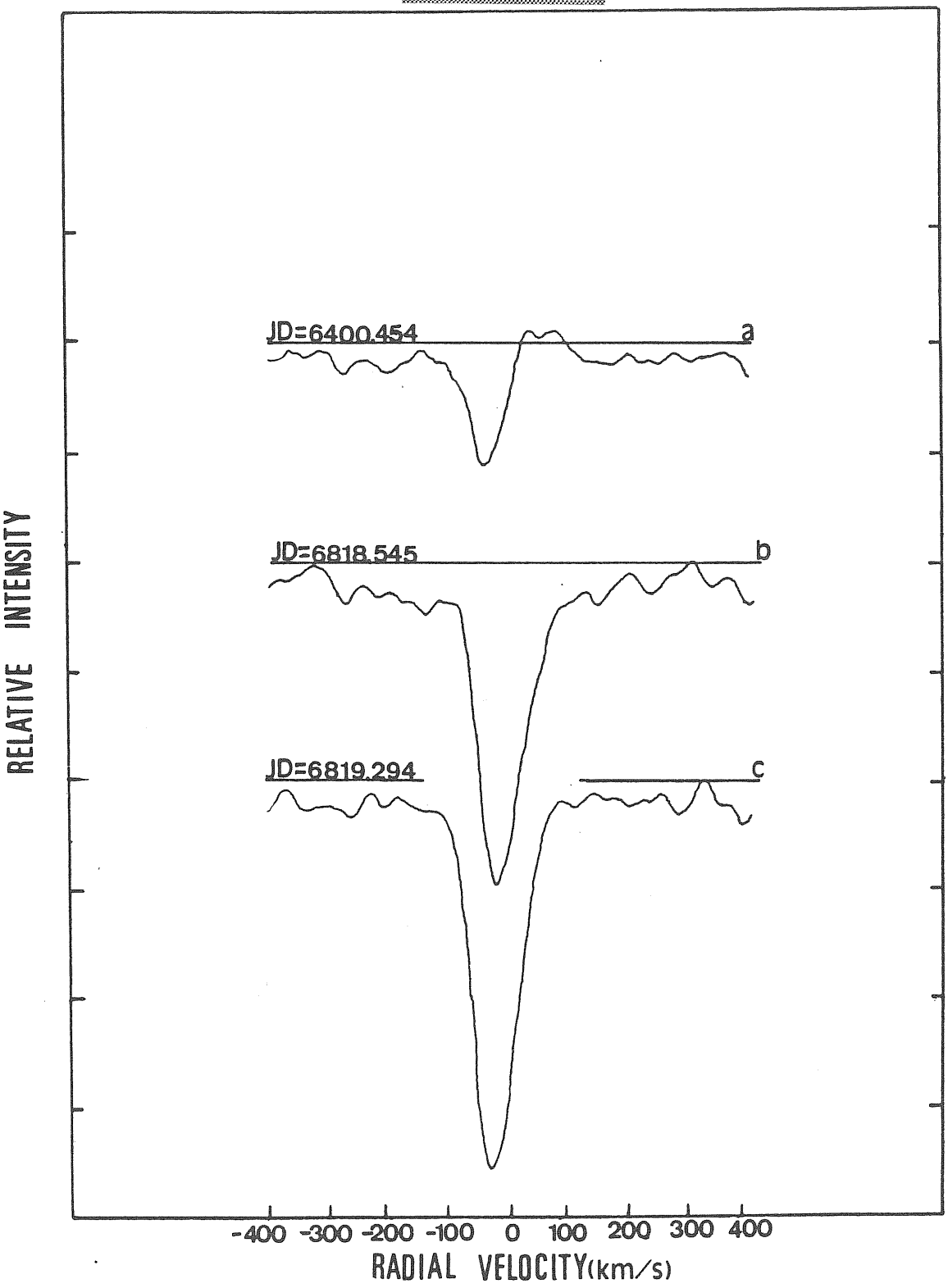
JD=6400.454
a
JD=6818.545
b
JD=6819.294
c
RELATIVE INTENSITY
-400 -300 -200 -100 0 100 200 300 400
RADIAL VELOCITY(km/s)

FIGURE 4

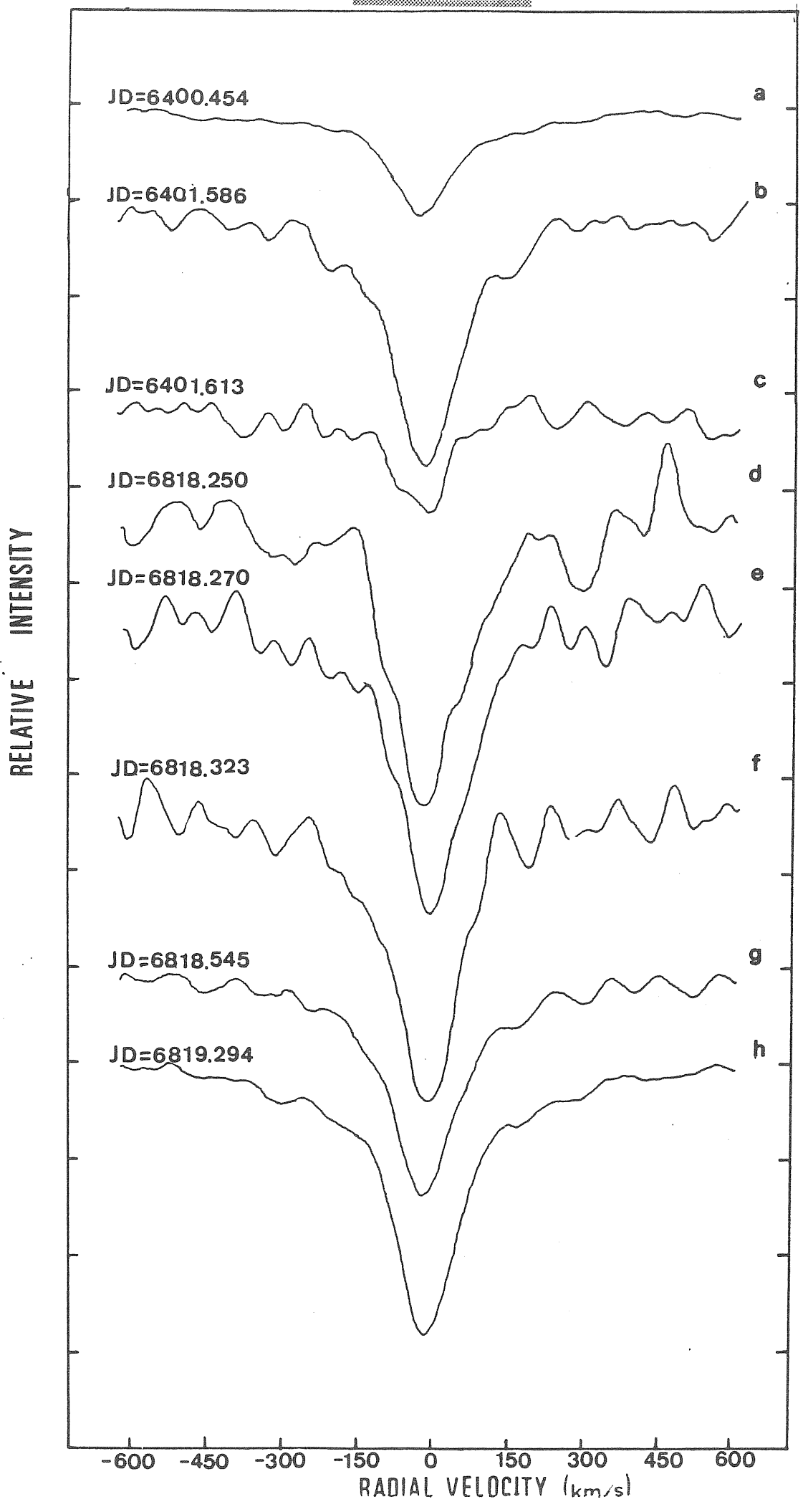
JD=6400.454
a
JD=6401.586
b
JD=6401.613
c
JD=6818.250
d
JD=6818.270
e
JD=6818.323
f
JD=6818.545
g
JD=6819.294
h
RELATIVE INTENSITY
-600
-450
-300
-150
0
150
300
450
600
RADIAL VELOCITY (km/s)

FIGURE 5

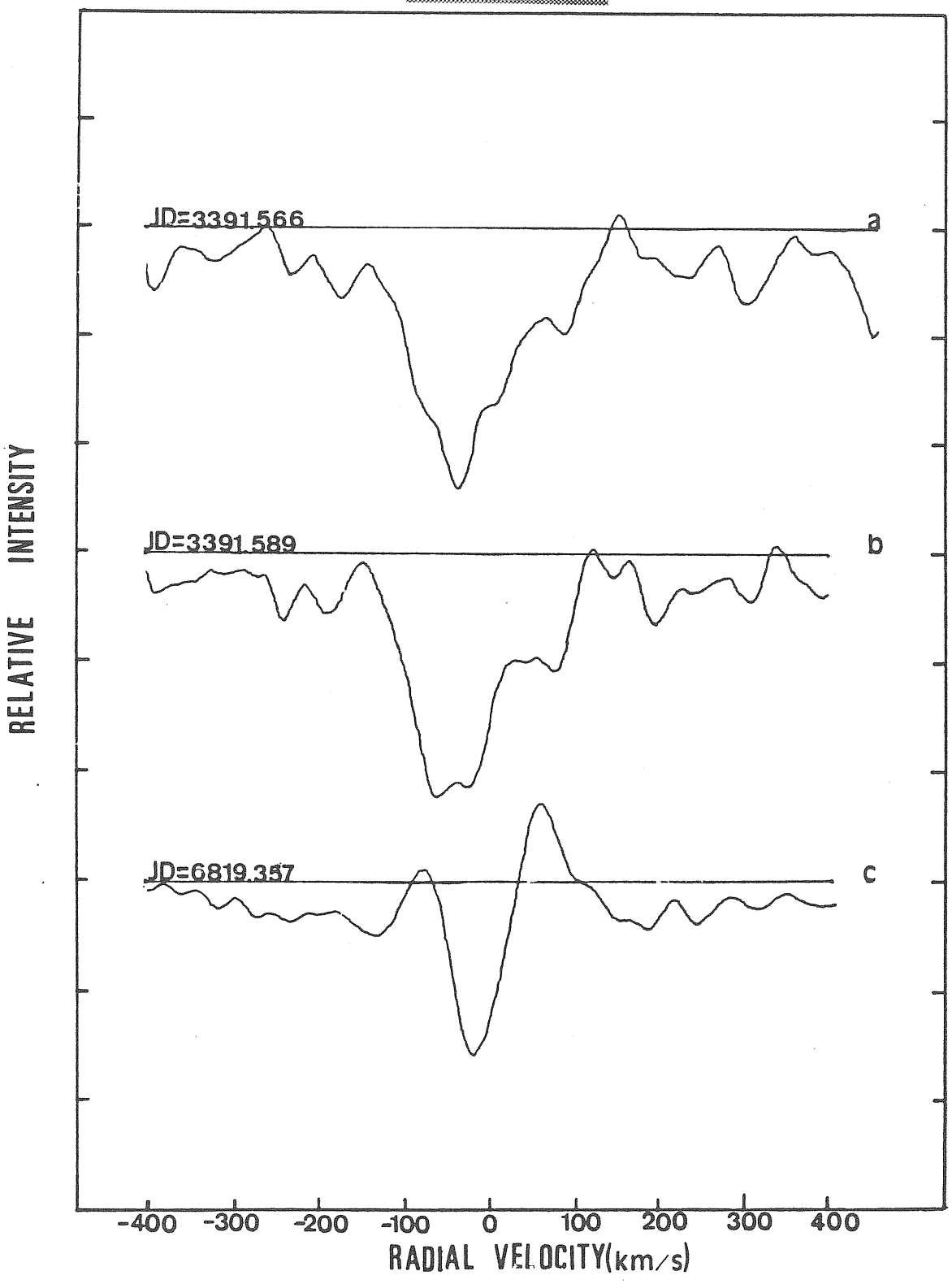
JD=3391.566
a
JD=3391.589
b
JD=6819.357
c
RELATIVE INTENSITY
-400
-300
-200
-100
0
100
200
300
400
RADIAL VELOCITY(km/s)

FIGURE 6

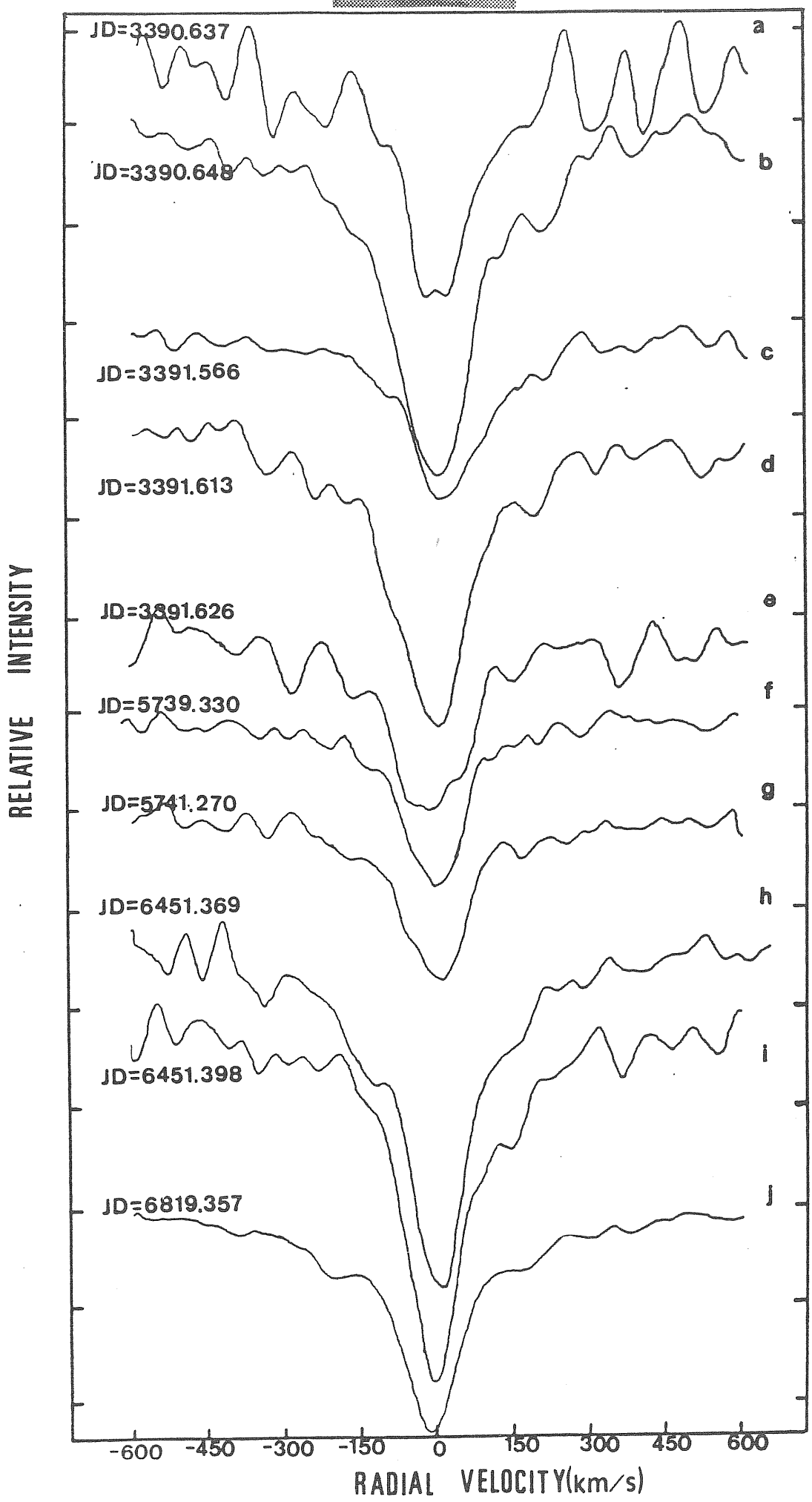
JD=3390.637
a
JD=3390.648
b
JD=3391.566
c
JD=3391.613
d
JD=3391.626
e
JD=5739.330
f
JD=5741.270
g
JD=6451.369
h
JD=6451.398
i
JD=6819.357
j
RELATIVE INTENSITY
-600
-450
-300
-150
0
150
300
450
600
RADIAL VELOCITY(km/s)

Table 4. Radial velocities of the H alpha and H beta lines relative to the center of mass velocities of the program stars.

HD 199478

	JULIAN DATE (2440000+)										
	0830.348	0830.386	0830.415	0834.423	0836.461	0836.506	0931.234	0933.316	6400.331	6402.290	6639.414
	RV(km/s)										
H Beta	31.5	36.7	32.1	39.2	21.3	25.3	24.7	13.8	- 4.2	-16.3	-
H Alpha	-	-	-	-	73.7	79.1	-	-	-	-	73.9

HD 21291

	JULIAN DATE (2440000+)							
	6400.454	6401.586	6401.613	6818.250	6818.270	6818.323	6818.545	6819.294
	RV(km/s)							
H Beta	-17.8	- 5.5	-11.3	-13.6	3.3	- 0.2	- 9.3	-13.4
H Alpha	-26.6	-	-	-	-	-	-20.3	-19.7

HD 21389

	JULIAN DATE (2440000+)										
	3390.637	3390.684	3391.566	3391.589	3391.613	3391.626	5739.330	5741.270	6451.369	6451.398	6819.357
	RV(km/s)										
H Beta	- 2.1	2.6	-11.8	-	3.8	- 1.8	- 4.7	10.0	9.7	- 7.8	- 7.0
H Alpha	-	-	-48.8	-38.1	-	-	-	-	-	-	-13.3

Table 5. Measured radial velocity differences between the average values of the radial velocities of Si II and Fe II lines.

Star	JULIAN DATE (2440000+) 0830.348	0830.386	0830.415	0834.423	0836.461	0836.506	0931.234	0933.316	6400.331	6402.290	6639.414
	RV(km/s)										
HD199478	3.9	6.3	1.9	4.5	3.3	0.4	0.8	7.1	2.7	2.5	0.6

Star	JULIAN DATE (2440000+) 6400.454	6401.586	6401.613	6818.250	6818.270	6818.323	6818.545	6819.294
	RV(km/s)							
HD21291	5.8	0.8	0.0	3.7	3.2	1.7	0.2	0.1

Star	JULIAN DATE (2440000+) 3390.637	3390.684	3391.566	3391.589	3391.613	3391.626	5739.330	5741.270	6451.369	6451.398	6819.357
	RV(km/s)										
HD21389	- 6.4	- 5.8	2.4	-	3.7	- 1.0	- 2.7	2.7	0.9	5.7	- 0.3

Table 6. Observed average quantities of the Mg II 4481.1 and He I 4471.5 lines.

Star	Element	Wav. obs. (A)	Eqw. (A)	Depth	Full Band width(A)	Halfwidth Blue part(A)	Halfwidth Red part(A)
HD 199478							
	Mg II	4480.9	1.0	- 0.5	1.5	0.8	0.7
	He I	4471.1	0.9	- 0.5	1.5	0.6	0.9
HD 21291							
	Mg II	4481.0	0.7	- 0.5	1.3	0.6	0.7
	He I	4471.4	0.3	- 0.3	1.2	0.6	0.6
HD 21389							
	Mg II	4481.1	1.1	- 0.8	1.3	0.6	0.7
	He I	4471.4	0.4	- 0.3	1.3	0.6	0.7

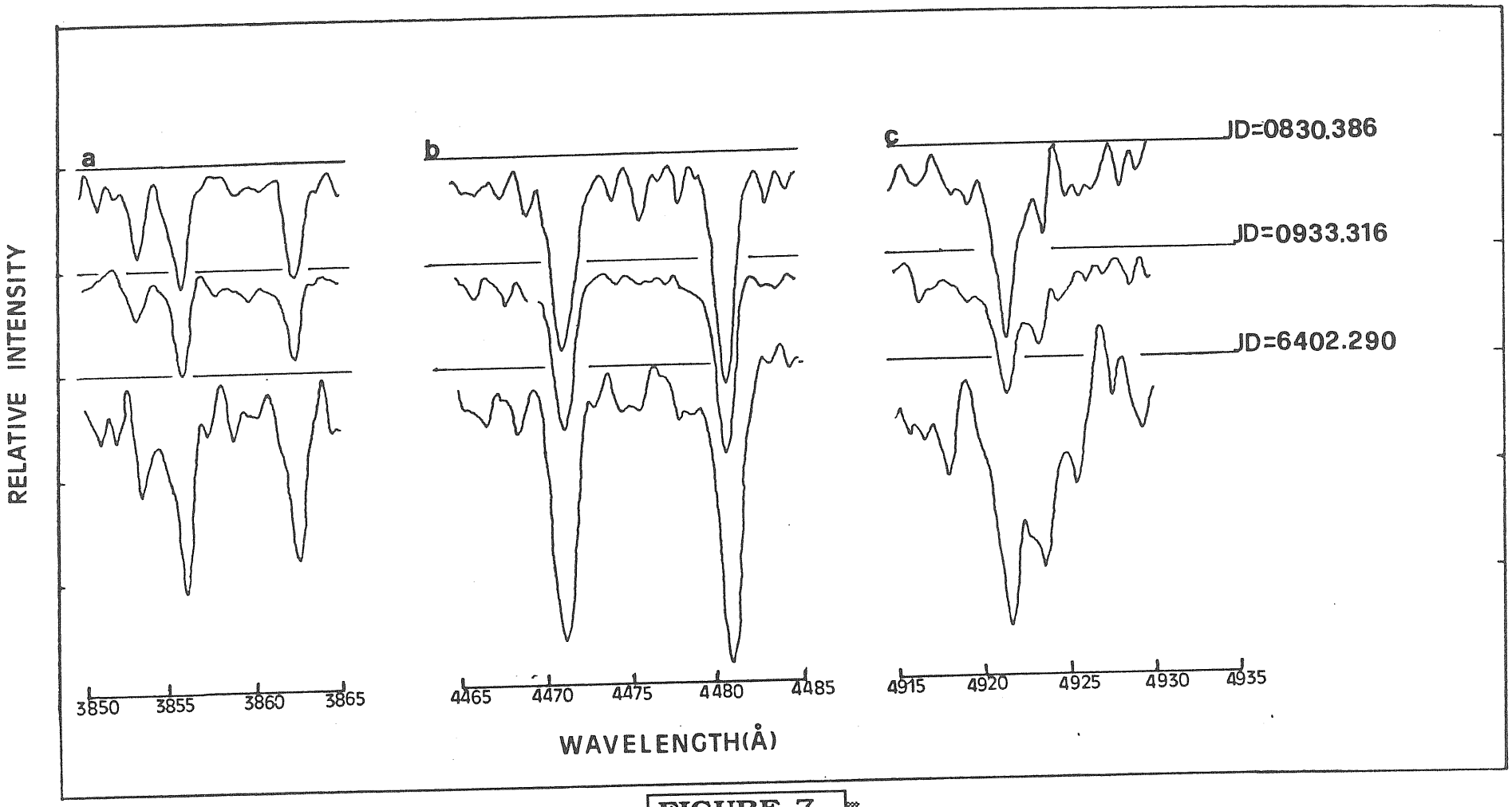
RELATIVE INTENSITY
a
b
c
JD=0830.386
JD=0933.316
JD=6402.290
3850
3855
3860
3865
4465
4470
4475
4480
4485
4915
4920
4925
4930
4935
WAVELENGTH(Å)

FIGURE 7

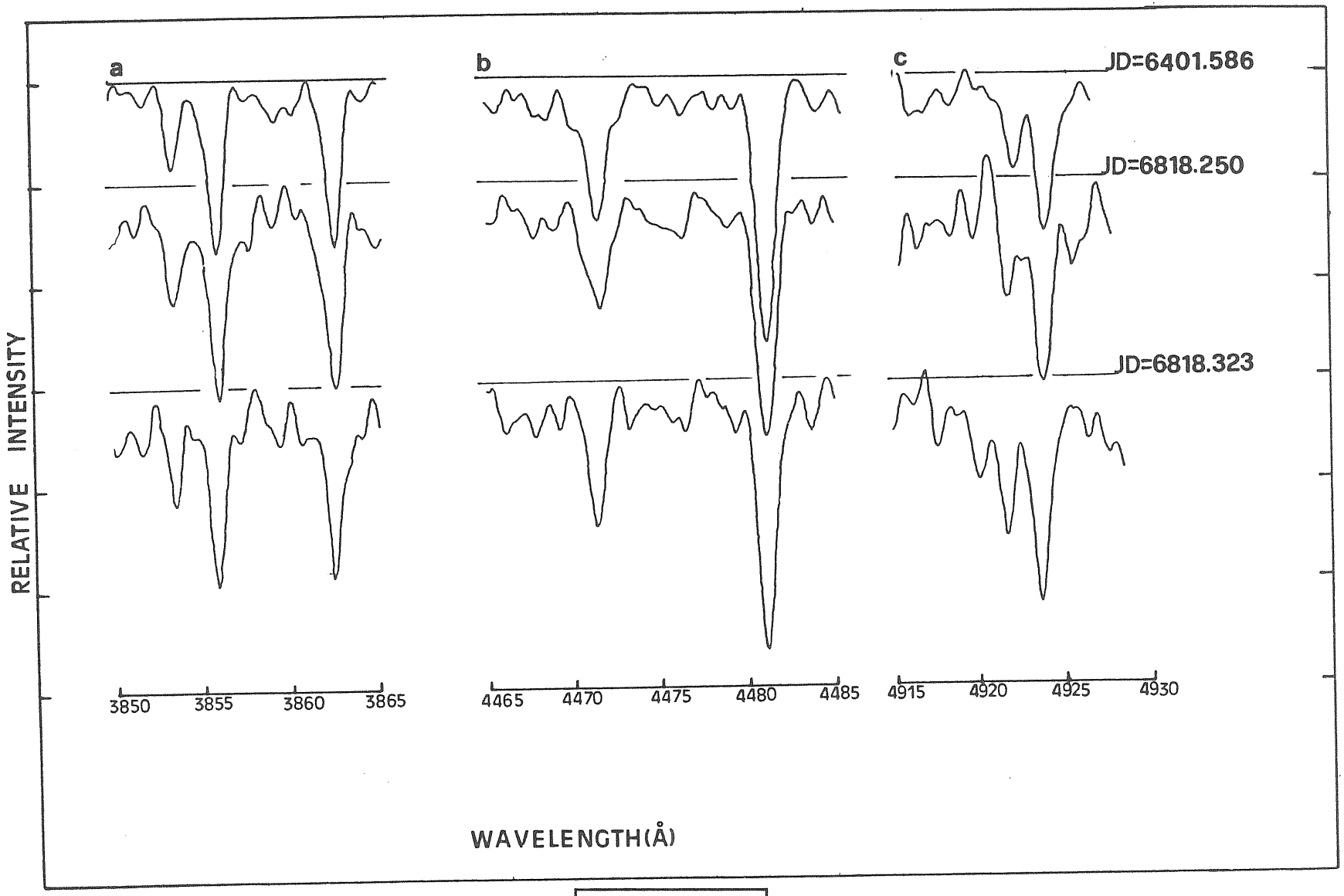
a
b
c
JD=6401.586
JD=6818.250
JD=6818.323
RELATIVE INTENSITY
3850
3855
3860
3865
4465
4470
4475
4480
4485
4915
4920
4925
4930
WAVELENGTH(Å)

FIGURE 8

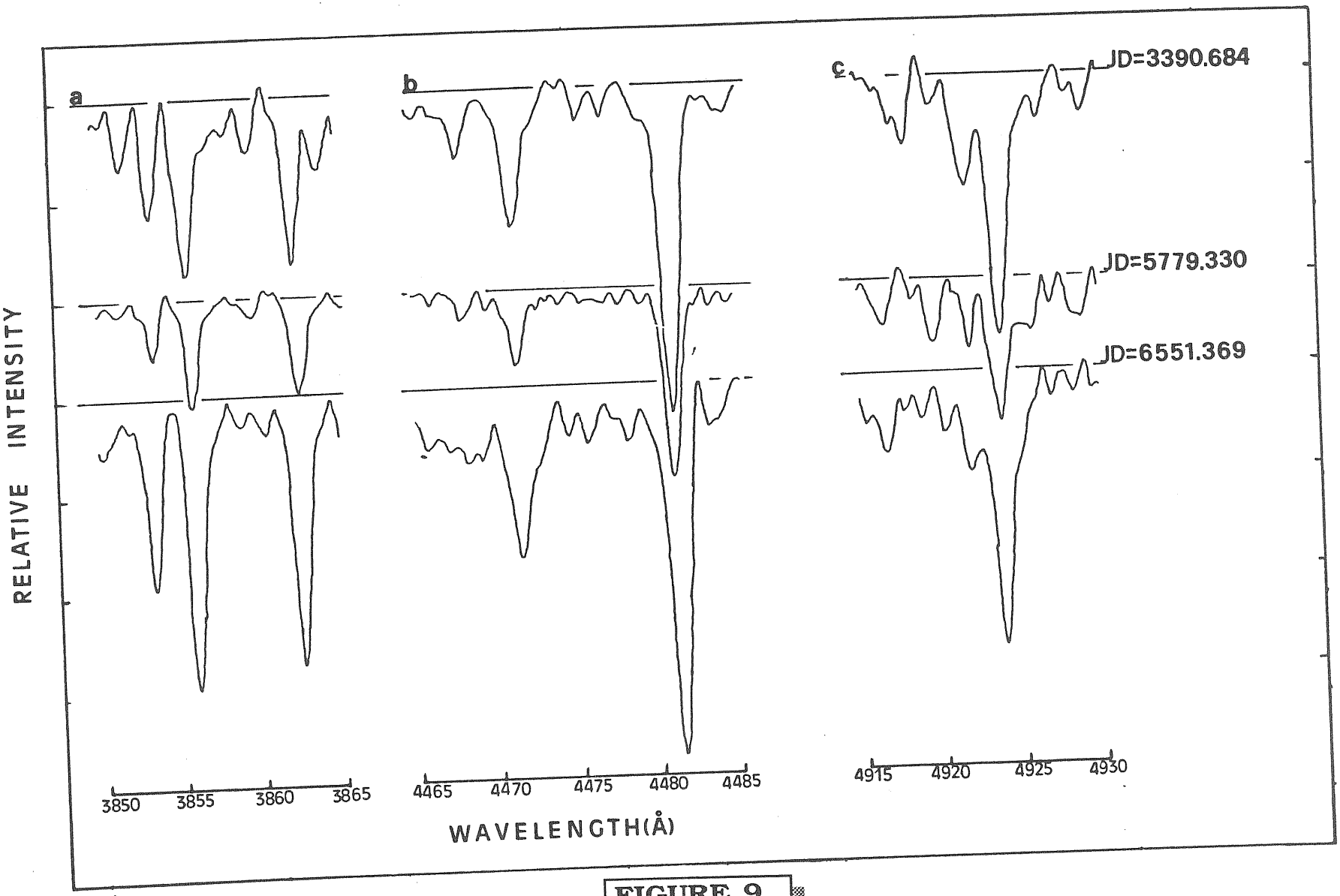
a
b
c
JD=3390.684
JD=5779.330
JD=6551.369
RELATIVE INTENSITY
3850
3855
3860
3865
4465
4470
4475
4480
4485
4915
4920
4925
4930
WAVELENGTH(Å)

FIGURE 9

Table.7 Assigned optical depths for line or line groups taken from Zvereva et al. (1984)

Line or line groups	log
H_α	-1.10
H_β	-1.02
H_γ	-0.98
H_δ	-0.92
H(8-10)	-0.80
H(13-18)	-0.64
Mg II	-0.40
Si II	-0.18
TiII,Fe II	-0.15
He I	0.0

FIGURE 10

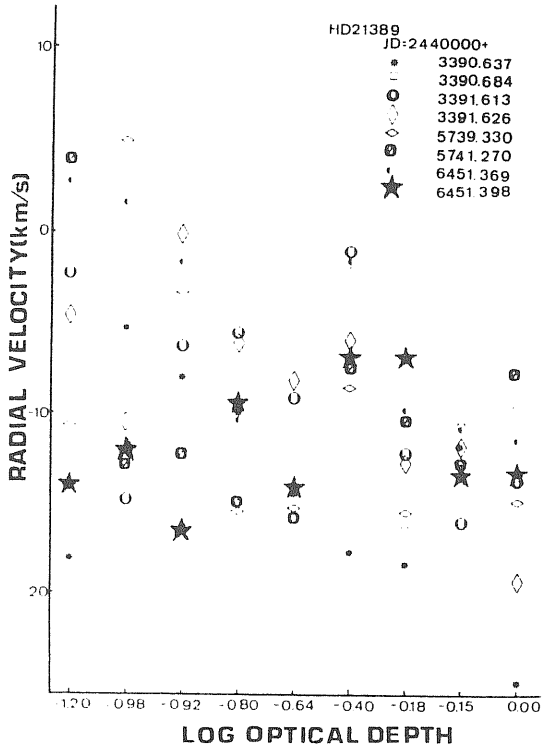
HD21389
JD:2440000+
3390.637
3390.684
3391.613
3391.626
5739.330
5741.270
6451.369
6451.398
RADIAL VELOCITY(km/s)
LOG OPTICAL DEPTH
a

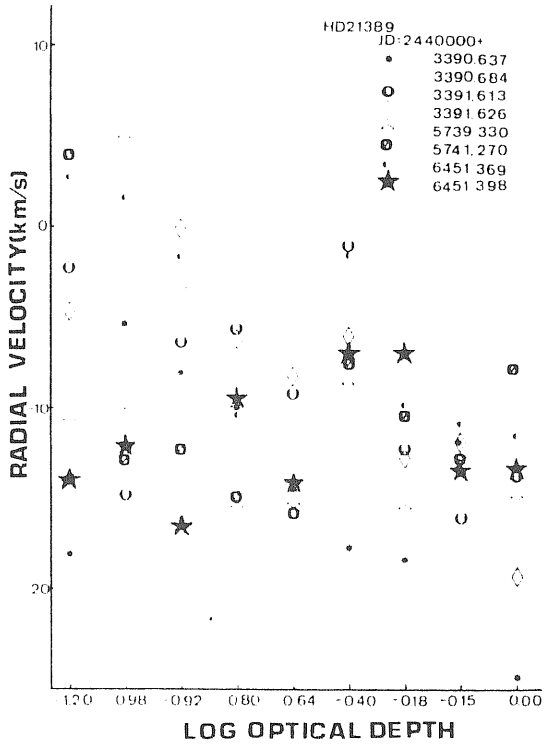
HD21389
JD:2440000+
3390.637
3390.684
3391.613
3391.626
5739.330
5741.270
6451.369
6451.398
RADIAL VELOCITY(km/s)
LOG OPTICAL DEPTH
b

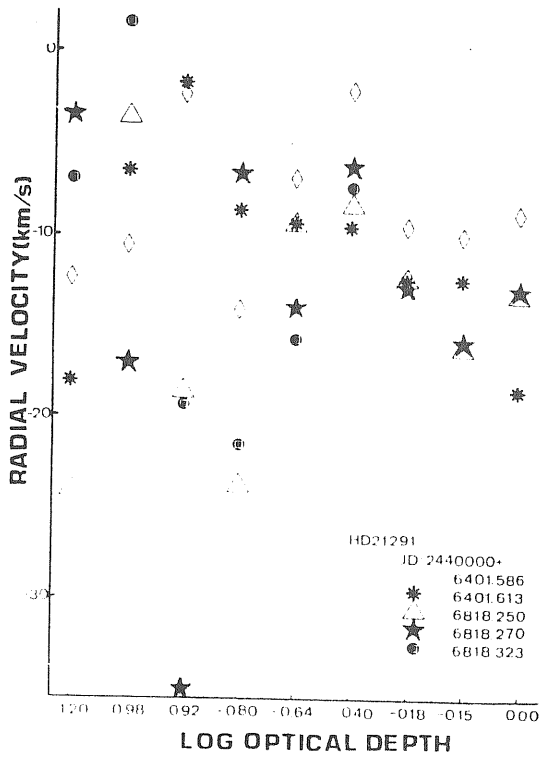
HD21291
JD 2440000+
6401.586
6401.613
6818.250
6818.270
6818.323
RADIAL VELOCITY(km/s)
LOG OPTICAL DEPTH
c

Table 8. Observed quantities of the unidentified interstellar features.

Interstellar band	HD 199478 Ave. Eqw. (A)	HD 199478 Ave. Depth (A)	HD 199478 Ave. Bw. (A)	HD 21291 Ave. Eqw. (A)	HD 21291 Ave. Depth (A)	HD 21291 Ave. Bw. (A)	HD 21389 Ave. Eqw. (A)	HD 21389 Ave. Depth (A)	HD 21389 Ave. Bw. (A)
5780	0.2	-0.1	1.9	0.3	-0.9	2.5	0.4	-0.2	2.3
5797	0.1	-0.1	1.2	0.1	-0.1	1.7	0.1	-0.1	1.5
6614	0.2	-0.1	1.7	0.1	-0.1	1.4	0.1	-0.1	1.5

IV.The UV spectra

IV.1.HD 199478

We present four longwave and two shortwave range spectra of this supergiant taken with one year interval.

Si IV lines of HD 199478 were quite asymmetric and specially 1394 is strongly blended.The line profiles change significantly between the two spectra presented in Figure 11 a, b.From the same figure we see that the neighbouring lines also present time variation.C IV lines were unusually weak and like Si IV blended with Fe which exhibited some variation in the line profile (Figure 11c).

Al III (UV1) lines were present in the vicinity of strong Fe III lines, blue shifted and slightly asymmetric.Similarly Fe III (UV34) lines were rather weaker than the other multiplet lines of Fe III, blue shifted and symmetric. Slight profile variations are shown Figures 11 d,e,f respectively.The most interesting features of the UV spectra of HD 199478 undoubtly are the Mg II (UV1) lines which presented double peak absorption components; 2802 line was also accompanied with a weak and highly variable emission red wing (Figure 11 g). Line profiles, relative depths and radial velocities of these lines varied substantially.

Si II (UV1,2,3), C II (UV1), Al II (UV1) lines were strong symmetric and blue shifted.Measured center radial velocities decreased between two spectra taken with approximately one year interval, although edge velocities

remained the same.Similar variation was not seen with the lines of Fe III, Al III and Fe II.Also Mg II lines revealed same variation as Si II.It is interesting to remark here that the relative depths of the blue shifted absorption components vary inversely with the radial velocities of the lines. HD 199478 is heavily reddened and the interstellar components of Mg I 2852, C II and Si II lines are strong.Table 10 presents measured values of the selected lines.

IV.2.HD 21291

HD 21291 is one of the supergiants in our program which has been studied very little in the UV region.Only C IV lines and some selected wavelength ranges are analyzed by Underhill (1982).This star has many common similarities with HD 199478 as we will see from a close look to it's spectra.

Si IV lines of HD 21291 are blended as in the case of HD 199478.Infact when we compare the relative intensities of the Si IV 1394 with Si IV 1402 ,although the first line is intrinsicaly more strong than the second one, the large difference is probably due to blending in 1394, which generally causes erroneus edge velocity measurements.Lines of Si IV were asymmetric and blue shifted.Si IV 1402 line is splitted into two, possibly with the blending of metals specially Fe II.Line profiles at the centers changed substantially (Figure A 12a,b).Similar to Si IV ,C IV lines are also blended and their presence was doubtful, because in this range of the spectra lines of Fe III, Ni III, P II were

quite strong and presented variability in their profiles (Figure 12.c).

Figure 12.d presents Al III (UV1) lines which are asymmetric and unshifted.Some variations are observed in the line centers.Fe III (UV34), Figure 12.e,f were similar to those of Al III lines but slightly blue shifted. As we see from the figure the intensities of the other Fe III multiplet lines are comparable to that of Fe III (UV34).There were no profile variations for Fe III lines.Like for HD 199478, most interesting features of the UV spectra of HD 21291 were Mg II (UV1) lines (Figure 12.g).These lines exhibited double peak absorption components with strong variation in the line profiles.Again like the case of HD 199478, the relative intensity and the radial velocity of the blue shifted component vary inversely i.e. when the central depth of the line decreases the line is more blue shifted.Also as seen from the same figure the last spectrum taken in 1980 shows that 2802 line has a weak emission red wing, so it displays a P Cygni profile.

When we compare two short wavelength range spectra of HD 21291, it is interesting to note that the lines of Si II (UV1,2,3), C II (UV1) , and C I (UV1) were blue shifted in 1979, but not in the 1980 spectrum.Similarly the measured blue edge velocities of these lines diminished within one year.At the same time Al II (UV1) ,P II (UV1) lines presented no variation.He II (Bal. α) line was highly blue shifted in both

spectra.

In the long wavelength range UV spectra the lines of Fe II (UV1,2,3) presented slight changes in their radial velocities.In the spectrum LWR 3925 which was secured eight days later than LWR 3848 the Fe II lines diminished in radial velocities.In the last spectrum (1980) we see that again they are all blue shifted.As we have noted several times this star was closely associated with a nebulosity so interstellar lines were very strong and sharp.Table 11 presents the measured values of the selected lines.

IV.3.HD 21389

In this research two short wavelength and two long wavelength spectra of HD 21389 were presented.HD 21389 presented a large amount of narrow metallic lines through the whole spectral range very similar to the Be/shell star HD 193182. Underhill (1980) analyzed the C IV lines of this star and Praderie et al.(1980) studied HD 21389; no other detailed analysis had been carried out in the UV range.

The presence of the Si IV and C IV lines are very doubtful in the spectra of HD 21389.As seen from Figure 13a,b,c the spectral region where Si IV and C IV lines should be present is filled with quite narrow and strong ,firstly and secondly ionized ion lines.We would like to note here that Underhill (1980) published a spectrum of this star taken nearly a week later than our last observed spectrum where C IV lines had presented very narrow unshifted emission components.

Al III (UV1) and Fe III (UV34) lines were symmetric, slightly blue shifted and again accompanied with rather strong unshifted metal lines of first and second ionization levels.There were no significant profile variations for these lines (Figure 13d,e,f).Mg II (UV1) lines, Figure 13.g, are composed from double peak absorption components; we observe slight changes in the line profiles.No emission red wing was present although the wings of the unshifted components presented variation.The lines of Si II (UV2,3) and Al II (UV1) were very strong and blue shifted with a time variation in the radial velocities between two spectra.Similar variation shown by the O I lines.P II (UV1), C I (UV2,3), Si (UV1) and Fe II (UV1,2,3) lines were unshifted in both spectra.

When we compare our spectral measurements with the ones presented by Praderie et al. (1980) there are important similarities and differences in some aspects.According to general conclusion of Praderie et al.(1980), only the profiles of resonance lines of abundant once ionized elements were blue shifted, Al III, O I, and C I lines were not.Our measurements revealed that the O I lines were strongly blue shifted and exhibited notable time variation within a week.Also Mg II (UV1) lines presented by Praderie et al. (1980), where the observation date was 1978, exhibited clearly two blue shifted components although in our spectra (1979) this second blue shifted component was absent.We present the measured values of the spectral lines in the Table 12.

Table and Figure captions,

Table 9.Ultra-violet data for program supergiants.

Figure 11.Some selected UV lines of HD 199478.

Table 10.UV spectral measurements of HD 199478.

Figure 12.Same as previous figure;for HD 21291.

Table 11.Same as previous table; for HD 21291.

Figure 13.Same as previous figure: for HD 21389.

Table 12.Same as previous table; for HD 21389.

Table 9 .Ultra-Violet data for the Supergiants.

Star name	Spectrum	Year	Day	Beg. U.T. hh:mm	Exp. Time mm:ss
HD 199478	SW 9414	1980	180	20:48	180:00
	SW15552	1981	326	17:32	135:00
	LW 8159	1980	183	20:21	25:00
	LW 9319	1980	321	18:39	25:00
	LW 9320	1980	321	19:28	19:30
	LW12033	1981	326	16:58	20:00
HD 21291	SW 4264	1979	046	07:56	50:00
	SW 8087	1980	060	12:22	46:00
	LW 3848	1979	055	22:42	14:00
	LW 3925	1979	063	10:17	07:00
	LW 9317	1980	321	14:48	06:30
HD 21389	SW 4301	1979	050	18:47	100:00
	SW 4399	1979	057	14:49	200:00
	LW 3801	1979	050	20:34	16:00
	LW 3875	1979	057	18:13	32:00
	LW 5992	1979	304	08:57	25:00

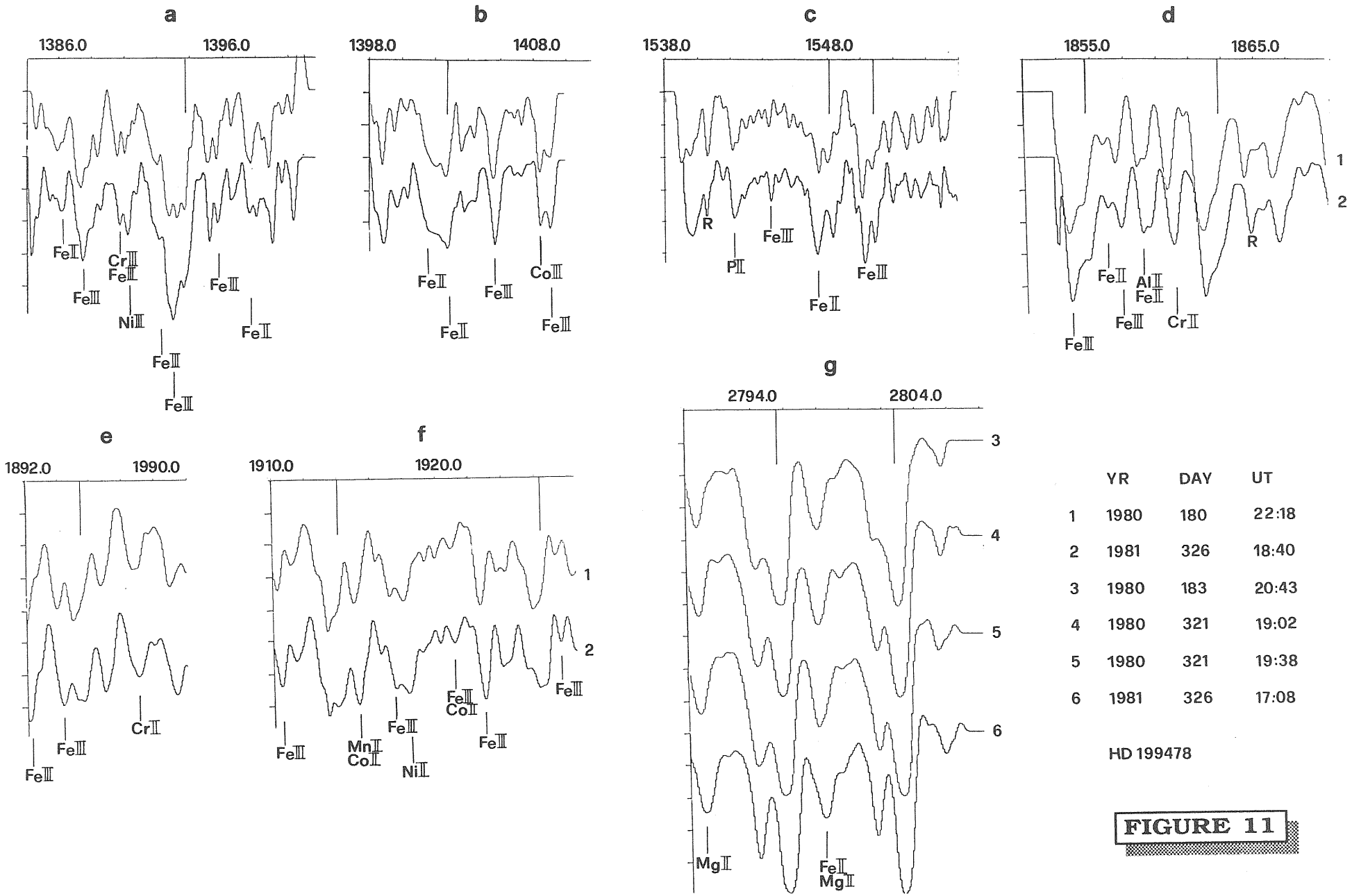

	YR	DAY	UT
1	1980	180	22:18
2	1981	326	18:40
3	1980	183	20:43
4	1980	321	19:02
5	1980	321	19:38
6	1981	326	17:08

HD 199478

FIGURE 11

Table I.10.UV spectral measurements of HD 199478

Element	Multip.	Vc	Vedg	EQW	FBWC	R/V	Remarks
Si IV	1	-22.0	-412.9	1.1	1.3	0.64	1
		unsh.	-403.4	1.6	2.1	0.70	2
Al III	1	-19.1	-146.6	0.5	1.0	0.74	1
		-63.7	-150.9	0.6	0.8	0.85	2
Fe III	34	-31.7	- 93.4	0.6	0.9	1.00	1
		-22.8	-107.4	0.6	1.0	0.93	2
Mg II							
	1	Vc	Vedg	EQW	DEPTH	FBWC	R/V	Remarks
		-193.3	-277.6	0.60	-0.6	1.0	0.89	3
		unsh.	-120.8	1.70	-1.0	1.5	0.68	
		149.5	170.5	<0.10	<0.1	-	0.74	
		-191.5	-246.8	0.70	-0.7	1.0	0.79	4
		unsh.	- 97.3	1.60	-1.3	1.4	0.56	
		142.7	202.1	0.10	0.3	0.6	1.40	
		-178.3	-293.3	0.80	-0.7	1.1	0.76	5
		unsh.	- 94.6	1.60	-1.2	1.3	0.62	
		185.2	218.9	<0.10	<0.1	-	-	
		-153.4	-208.2	0.80	-0.8	0.9	0.77	6
		unsh.	- 98.9	1.60	-1.1	1.3	0.64	
		142.2	233.3	<0.10	<0.10	-	-	

Table I.10 continued

Element	Mult.	Vc	Vedg	Remarks
Si II	3	- 52.7	-316.4	1
		- 20.8	-257.4	2
C II	1	- 22.3	-285.9	1
		- 18.1	-290.4	2
Si II	2	- 41.9	-240.7	1
		- 5.9	-248.6	2
Al II	1	- 6.6	-289.5	1
		- 3.0	-303.5	2
O I	1	- 42.3	-	1
		- 32.1	-	2
P II	1	- 31.4	-	1
		- 11.2	-	2
C I	3	- 34.1	-	1
		- 4.6	-	2
C I	2	- 28.1	-	1
		- 15.4	-	2
Si II	1	- 38.8	-	1
		- 11.2	-	2
He II	(Ba.α)	- 73.1	-	1
		- 54.9	-	2
Fe II	3	- 35.0	-193.3	3
		- 10.0	-151.9	6
Fe II	2	- 27.5	-193.3	3
		- 37.9	-121.6	6
Fe II	1	- 19.9	-141.2	3
		- 31.2	-133.2	6

Notes: Vc=Central velocity, Vedg= Edge velocity measured from the blue edge of the fitted gaussian line (km/s), FBWC=Full band width on the continuum (km/s), R/V=Ratio of the red and blue wings on the continuum. Depth=Central depth of the fitted line, positive values corresponds to emission in continuum units.

Remarks:

	YR	DAY	U.T.
1]	1980	180	22:18
2]	1981	326	18:40
3]	1980	183	20:43
4]	1980	321	19:02
5]	1980	321	19:38
6]	1981	326	17:08

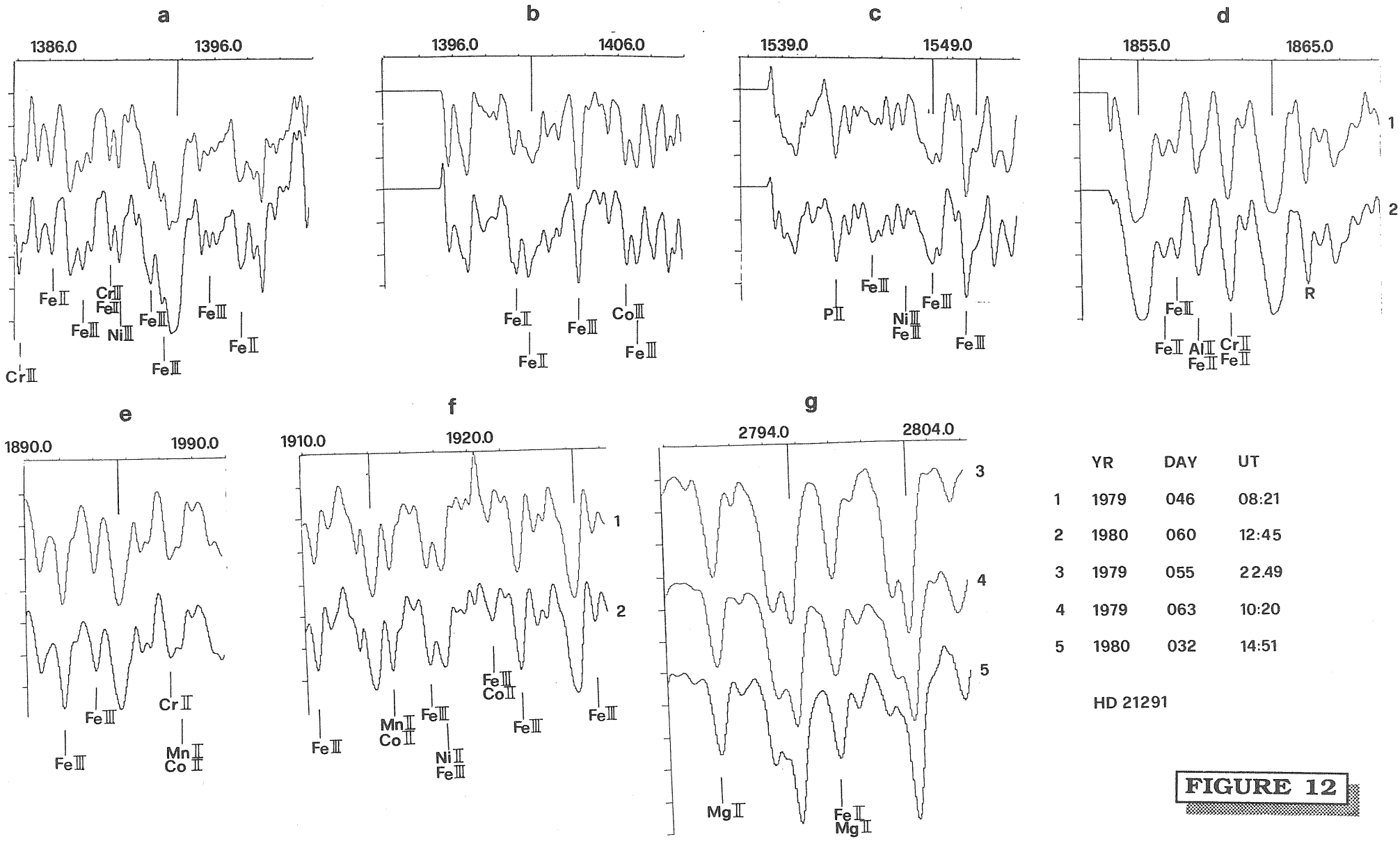

	YR	DAY	UT
1	1979	046	08:21
2	1980	060	12:45
3	1979	055	22.49
4	1979	063	10:20
5	1980	032	14:51

HD 21291

FIGURE 12

Table I.11.UV spectral measurements of HD 21291

Element	Multip.	Vc	Vedg	EQW	FBWC	R/V	Remarks
Si IV	1	-79.7	-249.1	1.2	1.3	0.81	1
		-39.6	-189.8	1.2	1.2	0.78	2
Al III	1	unsh.	-160.8	0.9	0.9	1.00	1
		unsh.	-170.1	0.8	0.9	0.85	2
Fe III	34	-10.9	- 94.6	0.9	1.2	0.80	1
		-10.3	- 96.4	0.8	1.1	0.75	2
Mg II							
	1	Vc	Vedg	EQW	DEPTH	FBWC	R/V Remarks
		-126.7	-177.6	0.7	-0.7	0.8	0.74 3
		unsh.	- 73.7	1.1	-0.9	1.1	0.59
		-130.2	-181.4	0.6	-0.6	0.8	0.79 4
		unsh.	- 71.3	1.1	-1.0	1.0	0.55
		-159.7	-216.4	0.5	-0.4	1.0	0.88 5
		unsh.	- 51.6	1.0	-1.0	0.9	0.82
		200.2	254.0	0.2	0.3	0.8	1.40

Table : I.11 continued

Element	Mult.	Vc	Vedg	Remarks
Si II	3	- 26.4	-194.3	1
		unsh.	-154.2	2
C II	1	- 42.0	-218.8	1
		unsh.	-162.1	2
Si II	2	- 17.9	-200.7	1
		unsh.	-183.6	2
Al II	1	- 7.2	-145.8	1
		- 8.9	-122.3	2
O I	2	- 30.0	-	1
		- 16.1	-	2
P II	1	- 25.4	-	1
		- 25.4	-	2
C I	3	- 18.7	-	1
		- 15.6	-	2
C I	2	- 22.8	-	1
		unsh.	-	2
Si II	1	- 13.9	-	1
		unsh.	-	2
He II	(Ba.α)	- 62.4	-	1
		- 64.0	-	2
Fe II	3	- 28.3	-191.7	3
		- 19.7	-116.9	4
		- 50.2	-111.6	5
Fe II	2	- 46.1	-156.6	3
		- 23.9	-104.3	4
		- 39.1	-144.9	5
Fe II	1	- 16.3	-126.8	3
		unsh.	-115.7	4
		- 28.8	-120.6	5

Notes: Vc=Central velocity, Vedg= Edge velocity measured from the blue edge of the fitted gaussian line (km/s), FBWC=Full band width on the continuum (km/s), R/V=Ratio of the red and blue wings on the continuum. Depth=Central depth of the fitted line, positive values corresponds to emission in continuum units.

Remarks:

	YR	DAY	U.T.
1]	1979	046	08:21
2]	1980	060	12:45
3]	1979	055	12:45
4]	1979	064	10:20
5]	1980	032	14:51

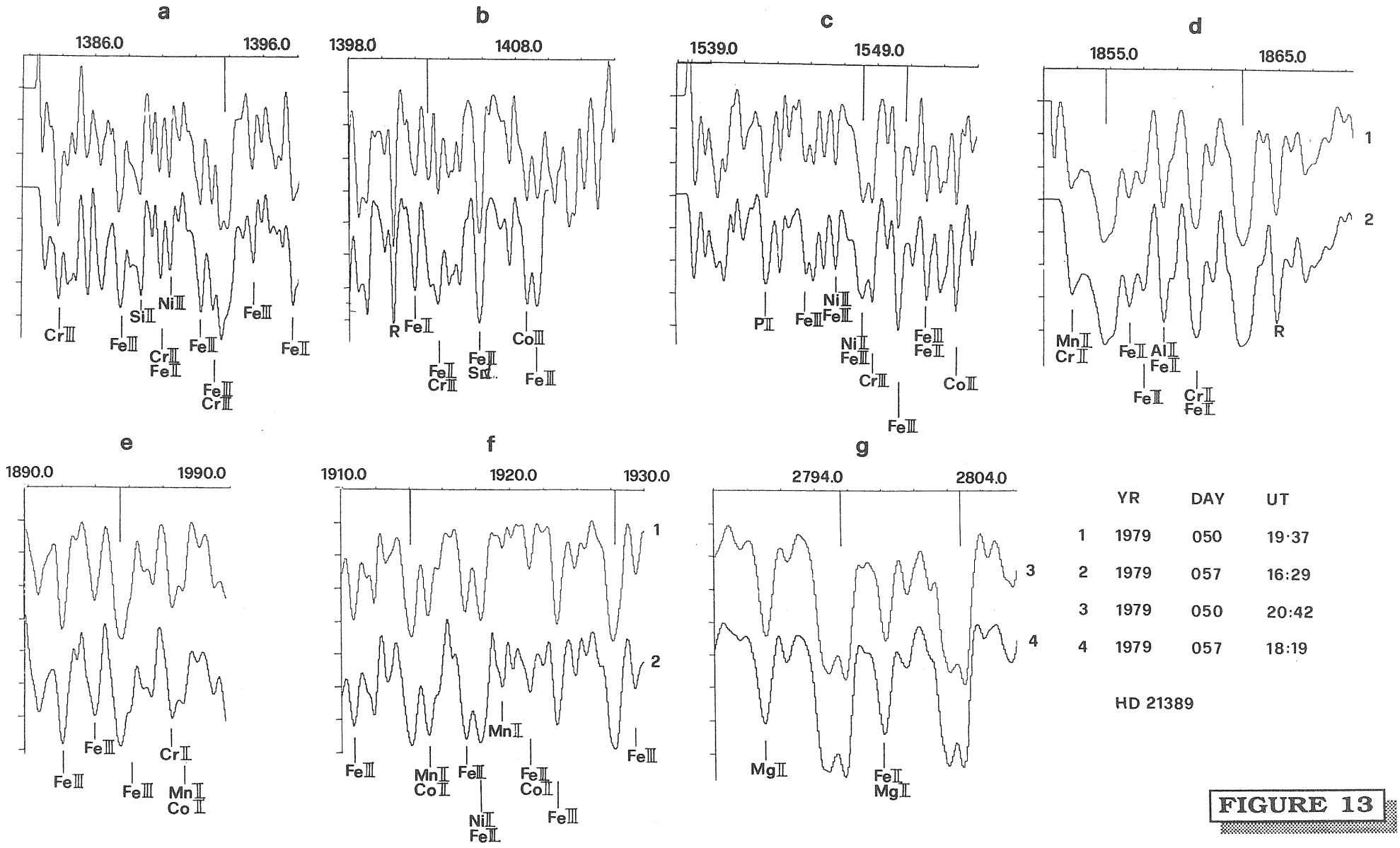

	YR	DAY	UT
1	1979	050	19·37
2	1979	057	16:29
3	1979	050	20:42
4	1979	057	18:19

HD 21389

FIGURE 13

Table I.12.UV spectral measurements of HD 21389

Element	Multip.	Vc	Vedg	EQW	FBWC	R/V	Remarks
Al III	1	-34.9	-116.9	1.5	1.6	1.00	1
		-36.1	-122.4	1.4	1.6	1.00	2
Fe III	34	-20.5	- 81.2	0.9	0.9	0.78	1
		- 5.8	- 82.2	0.9	1.0	0.93	2

Mg II

1	Vc	Vedg	EQW	DEPTH	FBWC	R/V	Remarks
	-117.9	-186.9	1.0	-0.9	1.1	0.74	3
	unsh.	- 60.2	1.0	-1.0	1.0	0.73	
	-123.4	-198.2	1.1	-0.8	1.1	0.65	4
	unsh.	- 72.9	1.0	-1.0	1.0	0.70	

Element	Mult.	Vc	Vedg	Remarks
Si II	3	-	-323.3	1
		- 59.3	-349.2	2
C II	1	unsh.	-249.5	1
		unsh.	-284.6	2
Si II	2	-115.5	-315.1	1
		- 55.6	-266.4	2
Al II	1	-116.6	-206.2	1
		- 89.8	-307.4	2
O I	1	-117.9	-	1
		- 79.1	-	2

Notes: Vc=Central velocity, Vedg= Edge velocity measured from the blue edge of the fitted gaussian line (km/s), FBWC=Full band width on the continuum (km/s), R/V=Ratio of the red and blue wings on the continuum. Depth=Central depth of the fitted line, positive values corresponds to emission in continuum units.

Remarks:

	YR	DAY	U.T.
1]	1979	050	19:37
2]	1979	057	16:29
3]	1979	050	20:42
4]	1979	057	18:19

APPENDIX II:The Formation of shell lines according to Kogure (1977).

We suppose that a shell star is a B-type star having an envelope concentrated toward the equatorial plane and seen nearly equator-on.The envelope has a velocity field,so that we first divide the whole envelope into a definite number of zones ,as has been done by Sobolev(1947).Each zone is specified by a number k(k=0,∓1,∓2,.....) and has a equal line-of-sight velocity v_k given by

$$v_k = 2kv_D \qquad (1)$$

where v_D denotes the thermal Doppler velocity and the factor 2 comes from the effective width of a line formed in a single zone.The k-th velocity zone can absorb or emit the 2n-radiation of Balmer series at the wavelength

$$\lambda_{2n}(k) = \lambda_{2n}(0)(1 + v_k/c) \qquad (2)$$

where $\lambda_{2n}(0)$stand for the wavelength at the respective line center. For the k-th velocity zone the screening factor $\beta(k)$is defined as the fractional area of the stellar disk that is screened by the k-th velocity zone lying in front of it.Furthermore,we define the following quantities:

$I_{2n}(k)$:the emergent intensity of the 2n-radiation at the surface of the k-th

velocity zone toward the direction of an observer,

$I^*_{2n}(k)$:the stellar emergent intensity at the surface

directed to the observer,

$\pi F^{*}_{c,2n}$:the stellar emergent flux in the continuum adjacent to the 2n-radiation

The spectral width of these three quantities is assumed to be $2\Delta_D$ in angstrom, where Δ_D corresponds to the mean thermal Doppler velocity in equation(1). In addition we define :

A^{*} :the projected area of the stellar disk seen from the observer,

$\sigma(k)$:the projected area of the k-th velocity zone,

$\sigma_d(k)$:the part of $\sigma(k)$ that screens the stellar disk,

$\sigma_e(k)$:the part of $\sigma(k)$ that extends outside the stellar disk.

For σ's we have

$$\sigma(k) = \sigma_d(k) + \sigma_e(k) \tag{3}$$

and

$$\sigma_d(k) = \beta(k) A^{*}. \tag{4}$$

With the aid of these symbols and assumptions for simplification, we can write the residual intensity $r_{2n}(k)$ at the wavelength of the 2n-radiation in the form

$$r_{2n}(k) = \frac{1}{\pi F^{*}_{c,2n} A^{*}} \left[\int_{\sigma_d(k)} \left\{ I_{2n}(k) + I^{*}_{2n}(k) \exp[-\tau(Hn, k)] \right\} d\sigma \right.$$
$$\left. + \int_{A^{*} - \sigma_d(k)} I^{*}_{2n}(k) d\sigma + \int_{\sigma_e(k)} I_{2n}(k) d\sigma \right] \tag{5}$$

where $\tau(H_n,k)$ denotes the optical thickness of the k-th zone in the 2n-radiation at the projected surface element $d\sigma$. Each term in equation (5) has the following implication: the integrand in the first integral denotes the intensity of radiation emerging through the outer surface of the k-th velocity zone lying in front of the stellar disk. The integration covers the area $\beta(k)A^*$ in the stellar disk. The second integral indicates the intensity of λ_{2n} (k)-radiation emitted from the part of stellar disk that is not screened by the k-th zone. The third integral term in equation (5) gives the radiation intensity at the same wavelength emitted from the surface of the k-th velocity zone outside the stellar disk. This part of the radiation mainly contributes to the formation of the emission components. In equation (5) we have neglected the contribution from the continuous emission of the envelope. For the purpose of simplifying equation (5), we first define the average surface intensity of the k-th velocity zone by

$$\pi F_{2n}(k) = \frac{1}{\sigma(k)} \int_{\sigma(k)} I_{2n}(k)\, d\sigma \qquad (6)$$

and

$$\pi F_{2n}^*(k) = \frac{1}{A^*} \int_{A^*} I_{2n}^*(k)\, d\sigma = I_{2n}^*(k) \qquad (7)$$

The last equality of the equation (7) holds if the limb darkening, gravity darkening, and Doppler shift due stellar

rotation are ignored. Secondly,we suppose that the projected area $\beta(k)$ on the stellar disk is also divided into m-parts $\beta_i(k)$ $(i=1,2,....)$ with the respective optical thickness $\tau(H_n,k)$. Equation (5)then reduces to the form

$$r_{2n}(k)=\frac{F_{2n}(k)}{F^*_{c,2n}}\left[\beta(k)+\frac{\sigma_e(k)}{A^*}\right]+r^*_{2n}(k)\left\{\sum_{i=1}^{m}\beta_i(k)\exp[-\tau_i(H_n,k)]+1-\beta(k)\right\} \quad (8)$$

where

$$\beta(k)=\sum_{i=1}^{m}\beta_i(k) \quad (9)$$

and

$$r^*_{2n}(k)=\frac{F^*_{2n}(k)}{F^*_{c,2n}} \quad (10)$$

being the residual intensity of the broad stellar absorption at $\lambda_{2n}(k)$ and we usually have $r^*_{2n}(k)=1$ for $n\gtrsim 20$. The first part of equation (8) yields the profile of the emission component , while the second part gives the profile of shell absorption superimposed on the emission component and stellar absorption profile.

Next we consider some extreme cases.Let a star in question have a sufficiently developed envelope.For the lower members of the Balmer series,we may put,for the main part of the line profile,

$$\tau_i(H_n,k)\gg 1$$

and

$$F_{2n}(k)\gtrsim F^*_{c,2n}$$

In this case ,equation (8)can be written as

$$r_{2n}(k) \simeq \frac{\sigma(k)}{A^*} \frac{F_{2n}(k)}{F^*_{c,2n}} + r^*_{2n}(k)[1-\beta(k)] \qquad (11)$$

This gives the main part of the profiles,i.e.,the central deep absorption corresponds to the values of k for which $\sigma(k)/A^* \ll 1$ and $1-\beta(k) \ll 1$, whereas the strong emission appears for the values of k where $\sigma(k)/A^* \gg 1$ in equation(11).

For the higher members ,on the contrary,we may put

$$F_{2n}(k) \ll F^*_{c,2n} \quad ,$$

and then ,we have from equation(8)

$$r_{2n}(k) \simeq r^*_{2n}(k) \left\{ \sum_{i=1}^{m} \beta_i(k) \exp[-\tau_i(H_n,k)] + 1 - \beta(k) \right\} \qquad (12)$$

Equation (12)implies that the profiles of shell absorption in higher members of the Balmer can be determined fairly freely from from the internal radiation field of the envelope.

For the highest members of the Balmer series,for which we can assume

$$\tau_i(H_n,k) \ll 1,$$

equation(12)is furthermore approximated as

$$r_{2n}(k) \simeq r^*_{2n}(k)\left[1 - \sum_{i=1}^{m} \beta_i(k)\tau_i(H_n,k)\right] \qquad (13)$$

Finally ,the optical thickness $\tau_i(H_n,k)$ can be reduced to $\tau_i(H_\alpha,k)$ by the relation

$$\tau_i(H_n,k) = \tilde{\omega}_n \tau_i(H_\alpha,k) \qquad (14)$$

where

$$\tilde{\omega}_n = \frac{\nu_{2n} B_{2n}}{\nu_{23} B_{23}}$$

B_{23} , B_{2n} being the Einstein coefficients for the respective transition. Approximate formula for $\tilde{\omega}_n$ is given in the footnote of Kogure(1975).

The residual intensities $r_{2n}(k)$ given by equation (12) provide a method to derive the envelope parameters $\beta_i(k)$ and $\tau_i(H_\alpha,k)$($k=0\mp1,\mp2,\ldots\ldots\ldots,i=1,2\ldots$) from the observed profiles of shell lines in intermediate and higher members of the Balmer series.When no appreciable Balmer progression appears, this procedure is much simplified, since the central residual intensities of shell lines correspond to the same velocity zone of,say,k=0.We consider such cases for a while and omit the suffix k from the formulae.

In addition ,for a large part of observed stars, comparison with observation can be made by simplest cases of m=1 or 2 in equation (12) .The approximate formulae for these cases are written as follows:

i]Case of m=1 (the single-layer approximation): This expression has been already obtained by Kogure (1975).

$$1 - \frac{r_{2n}}{r^*_{2n}} = \beta \left\{ 1 - \exp\left[- \tilde{\omega}_n \tau(H_\alpha) \right] \right\} \qquad (15)$$

ii]Case of m=2(the double-layer approximation):

$$1-\frac{r_{2n}}{r_{2n}^{*}}=\beta_1\{1-\exp[-\tilde{\omega}_n\tau_1(H_\alpha)]\}+\beta_2\{1-\exp[-\tilde{\omega}_n\tau_2(H_\alpha)]\} \quad (16)$$

and

$$\beta=\beta_1+\beta_2 \quad (17)$$

For the purpose of fitting observation, we first draw a family of curves

$$1-\frac{r_{2n}}{r_{2n}^{*}}=\beta(1-e^{-x}) \quad (18)$$

with different values of β $(0<\beta<1)$ on the plane of $(1-r_{2n}/r_{2n}^{*})$ versus logx. Next we plot the observed values of $(1-r_{2n}/r_{2n}^{*})$ against the abscissa log $\tilde{\omega}_n$. In the single-layer approximation , we search for the best value of β and the coordinate of logx=0 on the abscissa log $\tilde{\omega}_n$ by a suitable horizontal shift of the curve (.18).The optical thickness is then given by the relation

$$\log\tau(H_\alpha)=-\log\tilde{\omega}_n \quad (19)$$

In the double -layer approximation, the fitting can be made as a composition of two different layers by a trial-and-error method ,or by the least-squares method.The two layers,thus found and designated as layers 1 and 2 ,have a different combinations of β and $\tau(H_\alpha)$.We shall call layer 1 for the layer

having larger optical thickness i.e., $\tau_1(H_\alpha) > \tau_2(H_\alpha)$. That is, layer 1 is the layer which contributes to the formation of shell lines in the highest part of the Balmer series. On the positional relation of layers 1 and 2, a further study on the shell line profiles is needed, though a crude information will be obtained by the measurement of the widths of shell lines.

ASTRONOMY & ASTROPHYSICS
SUPPLEMENT SERIES

Astron. Astrophys. Suppl. Ser. **75**, 79-92 (1988)

Spectra and radial velocities of white supergiants (*)

L. Denizman ([1]) and M. Hack ([2,**])

([1]) International School for Advanced Studies (I.S.A.S.), Trieste, Italy
([2]) Department of Astronomy, University of Trieste, Italy

Received October 8, 1987, accepted March 29, 1988

Summary. — The visual spectra of two late B (HD 199478 and HD 21291) and one early A (HD 21389) type nebulosity related supergiants are presented. Line profiles of hydrogen and metals are described extensively and compared with early observations. Also Balmer progression and radial velocity *versus* optical depth diagrams have been constructed. During the observational period hydrogen and metallic line profiles and their radial velocities exhibited variations which were rather similar to those observed in Be stars.

Key words : supergiants — atmospheres of supergiants.

1. Introduction.

As it was suggested by several previous investigations (Rosendhal, 1970 ; Rosendhal and Wegner, 1970 ; Rosendhal, 1973 ; Aydin, 1972 ; Zvereva *et al.*, 1984) there is need for continuous observations of early type supergiants for understanding the line variability, the kinematic properties, the large-scale and small-scale motions in their atmospheres.

The aim of this work is to present the results of the observations of optical spectra for three supergiants which seem to be related to nebulosity and distinguished from other supergiants in having a definite affinity with Be stars. The program stars and their basic data are given in table I. It has been noted by Zvereva *et al.* (1984) that two of them, HD 21389 and HD 21291 may be the first samples of late-B and A-type supergiants, which have atmospheres dominated by radial pulsation-type motions. This study includes another object HD 199478, which is similar to the other two.

2. Observations and data analysis.

2.1 THE OBSERVATIONS. — All the program stars have been observed at the Haute-Provence observatory. In this work, 30 spectrograms obtained at the coudé spectrograph of the 152 cm telescope at 7, 12, 20 Å/mm reciprocal dispersions and at the 193 cm telescope at 10.6 Å/mm with the ISIS (CCD) spectrograph (Gillet *et al.*, 1986) device, are analysed. The whole spectral region ranges from 3300 Å to 6800 Å. Table II gives the list of spectra and the dates of observation for the red and blue plates.

2.2 DATA PROCESSING. — The photographic material was digitized with the Perkins Elmer PDS 1010A digital microdensitometer of the Astronomical Observatory of Trieste. Five scans were performed on all plates in order to digitize the upper and lower plate fog and wavelength reference spectra, and the stellar spectrum. The scanning step was set to 5 microns. With the same setting of the PDS exposure-calibration plates were scanned by a raster which was perpendicular to the dispersion axis. The origin of this raster scan was chosen as a known suitable line of the wavelength reference spectrum so each scan of the raster included one full series of exposure calibration levels at the wavelength corresponding to the current scan origin. The interscan distance was set to 100 Å for the blue plates and 200 Å for the red plates.

The digitized spectrograms were then reduced to linearized exposure-wavelength data arrays by means of the ELSPEC/11 interactive spectrogram processing package of the ASTRONET pole of Trieste (Pasian *et al.*, 1982).

The wavelength calibration was performed by means of a fourth order polynomial fit of the current wavelengths and abscissae of the lines recovered in the upper and lower wavelength reference spectra. The upper and lower calibrations were then interpolated at

Send offprint requests to : L. Denizman.

(*) Based on the observations secured at the Haute Provence Observatory.

(**) Visiting Astronomer at the Astronomical Observatory of Trieste.

the current ordinate of the stellar spectrum to remove the wavelength offset due to local misalignment of the stellar spectrum with respect to the scanning axis of the microdensitometer and to improve the total accuracy. The typical accuracy of the wavelength calibration as estimated through the residuals of the polynomial fit is on the order of 0.02 Å.

The exposure calibration was performed by means of the coefficients of the second order polynomial fit of the logarithm of the exposure to the Baker density measured on the calibration plate. The plate fog parallel to the stellar spectrum was subtracted from the raw stellar spectrum. The coefficients used for the exposure linearization were computed through the coefficients obtained from the two exposure calibration scans corresponding in wavelength to the Hα line for the red plates and Hβ line for the blue ones. The exposure calibration error as estimated through the residuals of the polynomial fit is typically around 3-2 %. The normalization to the continuum was performed by means of a cubic spline fit of the series of nominal continuum data obtained by averaging the current stellar spectrum in a series of selected spectral windows interactively. Then heliocentric correction was applied to every spectrum and line parameters were measured interactively and from the plots. The total measurement accuracy of this standard data reduction was estimated to be 0.8 km/s in radial velocities and 2 % in the relative intensities. The average total error of the radial velocities, obtained by fitting line-parameters is typically around 1.6 km/s.

The ISIS image has been processed at the Haute Provence Observatory with IHAP software ; then the calibrated and heliocentricly corrected image has been transformed by a special procedure which converts FITS format to standard ELSPEC file (Castelli F. *et al.*, 1986).

3. The spectra.

3.1 HYDROGEN LINES. — The hydrogen lines of the program stars are sharp with Balmer series visible up to about $n = 22$. Line profiles, radial velocities and equivalent widths are variable for all the program stars. The measured average Balmer discontinuities D for the program stars are the following : for HD 199478 $D = 0.19$, for HD 21291 $D = 0.23$, for HD 21389 $D = 0.27$ where

$$D = (\log I\,[3650\,(\mathrm{A}) +] - \log I\,[3650 -]) . \quad (1)$$

The measured radial velocities and average equivalent widths at the corresponding Julian date are given in tables IIIa, b, c. Table IV gives the radial velocities for the Hα and Hβ lines of hydrogen compared with the radial velocities of the center of mass of the program stars.

3.1.1 HD 199478. — The Hα profile of HD 199478 was first published by Rosendhal (1973). It was a double-peak emission with the component at the red edge weaker than the blue one with a central absorption at radial velocity + 68 km/s. We present four different Hα profiles. The first two of them which were observed during the same night show variable weak absorption components superimposed on a weak emission with Hα absorption at the radial velocities + 57.7 km/s for the first profile and + 63.1 km/s for the second one respectively (Figs. 1a, b). These superimposed weak components were not present on the other two profiles which were observed with one night interval with each other. The emission and the absorption components are stronger, and for these last two profiles Hα absorption radial velocities are + 56.3 km/s and + 57.9 km/s (Figs. 1c, d). Unfortunately these absorption components were affected by contribution of the terrestrial atmospheric absorption, although their bandwidths on the continuum suggest that the stellar hydrogen components are also present.

The Hβ line profiles and radial velocities show a sequence of variation during the observation period. In the case of HD 199478 the profiles shown in figures 2a, b, c which were secured on the same night show a contraction phase ; the profile given in figure 2d which was secured four nights later possibly presents the maximum of the contraction. In figures 2g, h the spectra which were secured with two nights interval represent a passage from contraction to expansion and lastly in figures 2i, j the profiles indicate expansion.

3.1.2 HD 21291. — Two Hα profiles of this star were analysed by Rosendhal (1973). The first one was an inverse P Cygni profile, while the second one was an asymmetric absorption profile which was extended towards the blue and a trace of weak emission was present on the red side of the absorption.

Three Hα profiles of HD 21291 are presented : the first one is an asymmetric, blue-shifted absorption profile, radial velocity − 33.4 km/s, with a weak emission component on the red edge which is similar to the first profile observed by Rosendhal. The weak equivalent width and the shape of the profile suggest a contribution by the emission component (Fig. 3a). The profiles shown in figures 3b, c were secured with one night interval. The first one shows an asymmetric absorption profile, the second one is more symmetric and both of them have no emission components ; the equivalent widths are greater than the first one and the radial velocities are lower (− 27.1 km/s and − 26.5 km/s, respectively).

The Hβ line profile and the radial velocity changes during the observational period, for HD 21291 are given in figure 4. The profile in figure 4a was observed during the same night as the Hα profile in figure 3a. It is symmetric and has wings up to $\mp$ 350 km/s and a radial velocity of − 24.6 km/s ; the equivalent width is the smallest among all our observed values. Figures 4b, c present the profiles secured on the same night, with one night interval with the previous one ; the last two profiles show a notable difference in their shapes and radial velocities, − 12.3 km/s and − 18.1 km/s respectively. Profiles given in figures 4d, e, f, g are taken on the same night, and show the fast variation of the star in expansion phase.

3.1.3 HD 21389. — This star is the most extensively studied one among the program stars. The Hα profiles of this star show a series of variations from pure emission to absorption, or to inverse P Cygni, or to direct P Cygni profiles. Aydin (1972) observed a contraction phase of this star as indicated by the radial velocity progression of the Balmer lines and by the inverse P Cygni profile of Hα. Later Rosendhal (1973) also analysed the Hα profiles of HD 21389 and noted a double-peak emission and a superimposed central absorption profile for Hα. Lastly Zvereva *et al.* (1984) observed a weak emission on both sides of the Hα on August 1978 and a P Cygni profile on February 1980.

In this work three Hα profiles of this star are presented. The first two profiles secured with one night interval show variable and asymmetric absorption components without any emission feature with radial velocities – 54.8 km/s and – 46.1 km/s. The third profile shows a double-peak emission with a blue shifted absorption component at – 19.3 km/s ; it is similar to that observed by Zvereva *et al.* on August 1978 (Figs. 5a, b, c).

Similar rapid variations for the Hβ profiles are observed for HD 21389. The profiles shown in figures 6a, b are observed on the same night ; the first profile presents a double-peak asymmetric absorption component, although the second profile looks more symmetric, and the radial velocities – 8.1 km/s and – 3.4 km/s respectively : a possible contraction phase. Profiles given in figures 6c, d, e which were secured on the same night present possibly an atmospheric expansion phase, although figures 6f, g which were secured with one night interval, represent a possible contraction phase. Lastly figures 6h, i, j, suggest again an expansion.

3.2 THE METALLIC LINES. — The metallic lines of the program stars also present variable profiles and radial velocities. The average velocity differences between the hydrogen lines ($n > 10$) and that of the metallic lines are also variable ; in some cases there is a notable difference, during some other nights the differences are very small. Differences between the average velocities of SiII and FeII for the program stars are given in table V. It seems that HD 21389 presents a change of the sign of the difference. This change was noted by Aydin (1972), and then by Zvereva *et al.* (1984). These observations indicate a change of the sign in a short time interval (hours). For HD 199478 and HD 21291 on the contrary all the measured differences were always positive. Some selected metallic line profiles of the program stars are presented as follows : SiII λλ3853.6, 3856.0, 3862.5 in figures 7a, 8a, 9a ; HeI λ4471.4 and MgII λ4481.1 in figures 7b, 8b, 9b ; HeI λ4921.9 and FeII λ4923.9 in 7c, 8c, 9c for HD 199478, HD 21291 and HD 21389, respectively. They show the variations clearly. Also the measured wavelengths, equivalent widths w, relative depths, full bandwidths on the continuum, and halfwidths on the continuum of HeI λ4471 and MgII λ4481 lines which are sensitive to the rotational broadening are given in table VI. These values confirm the $v \sin i$ values given in table I showing that HD 199478 is a faster rotator than the other two. Figures 10, 11, 12 present the measured radial velocities of the absorption cores of the lines *versus* optical depth, for HD 199478, HD 21291 and HD 21389, respectively. These diagrams have been prepared to display the differential line shifts pattern and compare them with the results of Zvereva *et al.* (1984). So we combined lines with similar formation depths into groups. Typical values of the assigned optical depths are given in table VII.

3.3 THE INTERSTELLAR LINES. — These stars are closely associated with nebulosities. Hence the interstellar CaII and NaI lines are sharp and strong. All the program stars presented also evidence for shell components as seen in β Ori (Barsukova *et al.*, 1983) but it was difficult to measure them with the available dispersions. Only one spectrogram of HD 199478 secured with the highest dispersion (7 Å/mm) shows clearly an extended blue flank for the CaIIK line up to – 102 km/s, and also there is another component with velocity + 39.1 km/s. For the same star NaID lines also show a component at radial velocity + 43.5 km/s. According to Munch (1957) HD 21291 had a very weak component at NaI 5890 line, with radial velocity – 35 km/s that was not possible to detect with our available data. The unidentified interstellar features such as λλ5780, 5797 and 6614 Å are observed in all the program stars. Their equivalent widths, relative depths and full bandwidths on the continuum are given in table VIII.

4. Conclusion.

One of the chief indications from the visible spectrum that outflow may be occurring in the envelopes of B-type supergiants is the fact that a Balmer progression is observed for Ia supergiants, i.e. the lines Hα, Hβ and Hγ tend to show more negative radial velocities than do the higher members of the Balmer series. This systematic trend is shown by most of the B-type supergiants that have been investigated in detail by Hutchings (1976a, 1980). Underhill (1982) concluded that the direction of the Balmer progression is never reversed for B supergiants. That is, the absorption cores of Hα, Hβ and Hγ never presented less negative velocities than the higher Balmer lines. However our observations confirmed the researches done by Aydin (1972) for HD 21389, and by Zvereva *et al.* (1984) and contradicted the above conclusion of Underhill (1982) because these supergiants do have inverse Balmer progressions, like Be stars (Ballereau and Hubert-Delplace, 1982 ; Denizman and Hack, 1988).

Furthermore, besides the Balmer progression variations, the observed Hα profiles and their long timescale variations are similar to those observed in Be stars as it was already noted by Harmanec (1982). The observed variations can be explained by macroscopic radial motions, or semiregular or irregular pulsation-type motions. Surely there is need of continuous and simultaneous observations in the optical and ultraviolet wavelength ranges of this kind of stars. An ultraviolet

research of these stars and their comparison with Be/shell stars is in progress.

Acknowledgements.

One of us (L.D.) would like to thank the director of the OAT Prof. G. Sedmak, the technical personnel of OAT, the computer center and ASTRONET staff for their hospitality and help during the preparation of this work. We also thank the director of the OHP M. P. Véron, and the technical personnel of the 152 cm and 193 cm telescopes for their continuous help and hospitality during the observations.

Our very special thanks to M. Felenbok from Meudon and M. D. Gillet from OHP for the ISIS image and its data processing, and to L. Rusconi for very useful discussions about ELSPEC and V. Doazan from Paris for her comments. This work is a part of a Ph. D. thesis at I.S.A.S. and supervised by Prof. M. Hack, director of the Astronomy Department of the Trieste University.

References

ABT, H. A. : 1957, *Astrophys. J.* **126,** 183.
AYDIN, C. : 1972, *Astron. Astrophys.* **19,** 369.
BALLEREAU, D. and HUBERT-DELPLACE, A. M. : 1982, The Be stars, *IAU Symp.* Eds. M. Jaschek-G. Groth (Reidel, Dordrecht) **98,** 171.
BARSUKOVA, E. A., LEBEDEVA, I. A. CHARGEISHUILI, K. B. and CHENTSOV, E. L. : 1983, *Bull. Sp. Ast. Obs.* (North Caucasus) **16,** 34.
BERNACCA, P. L., PERINOTTO, M. : 1970, *Publ. Obs. Padova Asiago,* No. **239.**
CASTELLI, F., CRIVELLARI, L. and MAGAZZU, M. : 1986, Local user note, No. **8,** OAT.
DENIZMAN, L. and HACK, M. : 1988, in preparation.
GILLET, D., GUÉRIN, J. and KOHLER, D. : 1986, notice d'utilisation No. **2,** OHP.
HARMANEC, P. : 1982, The Be stars, *IAU Symp.* Eds. M. Jaschek and H.-G. Groth (Reidel, Dordrecht) **98,** 279.
HUTCHINGS, J. B. : 1976a, *Astrophys.* **203,** 438.
HUTCHINGS, J. B. : 1980, *Astrophys. J.* **235,** 413.
MUNCH, D. : 1957, *Astrophys. J.* **125,** 42.
PASIAN, F., RUSCONI, L., SEDMAK, G. : 1982, *Publ. O.A.T.* Nos. **806** and **807.**
ROSENDHAL, J. D. : 1970a, *Astrophys. J.* **159,** 107.
ROSENDHAL, J. D. : 1973, *Astrophys. J.* **186,** 909.
ROSENDHAL, J. D. and WEGNER, G. : 1970, *Astrophys. J.* **162,** 547.
UNDERHILL, A. and DOAZAN, V. : 1982, B stars with and without emission lines, NASA SP-456.
ZVEREVA, E. B., ZEINALOV, S. K. and CHENTSOV, E. L. : 1984, *Izv. Spets. Astro. Obs.* **18,** 29.

TABLE I. — *Basic data for the program stars.*

	HD 199478	HD21291	HD21389
Spect. Type	B8 Ia	B9 Ia	A0 Ia
V(mag.)	5.69	4.23	4.58
B-V(mag.)	0.46	0.41	0.57
r(kpc.)	1.84	1.03	1.00
R(kpc.)	10.09	10.83	10.81
Vel.(km/s)	-16.00	-6.80	-6.00
Assoc. or Clust.	NGC 6991	CAM OB1	CAM OB1
Vsini(km/s)	49.00	15.00	8.00

Where V = apparent visual magnitude, B-V = observed B-V colour, r = distance from the sun, R = distance from the galactic center, Vel. = radial velocity of the star, Assoc. or clust. = stellar association or cluster to which the star may belong, $V \sin i$ = measured rotational velocity. $V \sin i$ values are taken from following researches : for HD 199478 from Rosendhal (1970), for HD 21291 from Bernacca *et al.* (1970), and for HD 21389 from Aydin (1972). Other values are taken from Humpreys (1970).

TABLE II. — *Available visual data for the program stars.*

Spectrogram	Emulsion	UT time	Julian day 2400000+
HD 199478			
(a)	(b)		
GB 338	IIaOch	20:18	40830.3487
GB 339	IIaOch	21:12	40830.3862
GB 340	IIaOch	21:54	40830.4154
GC 23	IIaOch	22:05	40834.4230
GB 380	IIaF	23:00	40836.4612
GB 381	IIaF	24:04	40836.5056
GB 726	IIaOch	17:38	40931.2344
GB 746	IIaOch	19:35	40933.3155
GB9062	IIaOch	19:57	46400.3314
GB9065	IIaOch	18:58	46402.2903
ISIS(CCD)	-	21:30	46637.3982
GA7253	IIIaF	21:53	46639.4141
HD 21291			
GB9064	IIIaF	22:47	46400.4537
GB9068	IIaOch	01:57	46401.5856
GB9069	IIaOch	02:36	46401.6127
GB9397	IIaOch	17:57	46818.2504
GB9398	IIaOch	18:25	46818.2698
GB9399	IIaOch	19:55	46818.3323
GB9403	IIIaF	25:01	46818.5448
GB9405	IIIaF	19:00	46819.2941
HD21389			
GB4136	IIaOch	03:17	43390.6372
GB4137	IIaOch	03:33	43390.6484
GB4142	O98-82	01:[illegible]	43391.5658
GB4143	O98-82	02:[illegible]	43391.5894
GB4144	IIaOch	02:42	43391.6130
GB4145	IIaOch	03:00	43391.6255
W 7486	IIaOch	19:53	45739.3298
W 7498	IIaOch	18:27	45741.2694
GB9116	IIaOch	20:48	46451.3693
GB9118	IIaOch	21:30	46451.3984
GB9406	IIIaF	20:30	46819.3566

(a)The dispersions of the spectra are the followings:
GB = 12 A/mm, GA =20 A/mm,GC = 7 A/mm, W= 10 A/mm, ISIS= 10 A/mm
(b)Effective Wavelength regions for emulsions are the followings:IIaoch 3600-5100 A, IIIaF and O98-82 4800-6700 A, for ISIS image centered on H_α and 50 A total width of the observational band.

TABLE IIIa. — *Measured radial velocities and average equivalent widths of HD 199478.*

Elem	Mult	Wav. Lab (A)	JULIAN DATE (2440000+) 0830.348	0830.386	0830.415	0834.423	0931.234	0933.316	6400.331	6402.290	Ave Eqw (A)
			Radial velocities(km/s)								
H 18	4	3691.6	-7.6	-16.8	-35.8	-19.8	-13.4	-23.0	-18.2	-31.0	0.8
H 17	3	3697.2	-35.5	-4.2	-26.9	-25.2	-18.9	-34.8	-15.7	-23.7	1.2
H 16	3	3703.9	-8.4	-11.2	-28.0	-	-13.7	-43.9	-1.0	-10.5	2.1
H 15	3	3712.0	-5.6	-29.5	-28.0	-29.5	-21.7	-1.1	-21.7	-1.1	1.5
H 14	3	3721.9	-6.2	-6.8	-31.5	-25.3	-41.0	-26.8	-26.9	-22.1	1.5
H 13	3	3734.4	-20.0	-27.9	-21.9	-21.9	-23.5	-21.9	-6.1	-12.5	1.8
H 12	2	3750.2	-	-12.9	-6.1	-31.2	-27.4	-32.7	-7.6	-20.2	1.7
H 11	2	3770.6	-	-5.6	-14.5	-23.8	-20.7	-25.4	-20.7	-11.3	1.6
H 10	2	3797.9	-12.2	-28.2	-27.7	-15.3	-15.4	-37.1	-1.2	-12.2	1.4
He I bl	22	3819.6	-1.7	-	-24.5	-32.2	-26.1	-33.8	-10.7	-15.3	0.8
H 9	2	3835.4	-1.4	-20.3	-4.2	-30.2	-30.2	-18.0	-13.4	-7.2	1.5
Si II	1	3853.7	-36.1	-26.6	-43.5	-45.1	-37.5	-42.0	-28.3	-37.4	0.2
Si II	1	3856.0	-20.6	-13.9	-27.6	-32.1	-24.6	-30.7	-15.4	-18.4	0.4
Si II	1	3862.6	-19.4	-28.7	-35.3	-27.7	-35.3	-30.8	-17.1	-18.1	0.4
H 8	2	3889.1	-8.2	-2.9	-13.0	-20.6	-7.0	-26.7	-28.2	-25.2	1.7
C II	4	3919.0	-32.3	-27.3	-19.3	-28.3	-17.8	-35.8	-	-26.8	0.1
C II	4	3920.7	-14.3	-26.3	-23.3	-20.0	-23.3	-47.4	-29.3	-36.8	0.2
Ca II	1	3933.7	-22.1	-13.9	-20.7	-19.2	-20.7	-22.3	-11.8	-10.3	1.1
He I	5	3964.7	-21.8	-11.8	-32.8	-44.6	-22.4	-43.2	-46.2	-38.7	0.3
Ca II	1	3968.5	-13.3	-17.7	-20.7	-22.2	-11.9	-20.7	-13.3	-25.2	0.8
H Epsl	1	3970.1	-5.6	-5.7	-19.0	-33.8	-8.6	-30.8	-14.5	-35.3	1.4
He I	55	4009.3	-25.7	-24.8	-4.7	-29.0	-21.7	-33.4	-12.9	-29.2	0.2
He I bl	18	4026.3	-26.0	-32.6	-23.5	-35.9	-24.9	-35.2	-36.6	-37.8	0.6
H Delt	1	4101.7	-4.0	-0.3	-10.9	-9.4	-13.8	-23.8	-22.4	-26.7	1.6
He I	16	4120.8	-7.6	-0.5	-33.5	-26.3	-20.6	-19.1	-4.9	-10.4	0.2
Si II	3	4128.1	-35.8	-7.1	-19.6	-25.3	-26.7	-33.8	-18.2	-15.3	0.4
Si II	3	4130.9	-11.1	-22.8	-27.2	-30.0	-18.7	-24.3	-22.9	-28.6	0.5
He I	53	4143.8	-10.9	-15.0	-18.1	-39.3	-32.3	-29.5	-26.6	-37.9	0.4
Fe II	27	4233.2	-16.0	-29.8	-21.6	-41.0	-45.2	-50.8	-32.5	-29.9	0.3
H Gamm	1	4340.5	0.4	13.2	-13.4	-22.9	-3.9	-14.8	-16.1	-3.6	1.7
Fe II	27	4351.8	-47.3	-56.7	-45.9	-57.9	-43.1	-57.9	-22.9	-33.7	-
He I	51	4387.9	-16.8	-30.8	-15.3	-23.3	-7.2	-23.3	-35.7	-19.2	0.3
He I	14	4471.5	-4.2	-30.4	-5.7	-24.1	-16.2	-21.5	-25.4	-20.2	0.9
Mg II	4	4481.1	-11.9	-18.0	-25.7	-19.1	-6.0	-20.5	-25.8	-16.5	1.0
Fe II	37	4515.3	-	-7.8	-	-14.4	-	-12.0	-8.1	-39.4	-
Fe II	38	4549.5	-29.5	-16.5	-30.9	-43.7	-27.2	-30.9	-32.1	-23.1	0.2
Fe II	37	4555.9	-20.1	-26.2	-30.2	-34.0	-28.9	-	-21.2	-10.7	-
Fe II	38	4583.8	-	-23.7	-35.0	-28.4	-15.8	-42.3	-33.5	-26.1	0.2
Fe II bl	37	4629.3	-29.7	-30.7	-16.0	-	-31.9	-53.4	-2.2	-21.7	0.1
He I	12	4713.1	-13.9	-10.5	-11.4	-10.4	-20.4	-20.4	-30.4	-31.6	0.7
S II	9	4815.5	-32.1	-30.2	-18.7	-	-21.2	-20.2	-38.3	-7.6	0.2
H Beta	1	4861.3	15.5	20.7	16.1	23.2	8.7	-2.2	-20.2	-32.3	1.9
He I	48	4921.9	-	-18.2	-18.4	-	-22.0	-25.6	-18.4	-22.0	0.6
Fe II	42	4923.9	-	-17.8	-46.6	-	-13.2	-28.7	-32.2	-23.9	0.7

Elem.	Mult.	Wav. Lab. (A)	JULIAN DATE (2440000+) 0836.461	0836.506	6639.414	Ave Eqw (A)
			Radial velocities(km/s)			
H Beta	1	4861.3	5.3	9.3	-	-
He I	48	4921.9	-25.2	-22.0	-30.3	-
Fe II	42	4923.9	-13.0	-23.9	-48.7	-
He I	4	5015.7	-6.7	-16.9	-20.0	0.1
Fe II	42	5018.4	-23.6	-17.8	-18.7	0.1
S II	7	5032.4	-16.9	-	-18.7	0.1
Si II	5	5041.1	-	-40.0	-31.4	0.2
Si II	5	5056.0	-9.6	-2.3	-24.4	0.2
Fe II	42	5169.0	-25.0	-16.5	-25.8	0.2
S II	6	5428.6	-21.0	-17.0	-28.7	0.2
S II	6	5432.8	-19.5	-27.3	-41.2	0.1
S II	6	5453.8	-14.8	-29.4	-12.2	0.3
S II	14	5640.0	-5.4	-13.6	-18.7	0.1
S II	14	5647.0	-22.8	-20.8	-23.6	0.2
N II	3	5666.6	-28.6	-38.9	-13.1	0.1
N II	3	5679.6	-4.0	-7.9	-	0.1
Fe II	24	5779.7	-22.9	-7.4	-	0.2
He I bl	11	5875.7	-2.9	-10.1	-27.0	0.6
Na I	1	5890.0	-15.3	-17.5	-14.9	0.6
Na I	1	5895.9	-13.7	-12.1	-18.5	0.5
Si II	4	5957.6	-	-8.0	-49.1	0.1
Si II	2	6347.1	-18.4	-16.3	-27.4	0.6
Si II	2	6371.4	-25.3	-13.2	-20.4	0.4
Ne I	1	6402.2	-18.8	-7.9	-41.2	0.1
H Alph	1	6562.8	57.7	63.1	57.9	0.1
C II	2	6578.0	-15.0	-26.0	-18.7	0.2
C II	2	6582.9	-34.7	-9.3	-20.2	0.2
He I	46	6678.2	-18.1	-22.6	-18.2	0.5

TABLE IIIb. — *Measured radial velocities and average equivalent widths of HD 21291.*

Elem	Mult.	Wav Lab (A)	JULIAN DATE (2440000+) 6401.586	6401.613	6818.250	6818.270	6818.323	Ave Equ (A)
			Radial velocities(km/s)					
H 18	4	3691.6	0.9	- 3.8	- 4.5	-13.4	-18.0	0.8
H 17	3	3697.2	- 1.8	- 6.3	- 4.5	- 4.6	-12.0	1.6
H 16	3	3703.9	- 9.1	- 7.5	- 4.2	-24.5	-18.5	0.8
H 15	3	3712.0	- 7.2	- 8.3	- 1.1	- 1.0	-18.6	0.8
H 14	3	3721.9	- 7.6	-16.0	-28.1	-26.6	-18.3	1.3
H 13	3	3734.4	-14.0	-13.8	-13.2	-14.0	- 9.2	0.9
H 12	2	3750.2	- 4.5	-13.4	- 4.3	-18.2	- 5.7	1.3
H 11	2	3770.6	-11.6	-11.2	- 1.6	-25.3	-31.0	1.3
H 10	2	3797.9	-	- 3.0	-10.6	- 1.9	-38.4	1.0
He I bl	22	3819.6	-23.0	-19.7	-24.5	-16.7	-22.9	0.2
H 9	2	3835.4	-14.9	- 5.5	-27.9	- 5.3	-16.2	1.2
Si II	1	3853.7	-14.0	-14.2	-31.4	- 5.4	- 8.1	0.2
Si II	1	3856.0	- 7.8	-12.7	- 1.3	-16.6	-15.0	0.5
Si II	1	3862.6	- 2.6	-21.2	- 7.9	-17.0	-13.7	0.3
H 8	2	3889.0	-13.3	-17.4	-32.7	-12.7	-10.0	1.0
C II	4	3919.0	- 4.3	-	-38.8	-15.8	-17.5	0.1
C II	4	3920.7	- 3.8	-	- 0.5	-	-23.0	0.1
Ca II	1	3933.6	- 5.1	-15.3	-17.8	-10.3	-13.3	0.6
He I	5	3964.7	- 7.3	-25.5	- 8.9	- 4.8	-20.9	0.1
Ca II	1	3968.5	-11.3	-10.7	-13.1	- 8.5	-16.1	0.5
H Epsl	1	3970.1	- 3.6	- 9.7	-11.6	- 5.6	-17.3	1.0
He I	55	4009.3	- 0.2	-14.0	- 5.6	-11.2	- 9.7	0.1
He I bl	18	4026.3	-16.6	- 1.5	-20.2	-14.5	-20.2	0.2
H Delt	1	4101.7	- 2.3	- 1.7	-18.6	-35.0	-19.3	0.9
He I	16	4120.8	-13.2	-59.1	- 2.5	-14.5	-26.2	0.2
Si II	3	4128.1	- 5.8	- 1.0	-20.4	- 6.4	- 6.4	0.3
Si II	3	4130.9	-16.7	-12.7	- 1.6	-18.5	-12.8	0.3
He I	53	4143.8	- 4.1	- 2.5	-14.9	-14.8	-10.6	0.1
Fe II	27	4173.5	- 2.3	-	-12.4	-19.5	- 6.7	0.1
Fe II	28	4178.9	- 7.0	-17.7	- 7.6	-17.6	-12.3	0.2
Fe II	27	4233.2	-10.4	-20.5	- 9.1	-14.3	-17.2	0.2
Fe II	27	4303.2	- 5.9	- 7.3	-10.1	-22.2	- 5.9	0.2
H Gamm	1	4340.5	-10.5	- 6.4	- 3.5	-17.1	1.7	1.3
He I	51	4387.9	- 5.7	-40.3	-10.9	-10.9	-19.1	0.3
He I	14	4471.5	- 1.2	-46.5	- 1.7	- 5.7	-10.8	0.2
Mg II	4	4481.1	- 2.1	- 9.6	- 8.3	- 6.2	- 7.3	0.6
Fe II	37	4515.3	-20.8	-22.6	- 2.9	- 1.7	-	0.4
Fe II	38	4549.5	- 2.8	- 6.5	-24.2	-21.5	-10.4	0.3
Fe II	37	4555.9	-13.9	- 8.3	-31.1	-18.3	- 9.4	0.4
Fe II	38	4583.8	-10.6	- 3.3	-16.9	- 4.2	-18.1	0.2
Fe II bl	37	4629.3	-14.1	-	-17.8	-25.6	-11.5	0.2
He I	12	4713.1	-16.7	-	- 7.7	-11.3	- 5.2	0.1
H Beta	1	4861.3	-12.3	-18.1	-20.4	- 3.5	- 7.0	0.9
He I	48	4921.9	- 3.9	- 5.1	-20.5	-19.4	-22.2	0.2
Fe II	42	4923.9	-11.5	-12.8	-29.7	-14.3	-24.1	0.9

Elem.	Mult.	Wav.Lab. (A)	JULIAN DATE (2440000+) 6400.454	6818.545	6819.294	Ave. Equ (A)
			Radial velocities(km/s)			
H Beta	1	4861.3	-24.6	-16.1	-20.2	-
He I	48	4921.9	-11.1	- 2.7	- 8.6	-
Fe II	42	4923.9	-10.7	-10.7	-10.5	0.3
He I	4	5015.7	- 2.7	- 9.8	- 3.8	0.1
Fe II	42	5018.4	- 8.9	-15.2	- 3.4	0.3
Si II	5	5041.1	-10.3	-15.2	-10.7	0.2
Si II	5	5056.0	- 4.4	- 8.1	- 6.9	0.3
Fe II	42	5169.0	-11.6	-16.3	-10.7	0.4
Fe II	49	5234.6	- 7.3	- 5.0	-14.0	0.2
Fe II	49	5276.0	-11.8	-10.6	-10.8	0.2
Fe II	49	5316.6	-16.5	-12.2	-12.0	0.3
He I bl	11	5875.7	- 0.9	- 4.0	- 1.1	0.3
Na I	1	5890.0	- 8.7	-10.3	- 7.5	0.4
Na I	1	5895.9	- 7.8	- 5.9	-10.9	0.3
Si II	4	5957.6	- 2.0	- 8.0	-11.1	0.1
Si II	2	6347.1	- 1.5	- 9.7	-10.7	0.5
Si II	2	6371.4	- 8.6	-16.7	-11.3	0.4
H Alph	1	6562.8	-33.4	-27.1	-26.5	0.6
C II	2	6578.0	- 9.4	-11.8	- 7.1	0.1
C II	2	6582.9	-13.7	- 8.0	- 3.7	0.1
He I	46	6678.2	-10.9	-10.1	-15.4	0.3

TABLE IIIc. — *Measured radial velocities and average equivalent widths for HD 21389.*

Elem.	Mult.	Wav. Lab. (A)	JULIAN DATE (2440000+) 3390.637	3390.684	3391.613	3391.626	5739.330	5741.270	6451.369	6451.398	Ave Eqw (A)
			Radial velocities(km/s)								
H 18	4	3691.6	-34.1	-10.2	- 3.8	-11.8	- 6.9	-26.2	-11.1	-17.6	0.7
H 17	3	3697.2	- 9.3	-31.6	-28.5	-12.6	- 1.3	-12.3	- 9.2	- 8.6	1.2
H 16	3	3703.9	- 5.8	-15.3	-16.0	- 1.9	- 1.0	-24.8	- 5.1	-17.9	0.7
H 15	3	3712.0	- 4.2	-12.1	- 1.0	-20.0	-16.7	-20.1	-14.2	-17.4	1.3
H 14	3	3721.9	-31.5	- 4.7	- 3.1	- 1.6	-47.3	-11.0	- 8.9	- 3.1	1.3
H 13	3	3734.4	- 1.4	- 7.2	- 3.0	- 1.4	-18.8	- 0.2	- 3.5	-20.0	1.0
H 12	2	3750.2	- 1.4	-12.3	- 0.2	- 1.4	- 7.6	- 9.2	-15.0	- 6.5	1.2
H 11	2	3770.6	- 5.1	- 8.2	- 6.6	-22.2	- 1.9	- 9.8	-24.1	- 9.5	1.7
H 10	2	3797.9	- 0.9	- 7.6	- 6.0	- 7.6	-23.1	-15.3	-16.4	-11.4	1.2
He I bl	22	3819.6	-39.9	- 1.4	- 5.6	-48.9	-12.3	- 7.5	-17.1	- 3.6	0.3
H 9	2	3835.4	- 8.5	- 4.2	-10.3	- 6.0	-11.8	-24.1	- 7.8	- 3.5	1.2
Si II	1	3853.7	-28.3	-22.0	-11.5	-13.0	-14.5	-28.3	-15.3	- 5.6	0.3
Si II	1	3856.0	-13.9	-12.3	-10.8	-21.5	-24.5	- 0.8	-11.8	-11.1	0.4
Si II	1	3862.6	-20.1	-17.1	-14.0	-14.1	-21.6	- 7.9	- 7.5	- 6.2	0.4
H 8	2	3889.1	-20.6	-11.5	- 0.6	- 4.8	-11.5	- 5.5	- 7.0	-13.4	1.2
C II	4	3919.0	-28.3	-14.8	-32.8	-	-14.8	-17.5	-25.4	-46.9	0.4
C II	4	3920.7	- 9.8	-	-18.8	-29.3	- 9.8	-29.0	- 5.6	-27.6	-
Ca II	1	3933.7	-13.3	- 7.3	- 8.8	-13.3	- 5.8	- 8.8	- 8.5	-11.6	0.8
He I	5	3964.7	- 4.6	-28.3	-16.3	- 7.6	-15.4	-19.2	-20.9	-40.3	0.2
Ca II	1	3968.5	-16.3	-11.8	- 7.4	-20.7	-19.2	-11.8	-14.0	- 6.1	0.6
H Epsl	1	3970.1	- 5.6	- 5.6	- 5.6	- 6.1	- 5.8	- 6.2	- 8.4	-14.8	1.2
He I	55	4009.3	-29.0	- 7.0	- 7.1	-33.2	- 5.3	- 2.6	- 2.4	- 5.6	0.4
He I bl	18	4026.3	-17.6	-10.3	-17.6	-22.0	-10.3	- 1.5	-15.0	-24.1	0.2
H Delt	1	4101.7	- 8.1	- 2.3	6.3	- 0.9	- 3.4	-12.3	- 1.7	-16.5	1.5
He I	16	4120.8	-19.4	-16.6	-28.8	-10.7	-24.9	-10.7	- 2.2	-12.0	0.1
Si II	3	4128.1	-18.1	-13.8	-12.4	- 5.3	-12.4	- 5.3	- 3.4	- 7.4	0.4
Si II	3	4130.9	-11.6	-17.2	-12.9	-10.1	- 4.4	-10.2	-11.0	- 7.4	0.3
Fe II	27	4173.5	- 6.8	-11.2	- 9.8	- 9.8	-18.3	- 9.8	-18.9	-19.7	0.3
Fe II	28	4178.8	- 7.5	- 6.1	-29.4	- 9.1	- 8.9	- 0.4	- 0.5	-14.5	0.3
Fe II	27	4233.2	- 6.3	-11.9	-14.6	-18.8	-10.4	-18.9	-15.3	-13.2	0.4
Fe II	27	4303.2	-16.9	-17.0	- 7.5	- 8.0	- 6.1	-18.4	- 7.4	-14.3	0.3
H Gamm	1	4340.5	- 5.3	- 1.2	-14.7	-10.5	4.9	-12.9	1.5	-12.2	1.6
He I	51	4387.9	-	- 7.2	-	-20.2	-23.3	- 8.5	-11.1	- 1.9	0.3
He I	14	4471.5	-	- 1.7	- 3.1	- 4.4	-14.9	- 4.4	-10.6	-10.7	0.3
Mg II	4	4481.1	-17.8	- 2.1	- 1.1	- 6.0	- 8.7	- 7.6	- 1.7	- 7.0	0.8
Fe II	37	4515.3	-10.7	-17.2	-19.0	- 5.5	-13.8	- 4.2	- 9.1	-12.7	0.2
Fe II	38	4549.5	- 7.5	-11.4	-19.2	-16.2	-20.4	-17.9	-10.2	-14.7	0.7
Fe II	37	4555.9	-22.5	- 4.4	-14.6	-10.9	-17.4	- 7.2	- 5.1	-15.3	0.3
Fe II	38	4583.8	-26.1	-17.0	-16.3	-10.7	-10.7	- 9.4	-12.8	-12.8	0.4
Fe II bl	37	4629.3	-12.9	- 2.7	-11.6	-19.3	- 7.0	-29.4	-11.2	- 7.6	0.3
H Beta	1	4861.3	- 8.1	- 3.4	- 2.2	- 4.6	-10.7	4.0	3.7	-13.8	1.5
He I	48	4921.9	-38.7	- 5.2	-17.2	- 7.7	-12.4	-	-13.1	- 7.6	0.2
Fe II	42	4923.9	- 2.4	- 8.4	-18.5	- 9.5	-14.3	-	-16.1	- 8.2	0.4

Elem.	Mult.	Wav. Lab. (A)	JULIAN DATE (2440000+) 3391.566	3391.589	6819.357	Ave Eqw (A)
			Radial velocities(km/s)			
H Beta	1	4861.3	-17.8	-	-13.0	-
He I	48	4921.9	-	-	-13.6	-
Fe II	42	4923.9	- 8.4	-	-10.5	-
He I	4	5015.7	- 3.8	-	-15.5	0.1
Fe II	42	5018.4	-16.0	-	-10.6	0.3
Si II	5	5041.1	-11.5	-	-15.2	0.2
Si II	5	5056.0	-13.4	-	-11.5	0.3
Fe II	42	5169.0	-22.[illegible]	-	-12.0	0.4
Fe II	49	5234.6	-22.[illegible]	-	-11.9	0.2
Fe II	49	5276.0	-11.5	- 2.8	-10.8	0.2
Fe II	49	5316.6	- 5.0	- 8.9	-12.3	0.3
He I bl	11	5875.7	- 3.2	-10.2	- 5.1	0.3
Na I	1	5890.0	- 5.1	- 9.5	-13.3	0.6
Na I	1	5895.9	- 7.6	- 9.1	- 8.3	0.6
Si II	4	5957.6	-20.4	-15.0	-14.3	0.7
Si II	2	6347.1	- 1.5	-12.6	-13.6	0.7
Si II	2	6371.4	-12.1	-16.0	- 3.0	0.5
H Alph	1	6562.8	-54.8	-46.1	-19.3	0.4
He I	46	6678.2	- 5.6	-12.0	- 8.3	0.3

TABLE IV. — *Radial velocities of the Hα and Hβ lines relative to the center of mass velocities of the program stars.*

HD 199478

	JULIAN DATE (2440000+)										
	0830.348	0830.386	0830.415	0834.423	0836.461	0836.506	0931.234	0933.316	6400.331	6402.290	6639.414
	RV(km/s)										
H Beta	31.5	36.7	32.1	39.2	21.3	25.3	24.7	13.8	- 4.2	-16.3	-
H Alpha	-	-	-	-	73.7	79.1	-	-	-	-	73.9

HD 21291

	JULIAN DATE (2440000+)							
	6400.454	6401.586	6401.613	6818.250	6818.270	6818.323	6818.545	6819.294
	RV(km/s)							
H Beta	-17.8	- 5.5	-11.3	-13.6	3.3	- 0.2	- 9.3	-13.4
H Alpha	-26.6	-	-	-	-	-	-20.3	-19.7

HD 21389

	JULIAN DATE (2440000+)										
	3390.637	3390.684	3391.566	3391.589	3391.613	3391.626	5739.330	5741.270	6451.369	6451.398	6819.357
	RV(km/s)										
H Beta	- 2.1	2.6	-11.8	-	3.8	- 1.8	- 4.7	10.0	9.7	- 7.8	- 7.0
H Alpha	-	-	-48.8	-38.1	-	-	-	-	-	-	-13.3

TABLE V. — *Measured radial velocity differences between the average values of the radial velocities of SiII and FeII lines.*

Star	JULIAN DATE (2440000+)										
	0830.348	0830.386	0830.415	0834.423	0836.461	0836.506	0931.234	0933.316	6400.331	6402.290	6639.414
	RV(km/s)										
HD199478	3.9	6.3	1.9	4.5	3.3	0.4	0.8	7.1	2.7	2.5	0.6

Star	JULIAN DATE (2440000+)							
	6400.454	6401.586	6401.613	6818.250	6818.270	6818.323	6818.545	6819.294
	RV(km/s)							
HD21291	5.8	0.8	0.0	3.7	3.2	1.7	0.2	0.1

Star	JULIAN DATE (2440000+)										
	3390.637	3390.684	3391.566	3391.589	3391.613	3391.626	5739.330	5741.270	6451.369	6451.398	6819.357
	RV(km/s)										
HD21389	- 6.4	- 5.8	2.4	-	3.7	- 1.0	- 2.7	2.7	0.9	5.7	- 0.3

TABLE VI. — *Observed average quantities of the MgII 4481.1 and HeI 4471.5 lines.*

Star	Element	Wav. obs. (A)	Equ. (A)	Depth	Full Band width(A)	Halfwidth Blue part(A)	Halfwidth Red part(A)
HD 199478							
	Mg II	4480.9	1.0	- 0.5	1.5	0.8	0.7
	He I	4471.1	0.9	- 0.5	1.5	0.6	0.9
HD 21291							
	Mg II	4481.0	0.7	- 0.5	1.3	0.6	0.7
	He I	4471.4	0.3	- 0.3	1.2	0.6	0.6
HD 21389							
	Mg II	4481.1	1.1	- 0.8	1.3	0.6	0.7
	He I	4471.4	0.4	- 0.3	1.3	0.6	0.7

TABLE VII. — *Assigned optical depths for line or line groups taken from Zvereva et al. (1984).*

Line or line groups	log τ
H_α	-1.10
H_β	-1.02
H_γ	-0.98
H_δ	-0.92
H(8-10)	-0.80
H(13-18)	-0.64
Mg II	-0.40
Si II	-0.18
TiII,Fe II	-0.15
He I	0.0

TABLE VIII. — *Averaged equivalent widths, relative depths, and full bandwidths on the continuum of the unidentified interstellar features.*

Interstellar band	Eqw. (A)	HD 199478 Depth (A)	Bw. (A)
5780	0.2	-0.1	1.9
5797	0.1	-0.1	1.2
6614	0.2	-0.1	1.7
		HD 21291	
5780	0.3	-0.9	2.5
5797	0.1	-0.1	1.7
6614	0.2	-0.1	1.4
		HD 21389	
5780	0.4	-0.2	2.3
5797	0.1	-0.1	1.5
6614	0.1	-0.1	1.5

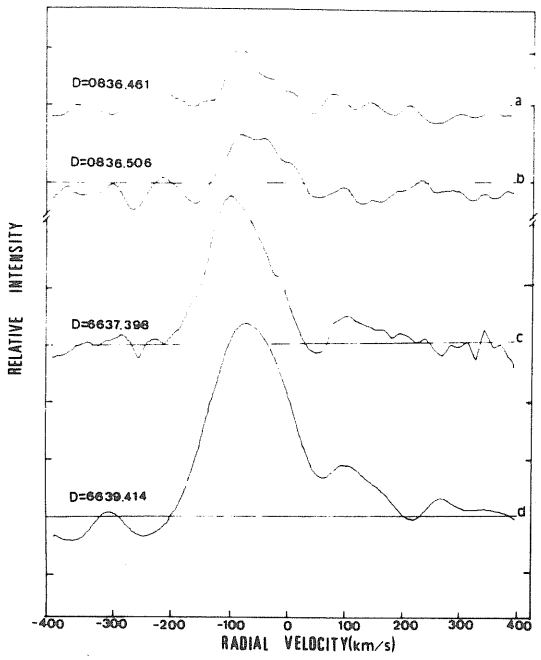

FIGURE 1. — Hα profiles of HD 199478. *X* axis gives the relative radial velocity with heliocentric correction and *Y* axis gives the relative intensity. Solid lines are continuum and each level corresponds to 0.1 difference in relative intensity. JD = 2440000 + .

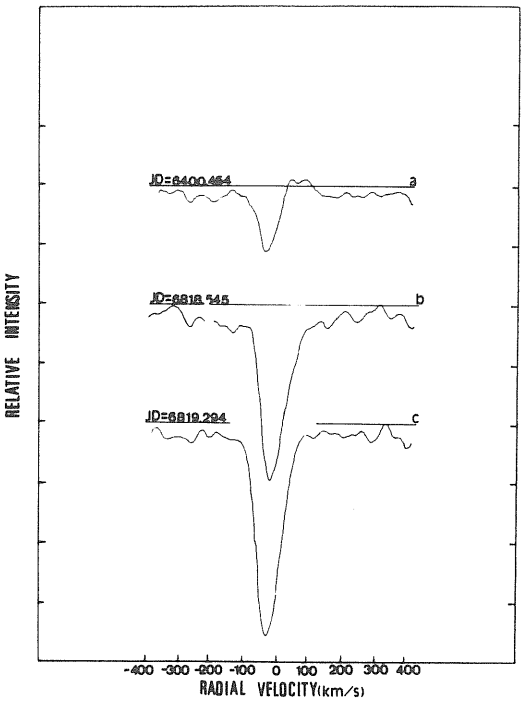

FIGURE 3. — Hα profiles of HD 21291 ; same as figure 1.

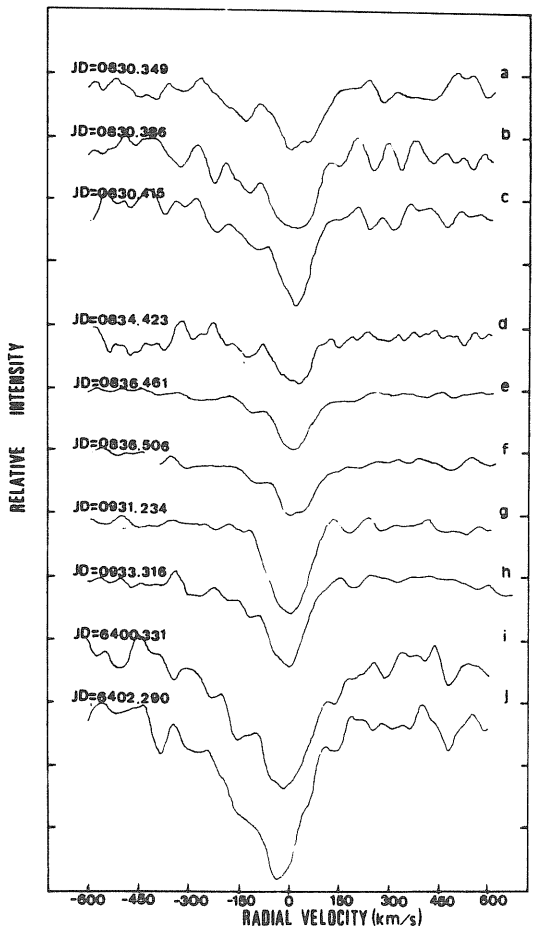

FIGURE 2. — Hβ profiles of HD 199478. Same axis as figure 1, but each level corresponds to 0.2 difference in relative intensity. JD = 2440000 + .

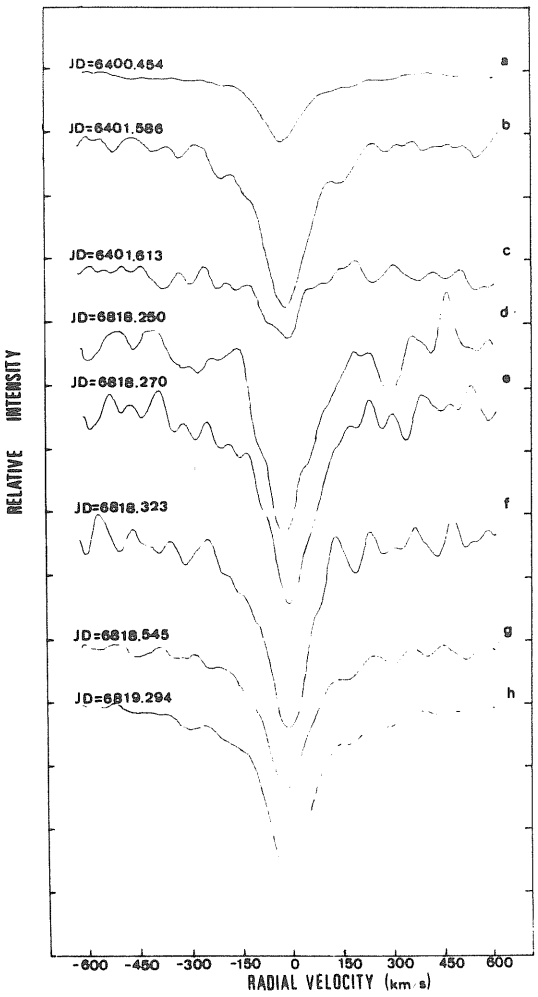

FIGURE 4. — Hβ profiles of HD 21291 ; same as figure 2.

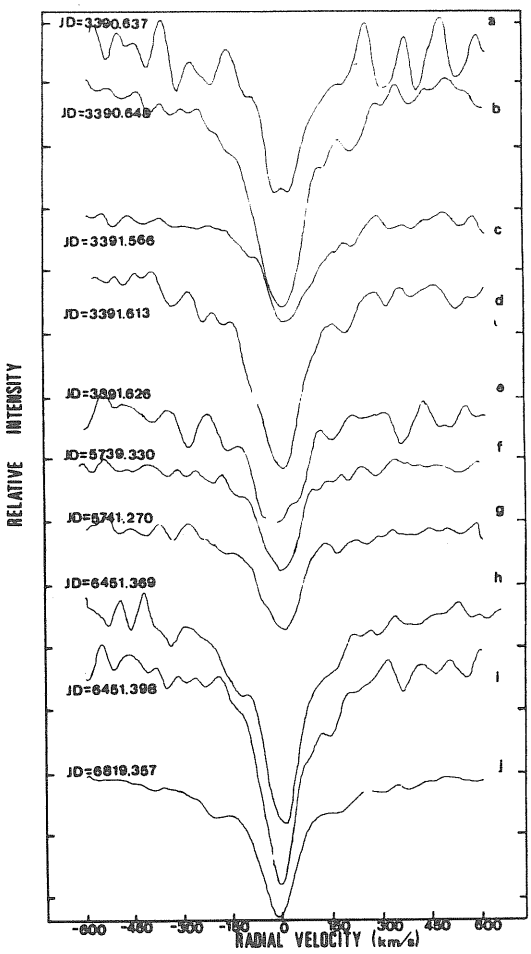

FIGURE 6. — Hβ profiles of HD 21389 ; same as figure 2.

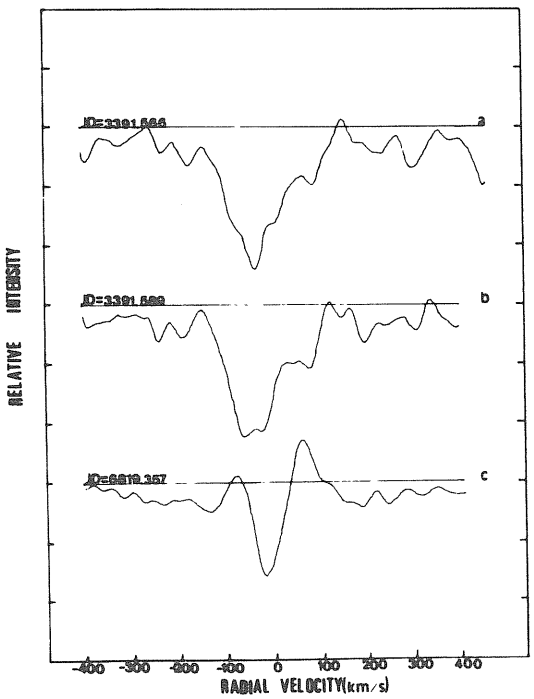

FIGURE 5. — Hα profiles of HD 21389 ; same as figure 1.

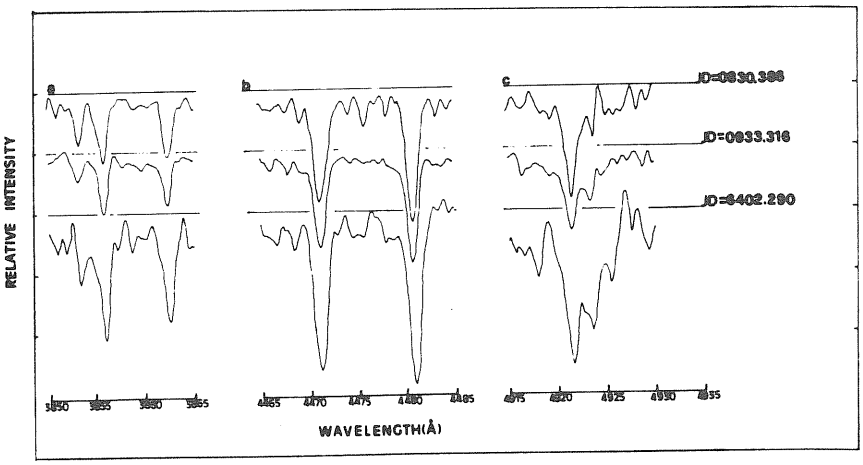

FIGURE 7. — Some selected lines of HD 199478: *X* axis gives heliocentrically corrected wavelengths in Angström. Each level corresponds to 0.2 difference in relative intensity and continua are marked with a solid line. JD = 2440000 + . a) SiII λλ3853.6, 3856.0, 3862.5 ; b) HeI λ4471.4 and MgII λ4481.1 ; c) HeI λ4921.9 and FeII λ4923.9.

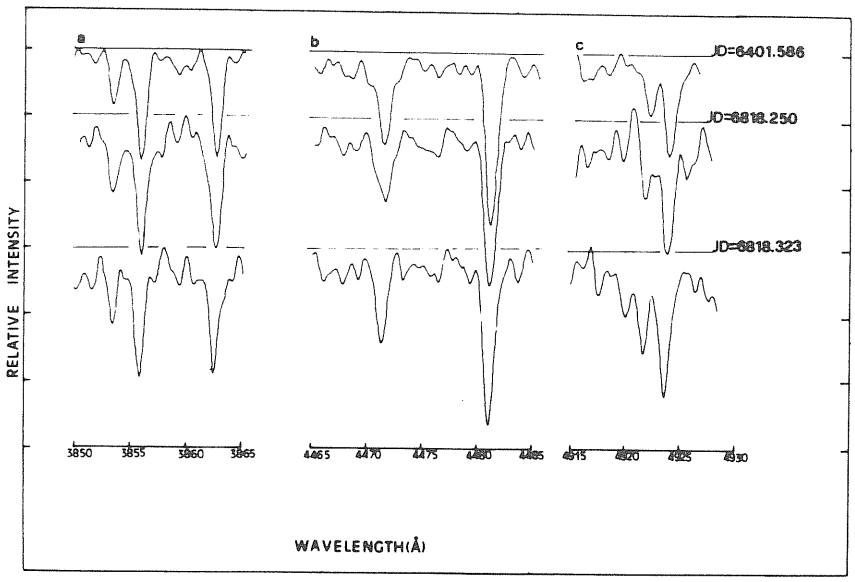

FIGURE 8. — Some selected lines for HD 21291. Same as figure 7.

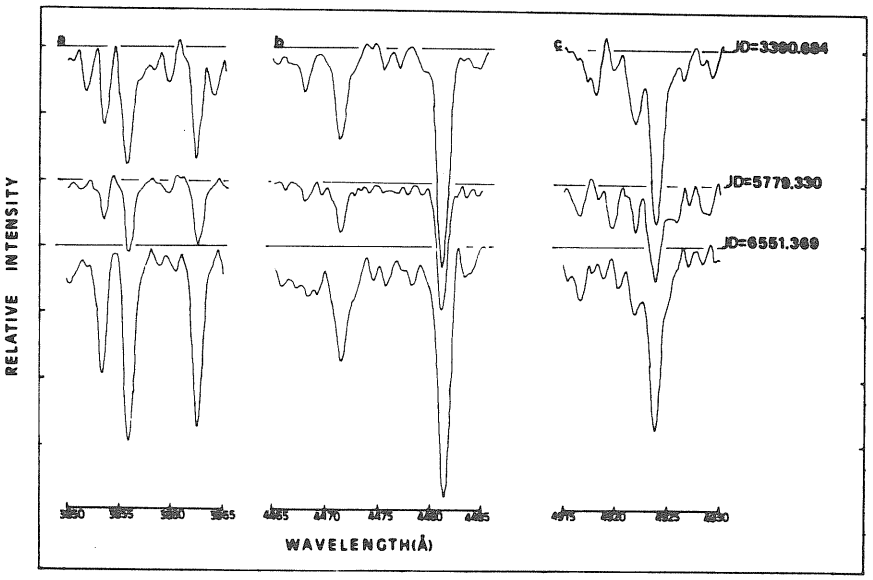

FIGURE 9. — Some selected lines for HD 21389. Same as figure 7.

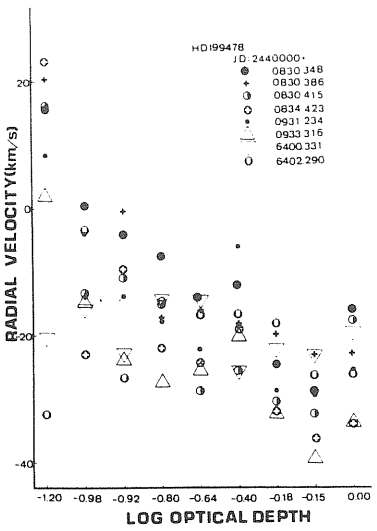

FIGURE 10. — Measured radial velocities *versus* log optical depth for HD 199478.

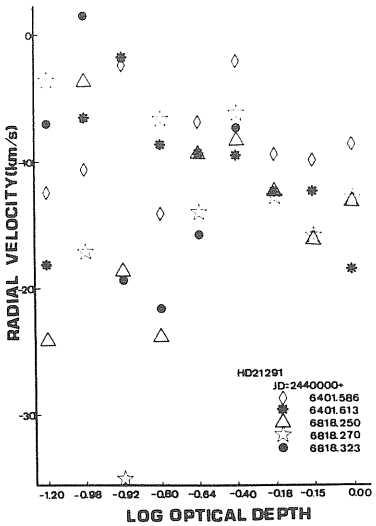

FIGURE 11. — Same as previous figure but for HD 21291.

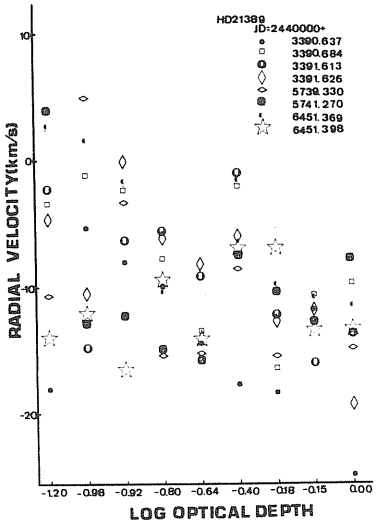

FIGURE 12. — Same as previous figure but for HD 21389.